

MECHANISMS OF PATHOLOGICAL ADIPOGENESIS

Role of ghrelin and ionic mechanisms in the
adipogenic differentiation of bone

MARINE BASTIEN

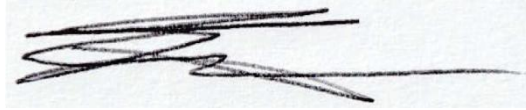
A thesis submitted in partial fulfillment of the requirements of Liverpool John Moores
University for the degree of Philosophiæ Doctor

May 2019

University statement

I declare that the work presented in this thesis is my own and has not been submitted for a comparable academic award.

Signed

A handwritten signature in black ink, consisting of several overlapping, fluid strokes that form a stylized, somewhat abstract shape.

Date: 26/04/2019

Summary

Although adipose tissue plays important physiological roles, the increase in adiposity with aging is a common feature in several pathologies, including some forms of osteoporosis. Ion channels and ghrelin signalling have been shown to be involved in regulating many cell processes such as proliferation, differentiation and apoptosis, particularly in bone. This thesis investigated the roles of ghrelin and ion channels in the adipogenic differentiation of 7F2 preosteoblastic cells. The amount of Oil Red O stain increased by 135%, and the mRNA expression of two adipocytic markers, PPAR γ (5.46 ± 0.22 ; $p = 0.024$) and C/EBP α (25.3 ± 0.21 ; $p = 0.0048$), was higher in 7F2 cells cultured with adipogenic medium compared with basal medium, indicating that 7F2 cells differentiated into adipocytes. 7F2 cells also expressed previously unreported variant isoforms of ghrelin at the mRNA level; these variants isoforms were much more abundant than native ghrelin. 7F2 cells also express the other key genes from ghrelin signalling, i.e. *Ghsr* and *Mboat4*, suggesting that ghrelin or its variant isoforms may have autocrine/paracrine effects in these cells. Ghrelin mRNA expression was higher in 7F2 cells treated with basal medium + 200 nM ghrelin (144.84 ± 0.58) and adipogenic medium + 200 nM ghrelin (123.07 ± 0.33) compared with cells cultured with basal medium alone ($p = 0.01$), and adipogenic medium alone (0.79 ± 0.40 ; $p = 0.0089$), respectively. Treatment with 20 nM and 200 nM ghrelin had no significant effect on lipid content and on osteoblastic and adipocytic markers mRNA levels ($p > 0.05$). On the contrary, cell numbers were lower in 7F2 cells cultured with the voltage-gated K⁺ channel blocker tetraethylammonium, and lipid droplets inside 7F2 cell-derived adipocytes were smaller compared with cells cultured with adipogenic medium alone, suggesting that voltage-gated K⁺ channels are involved in regulating cell proliferation and adipogenic differentiation. 7F2 cells and 7F2 cell-derived adipocytes expressed the K_{ATP} channel subunits *Kcnj8* and *Sur2B*, and the BK channel subunits *Kcnma1* and *Kcnmb2*. 12 types of functional ion channels were detected in electrophysiology experiments but could not be identified. In conclusion, ghrelin treatment did not inhibit adipogenic differentiation in 7F2 cells, but 7F2 cells expressed previously unreported variant isoforms of ghrelin and ion channels which may play important roles in regulating osteoblast functions and adipogenic differentiation. Future work is required to confirm the presence of ghrelin variants at the protein level, and to study the roles of these variants and ionic mechanisms in bone metabolism. A better understanding of the mechanisms underlying pathological adipogenesis in bone may provide interesting therapeutic targets for disorders such as osteoporosis.

Table of contents

University statement.....	i
Summary.....	ii
Table of contents.....	iii
Acknowledgements	xi
List of figures and tables.....	xii
Abbreviations.....	xvii
Chapter 1 – Introduction.....	1
1.1. Outline	2
1.2. Bone.....	3
1.2.1. Functions of bone	3
1.2.2. Bone remodelling	4
1.2.3. Bone marrow adipose tissue	7
1.2.4. Mesenchymal stem cells	8
1.2.4.1. Definition.....	8
1.2.4.2. Osteogenesis and adipogenesis	8
1.2.4.2.1. Osteogenic differentiation of BMSCs.....	8
1.2.4.2.2. Adipogenic differentiation of BMSCs.....	9
1.3. Osteoporosis	10
1.3.1. Definition of osteoporosis.....	10
1.3.2. Osteoporosis: obesity of the bone?	12
1.3.1. Treatments for osteoporosis	14
1.4. Ghrelin	15
1.4.1. Ghrelin signalling: an overview.....	15
1.4.1.1. Ghrelin.....	15
1.4.1.2. Growth Hormone Secretagogue Receptor (GHSR)	16
1.4.1.3. Ghrelin-O-acyltransferase (GOAT)	18
1.4.2. Ghrelin is much more than a ‘hunger hormone’	20

1.4.2.1.	Ghrelin and bone.....	21
1.4.2.2.	Ghrelin and adipogenesis	23
1.5.	Ion channels	24
1.5.1.	Potassium channels and membrane potential	25
1.5.2.	Ion channels and bone.....	26
1.5.2.1.	Potassium channels and osteoblasts	27
1.5.2.2.	Potassium channels and adipocytes	29
1.6.	Hypothesis, aims and experimental strategies	30
Chapter 2 – Materials and Methods		32
2.1.	Cell culture	33
2.1.1.	Routine cell culture.....	33
2.1.2.	Adipogenic differentiation of 7F2 cells.....	33
2.1.2.1.	Adipogenic differentiation medium	33
2.1.2.2.	Adipogenic differentiation for Oil Red O staining assay	34
2.1.2.3.	Adipogenic differentiation for RT-PCR analysis.....	34
2.2.	Cell counting.....	35
2.3.	Molecular biology.....	35
2.3.1.	RNA extraction and DNase treatment	35
2.3.2.	Reverse transcription	36
2.3.3.	Polymerase chain reaction (PCR)	37
2.3.4.	Gel electrophoresis	38
2.3.5.	Quantitative PCR (qPCR)	38
2.3.6.	Sequencing	40
2.3.6.1.	Gel extraction of PCR products.....	40
2.3.6.2.	Sanger sequencing.....	41
2.3.6.3.	Analysis of sequencing data.....	41
2.3.7.	Statistical analysis	41
2.4.	Electrophysiology	42
2.4.1.	Physiological recording solution.....	42

2.4.2. Electrode fabrication.....	43
2.4.3. Electrophysiology apparatus	43
2.4.4. Patch-clamp methodology	44
2.4.4.1. Single-channel patch-clamp.....	44
2.4.4.2. Perforated patch-clamp.....	45
2.4.5. Data acquisition and analysis	46
Chapter 3 – Protocol optimisation for the differentiation of murine 7F2 osteoblast-like cells into adipocytes.....	47
3.1. Introduction	48
3.1.1. <i>In vitro</i> differentiation into adipocytes.....	48
3.1.2. Chapter objectives and experimental strategies	50
3.2. Materials and Methods	52
3.2.1. Cell culture and adipogenic differentiation of 7F2 cells.....	52
3.2.2. Molecular biology.....	52
3.2.2.1. RNA extraction, DNase treatment and reverse transcription.....	52
3.2.2.2. PCR.....	52
3.2.2.2.1. Oligonucleotide primers: house-keeping and differentiation marker genes.....	52
3.2.2.2.2. PCR reaction compositions and conditions	52
3.2.2.3. Gel electrophoresis.....	54
3.2.2.4. Quantitative PCR.....	54
3.2.3. Statistical analysis	54
3.3. Results	55
3.3.1. Length of treatment.....	55
3.3.2. Seeding density has a strong effect on adipogenic trans-differentiation.....	55
3.3.3. Insulin failed to further stimulate adipogenic trans-differentiation.....	56
3.3.4. Adipogenic treatment: final protocol	56
3.3.4.1. Adipogenic treatment increases lipid content and decreases cell number	56

3.3.4.2. mRNA expression levels of adipogenic markers increase while mRNA expression levels of osteoblastic markers decrease	57
3.4. Discussion	59
3.4.1. Adipogenic differentiation of 7F2 cells.....	59
3.4.2. Chapter conclusions	60
Chapter 4 – 7F2 osteoblast-like cells and 7F2 cell-derived adipocytes express <i>Ghsr</i> , <i>Mboat4</i> and several isoforms of <i>Ghrl</i>	77
4.1. Introduction	78
4.1.1. Ghrelin: one gene that encodes a variety of peptides.....	78
4.1.1.1. Structure of the ghrelin gene.....	78
4.1.1.2. Alternative splicing of the ghrelin gene	79
4.1.2. Chapter hypothesis, objectives and experimental strategies.....	81
4.2. Materials and Methods	82
4.2.1. Adipogenic differentiation and ghrelin treatment of 7F2 cells	82
4.2.2. Molecular biology	82
4.2.2.1. RNA extraction, DNase treatment and reverse transcription.....	82
4.2.2.2. PCR.....	82
4.2.2.2.1. Oligonucleotide primers: house-keeping and ghrelin signalling genes	82
4.2.2.2.2. PCR reaction compositions and conditions	82
4.2.2.3. Gel electrophoresis.....	83
4.2.2.4. Gel extraction of PCR products and sequencing.....	83
4.2.2.5. Quantitative PCR.....	84
4.2.3. Statistical analysis	84
4.3. Results	85
4.3.1. 7F2 cells express <i>Ghrl</i> , <i>Ghsr</i> , and <i>Mboat4</i>	85
4.3.2. mRNA expression of ghrelin signalling system is responsive to adipogenic medium and exogenous ghrelin	85
4.3.3. Identification of ghrelin variant expressed in 7F2 cells	86
4.3.3.1. Ghrelin mRNA retains several introns in 7F2 cells	86

4.3.3.2. Sequencing data.....	88
4.3.4.3. Prediction of protein structure.....	88
4.4. Discussion	90
4.4.1. 7F2 cells express <i>Ghsr</i> , <i>Mboat4</i> , and variant isoforms of <i>Ghrl</i>	90
4.4.2. Ghrelin treatment promotes ghrelin mRNA expression	92
4.4.3. Chapter conclusions	93
Chapter 5 – The influence of ghrelin and K ⁺ channel ligands on adipogenic differentiation of 7F2 cells.....	104
5.1. Introduction	105
5.1.1. K _{ATP} channels	105
5.1.2. BK channels.....	108
5.1.3. Chapter hypothesis, objectives and experimental strategy.....	109
5.2. Materials and Methods	111
5.2.1. Cell culture.....	111
5.2.1.1. Adipogenic differentiation and ghrelin treatment of 7F2 cells.....	111
5.2.1.2. Cell counting.....	111
5.2.1.3. Inhibition of GHSR	111
5.2.1.4. Treatment with tetraethylammonium (TEA).....	111
5.2.1.5. Treatment with diazoxide	111
5.2.2. Molecular biology	112
5.2.2.1. RNA extraction, DNase treatment and reverse transcription.....	112
5.2.2.2. PCR.....	112
5.2.2.2.1. Oligonucleotide primers	112
5.2.2.2.2. PCR reaction compositions and conditions	112
5.2.2.2.4. Gel electrophoresis	113
5.2.2.3. Quantitative PCR.....	114
5.2.3. Statistical analysis	114
5.3. Results	115
5.3.1. Effects of ghrelin on 7F2 cells and 7F2 cell-derived adipocytes	115

5.3.1.1. Effects of ghrelin on cell number	115
5.3.1.2. Effects of ghrelin on adipogenic differentiation	115
5.3.1.2.1. Effect on lipid content.....	115
5.3.1.2.2. Effect on differentiation marker mRNA expression.....	116
5.3.1.2.3. The effects of ghrelin in 7F2 cells may be mediated by GHSR.....	117
5.3.1.3. Ionic mechanisms in 7F2 cells and 7F2 cell derived adipocytes, and the effects of ghrelin on these.....	118
5.3.1.3.1. K _{ATP} channels	118
5.3.1.3.2. BK channel.....	119
5.3.2. Pharmacological modulation of K ⁺ channels: effect on adipogenesis.....	119
5.3.2.1. Effects of TEA.....	119
5.3.2.1.1. TEA decreases the amount of lipids in 7F2-cell derived adipocytes	119
5.3.2.1.2. TEA decreases cell proliferation.....	120
5.3.2.2. Effects of diazoxide on 7F2 cell adipogenic differentiation.....	120
5.4. Discussion	122
5.4.1. Ghrelin treatment affects 7F2 cell differentiation, but not proliferation	122
5.4.2. Potassium channel ligands modulate proliferation and adipogenic differentiation of 7F2 cells.....	124
5.4.2. Chapter conclusions	126
Chapter 6 – A comparison of the electrophysiological characteristics of osteoblasts and adipocytes, and the effects of ghrelin on these	156
6.1. Introduction	157
6.1.1. Ionic mechanisms in ghrelin signalling	157
6.1.2. Chapter objectives and hypothesis.....	158
6.2. Materials and Methods	159
6.2.1. Adipogenic differentiation and ghrelin treatment of 7F2 cells	159
6.2.2. Electrophysiology.....	159
6.3. Results	160
6.3.1. Small conductance currents	163

6.3.1.1. Current 1.....	163
6.3.1.2. Current 2.....	163
6.3.1.3. Current 3.....	163
6.3.1.4. Current 4.....	164
6.3.1.5. Current 5.....	164
6.3.2. Intermediate conductance currents	164
6.3.2.1. Current 6.....	164
6.3.2.2. Current 7.....	164
6.3.3. Large conductance currents.....	165
6.3.3.1. Current 8.....	165
6.3.3.2. Current 9.....	165
6.3.4. Rectifying currents.....	165
6.4. Discussion	167
6.4.1. Problems encountered while recording electrophysiological data.....	167
6.4.2. Ion channel candidates.....	168
6.4.2.1. Currents detected only in 7F2 osteoblast-like cells.....	169
6.4.2.2. Currents detected only in 7F2 cells treated with ghrelin.....	170
6.4.2.13. Currents detected in 7F2 cells both in absence and in presence of ghrelin.....	171
6.4.3. Chapter conclusions	173
Chapter 7 – General discussion and conclusions	216
7.1. Summary of Key Findings.....	217
7.2. Discussion of findings.....	218
7.3. Limitations and assumptions.....	221
7.3.1. Cell culture assays	221
7.3.2. Molecular biology	222
7.3.3. Electrophysiology.....	222
7.4. Recommendations for future work	223
7.5. Concluding statement.....	225

Chapter 8 – Appendix	227
8.1. Oligonucleotide primers.....	228
8.1.1. Oligonucleotide primers for house-keeping genes.....	228
8.1.2. Oligonucleotide primers for differentiation markers.....	230
8.1.3. Oligonucleotide primers for ghrelin signalling genes	234
8.1.4. Oligonucleotide primers for ghrelin signalling genes	236
8.1.5. Oligonucleotide primers for ion channels.....	240
8.2. Sequencing of <i>Ghrl</i> PCR products	245
Chapter 9 – References	257

Acknowledgements

First of all, I would like to thank my three supervisors, Dr Neil Henney, Dr Andrew Evans and Dr James Downing, for their help and support, on a daily basis and during the writing stage of my PhD. I am very grateful for their advice and encouragement.

I would also like to thank Dr. Daniel Graham, Dr. Jerry Bird, Dr. John Hall, Paul Mintz and the staff at the School of Pharmacy and Biomolecular Sciences for their time and assistance. I must also thank Stephen Broadfoot for providing a quiet lab where to perform electrophysiological recording.

Finally, I would like to thank my family and Antonin for their encouragement and unwavering support.

List of figures and tables

Figures

Fig 1.1	Cellular activities supporting bone remodelling	6
Fig 1.2	Parameters that influence circulating levels of ghrelin	16
Fig 1.3	Posttranslational modifications of ghrelin	20
Fig 1.4	Main physiological activities of ghrelin	21
Fig 1.5	K ⁺ channel subfamilies	25
Fig 2.1	All bands with exact DNA quantity	38
Fig 2.2	Statistical analysis of data	42
Fig 2.3	Example of 7F2 cells before and after recording	45
Fig 3.1	Oil Red O staining and quantification after 2, 4 and 7 days of treatment	61-62
Fig 3.2	Effect of seeding density on the trans-differentiation of 7F2 cells	63-66
Fig 3.3	Effects of 5 µg/ml insulin on adipogenic differentiation	67-68
Fig 3.4	Effect of adipogenic treatment on 7F2 cell lipid content and cell number	69-71
Fig 3.5	Effect of adipogenic medium on the mRNA expression of differentiation markers	72-74
Fig 3.6	No RT controls for differentiation markers	75
Fig 4.1	From the mouse ghrelin gene to mature peptide	79
Fig 4.2	RT-PCR for the genes from ghrelin signalling	95
Fig 4.3	qRT-PCR analysis of <i>Ghrl</i> expression in 7F2 cells treated with ghrelin	96
Fig 4.4	qRT-PCR analysis of <i>Ghsr</i> expression in 7F2 cells treated with ghrelin	97
Fig 4.5	qRT-PCR analysis of <i>Mboat4</i> expression in 7F2 cells treated with ghrelin	98
Fig 4.6	Characterisation of the ghrelin variant expressed in 7F2 cells by	99-101

	RT-PCR analysis	
Fig 4.7	No RT controls for the ghrelin variants	102-103
Fig 5.1	K _{ATP} channel structure	107
Fig 5.2	BK channel structure	109
Fig 5.3	Effects of 20 nM ghrelin on cell numbers	127
Fig 5.4	Effects of 20 nM ghrelin on the lipid content	128-129
Fig 5.5	Effects of 200 nM ghrelin on lipid content	130-131
Fig 5.6	RT-PCR analysis of differentiation markers in 7F2 cells treated with 20 nM ghrelin	132
Fig 5.7	qRT-PCR analysis of differentiation markers in 7F2 cells treated with 20 nM and 200 nM ghrelin	133-136
Fig 5.8	Role of GHSR in the effects of ghrelin on the adipogenic differentiation of 7F2 cells: RT-PCR analysis	137
Fig 5.9	Role of GHSR in the effects of ghrelin on the adipogenic differentiation of 7F2 cells: qRT-PCR analysis	138-139
Fig 5.10	No RT controls for the differentiation markers	140-141
Fig 5.11	RT-PCR analysis for the K _{ATP} channel subunits	142
Fig 5.12	qPCR analysis for K _{ATP} channel subunits	143-144
Fig 5.13	RT-PCR analysis for the BK channel subunits	145
Fig 5.14	qPCR analysis for <i>Kcnma1</i>	146
Fig 5.15	Effects of TEA on 7F2 cell adipogenic differentiation	147-151
Fig 5.16	Effects of TEA of cell numbers	152
Fig 5.17	Effects of diazoxide on the adipogenic differentiation of 7F2 cells	153-155
Fig 6.1	Ghrelin inhibits insulin secretion via activation of Kv2.1	158
Fig 6.2	Patch configurations for electrophysiological recording	174
Fig 6.3	Current 1 in 7F2 cells cultured with adipogenic medium + 20 nM ghrelin	175-176
Fig 6.4	Current 1 in 7F2 cells cultured with basal medium + 20 nM ghrelin	177-178

Fig 6.5	Current 2 in 7F2 cells cultured with adipogenic medium + 20 nM ghrelin	179-180
Fig 6.6	Current 2 in 7F2 cells cultured with basal medium + 20 nM ghrelin	181
Fig 6.7	Current 3 in 7F2 cells cultured with basal medium	182-183
Fig 6.8	Current 3 in 7F2 cells cultured with adipogenic medium + ghrelin (cell-attached)	184-185
Fig 6.9	Current 3 in 7F2 cells cultured with adipogenic medium + ghrelin (excised inside-out)	186-187
Fig 6.10	Current 3 in 7F2 cells cultured with basal medium + ghrelin (excised inside-out)	188-189
Fig 6.11	Current 4 in 7F2 cells cultured with basal medium	190-191
Fig 6.12	Current 5 in 7F2 cells cultured with basal medium	192-193
Fig 6.13	Current 5 in 7F2 cells cultured with adipogenic medium	194-195
Fig 6.14	Current 5 in 7F2 cells cultured with adipogenic medium + ghrelin	196-197
Fig 6.15	Current 6 in 7F2 cells cultured with adipogenic medium + ghrelin	198-199
Fig 6.16	Current 7 in 7F2 cells cultured with basal medium + ghrelin	200-201
Fig 6.17	Current 8 in 7F2 cells cultured with basal medium (cell-attached)	202-203
Fig 6.18	Current 8 in 7F2 cells cultured with basal medium (excised inside-out)	204-205
Fig 6.19	Current 9 in 7F2 cells cultured with basal medium + ghrelin	206-207
Fig 6.20	Current 10 in 7F2 cells cultured with basal medium	208-209
Fig 6.21	Current 10 in 7F2 cells cultured with adipogenic medium + ghrelin	210-211
Fig 6.22	Current 11 in 7F2 cells cultured with adipogenic medium	212-213
Fig 6.23	Current 12 in 7F2 cells cultured with adipogenic medium + ghrelin	214-215
Fig 8.1	Primers and amplification sequences for house-keeping genes.	229

Fig 8.2	Primers and amplification sequences for differentiation markers.	231-233
Fig 8.3	Primers and amplification sequences for ghrelin signalling components.	235
Fig 8.4	Primers and amplification sequences for the various regions of the ghrelin gene	238-239
Fig 8.5	Primers and amplification sequences for ion channels	241-244
Fig 8.6	Sequencing of the 741 bp band from PCR with primers located on exons 1 and 3	246-248
Fig 8.7	Sequencing of the 315 bp band from PCR with primers located on exons 2 and 3	249-250
Fig 8.8	Sequencing of the 924 bp band from PCR with primers located on exons 4 and 5	251-253
Fig 8.9	Sequencing of the 2088 bp band from PCR with primers located on exons 3/4 and 5	254-256

Tables

Table 1.1	Subtypes of osteoporosis	11
Table 1.2	Various types of therapies against osteoporosis	15
Table 2.1	Reverse transcription reaction composition	36
Table 2.2	Reverse transcription reaction conditions	37
Table 2.3	PCR reaction composition	37
Table 2.4	qPCR reaction composition	39
Table 2.5	qPCR cycling conditions	39
Table 2.6	Composition of electrophysiological solutions	43
Table 3.1	PCR reaction conditions	53
Table 4.1	PCR reaction conditions	83
Table 5.1	PCR reaction conditions	113
Table 6.1	Summary of electrophysiology recordings	161
Table 6.2	List of the currents detected	161

Table 6.3	Summary of the characteristics of the currents detected	162
Table 8.1	Oligonucleotide primer details for differentiation markers	228
Table 8.2	Oligonucleotide primer details for differentiation markers	230
Table 8.3	Oligonucleotide primer details for ghrelin signalling components	234
Table 8.4	Names, sequences and location of primers	236
Table 8.5	Expected product size for each tested sets of primers	237
Table 8.6	Oligonucleotide primer details for ion channels	240

Abbreviations

ADP	Adenosine diphosphate
ALP	Alkaline phosphatase
AM	Adipogenic medium
aP2	Adipocyte protein 2
ATF4	Activating transcription factor 4
ATP	Adenosine triphosphate
BK	Large conductance, calcium-activated K channel
BM	Basal medium
BMAT	Bone marrow adipose tissue
BMD	Bone mineral density
BMP	Bone morphogenetic protein
BMSC	Bone marrow stromal cell
BMU	Bone multicellular unit
Cbfa1	Core-binding factor alpha 1
C/EBP α	CCAAT/enhancer binding protein- α
C/EBP β	CCAAT/enhancer binding protein- β
C/EBP δ	CCAAT/enhancer binding protein- δ
cDNA	Complementary deoxyribonucleic acid
ClC	Chloride channel
CMKLR1	Chemokine-like receptor 1
CNS	Central nervous system
COX	Cyclooxygenase
CREB	cAMP response element-binding protein
DLS	D-[Lys3] GHRP-6
DMEM	Dulbecco's modified Eagle medium
DMSO	Dimethyl sulfoxide
DNA	Deoxyribonucleic acid
dNTP	Deoxyribonucleotide triphosphate
DPBS	Dulbecco's phosphate buffered saline
Eag	Ether-à-go-go
EDTA	Ethylenediaminetetraacetic acid
EEF2	Eukaryotic translation elongation factor 2
ERK1/2	Extracellular signal-regulated kinases 1/2
FBS	Fetal bovine serum

GGDT	Ghrelin gene-derived transcript
GH	Growth hormone
Ghrl	Ghrelin
GHS	Growth hormone secretagogue
GHSR	Growth hormone secretagogue receptor
Glut4	Glucose transporter type 4
GOAT	Ghrelin <i>O</i> -acyltransferase
GOI	Gene of interest
GPCR	G protein-coupled receptor
HCl	Hydrochloric acid
HEPES	4-(2-hydroxyethyl)-1-piperazineethanesulfonic acid
HK	House-keeping gene
HRT	Hormone replacement therapy
I	Current
IBMX	isobutylmethylxanthine
IGF-1	Insulin-like growth factor 1
IKCa	Intermediate-conductance calcium-activated potassium channel
IKDR	Delayed rectifier potassium current
K2P	2-pore domain potassium channel
K _{ATP}	ATP-dependent potassium channel
KCa	Calcium-activated potassium channel
KIR	Inward rectifier potassium channel
KOH	Potassium hydroxyde
K _v	Voltage-regulated potassium channel
Mboat4	Membrane-bound <i>O</i> -acyltransferase 4
MEM- α	Alpha-minimum essential medium
mRNA	Messenger RNA
MSC	Mesenchymal stem cell
NaOH	Sodium hydroxyde
NBD	Nucleotide binding domain
NDP	Nucleoside-diphosphate
NSAID	Non-steroidal anti-inflammatory drug
ORF	Open reading frame
OSE 2	Osteoblast-specific element 2
Osf2	Osteoblast-specific transcription factor 2
Osx	Osterix

OX1R	Orexin receptor 1
PBS	Phosphate buffered saline
PCR	Polymerase Chain Reaction
PFA	Paraformaldehyde
PGD	Pore-gate domain
PGE2	Prostaglandin E2
PKA	Protein kinase A
Po	Open probability
Popen	Open probability
PPAR γ	Peroxisome proliferator-activated receptor- γ
PTH	Parathyroid hormone
qRT-PCR	Quantitative Reverse Transcription-Polymerase Chain Reaction
RANKL	Receptor activator of nuclear factor kappa B ligand
RCK	Regulator of potassium conductance
RNA	Ribonucleic acid
RT	Reverse transcription
RT-PCR	Reverse Transcription-Polymerase Chain Reaction
Runx2	Runt-related transcription factor 2
SB Buffer	Sodium-borate buffer
SD	Standard deviation
SEM	Standard error of the mean
SERM	Selective estrogen receptor modulator
shRNA	Small hairpin ribonucleic acid
siRNA	Small interfering ribonucleic acid
SSC	Skeletal stem cell
SUR	Sulphonylurea receptor
TEA	Tetraethylammonium
TGF	Transforming growth factor
TMD	Transmembrane domain
TRPV	Transient receptor potential, vanilloid-type
V	Voltage
VDCC	Voltage-dependent calcium channel
VRAC	Volume-regulated anion channel
VSD	Voltage-sensor domain

Chapter 1 - Introduction

1.1. Outline

While adipose tissue plays an essential role in many physiological processes, pre-terminal differentiation or trans-differentiation of mature mesenchymal cell phenotypes into adipocytes within different tissues is proposed to be a common feature of certain pathologies, including osteoporosis, cancer or age-associated immune senescence. Adipose tissue is an important regulator of bone metabolism via the secretion of factors that can regulate bone homeostasis by direct and indirect mechanisms (Ali *et al.*, 2013). Bone is a multifunctional, dynamic tissue that is constantly remodelled; bone homeostasis is a result of the balance between two processes: bone resorption and bone formation. Both these processes depend on the proliferation, differentiation and functions (resorption/mineralisation) of specialised bone cells, osteoclasts and osteoblasts. Any interference with any of these key physiological processes can result in unbalanced bone resorption or formation, leading to bone disorders. Bone marrow contains adipose tissue, which participates in regulating bone homeostasis, but is also associated with several bone disorders, such as osteoporosis. Osteoporosis is one of the most common bone disorders, affecting over 3 million people in the United Kingdom; the economic cost of fragility fractures was estimated at £3,497 million in 2010 (Svedbom *et al.*, 2013). Osteoporosis is associated with decreased osteoblast formation and activity, and increased adipogenesis. There are several risk factors for osteoporosis, such as long-term glucocorticoid therapy (Briot and Roux, 2015). Various treatments are already available, but they are not adapted for every patient, so it is necessary to develop new treatments. Prevention is also an important aspect of osteoporosis management, and understanding the mechanisms of the pathology can help with that. There are many factors regulating bone homeostasis; in particular, hormones from energy metabolism, such as ghrelin, play a central role. Ghrelin, which was first discovered in 1999 for its actions in stimulating growth hormone (GH) release and appetite (Kojima *et al.*, 1999; Wren *et al.*, 2000), plays many roles in peripheral tissues, including bone and adipose tissues, regulating osteoblast and adipocyte proliferation and differentiation (Delhanty *et al.*, 2014a; Müller *et al.*, 2015). Although mice deficient in ghrelin (*Ghrl*^{-/-}) or ghrelin receptor (*Ghsr*^{-/-}) have unaltered bone mineral density (BMD) (Sun *et al.*, 2003, 2004), their bone microarchitecture is modified: *Ghsr*^{-/-} mice have lower trabecular bone mass, while *Ghrl*^{-/-} mice have lower cortical bone mass (Delhanty *et al.*, 2014b; a). The role of ion channels in bone homeostasis is now well established; numerous ion channels are expressed in mesenchymal stem cells (MSCs), osteoblast precursors and

osteoblasts. A large number of studies have demonstrated that ion channels, and particularly potassium (K⁺) channels, regulate cell proliferation, differentiation and functions in bone MSCs (Tao *et al.*, 2008), osteoblasts (Henney, 2008; Henney *et al.*, 2009; Li, 2012), osteoclasts (Yeon *et al.*, 2015) and adipocytes (Zhang *et al.*, 2012). Mutations in ion channels can be involved in some pathologies called channelopathies, including in bone; for example, mutations in the chloride transporter CLC-7 are associated with osteopetrosis, and this channel may be a therapeutic target against osteoporosis (Zhao *et al.*, 2009; Schulz *et al.*, 2010). Finally, K⁺ channels are also involved in mediating ghrelin signalling (Dezaki *et al.*, 2007). The work presented in this thesis focuses on the role of ghrelin and ionic mechanisms in the adipogenic transdifferentiation of murine 7F2 cells as a model for the adipogenesis of osteoblast precursors.

1.2. Bone

Bone is a multifunctional organ, playing important mechanical and metabolic roles. Bone is a dynamic tissue; it is constantly renewed through a process called remodelling, which involves bone resorption by specialised cells called osteoclasts, followed by new bone formation by osteoblasts. In addition to osteoblasts and osteoclasts, bone also contains various other cells, including haematopoietic stem cells, MSCs, osteocytes, lining cells, and adipocytes (Contador *et al.*, 2015); these cells communicate with and influence each other (Datta *et al.*, 2008). Osteoblasts and adipocytes originate from the same precursors, the MSCs.

1.2.1. Functions of bone

Bone plays several important mechanical roles: as a skeleton it is essential for locomotion, providing structure and support for the body and enabling mobility. It also provides protection for important organs such as the brain, protected by the skull, and the heart, protected by the ribcage. Bone is composed of two types of bone tissues: cortical bone and trabecular bone. Cortical bone is compact and forms the outside part of bones. Trabecular bone forms the internal part of bones, is less dense than cortical bone, and frequently contains myeloid tissue, where haematopoiesis occurs (Porter and Calvi, 2008).

Bone also plays important metabolic roles. Bone functions as a mineral store and is a vital player of the calcium-phosphate homeostasis, storing these two minerals and releasing them in the circulation during the process of bone resorption. Bone stores

lipids via the bone marrow adipocytes. There are multiple regulatory links between bone and energy metabolism: bone metabolism is both a target and a regulator of energy metabolism via direct and indirect mechanisms, hormones acting systemically and/or cytokines acting locally. Osteoblasts, via secreted undercarboxylated osteocalcin, increase pancreatic β -cell proliferation, insulin secretion, and insulin sensitivity (Hauschka *et al.*, 1989; Lee *et al.*, 2007; Ferron *et al.*, 2008; Brennan-Speranza and Conigrave, 2015). Osteoblasts also possess insulin receptors, and insulin signalling is necessary for osteoblasts, directly stimulating cell proliferation, differentiation and survival (Ferron *et al.*, 2010; Fulzele *et al.*, 2010; Clemens and Karsenty, 2011; Pramojane *et al.*, 2014). Bone marrow adipocytes, via adipokines such as leptin and adiponectin, also participate in the regulation of energy metabolism (Karsenty, 2006; Cawthorn *et al.*, 2014). Another energy metabolism-regulating hormone, ghrelin, influences bone homeostasis via direct and indirect mechanisms (see section 1.4.2.1).

1.2.2. Bone remodelling

Bone remodelling allows for repairing microdamage, healing fractures, and regulating calcium-phosphorus homeostasis. Bone remodelling involves bone resorption by osteoclasts followed by new bone formation by osteoblasts (see figure 1.1); these two processes are tightly coupled and balanced (Delhanty *et al.*, 2014a). Bone remodelling is achieved by the cooperative and sequential work of several bone cell types, including osteoblasts, osteocytes, bone lining cells and osteoclasts, which are organised in specialised units called bone multicellular units (BMUs) (Zhou *et al.*, 2010). Osteoblast and osteoclast differentiation and functions are regulated by multiple factors including cytokines acting locally, hormones acting systemically, neurotransmitters, and mechanical stimuli (Harada and Rodan, 2003; Teitelbaum and Ross, 2003; Hu *et al.*, 2017).

Osteoblasts play a central role in forming and maintaining skeletal architecture: they are responsible for bone formation through the secretion of the organic components of bone matrix in the form of a complex mixture of bone matrix proteins, also called osteoid; they also regulate the differentiation and function of osteoclasts. Osteoblasts are located on bone surfaces, usually in a single layer (Marks and Odgren, 2002; Mackie, 2003).

Osteoblasts are derived from MSCs, also called skeletal stem cells (SSCs) or bone marrow stromal cells (BMSCs), which can be found in the bone marrow stroma and

periosteum (Harada and Rodan, 2003). MSCs are capable of differentiating into multiple lineages, including osteoblasts and adipocytes. The osteogenic differentiation of MSCs and osteoblasts are tightly regulated by a number of transcription factors, growth factors and hormones (Aubin and Triffitt, n.d.; Wang *et al.*, 2016; van de Peppel *et al.*, 2017), such as parathyroid hormone (PTH), oestrogens, transforming growth factor- β (TGF- β), bone morphogenetic proteins (BMPs), insulin, and ghrelin (Lee *et al.*, 2000; Gimble, 2011; Delhanty *et al.*, 2014a; Pramojane *et al.*, 2014). Some of these factors, such as TGF- β and BMPs, are secreted by osteoblasts and sequestered in bone matrix; they are released during osteoclastic resorption (Mackie, 2003).

Between 60 and 80% of osteoblasts recruited to a resorption pit die by apoptosis within 200 days (Jilka *et al.*, 1999, 2007; Manolagas and Parfitt, 2010); some of the osteoblasts become quiescent bone-lining cells, which cover inactive, non-remodelling bone surfaces and communicate with each other via gap junctions. They are responsible for immediate release of calcium from the bone and most likely participate in bone remodelling (Miller *et al.*, 1989). Bone lining cells prevent the direct interaction between osteoclasts and bone matrix on non-remodelling bone surfaces, where bone resorption should not occur (Florencio-Silva *et al.*, 2015). Bone lining cells also constitute a major source of osteoblasts in adults (Matic *et al.*, 2016); they can be induced to proliferate and differentiate into osteogenic cells, and participate in bone remodelling.

The remaining osteoblasts become surrounded with bone and differentiate into osteocytes, which progressively stop secreting osteoid. Osteocytes represent approximately 90% of the cells in bone (Manolagas and Parfitt, 2010). They are not isolated cells; they are located in lacunae and form a network throughout mineralised bone matrix, communicating with each other via gap junctions and canaliculi throughout bone. Osteocytes can also communicate with osteoblasts on the bone surface (Marks and Odgren, 2002; Mackie, 2003), participating in regulation of bone remodelling (Komori, 2013). They participate in mechanosensation and paracrine signalling to regulate bone remodelling in response to mechanical strain and fatigue damage (Marotti, 2000; Zhao *et al.*, 2002; Han *et al.*, 2004), in particular via K⁺ channels (Gu *et al.*, 2001a).

Chapter 1 – Introduction

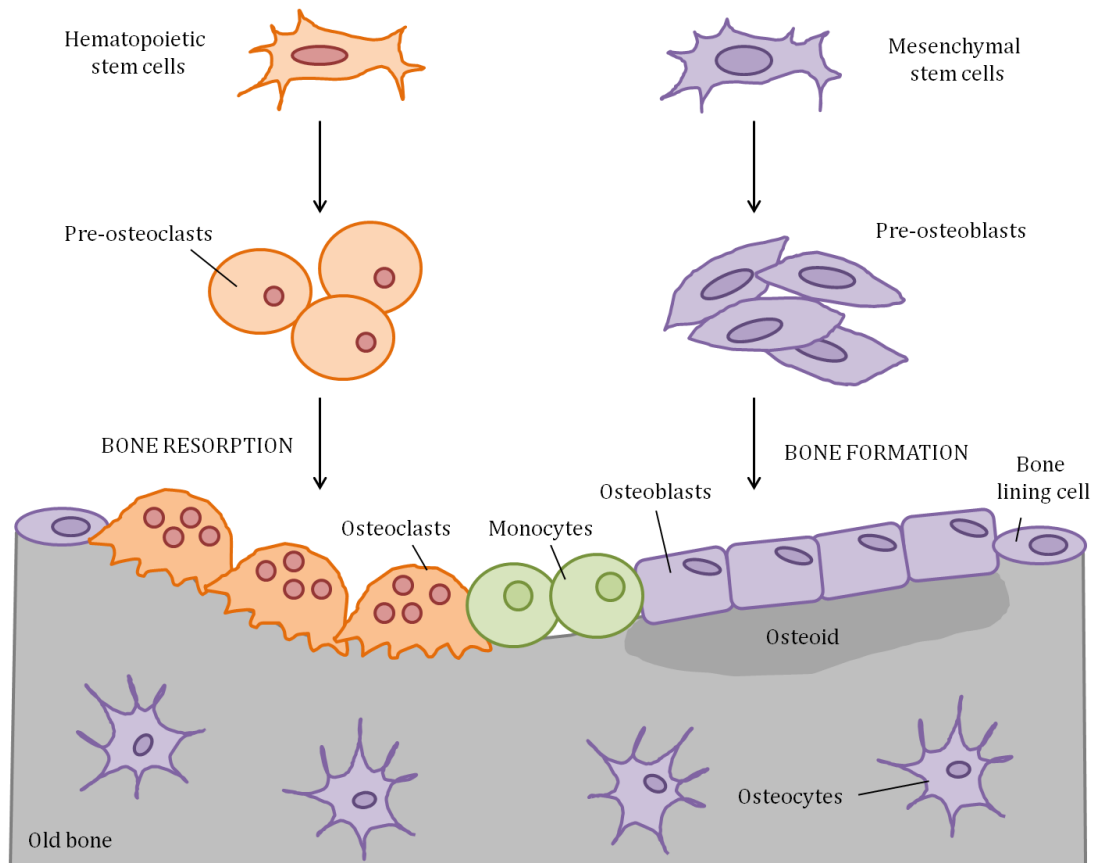


Figure 1.1: Cellular activities supporting bone remodelling

Bone is resorbed by osteoclasts, which result from the fusion of several mononuclear precursors originating from haematopoietic stem cells. Osteoclasts are large, multinucleated cells that form resorption pits in the bone matrix by secreting acids and enzymes that degrade the bone (Blair *et al.*, 2005; Lampiasi *et al.*, 2016). After resorbing bone, osteoclasts undergo apoptosis. Then, osteoblasts, which originate from MSCs, produce new osteoid matrix and promote mineralisation. 60-80% of the osteoblasts recruited to a resorption pit die by apoptosis (Jilka *et al.*, 1999, 2007; Manolagas and Parfitt, 2010); others become small, quiescent lining cells; and the remaining osteoblasts become surrounded with bone and differentiate into osteocytes. Adapted from (Lian *et al.*, 2012).

In healthy adults, bone resorption and bone formation are well-balanced; however, with aging and other risk factors such as glucocorticoid therapy, these two processes become unbalanced, leading to bone loss and increasing the risk of developing osteoporosis (see section 1.3.1).

1.2.3. Bone marrow adipose tissue

In addition to bone resorbing and bone forming cells, bone contains adipocytes. Like osteoblasts, adipocytes originate from MSCs. Bone marrow adipogenesis is both a physiological and pathological process; it occurs throughout the entire life of all mammals (Rosen *et al.*, 2009; Hardouin *et al.*, 2016). Around the time of birth, bone cavities mainly contain active haematopoietic cells in the marrow; but in adults, human bone marrow adipose tissue (BMAT) represents between 50% and 70% of total bone marrow volume and 5% of total body fat mass (Hardouin *et al.*, 2016). Bone marrow adipogenesis accelerates during aging, especially after menopause for women. Similarly, in rodents, BMAT is present in adults (Lecka-Czernik, 2012; Wang *et al.*, 2013) and increases with aging (Pittenger *et al.*, 1999; Sadie-Van Gijsen *et al.*, 2013).

Adipose tissue functions as an energy store and a secretory organ; adipocytes can secrete various adipokines such as leptin and adiponectin, but also free fatty acids and inflammatory cytokines (Hardouin *et al.*, 2016). These molecules participate in the regulation of energy metabolism and inflammation (Hardouin *et al.*, 2016). Until recently, the functions of BMAT were unknown; it has been the focus of several studies in the recent years. In humans, BMAT has often been considered as a “filling” tissue, filling the void left by bone during aging (Rosen *et al.*, 2009). However, bone marrow adipocytes are now known to play an important role in fat-bone interactions, by secreting paracrine and autocrine factors (Rosen *et al.*, 2009; Cawthorn *et al.*, 2014; Suchacki *et al.*, 2016) that may interfere with haematopoiesis and bone remodelling (Corre *et al.*, 2004). Bone is both a target and a regulator of energy metabolism; leptin and adiponectin can modulate bone mass via direct and indirect mechanisms (Justesen *et al.*, 2001; Verma *et al.*, 2002). BMAT seems to be an important factor of bone alterations (Hardouin *et al.*, 2016), and increased BMAT is associated with BMD loss in aging, menopause, and with several chronic conditions, including diabetes, anorexia nervosa and osteoporosis (Cawthorn *et al.*, 2014; Hardouin *et al.*, 2016). The secretory role of adipocytes in regulation of haematopoiesis may also be involved in the pathophysiology of myeloma (Reagan *et al.*, 2015) and bone metastases (Hardaway *et al.*, 2014; Morris and Edwards, 2016).

In mice, the functions of BMAT are less clear. Some studies indicate that marrow adipocytes may be metabolically inert (Duque, 2007), suggesting that MSCs may differentiate into adipocytes “by default”, because they cannot differentiate into other cell types, in particular osteoblasts; this suggests that in mice, BMAT functions as a “filling” tissue. However, other studies demonstrate that on the contrary, bone marrow

adipocytes are metabolically active and can induce differentiation of more MSCs into adipocytes (Lecka-Czernik *et al.*, 2002), preventing them to differentiate into other cell types, especially osteoblasts. This is supported by studies that have demonstrated that the adipogenic transcription factor PPAR γ can inhibit osteoblastic differentiation (see section 1.3.2). Also, in mice under caloric restriction, BMAT significantly contributes to serum adiponectin levels (Cawthorn *et al.*, 2014).

1.2.4. Mesenchymal stem cells

1.2.4.1. Definition

MSCs are a group of fibroblast-like stem cells located in the non-hematopoietic compartment of the bone marrow. These cells have the potential to replace or restore the function of damaged tissues; they can differentiate into various lineages and can incorporate into a variety of tissues, including bone, cartilage, muscle and lung (Deng *et al.*, 2007; Kassem *et al.*, 2008). Under appropriate conditions *in vitro*, MSCs can differentiate into various mesoderm cell types, including osteoblasts, adipocytes, chondrocytes, hepatocytes, cardiomyocytes, and neuronal cells (Pittenger *et al.*, 1999; Bianco *et al.*, 2001; Abdallah *et al.*, 2005; Deng *et al.*, 2007), making MSCs a promising cell source for tissue engineering and regenerative medicine.

1.2.4.2. Osteogenesis and adipogenesis

Osteogenesis and adipogenesis are both tightly regulated processes, controlled by lineage-specific transcription factors that can induce MSC differentiation. MSC differentiation is also controlled by a variety of growth factors, hormones, extracellular matrix components and mechanical stimuli (Steward and Kelly, 2015; Wang *et al.*, 2016). Genetic and “micro-environmental” approaches have been used to identify several osteogenic and adipogenic transcription factors and signalling pathways.

1.2.4.2.1. Osteogenic differentiation of BMSCs

Osteogenesis is a tightly regulated process that is characterised by a sequence of events: the commitment of osteoprogenitors cells, differentiation into pre-osteoblasts and differentiation into mature osteoblasts whose function is to synthesise bone matrix that becomes progressively mineralised. These steps are controlled by several transcription factors such as runt-related transcription factor 2 (Runx2, also named Osf2/Cbfa1) (Marie, 2008). Other transcription factors, such as Osterix, β -catenin and ATF4, act downstream of Runx2 and play an important role in osteoblastogenesis.

Runx2 is the major transcription factor controlling osteoblast commitment and differentiation; it is both necessary and sufficient for MSC differentiation into osteoblasts (Marie, 2008). Runx2 activates gene expression by binding to the Runx consensus sequence (PuACCPuCA), also named osteoblast specific element 2 (OSE2), in the promoters of osteoblast-specific genes such as osteocalcin, type I collagen, osteopontin, and bone sialoprotein (Marie, 2008). Overexpression of Runx2 in non-osteoblastic cells (such as observed in MC3T3-E1 calvarial cells) or in adipose-tissue-derived MSCs (as in AD-MSCs) stimulates osteoblastic differentiation, increasing the expression of osteocalcin, bone sialoprotein and type I collagen; overexpression of Runx2 also promotes mineralisation (Ducy *et al.*, 1997; Otto *et al.*, 1997; Zhang *et al.*, 2006). On the contrary, deletion of Runx2 inhibits the differentiation of MSCs into osteoblasts (Ducy *et al.*, 1997; Komori *et al.*, 1997). Komori *et al.* (1997) have shown that homozygous Runx2 mutant mice die just after birth, and completely lack mature osteoblasts and mineralised bone. Osterix is another important osteogenic transcription factor specifically expressed by osteoblasts in all developing bones, required for osteoblast differentiation and bone formation (Nakashima *et al.*, 2002; Zhou *et al.*, 2010). In *Osx* null mice, mesenchymal cells cannot differentiate into mature osteoblasts and cannot deposit bone matrix, even though Runx2 is expressed. Interestingly, Runx2 null mice do not express Osterix, indicating that this transcription factor acts downstream of Runx2 (Nakashima *et al.*, 2002).

1.2.4.2.2. Adipogenic differentiation of BMSCs

Like osteogenesis, adipogenesis is a tightly regulated process, occurring in multiple steps. BMSCs first have to commit to the adipogenic cell lineage by differentiating into preadipocytes, then terminally differentiate into mature, functional adipocytes. In mice, there is an additional step, the clonal expansion of preadipocytes which divide once or twice (Rosen and MacDougald, 2006), followed by withdrawal from cell cycle and terminal differentiation (Ali *et al.*, 2013). In humans, preadipocytes do not divide before terminal differentiation (Rosen and MacDougald, 2006).

Adipogenesis is regulated by multiple transcription factors in sequential activation; the CCAAT/enhancer-binding proteins C/EBP β , C/EBP δ and C/EBP α and peroxisome proliferator-activated receptor γ (PPAR γ) play a central role in adipogenic differentiation. At the first stage of adipogenesis, extracellular signals induce the expression of C/EBP β and C/EBP δ in preadipocytes. These two transcription factors then promote the expression of PPAR γ and C/EBP α , which are considered to be the

master transcriptional regulators of adipogenesis. PPAR γ and C/EBP α form a positive feedback loop, increasing and maintaining their expression, and promoting terminal differentiation by activating genes that are required for the withdrawal of adipocytes from the cell cycle, and for the function and maintenance of mature adipocytes (Gregoire, 2001; Ali *et al.*, 2013).

There is a complex relationship between bone and adipose tissue; adipocytes secrete various molecules that regulate bone metabolism and skeletal homeostasis. Various bone disorders are associated with altered bone formation, including osteoporosis, Paget's disease of bone and osteoarthritis. The differentiation of the osteoblast precursors, the BMSCs, is also often altered in various bone disorders, particularly osteoporosis (Bianco *et al.*, 2008); increased adipogenic differentiation of BMSCs at the expense of osteoblastogenesis has been associated with osteoporosis (Gao *et al.*, 2014; Greco *et al.*, 2015).

1.3. Osteoporosis

1.3.1. Definition of osteoporosis

Osteoporosis is a major public health problem; it is a common metabolic bone disease characterised by excessive bone resorption and increased bone fragility that result from increased osteoclastogenesis and increased marrow adipogenesis at the expense of osteoblastogenesis (Bethel *et al.*, 2013). Fragility fractures represent the main clinical consequence of osteoporosis and are associated with pain, suffering, disability and can even lead to death for the affected patients due to complications. This silent disease has no symptom until fragility fracture occurs. Osteoporosis affects one in three women and one in five men after 50 years of age; more than 3 million people in the United Kingdom are estimated to have osteoporosis. There are more than 500,000 fractures every year associated with osteoporosis (National Osteoporosis Society, 2018). In 2010, a study estimated that approximately 536,000 fragility fractures occurred in the UK, and the economic cost of incident and previous fragility fractures was estimated at £ 3,497 million for the same year. Up to 20% of patients with osteoporosis die after hip fractures, and 40% can no longer live independently (Manolagas, 2000). As the population ages, it was estimated that in 2025, there will be approximately 682,000 fragility fractures, and the cost will represent £ 5,465 million (Svedbom *et al.*, 2013). There are several subtypes of osteoporosis (Clunie and Keen, 2014; Morimoto *et al.*, 2017) (see table 1.1).

Subtype		Causes
Primary osteoporosis	Type I (postmenopausal osteoporosis)	Loss of oestrogen, increased bone resorption
	Type II (senile osteoporosis)	Unbalanced bone remodelling
Secondary osteoporosis		Other conditions (hormonal imbalance, hyperparathyroidism, diabetes mellitus), iatrogenic (glucocorticoid therapy), idiopathic

Table 1.1: Subtypes of osteoporosis

Type II osteoporosis generally occurs after the age of 70 and affects women twice as frequently as men (Marchigiano, 1997; Bartl and Bartl, 2017).

Osteoblasts, osteoclasts and bone marrow adipocytes are directly involved in the pathophysiology of osteoporosis. The differentiation and functions of these cells is affected by several factors, such as aging, sex, or glucocorticoid therapy. Age and female sex increase the risk of developing both obesity and types I and II osteoporosis; several epidemiologic and clinical studies have shown that a high level of fat mass might be a risk factor for osteoporosis and fragility fractures (Zhao *et al.*, 2008; Kim *et al.*, 2010; Compston *et al.*, 2014; Greco *et al.*, 2015). Aging is associated with decreased osteoblast numbers and activity, increased osteoclast differentiation and increased bone marrow adiposity in humans (Hardouin *et al.*, 2016) and rodents (Pittenger *et al.*, 1999; Sadie-Van Gijzen *et al.*, 2013). MSCs differentiation has been shown to be age-dependent. Many *in vitro*, *in vivo* and clinical studies have shown that bone marrow adipocytes can directly modulate osteoblastogenesis and osteoclastogenesis through the release of paracrine factors (Hardouin *et al.*, 2016), especially the two adipokines leptin and adiponectin, which can modulate bone mass through direct and indirect mechanisms (Gimble, 2011; Kawai *et al.*, 2012; Naot and Cornish, 2014). In female patients, the expression levels of the adipogenic marker PPAR γ increase with aging, while the expression levels of the osteogenic marker Runx2 decrease. However, this effect is not observed in male patients (Jiang *et al.*, 2008).

Glucocorticoid-induced osteoporosis is the most common form of secondary osteoporosis (Briot and Roux, 2015). Glucocorticoids, which are corticosteroid drugs that are widely used to treat diseases such as rheumatoid arthritis, lupus erythematosus, asthma and lung disorders (Schatz and Hamilos, 1995; Goldstein *et al.*, 1999; Toogood, 2004), are associated with rapid bone loss and increased risk of fractures (Briot and Roux, 2015). This is due to several factors: the underlying inflammation treated by glucocorticoids plays a role in bone fragility (Staa *et al.*, 2006; Roux, 2011; Briot and Roux, 2015); glucocorticoids inhibit bone formation and accelerate bone resorption, leading to bone loss and decreased BMD rapidly after the beginning of therapy; and bone quality is also altered, making the bones more fragile. Some 10% of bone mass can be lost in the first year of glucocorticoid therapy (Morimoto *et al.*, 2017).

1.3.2. Osteoporosis: obesity of the bone?

As osteoblasts and adipocytes originate from the same MSC precursors, it has been hypothesized that an unbalanced adipogenesis at the expense of osteoblastogenesis could be involved in the pathophysiology of bone disorders, especially osteoporosis (Greco *et al.*, 2015). This theory is known as the “fat theory” for osteoporosis and is supported by experimental and clinical studies. Increased bone marrow adipogenesis is associated with several types of osteoporosis, particularly the forms associated with aging, menopause, or glucocorticoid treatment (Moerman *et al.*, 2004; Hardouin *et al.*, 2016).

MSCs derived from osteoporotic patients differentiate preferentially into adipocytes, instead of osteoblasts (Nuttall and Gimble, 2004; Rosen and Bouxsein, 2006; Rodriguez *et al.*, 2008). Similarly in mice with glucocorticoid-induced osteoporosis, BMSCs preferentially differentiate into adipocytes; this may be due to alterations of epigenetic markers in the promoter of regulatory genes such as PPAR γ (Zych *et al.*, 2013; Zhang *et al.*, 2015).

MSC differentiation is regulated by a variety of factors in the cell microenvironment, leading to the activation of signalling cascades that generally converge on two key transcription factors: PPAR γ for adipogenesis and Runx2 for osteoblastogenesis. Many studies have demonstrated that factors that induce adipogenesis inhibit osteoblastogenesis (Beresford *et al.*, 1992; Dorheim *et al.*, 1993; Muruganandan *et al.*, 2009) and vice versa (Gimble *et al.*, 1995; Hong *et al.*, 2005). Also, some signalling pathways are involved in regulation of both differentiation lineages, including Wnt

signalling (Hofmann, 2000; Willert *et al.*, 2003; Leclerc *et al.*, 2008; Piters *et al.*, 2008; Colaianni, 2014; Jing *et al.*, 2015; Yuan *et al.*, 2015), chemerin/CMKLR1 signalling (Muruganandan *et al.*, 2010, 2011), ERK1/2 signalling (Li *et al.*, 2016a) and Akt1 (Kawamura *et al.*, 2007). Typically, increased expression of one of the key regulators of adipogenesis and osteoblastogenesis, PPAR γ and Runx2, is accompanied by a decreased expression of the other (James, 2013). Furthermore, studies in animal models have shown that upregulated PPAR γ activity led to bone loss and increased marrow adiposity (Rzonca *et al.*, 2004; Sottile *et al.*, 2004). On the contrary, downregulated PPAR γ activity led to bone mass elevation; *ex vivo* culture of MSCs derived from the bones of PPAR $\gamma^{+/-}$ mice shows a decrease of the number of adipocytes and an increase of the number of osteoblasts (Akune *et al.*, 2004; Cock *et al.*, 2004). Liu *et al.* (2010) co-cultured primary fat cells or differentiated adipocytes with osteoblastic cells, and observed a decrease in two osteoblastic markers, Runx2 expression and alkaline phosphatase (ALP) activity. This was accompanied by an increase in two adipocytic markers, PPAR γ expression and adiponectin secretion. These results suggest that adipocytes can modulate osteoblast functions through the release of secretory products such as adiponectin, and that PPAR γ plays a key role in this process (Liu *et al.*, 2010). This is consistent with the fact that high circulating levels of adiponectin are associated with low BMD, and that treatment of bone MSCs with adiponectin inhibits osteogenesis in favour of adipogenesis (Abbott *et al.*, 2015).

Increased marrow adiposity is also associated with accelerated bone resorption. Some studies have shown that adipocytes may play a role in promoting osteoclast formation (Benayahu *et al.*, 1994; Kelly *et al.*, 1998, p.2; Sakaguchi *et al.*, 2000). This may be mediated, at least in part, by RANKL. RANKL expression is induced during adipogenesis, through the action of the adipogenic transcription factors C/EBP β and/or C/EBP δ . The number of RANKL-positive preadipocytes increases in bone marrow with aging, suggesting that increased marrow adipogenesis could influence osteoclastogenesis, accelerating bone resorption, and thus contributing to osteoporosis (Takeshita *et al.*, 2014).

Inter-conversion of osteoblasts into adipocytes has been demonstrated *in vitro* and may occur *in vivo*. Single cell MSC-derived clones can be induced to differentiate into adipocytes, then de-differentiate and re-differentiate into osteoblasts *in vitro* (Kim *et al.*, 2004). Mature adipocytes can be induced to transdifferentiate into osteoblastic cells under appropriate culture conditions (Justesen *et al.*, 2004) and inversely, mature osteoblasts can be induced to transdifferentiate into adipocytes (Nuttall *et al.*, 1998).

7F2 cells, which were isolated p53^{-/-} mouse bone marrow taken from the femur, are preosteoblast cells that can be induced to transdifferentiate into adipocytes (Thompson *et al.*, 1998). There is a correlation between the osteoadipogenic transdifferentiation of bone marrow cells and some bone metabolism diseases (Boskey and Coleman, 2010).

However, the fat theory for osteoporosis remains controversial. For example, the *in vivo* origin of bone-producing osteoblasts is not fully defined (Matic *et al.*, 2016); quiescent lining cells may be an important source of osteoblasts in adults. In addition, some histomorphometric studies demonstrate that bone mass and adipose tissue mass in the bone marrow can change in the same direction, suggesting that bone formation and adipocyte formation may be regulated independently (Tornvig *et al.*, 2001).

1.3.1. Treatments for osteoporosis

The current treatments include both pharmacological and non-pharmacological management; the latter include weight-bearing and muscle-strengthening exercises, as well as dietary and lifestyle changes to reduce risk factors (Henney, 2008; An *et al.*, 2016; Wang *et al.*, 2016) (see table 1.2). Exposure to sunlight is the main source of vitamin D, but supplementation may be necessary (Holick, 2009; Tella and Gallagher, 2014). Calcium supplementation is also often needed, as aging is associated with a negative calcium balance (Tella and Gallagher, 2014). Various pharmacological treatments are available. However, there is still need for new therapies, as these treatments can be costly, take a long time to be effective, and have adverse secondary effects. Biphosphonates for example may suppress bone turnover and lead to osteonecrosis of the mandible (Wang *et al.*, 2016). Also, HRT is not generally used because of its adverse effects, which include increased risks of breast cancer, strokes, and cardiovascular disease (National Osteoporosis Society, 2018). As osteoporosis results from imbalanced bone remodelling and is associated with increased marrow adipogenesis, new treatments that increase the number of osteoblasts and decrease the number of adipocytes may provide a cure for osteoporosis (Wang *et al.*, 2016). Getting a better understanding of pathological adipogenesis in bone marrow will help develop new treatments in the long term.

Medication	Effect
Biphosphonates (Briot and Roux, 2015)	Inhibit resorption
Teriparatide (Roux, 2010)	Stimulates osteoblast proliferation and mineralisation
Denusomab (Roux, 2010)	Targets RANKL, inhibits resorption
Hormone Replacement Therapy (HRT) (Rossouw <i>et al.</i> , 2002)	Compensates loss of oestrogen, inhibits resorption
Selective estrogen receptor modulators (SERMs): raloxifene (Yogui <i>et al.</i> , 2018; Zhang <i>et al.</i> , 2018)	Mimicks estrogen actions, inhibits resorption

Table 1.2: Various types of therapies against osteoporosis

The available treatments mainly target the symptoms and complications of osteoporosis, promoting bone formation and mineralisation, and inhibiting bone resorption.

1.4. Ghrelin

1.4.1. Ghrelin signalling: an overview

1.4.1.1. Ghrelin

Ghrelin is a 28 amino-acid peptide hormone mainly secreted in the stomach, by the oxyntic glands of the gastric fundus (Kojima *et al.*, 1999). Ghrelin was discovered in 1999 as the endogenous ligand for growth hormone secretagogue receptor (GHSR) 1a and it stimulates GH release from the anterior pituitary gland (Müller *et al.*, 2015). Ghrelin also regulates food intake, body weight, adiposity, and glucose metabolism, acting as a “hunger” hormone, signalling glucose metabolism status to the central nervous system (CNS) to adjust food intake and energy expenditure. Ghrelin secretion is influenced by the metabolic status (figure 1.2), and is regulated by many factors, including nutrients and other peptide hormones such as insulin and leptin (Delporte, 2013; Müller *et al.*, 2015; Sato *et al.*, 2015). Ghrelin needs to be modified postrationally to bind and activate the GHSR1a receptor; it is acylated by ghrelin *O*-acyltransferase (GOAT). Ghrelin, the GHSR and GOAT are highly conserved in vertebrates (Kojima and Kangawa, 2005; Gutierrez *et al.*, 2008). Ghrelin also plays direct roles in peripheral organs, including bone and adipose tissue.

Chapter 1 – Introduction

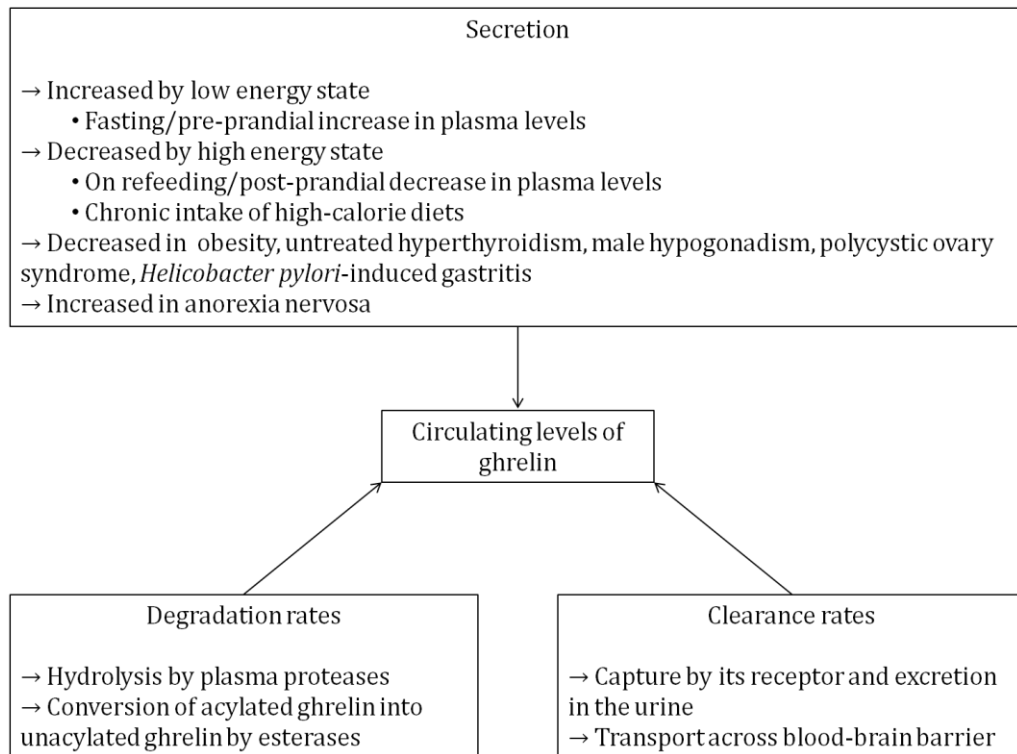


Figure 1.2: Parameters that influence circulating levels of ghrelin

Levels of circulating ghrelin depend on secretion, degradation rates and clearance rates. Ghrelin is secreted mainly by X/A-like cells in the stomach; secretion is regulated by energy state. Once released in the bloodstream, acylated ghrelin can be converted into unacylated ghrelin by esterases, and ghrelin can also be degraded by proteases. Following infusion, acylated ghrelin has a mean half-life of 9-11 minutes, whereas total ghrelin (acylated and unacylated) has a mean half-life of 35 minutes (Delporte, 2013). In mice, transport of both human and mouse ghrelin has been shown to be bidirectional; unacylated ghrelin transport rate is higher than that of acylated ghrelin (Banks et al., 2002; Rhea et al., 2018).

1.4.1.2. Growth Hormone Secretagogue Receptor (GHSR)

The discovery of the ghrelin receptor began with studies of growth hormone secretagogues (GHSs), which are small synthetic peptide and nonpeptide compounds that can stimulate the release of GH from the pituitary (Kojima *et al.*, 1999; Davenport *et al.*, 2005; Kaiya *et al.*, 2013). Some of these GHSs also stimulate appetite in mammals (Kaiya *et al.*, 2013). In 1996, GHSs were found to bind a G-protein coupled receptor (GPCR) that was named the growth hormone secretagogue receptor (GHSR) (Howard *et al.*, 1996); it has been found in both human and swine pituitary and hypothalamus. The GHSR is a rhodopsin-like GPCR with seven transmembrane domains, belonging to Family A (Davenport *et al.*, 2005). It is well conserved among vertebrates, including mammals, birds, and fish (Kojima and Kangawa, 2005).

The *Ghsr* gene contains two exons and one intron (McKee *et al.*, 1997; Petersenn *et al.*, 2001); the first exon encodes transmembrane domains 1 to 5, and the second exon encodes transmembrane domains 6 and 7 (Kojima and Kangawa, 2005). The promoter region of the gene contains no typical TATA, GC or CAAT boxes, but contains putative binding sites for several transcription factors, including part of an oestrogen response element (Iguchi *et al.*, 1999). Consistent with this, several studies have shown that GHSR gene expression can be upregulated by thyroid hormones (Kamegai *et al.*, 2001; Petersenn *et al.*, 2001) and oestrogens (Petersenn *et al.*, 2001). GHSR gene expression is also regulated by glucocorticoids: it was demonstrated to be inhibited by 10^{-7} M hydrocortisone in rat pituitary cells (Petersenn *et al.*, 2001), but stimulated by dexamethasone in pituitary gland of rats treated with 200 µg dexamethasone per day for 8 days (Tamura *et al.*, 2000).

In humans, swine and rats, there are two known mRNA isoforms for this receptor, GHSR1a and GHSR1b. Translation of the GHSR1a isoform produces the biologically active receptor that can be activated by acylated ghrelin; it arises from regular splicing of the gene, which removes the intron. GHSR1a consists of 366 amino acids in humans (Petersenn *et al.*, 2001) and of 364 amino acids in rats (McKee *et al.*, 1997) and mice; the third transmembrane domain is reportedly involved in ligand-binding (Smith *et al.*, 1999).

GHSR1b arises from alternative splicing in humans and swine; it contains the first exon and retains the intron, causing a single base translation frameshift and introducing a stop codon within the intron. This gives rise to a C-terminally truncated protein (Kaiya *et al.*, 2013). The corresponding protein consists of 289 amino acids (Petersenn *et al.*, 2001), and contains only the first five transmembrane domains plus a unique 24 amino acid “tail” encoded by the intron (Jeffery *et al.*, 2003). GHSR1b is pharmacologically inactive as no binding of the synthetic GHSs or ghrelin has been demonstrated. However, it may function to attenuate the activity of GHSR1a by heterodimerising with it (Callaghan and Furness, 2014). Although the main site of ghrelin synthesis is the stomach, the GHSR mRNA has been identified in a variety of tissues, including the stomach, heart, lung, pancreas, intestine, kidney, adipose tissues (Kojima *et al.*, 1999; Tschöp *et al.*, 2000, p.2000; Gualillo *et al.*, 2001; Shuto *et al.*, 2001), the hypothalamus, the pituitary (Guan *et al.*, 1997), and in the brainstem (Bailey *et al.*, 2000). Some studies did not detect GHSR mRNA in bone marrow (Guan *et al.*, 1997), but other indicates that GHSR1a is expressed both at the mRNA and the protein level in rat adipocytes, and that its expression increases with age (Choi *et al.*, 2003; Kim *et al.*, 2005).

1.4.1.3. Ghrelin-*O*-acyltransferase (GOAT)

In the circulation, ghrelin is present in two forms: acylated ghrelin (also named octanoylated ghrelin or acyl-ghrelin), and unacylated ghrelin (also named desacyl-ghrelin) (figure 1.3). Only a small proportion of circulating ghrelin is acylated; the majority of circulating ghrelin is unacylated (Hosoda *et al.*, 2000a; Delhanty *et al.*, 2012). Acylated ghrelin is rapidly deacylated in the serum by circulating esterases, without proteolysis (De Vriese *et al.*, 2004).

Ghrelin is the only known protein modified with an *O*-linked octanoyl side group, which is an 8-carbon fatty acid side chain; this modification occurs on its third serine residue which is conserved in all mammals (Kojima and Kangawa, 2005). This modification is critical for the role of ghrelin in regulating GH release, food intake, and lipid metabolism (Li *et al.*, 2016b): acylated ghrelin at nanomolar concentrations can bind and activate the GHSR1a, while it takes a much higher concentration of unacylated ghrelin to activate this receptor. As circulating levels of acylated ghrelin and unacylated ghrelin are comprised between 0.1 and 0.5 nmol/L, the concentration of unacylated ghrelin is too low to activate GHSR1a (Callaghan and Furness, 2014). Although unacylated ghrelin cannot bind and activate the GHSR1a in physiological circulating concentrations, it does have biological activities in multiple tissues such as adipose tissue, bone, skeletal muscles, heart, and pancreatic tissues; but the receptor(s) involved in these activities have not yet been identified (Callaghan and Furness, 2014). For example, unacylated ghrelin, as well as acylated ghrelin, can stimulate lipid accumulation in rat and human visceral adipocytes and rat bone marrow adipocytes (Thompson *et al.*, 2004; Kos *et al.*, 2009; Rodríguez *et al.*, 2009)

The enzyme responsible for acylation of ghrelin was identified by two separate research groups in 2008 (Gutierrez *et al.*, 2008; Yang *et al.*, 2008). Yang *et al.* (2008) identified 16 membrane-bound *O*-acyltransferase (MBOAT) proteins encoded by 11 genes in mice; endocrine cell lines were co-transfected with ghrelin and various MBOAT constructs. Only one member of the MBOAT family was capable of octanoylating ghrelin (Yang *et al.*, 2008); it was termed ghrelin *O*-acyltransferase (GOAT). In the same year, Gutierrez *et al.* (2008) identified GOAT in humans using gene-silencing experiments in human medullary thyroid carcinoma cells (TT cells), which have been shown to produce acyl ghrelin (Kanamoto *et al.*, 2011). Candidate genes were selected depending on several criteria: similarity to known acyltransferase sequences, existence of human homologues, and unknown gene function. 12 candidate genes were selected, most of which were orphan MBOATs. These candidate genes were

individually silenced by siRNA; silencing of one candidate, MBOAT4, using five distinct siRNAs, greatly reduced octanoyl ghrelin synthesis, while the knock down of the other candidate genes had no effect on the amount of octanoyl ghrelin. To confirm that MBOAT4 encoded the enzyme that acylates ghrelin, Gutierrez *et al.* cotransfected human embryonic kidney (HEK-293) cells with both the ghrelin gene and MBOAT4; 72h after transfection, the media from HEK-293 contained acyl ghrelin. Genetic disruption of the GOAT gene in mice led to a complete absence of acylated ghrelin in the circulation, further confirming that acylation of ghrelin is mediated by GOAT (Gutierrez *et al.*, 2008).

The predicted catalytic residues of mouse GOAT are asparagines-307 and histidine-338; when either of these residues is substituted with alanine, GOAT is unable to acylate ghrelin (Yang *et al.*, 2008). GOAT is conserved across vertebrate species; an amino-acid sequence comparison shows a ~90%-similarity between human, mouse and rat GOAT; and a ~60%-similarity between mammalian and zebrafish amino acid sequences (Gutierrez *et al.*, 2008). When GOAT cDNA from mouse, rat or zebrafish is co-transfected with human ghrelin in HEK-293 cells, ghrelin is acylated (Gutierrez *et al.*, 2008). This is consistent with the fact that acylation of ghrelin is critical for its function, and with the fact that the ghrelin sequence, and more particularly the active core that contains the serine 3 residue, is very well conserved in mammals, birds, and fish (Kojima and Kangawa, 2005; Yang *et al.*, 2008). Also, GOAT was found to be mainly expressed in the stomach, which is also the main source of ghrelin, as well as in peripheral tissues, such as breast, adipose tissue, lungs, muscles, kidneys, or pancreas (Lim *et al.*, 2011; Delhanty *et al.*, 2012). Thus, although a small proportion of circulating ghrelin is acylated, local concentrations of acylated ghrelin could be higher due to local acylation by GOAT.

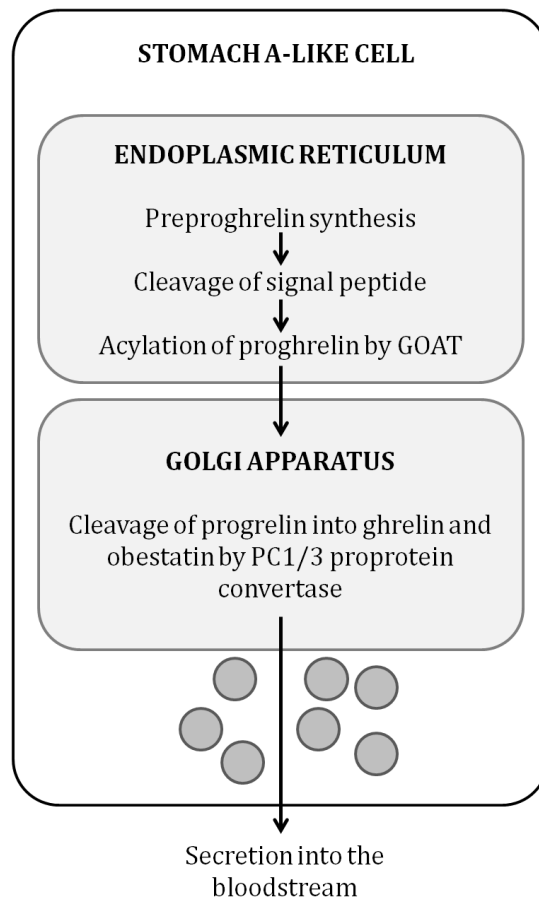


Figure 1.3: Posttranslational modifications of ghrelin

Ghrelin is mainly synthesised in the stomach, as preproghrelin. Preproghrelin is then processed to give rise to ghrelin and obestatin. Adapted from (Romero *et al.*, 2010).

1.4.2. Ghrelin is much more than a 'hunger hormone'

There is growing evidence that ghrelin plays a more complicated role than just regulating GH release and energy metabolism (figure 1.4). The ghrelin receptor GHSR is expressed in a variety of peripheral tissues and organs, including the stomach, heart, lung, pancreas, intestine, kidney, adipose tissues (Kojima *et al.*, 1999; Tschöp *et al.*, 2000; Gualillo *et al.*, 2001; Shuto *et al.*, 2001), bone marrow adipose tissue (Choi *et al.*, 2003), the arcuate nucleus (Arc) and ventromedial nucleus of the hypothalamus, in the pituitary (Guan *et al.*, 1997) and in the brainstem (Bailey *et al.*, 2000). It is also expressed by osteoblasts, both in primary cells and in cell lines, in human, mouse and rat (Fukushima *et al.*, 2005; Kim *et al.*, 2005; Maccarinelli *et al.*, 2005). As the stomach is the main source of circulating ghrelin, the wide tissue expression of its receptor suggests that ghrelin produced in and secreted from the stomach may have a variety of functions in addition to regulating GH secretion and food intake, through endocrine,

autocrine and/or paracrine signalling. Ghrelin is also expressed in a variety of tissues, including bone (Nikolopoulos *et al.*, 2010), and the ghrelin transcript can undergo alternative splicing; a number of isoforms have been identified in humans and mice (see Chapter 4). The expression pattern of ghrelin and existence of various ghrelin isoforms further suggest a role for ghrelin in processes other than GH release and energy metabolism. Consistent with this, ghrelin has been shown to play a role in many processes such as inflammation, cell proliferation, differentiation and apoptosis (Kim *et al.*, 2005; Maccarinelli *et al.*, 2005; Liang *et al.*, 2012), particularly in bone.

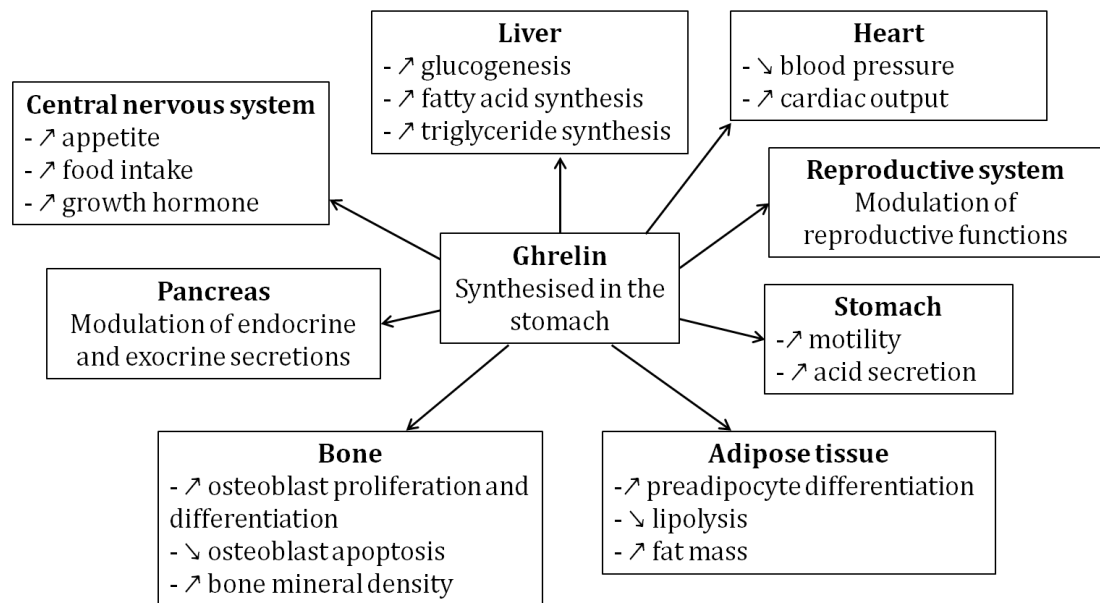


Figure 1.4: Main physiological activities of ghrelin

Ghrelin has a variety of functions in addition to stimulating growth hormone secretion and regulating energy metabolism. Adapted from (Delporte, 2013).

1.4.2.1. Ghrelin and bone

Several hormones from energy metabolism regulate bone homeostasis, including leptin, orexin, insulin, insulin-like growth factor 1 (IGF-1), adiponectin and ghrelin (Evans *et al.*, 2011; Delhanty *et al.*, 2014a; Wee and Baldock, 2014; Pizzorno, 2016b; a; Yue *et al.*, 2016). A large number of *in vitro* studies have shown that nanomolar concentrations of ghrelin stimulated proliferation and differentiation of both primary osteoblastic cells and osteoblastic cell lines across different species, including rats and humans (Fukushima *et al.*, 2005; Kim *et al.*, 2005; Maccarinelli *et al.*, 2005; Isabelle *et al.*, 2013). Ghrelin also inhibits apoptosis in osteoblastic cells (Kim *et al.*, 2005). Costa *et al.* (2011) showed that ghrelin had a strong mitogenic effect on human osteoblasts, but that effect was weaker in rat osteoblasts. Both ghrelin and its receptor GHSR1a have

been detected in rat osteoblasts (Fukushima *et al.*, 2005), suggesting that ghrelin has autocrine/paracrine effects in bone. The effects of ghrelin on osteoblasts appear to be mediated by GHSR1a (Kim *et al.*, 2005; Maccarinelli *et al.*, 2005; Isabelle *et al.*, 2013), accompanied by increased ALP activity, increased matrix mineralisation, and increased expression of osteoblast-specific genes, such as osteocalcin. Costa *et al.*, 2011 also showed that ghrelin increased osteoclastic bone resorption in rats, but did not alter osteoclast differentiation.

Ghrelin may also have biological effects in BMSCs. Ghrelin has been shown to stimulate BMSC proliferation in rats (Abdanipour *et al.*, 2018) and rabbits (Ye and Jiang, 2015). However, the effects of ghrelin on MSC lineage allocation are unclear. In murine embryo sarcoma cells (C3H10T1/2 cells) cultured with osteogenic differentiation medium, ghrelin downregulated ALP activity and osteoblast-specific gene expression, suggesting that ghrelin inhibited early osteogenic differentiation (Kim *et al.*, 2009). In C3H10T1/2 cells cultured with growth medium, ghrelin treatment increased PPAR γ and C/EBP α protein expression and suppressed Runx2 protein expression, suggesting that ghrelin may stimulate adipogenesis. However, when these cells were cultured with adipogenic medium, ghrelin did not promote adipogenic differentiation, as there was no increase in adipogenic gene expression and lipid content (Kim *et al.*, 2009). On the contrary, another study has demonstrated that ghrelin promoted osteoblastogenesis in rabbit MSCs (Ye and Jiang, 2015).

In vivo, ghrelin is also known to modulate osteoblast differentiation and function, both directly and indirectly via paracrine and endocrine mechanisms (Nikolopoulos *et al.*, 2010). Some of the effects of ghrelin may be associated with increased food intake, through the regulation of the GH-insulin-like growth factor (IGF) axis (Kim *et al.*, 2005), increased GH secretion and increased body weight stimulating bone formation due to the additional load. Ghrelin also has GH-independent effects on bone homeostasis, as chronic central administration of ghrelin increases bone mass through a mechanism independent of appetite regulation (Choi *et al.*, 2013), and intraperitoneal infusion of ghrelin increases BMD in GH-deficient rats (Fukushima *et al.*, 2005). Ghrelin also improves the repair of calvarial bone defects in rats, promoting the expression of osteoblastic markers such as ALP, osteocalcin, and type I collagen (Deng *et al.*, 2008; Nikolopoulos *et al.*, 2010).

Ghrelin signalling not only regulates osteoblast proliferation and differentiation; it is also necessary for normal bone formation (Ma *et al.*, 2015). GHSR-null mice exhibit a

low bone mass phenotype, with reduced bone formation; this phenotype is attenuated by restoring the expression of GHSR in osteoblasts. Ghrelin directly stimulates osteoblast differentiation via phosphorylation of cAMP response element-binding protein (CREB) and the expression of Runx2 (Ma *et al.*, 2015). In GHSR- and leptin-deficient mice, ghrelin has dual effects on osteoclastogenesis, inhibiting osteoclast progenitors directly but stimulating osteoclastogenesis via a systemic/central pathway; with aging, the osteoclastogenic effect of ghrelin is attenuated, revealing a protective effect of ghrelin on bone (van der Velde *et al.*, 2012). Another hormone, orexin, has been shown to regulate bone homeostasis in mice by peripheral mechanisms via orexin receptor 1 (OX1R) and ghrelin: OX1R-deficient mice exhibit high bone mass associated with a differentiation shift from marrow adipocytes to osteoblasts and with higher ghrelin expression in bone (Wei *et al.*, 2014).

These studies indicate that ghrelin is an important regulator of bone homeostasis and bone marrow function, via direct and indirect mechanisms, and acting on various cell types including BMSCs, osteoblasts and osteoclasts.

1.4.2.2. Ghrelin and adipogenesis

Ghrelin has been shown to affect adiposity through centrally and peripherally mediated signalling mechanisms (Müller *et al.*, 2015). Most *in vivo* studies show a stimulatory effect of ghrelin on adiposity. Pharmacological or genetic manipulation of ghrelin signalling affects adiposity and body weight: central and peripheral administration of ghrelin increases body weight and fat mass; intravenous and intra-bone marrow infusion of both acylated and desacyl ghrelin increase bone marrow adiposity, although these effects may be mediated by a receptor other than GHSR1a (Thompson *et al.*, 2004). In addition, suppression of arcuate GHSR expression induces a reduction in fat pad weight (Shuto *et al.*, 2002); mice lacking ghrelin or ghrelin receptors accumulate less fat mass than wild-type mice when on a high-fat diet (Wortley *et al.*, 2005; Zigman *et al.*, 2005). On the contrary, other studies reported that ablation of GHSR had no effect on body weight and fat mass in male mice fed with standard chow diet (Sun *et al.*, 2004; Zigman *et al.*, 2005) or in mice fed with a high fructose corn syrup (Ma *et al.*, 2013), but seemed to prevent age-associated obesity and insulin resistance by regulating fat metabolism in white and brown adipose tissues (Ma *et al.*, 2013; Müller *et al.*, 2015). Ghrelin also stimulates the expression of enzymes involved in fatty acid storage and downregulates genes controlling the rate-limiting step in fat oxidation; these effects are mediated by the sympathetic nervous system and some of them are independent of

food intake (Theander-Carrillo *et al.*, 2006). Ghrelin also acts centrally to promote hepatic lipid storage (Sangiao-Alvarellos *et al.*, 2009), inducing hepatic steatosis and increasing lipid droplet number and triacylglycerol content in a GHSR1a-dependent way (Davies *et al.*, 2009). However, the effect of peripheral ghrelin on adiposity is not uniform, suggesting tissue- and fat deposit-specific actions of ghrelin (Wells, 2009).

In vitro, the effects of ghrelin on adipogenesis are less clear. Some studies have shown that ghrelin directly stimulated the differentiation of rat preadipocytes, increasing the expression of PPAR γ and inhibiting lipolysis (Choi *et al.*, 2003). Another *in vitro* study showed that ghrelin gene products positively regulated adipogenesis (Giovambattista *et al.*, 2007). In contrast, other studies have shown that overexpression of ghrelin inhibited adipogenesis. Zhang *et al.* (2004) established a 3T3-L1 preadipocyte cell line overexpressing ghrelin, and observed that ghrelin significantly attenuated adipocyte differentiation, decreasing PPAR γ expression and stimulating cell proliferation. In the thymus, ghrelin and ghrelin receptor expression decrease during aging, and genetic ablation of ghrelin and its receptor leads to loss of thymic epithelial cells, while stimulating adipogenesis (Youm *et al.*, 2009). Acylated ghrelin increases thymic size and cellularity, reflecting an inhibition of adipose/fibrous differentiation while rejuvenating the epithelial/stromal microenvironment, leading to the expansion of the T-cell content (Dixit *et al.*, 2007). This indicates a reversal of age-dependent fatty involution (loss of epithelial function and T-cell production) that is associated with immune senescence (Taub *et al.*, 2010).

While ghrelin increases adiposity when infused in the bone marrow, it is not known which cell type is affected; ghrelin may promote the adipogenic differentiation of BMSCs, or the maturation of cells that are already committed to the adipogenic lineage. Alternatively, ghrelin may induce the trans-differentiation of cells that were already committed to the osteoblastic lineage.

1.5. Ion channels

Ion channels are transmembrane proteins that allow the principal cellular ions (sodium (Na⁺), potassium (K⁺), calcium (Ca²⁺) and chloride (Cl⁻)) to move through the plasma membrane at different rates by diffusing down their concentration gradients. There are a large number of ion channel subtypes in all cells, and they are involved in regulating important cell processes such as proliferation and differentiation, particularly in osteoblasts and adipocytes. Ion channels play important roles in bone metabolism and may be involved in the mechanisms of pathological adipogenesis.

1.5.1. Potassium channels and membrane potential

Potassium (K^+) channels in the cytoplasmic membrane are the most diverse class of ion channels, with over 80 genes identified. They are present in almost all cells, including both excitable and non-excitable cells, in a large number of tissues (Wang *et al.*, 2008). K^+ channels can be classified into 5 subcategories by function and structure: voltage-gated K^+ channels (K_V), Ca^{2+} - and Na^+ -activated K^+ channels (K_{Ca} and K_{Na}), inward-rectifier K^+ channels (K_{IR}), and 2-pore domain K^+ channels (K_{2P}) (figure 1.5).

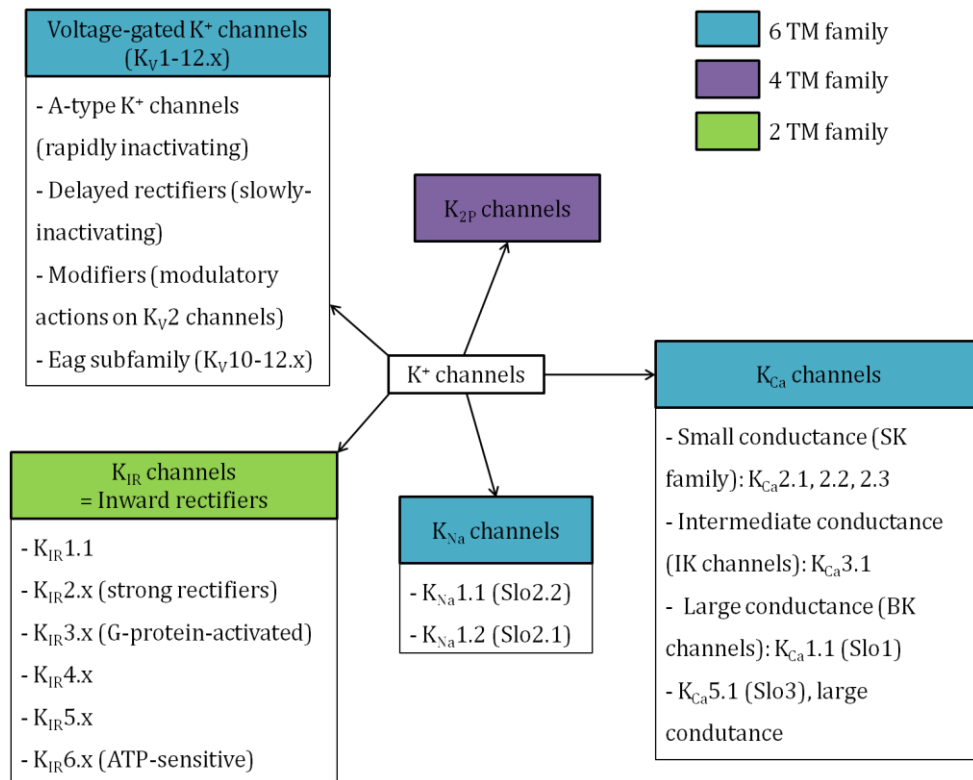


Figure 1.5: K^+ channels subfamilies

K_V channels are widely expressed in the nervous system and other tissues, including non-excitable cells, and may also regulate cell proliferation, cell migration and cell volume in a wide range of cell types. They display a large diversity as K_V channel subunits can form homomeric and heteromeric channels within each of the K_V 1, K_V 2, K_V 3, K_V 4 and K_V 7 subfamilies. The K_{2P} channels open across the physiological voltage-range and are regulated by chemical and physical factors, including neurotransmitters, post-translation modifications, second messengers, temperature and mechanical stretch. Some K_{2P} subunits can form heterodimers across subfamilies, further increasing the diversity of K^+ channels. Finally, the inward rectifiers have diverse physiological functions depending on their type and their location; similarly to voltage-gated K^+ channels, K_{IR} pore-forming subunits can form heteromeric channels within subfamilies, and are expressed in a wide variety of tissues (Hibino *et al.*, 2010; Alexander *et al.*, 2011a, 2017).

Membrane potential and ion channels are involved in transmitting signals via action potential in excitable cells such as neurons or myocytes, but they also play important roles non-excitable cells, regulating important processes such as cell proliferation, apoptosis, differentiation, migration, secretion and metabolism (Blackiston *et al.*, 2009; Capiod, 2011; Adams and Levin, 2013; Levin, 2013; Resende *et al.*, 2013).

1.5.2. Ion channels and bone

Sundelacruz *et al.* published two papers highlighting the role of membrane potential in the control of proliferation and differentiation of MSCs (Sundelacruz *et al.*, 2008, 2009). Working with human MSCs cultured in adipogenic or osteogenic differentiation media, they showed that MSC differentiation was inhibited by membrane depolarisation via high extracellular $[K^+]$ or ouabain treatment, which blocks the Na/K-ATPase transporter. On the contrary, MSC osteogenic differentiation was stimulated by membrane hyperpolarisation (Sundelacruz *et al.*, 2008). Hyperpolarisation occurred during both osteogenic and adipogenic differentiation; ion flux and changes in membrane potential have been associated with the control of proliferation and differentiation in various cell types (Binggeli and Weinstein, 1986; Levin, 2007). Proliferative and relatively immature cells tend to have depolarised membrane potentials, while terminally differentiated cells tend to have strongly hyperpolarised membrane potentials.

In bone, membrane potential and ion channels are involved in the regulation of proliferation and differentiation in various cell types, from BMSCs to differentiated cells such as osteoblasts, osteoclasts, and adipocytes, in various species, including humans, mice and rats.

There is good evidence that ion channels are involved in regulating the osteogenic and adipogenic differentiation of MSCs, including experiments with electrical stimulation and electromagnetic fields, and the numerous electrophysiological studies with MSCs from human, mice and rats, derived from bone or other tissues. Studies have shown that the electrical stimulation of adipose-derived MSCs enhanced osteogenic differentiation (Pelto *et al.*, 2013; Björninen *et al.*, 2014; Zhang *et al.*, 2016); this effect appeared to be mediated by voltage-gated channels as it was reduced with blockers of voltage-gated sodium, potassium and chloride channels, and completely nullified with a voltage-gated calcium channel blocker (Zhang *et al.*, 2016). Mechanical cues also regulate key processes in MSCs, including proliferation and differentiation, via ion

channels (Rawlinson *et al.*, 1996; Steward and Kelly, 2015; Chubinskiy-Nadezhdin *et al.*, 2017).

Osteoblasts, osteoblast-like cells and MSCs express a variety of ion channels which function in cooperation and regulate many aspects of osteoblast function, including proliferation, differentiation and mineralisation.

1.5.2.1. Potassium channels and osteoblasts

Osteoblasts, osteoblast-like cells and MSCs express an array of K⁺ channels, including voltage-gated K⁺ channels of the S4 family with six transmembrane domains (Li *et al.*, 2005, 2006), inward rectifier (Yellowley *et al.*, 1998), ATP-sensitive K⁺ channels (Moreau *et al.*, 1997; Henney, 2008), a two-pore domain K⁺ channel (Hughes *et al.*, 2006), and Ca²⁺-activated K⁺ channels of small-, intermediate- and large-conductance (Moreau *et al.*, 1997; Li *et al.*, 2005, 2006; Deng *et al.*, 2007; Henney, 2008; Hirukawa *et al.*, 2008; Henney *et al.*, 2009; Zhang *et al.*, 2014). A number of studies have demonstrated that K⁺ channels play a central role in the regulation of cell processes including proliferation, differentiation, mineralisation and secretion. The expression pattern of some of these K⁺ channels may be species-specific; for example, the intermediate-conductance Ca²⁺-activated channel is highly expressed in mouse and rat BMSCs (Deng *et al.*, 2007; Tao *et al.*, 2007), but not in human BMSCs (Heubach *et al.*, 2004; Li *et al.*, 2005). Also, the expression pattern may change with cell differentiation and maturation; in smooth muscle cells, cells that are at the proliferative stage express intermediate-conductance Ca²⁺-activated K⁺ channels, but when they become mature smooth muscle cells, these channels are replaced by large conductance channels (Köhler *et al.*, 2003; Tharp *et al.*, 2006). Finally, K⁺ channel expression and activity also vary with cell cycle progression (Deng *et al.*, 2007).

The human ether-à-go-go (hEag1 or Kv10.1) and the large-conductance calcium-activated (BK channel or KCa1.1) potassium channels putatively regulate the proliferation, the adipogenic and osteogenic differentiation of human BMSCs, and osteoblast functions (Zhang *et al.*, 2014). Pharmacological inhibition of either of these channels, or knockdown with specific shRNA, leads to reduced cell proliferation, decreasing the expression of the cell cycle regulatory proteins cyclin D1 and cyclin E and reducing the phosphorylation of ERK1/2 and Akt. Adipogenic differentiation of human BMSCs cultured with adipogenic medium is also reduced, as shown by the observed decrease in lipid accumulation and decreased PPAR γ expression. Inhibition of hEag1 or BK channels also decreases osteogenic differentiation of hBMSCs cultured

with osteogenic medium, with reduced *in vitro* mineralisation and osteocalcin expression (Zhang *et al.*, 2014).

The BK channel is also densely expressed in several human osteoblastic cells, including primary human osteoblasts and MG63 and SaOS-2 human osteoblast-like cell lines (Henney, 2008; Henney *et al.*, 2009; Li, 2012). These studies demonstrated that the BK channel is involved in regulation of proliferation and mineralisation. MG63 cells also express several K_{ATP} subunits: the pore-forming subunits Kir6.1 and Kir6.2, and the regulatory subunits SUR1 and SUR2B; pinacidil, which is a K_{ATP} channel opener, causes a significant increase in cell number (Henney, 2008). Both BK channel and K_{ATP} channels has been shown to also regulate osteocalcin secretion by MG63 cells (Moreau *et al.*, 1997).

In osteocytes, K^+ channels and voltage-dependent calcium channels (VDCCs) were shown to be involved in paracrine signalling and mechanotransduction (Gu *et al.*, 2001b; a). In osteoblasts, Ca^{2+} -activated K^+ channels regulate cell volume (Weskamp 2000) and resting membrane potential: KCa channel activation triggers membrane hyperpolarisation, balancing the depolarisation associated with $[Ca^{2+}]_i$ increases. The K^+ channels hence function as feedback regulators of $[Ca^{2+}]_i$ (Moreau *et al.*, 1996; Ravestloot *et al.*, 1990; Yellowley *et al.*, 1998). In particular, TREK-1, may be involved in the mechanotransduction in osteoblasts, controlling bone remodelling (Hughes *et al.*, 2006). TREK-1 is a member of the two-pore domain potassium channel family (K_{2P}); it is sensitive to membrane stretch, lysophospholipids, free fatty acids, temperature, intracellular pH, and anaesthetics. TREK-1, TREK2c and TRAAK expression was detected in human derived osteoblasts and MG63 cells; these three channels collectively form the lipid and mechanosensitive subfamily of mammalian K_{2P} channels (Patel and Honoré, 2002). Treatment with a TREK-1 blocker upregulated bone cell proliferation (Hughes *et al.*, 2006).

In mouse MSCs, intermediate-conductance Ca^{2+} -activated K^+ (IK_{Ca} or $KCa3.1$) and volume-sensitive Cl^- ($Clcn3$) channels have been shown to regulate cell proliferation (Tao *et al.*, 2008); blocking or silencing these channels reduced cell proliferation of mouse MSCs by 20-30%, decreasing the expression of cyclin D1 and cyclin E. The large-conductance Ca^{2+} -activated K^+ channel (BK channel) regulates MC3T3-E1 preosteoblast cell proliferation; BK channel knock-out significantly reduces cell number (Hei *et al.*, 2016).

Rat MSCs express several functional potassium channels, either alone or in combination: two delayed rectifier channels (Kv1.2 and Kv2.1), the BK channel (KCa1.1), an intermediate-conductance Ca^{2+} -activated K^+ channel (KCa3.1) and two transient K^+ channels (Kv1.4 and Kv4.3) (Li *et al.*, 2006; Deng *et al.*, 2007; Wang *et al.*, 2008). The expression of these potassium channels, in particular voltage-gated (Kv1.2 and Kv2.1) and calcium-activated potassium channels (KCa1.1 and KCa3.1), changed during cell cycle progression and played an important role in regulating this process. Membrane potential was shown to hyperpolarise during cell cycle progression, and this was associated with increased cell size. I_{KDR} decreased and I_{KCa} increased during progress from G_1 to S phase. This was associated with decreased expression levels of Kv1.2 and Kv2.1, and increased expression level of KCa3.1 during the cell cycle progression (Deng *et al.*, 2007). Pharmacological blockade of the voltage-gated channels (Kv) and Ca^{2+} -activated channels inhibited proliferation of cultured MSCs by arresting cell-cycle progression (Deng *et al.*, 2007; Wang *et al.*, 2008), and downregulation of Kv1.2, Kv2.1 and KCa3.1 with specific RNAi also inhibited cell proliferation (Deng *et al.*, 2007). Another study showed that the BK channel regulate rat osteoblast proliferation, differentiation and functions, using ROS17/2.8 osteoblasts: BK channel knockout significantly decreased cell number, the expression of osteoblastic markers Runx2, osteocalcin and osteopontin), and the ability to mineralise (Hei *et al.*, 2016).

1.5.2.2. Potassium channels and adipocytes

K^+ channels also regulate proliferation and adipogenic differentiation in MSCs and preadipocytes. Voltage-gated K^+ channels regulate the adipogenic differentiation of human BMSCs; blocking K_V currents with tetraethylammonium (TEA) significantly reduces lipid droplet formation and the expression of the adipogenic marker aP₂. You *et al.* (2013) showed that blocking Kv2.1 suppresses adipogenesis. The 3T3-L1 mouse preadipocytes have been shown to express the Ca^{2+} -activated intermediate conductance K^+ channel (KCa3.1), an inwardly rectifying potassium (Kir2.1) and the volume-sensitive chloride channel (Clcn3); KCa3.1 and Clcn3 participate in regulating cell proliferation (Zhang *et al.*, 2012). Finally, K_{ATP} channels also regulate proliferation and differentiation in rat preadipocytes (Wang *et al.*, 2007).

1.6. Hypothesis, aims and experimental strategies

The principle hypothesis of this thesis is 1) that ghrelin can inhibit adipogenic transdifferentiation in 7F2 cells, and 2) that potassium channels are involved in mediating ghrelin signalling in this process.

The overarching aim of this thesis was to provide a better understanding of the mechanisms underlying pathological adipogenesis in bone. In order to do this, this study investigated the effects of ghrelin on the adipogenic differentiation of osteoblast-like cells, and the role of potassium channels in that process. Indeed, recently, ghrelin has been shown to play an important role in regulating bone metabolism and adiposity, particularly in a context of pathological adipogenesis. It is also well established that ion channels, and particularly K⁺ channels, are also involved in regulating bone metabolism. Pathological adipogenesis is a common feature of several pathologies, including some forms of osteoporosis. Osteoporosis represents a major health problem, due to its high financial costs, its consequences on quality of life (reduced mobility, isolation) and the increased death risk due to serious fractures and associated complications. While various treatments are available, they are not recommended for every patient, and new treatments are still needed. Investigating the effects of ghrelin on the adipogenic trans-differentiation of 7F2 cells osteoblast-like cells, and the role of ionic mechanisms, particularly K⁺ channel, in this process, will provide a better understanding of pathological adipogenesis mechanisms in bone, which underlies several forms of osteoporosis, particularly glucocorticoid-induced osteoporosis. This research may, in the long term, lead to the development of drugs that will help prevent osteoporosis by targeting ghrelin signalling and ionic mechanisms. Numerous studies have shown that ghrelin stimulates osteoblastogenesis and adipogenesis; what about the effects of ghrelin on cells that are already committed to osteoblast lineage, but that can be induced into adipocytes, such as 7F2 cells? What are the roles of K⁺ channels in this process?

To answer these questions, the key objectives of this thesis were:

1) to optimise the protocol to differentiate 7F2 cells into adipocytes, to trigger efficient differentiation while still leaving room to observe a possible stimulatory effect of ghrelin; 2) to investigate the expression of key genes from ghrelin signalling (*Ghrl*, *Ghsr* and *Mboat4*) in 7F2 osteoblastic cells and adipocytes and to test the effects of ghrelin on these; 3) to test the effects of ghrelin and potassium channel ligands on 7F2 cell

Chapter 1 – Introduction

adipogenic differentiation; 4) to investigate and compare the electrophysiological properties of 7F2 cells and 7F2 cell-derived adipocytes, and to test the effects of ghrelin on these.

Chapter 2 – Materials and Methods

2.1. Cell culture

2.1.1. Routine cell culture

Minimum essential medium alpha (MEM- α) without ribonucleic or deoxyribonucleic acids, containing 2 mM L-glutamine, 1 nM sodium pyruvate and 50 mg/L ascorbic acid (Life Technologies, ThermoFisher Scientific) was supplemented with 10 % foetal bovine serum (FBS, Life Technologies, ThermoFisher Scientific). From here on, this will be referred to as basal medium.

The 7F2 immortalized murine preosteoblastic cell line was originally a gift from the Department of Child Health, School of Medicine, Cardiff University, and used at passages 12 to 28. Cells were cultured in 25 cm² tissue culture flasks in 4 ml basal medium and incubated at 37°C in 5% CO₂ humidified air. Medium was replaced every 2-3 days.

Confluent cultures were passaged weekly; cells were washed with 2 ml Dulbecco's phosphate buffered saline (DPBS; calcium- and magnesium-free, Gibco™, ThermoFisher Scientific) and detached with 500 μ l of trypsin-EDTA (0.25%) solution (trypsin from porcine pancreas, Gibco™, ThermoFisher Scientific). Cells were incubated with trypsin at 37°C for up to 5 minutes. When cells were detached, 2.5 ml of basal medium were added to stop the trypsinisation and cells were evenly suspended by gentle repeated pipetting. The suspension was then diluted in 7 mL basal medium (total volume 10 ml) and split at a 1:10 dilution in new culture flasks.

2.1.2. Adipogenic differentiation of 7F2 cells

2.1.2.1. Adipogenic differentiation medium

Dexamethasone and indomethacin were purchased from Sigma-Aldrich. Dexamethasone and indomethacin stock solutions were prepared in ethanol at a 1 mM concentration and at a 25 mM concentration respectively, and stored at -20°C for up to one year. Basal medium was supplemented with 50 μ M indomethacin and 100 nM dexamethasone (Sigma-Aldrich). From here on, this will be referred to as adipogenic medium. The composition of adipogenic medium was chosen based on the work by Thompson *et al.* (1998); here, MEM- α already contained 50 μ g/ml ascorbic acid, so no further supplementation was required.

2.1.2.2. Adipogenic differentiation for Oil Red O staining assay

7F2 cells were plated into 12-well tissue culture plates (Fisher Scientific) at a density of 2500 cells/cm² in adipogenic medium. Cells were incubated as usual for 7 days with medium replacement every 2-3 days. Digital photographs were taken daily under a microscope at 200x magnification to follow the apparition of lipid droplets within the cells.

A stock solution of 4% paraformaldehyde (PFA) was prepared by adding 10 g PFA powder to 250 ml 1x PBS (Gibco™, ThermoFisher Scientific). PFA was dissolved by heating the solution to 60°C. The solution was then filtered with Whatman paper and aliquoted to be frozen at -20°C. After 7 days of treatment, 7F2 cells were washed with DPBS, then fixated with 1 ml of 4% PFA solution per well. After 15 minutes at room temperature, 4% PFA was removed, the cells were washed twice with distilled water and air dried.

A 60 % Oil Red O : 40 % distilled water working solution was freshly prepared from a stock solution (0.25 g in 50 ml isopropanol) and filtered through coarse filter paper. Cells were stained with the working solution for 20 minutes at room temperature, then washed with 60 % isopropanol to remove excess stain and washed three times with distilled water. Photographs were taken under a microscope at a magnification of 200x. Oil Red O stain was extracted by adding 100% isopropanol to the cells for 30 minutes at room temperature, and quantified by transferring 100 µl from each well to a 96-well plate and measuring spectrophotometrically at 490 nm, using 100% isopropanol as blank.

2.1.2.3. Adipogenic differentiation for RT-PCR analysis

7F2 cells were cultured in 25 cm² flasks with adipogenic medium as described in section 2.1.1. After 7 days of culture, the cells were detached using trypsin as described previously. The cells were pelleted by centrifuging at 1,400 rpm for 5 minutes; then the medium was removed, the cell pellets were resuspended in 1 ml DPBS and transferred to 1.5 ml eppendorf tubes. The cells were pelleted again by centrifuging at 1,400 rpm for 5 minutes, DPBS was removed and the pellets were immediately frozen at -80°C for future RNA extraction and RT-PCR and qPCR analysis.

2.2. Cell counting

A Reichert Bright-Line haemocytometer (Sigma-Aldrich) and glass coverslip were cleaned with alcohol before use. The coverslip was moistened with water and fixed to the haemocytometer. The presence of Newton's refraction rings under the coverslip indicated proper adhesion.

7F2 cells were detached as above (see section 2.1.1). 50 μ l of cell suspension were mixed with 50 μ l of Trypan Blue (Sigma-Aldrich), staining dead cells in blue. 8 μ l of the mix was pipetted into each of the haemocytometer counting chambers, allowing the cell suspension to be drawn out by capillary action. At 100x magnification under a microscope, focus was made on the grid lines of the haemocytometer. Live cells were counted using a hand tally counter in 4 sets of 16 corner squares for each counting chamber, including the cells located on the left and top boundary lines, but not those on the right and bottom boundary lines.

The density of cell suspension was calculated by multiplying the average cell count from each of the sets of 16 corner squares by 10,000 (10^4) and by multiplying by 2 to correct for the 1:2 dilution from the Trypan Blue addition.

2.3. Molecular biology

2.3.1. RNA extraction and DNase treatment

Cells pellets were collected as described above (see section 2.1.2.3.). Cell pellets were thawed on ice and were resuspended in 1 ml Trizol (Invitrogen), pipetting repeatedly to lyse the cells. After 5 minutes at room temperature, 0.2 ml of cold chloroform (stored at 4°C; Sigma-Aldrich) was added and the microcentrifuge tubes were vortexed for 10 s, until the solution became pink. After 3 minutes at room temperature, the cell lysates were centrifuged at 14,000 rpm for 15 minutes at 4°C. The aqueous phase (500 μ l) was collected into new tubes.

500 μ l of cold isopropanol (stored at -20°C; Sigma-Aldrich) were added to each tube. After 10 minutes at room temperature, the tubes were centrifuged at 14,000 rpm for 30 minutes at 4°C.

The supernatant was removed. 500 μ l of 75% ethanol (stored at -20°C) were added to the tubes, which were then centrifuged at 14,000 rpm for 5 minutes at 4°C. The ethanol was removed and the pellets were air dried for 5-10 minutes. The pellets were then resuspended in 22 μ l of Ultrapure DNase/RNase-free distilled water (Invitrogen™,

ThermoFisher). 2 μl were used to measure the RNA concentration with a NanoDrop 2000 Spectrophotometer (Thermo Scientific), using Ultrapure DNase/RNase-free distilled water as blank. The concentration of the remaining 20 μl was then adjusted to a 1 $\mu\text{g}/\mu\text{l}$ concentration (1 γ).

mRNA was treated to remove possible DNA contaminant using the DNA-free™ DNA Removal Kit (Invitrogen™, ThermoFisher Scientific). A mix of 5 μl 10X buffer, 10 μl mRNA (10 μg), 1 μl DNase and 34 μl Ultrapure DNase/RNase distilled water was prepared, for a total volume of 50 μl . The mix was incubated at 37°C for 30 min, then 5 μl of DNase Inactive Reagent were added to stop the DNase; the samples were vortexed several times for 2 minutes at room temperature, then centrifuged at 14,000 rpm for 1.5 minutes. The DNA-free mRNA was transferred to a new tube for a final concentration of 0.2 γ (0.2 $\mu\text{g}/\mu\text{l}$). The remaining 1 γ mRNA was frozen at -80°C.

2.3.2. Reverse transcription

0.2 γ mRNA samples (see section 2.3.1) were thawed on ice. Reverse transcription was carried out with the High Capacity cDNA Reverse Transcription Kit (Applied Biosystems); compositions and conditions are detailed in tables 2.1 and 2.2 respectively. For no RT controls, the Multiscribe Reverse Transcriptase was replaced with 1 μl of nuclease-free water. The RT was run in a T100™ Thermal Cycler (Bio-Rad). After the reaction, 80 μl H₂O were added and cDNAs were stored at -20°C.

Components	Final concentrations	Volumes
10X RT Buffer	1 X	5 μl
25X dNTP 100 mM	1X	0.8 μl
Multiscribe Reverse Transcriptase		1 μl
RNA (0.2 $\mu\text{g}/\text{ml}$)		5 μl
Nuclease-free water		3.2 μl
Total volume		20 μl

Table 2.1: Reverse transcription reaction composition

Step	Temperature °C	Time
Step 1	25	10 min
Step 2	37	120 min
Step 3	85	5 min
Step 4	4	Indefinite

Table 2.2: Reverse transcription reaction conditions

2.3.3. Polymerase chain reaction (PCR)

Primers were designed from mouse gene sequences using FasterDB (Cancer Research Center of Lyon, CRCL) and Primer3 as follows: the FasterDB database was searched for genetic sequences in the mouse genome; part of mRNA sequences were selected so that they covered as many splicing isoforms as possible and copied into the ‘source sequence box’ of the web-based Primer3 primer design software. The software selected left and right primers for the given sequence without modification of the default software settings. Primer3-suggested primers were checked against the complete genetic sequence using the FasterDB ‘*in silico* PCR’ tool, to determine predicted amplicon sizes, especially when primer sequences were in different exons. Primers were obtained from Eurogentec (see Appendix, section 8.1 for primer details).

PCR of 50 µl were routinely performed, using Herculase II Fusion DNA Polymerase PCR kit (Agilent Technologies). The PCR reaction composition is detailed in table 2.3. Ultrapure DNase/RNase distilled water was used as a negative control and three house-keeping genes, *Hprt1*, *Eef2* and *Gapdh*, were used as positive controls.

Components	Final concentrations	Volumes
5X Herculase II Reaction Buffer	1 X	10 µl
dNTPs (100 mM; 25 mM each dNTP)	250 µM each dNTP	0.5 µl
Forward primer (10 µM)	0.2 µM	1 µl
Reverse primer (10 µM)	0.2 µM	1 µl
Herculase II Fusion DNA Polymerase		0.25 µl
cDNA		5 µl
Nuclease-free water		to 50 µl

Table 2.3: PCR reaction composition

2.3.4. Gel electrophoresis

The PCR amplification products were analysed by gel electrophoresis in 1% agarose gels. 1 L of 20X Sodium Borate (SB) buffer was prepared using 8 g NaOH (final concentration: 200 mM), 47 g Boric acid, and ddH₂O. For small gels, 0.75g of agarose were added to 75 ml 1X SB buffer; for large gels, 1.5 g of agarose were added to 150 ml 1X SB buffer. The agarose-containing buffer was warmed in a microwave until the agarose was dissolved; then SYBR Safe (Invitrogen) was added to stain DNA molecules. Electrophoresis ran at 200V for 20 minutes or at 100V for 40 minutes. Smartladder SF (Eurogentec) was used as a marker for each gel electrophoresis (Figure 2.1).

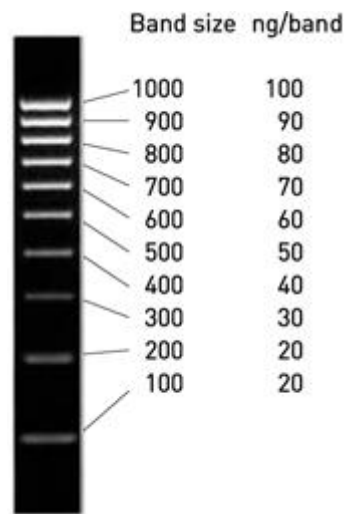


Figure 2.1: Smartladder SF DNA ladder

Using a standard loading of 5 µl, the bands correspond to an exact quantity of DNA, from 20 to 100 ng.

2.3.5. Quantitative PCR (qPCR)

qPCR was carried out using Rotor-Gene SYBR Green PCR kit (Qiagen). The reaction composition and conditions are detailed in tables 2.4 and 2.5 respectively. Reactions of 25 µl were performed; Ultrapure DNase/RNase-free distilled water was used as a negative control and three house-keeping (HK) genes, *Hprt1*, *Eef2* and *Gapdh* were used as positive controls. Oligonucleotide primers were the same as for RT-PCR (see Appendix, section 8.1 for primer details).

Chapter 2 – Materials and Methods

Components	Final concentrations	Volumes
2x Rotor-Gene SYBR Green	1 X	12.5 µl
PCR Master Mix		
Forward primer (10 µM)	1 µM	2.5 µl
Reverse primer (10 µM)	1 µM	2.5 µl
Template cDNA	≤ 100 ng	1 µl
RNase-free water		6.5 µl
Total volume		25 µl

Table 2.4: qPCR reaction composition

Step	Time	Temperature
PCR initial activation step	5 min	95°C
<i>Two-step cycling</i>		
Denaturation	5 s	95°C
Combined annealing/extension	10 s	60°C
Number of cycles	40	

Table 2.5: qPCR cycling conditions

For each qPCR assay, there were 3 or 4 replicate samples per condition (experimental or control), except when stated otherwise. In each qPCR assay, all the replicate samples were run in duplicates. Data were analysed using the relative C_T ($\Delta\Delta C_t$) method (Livak and Schmittgen, 2001; Schmittgen and Livak, 2008). Mean C_T values of house-keeping genes (*Hprt1*, *Eef2* or *Gapdh*) were subtracted from mean C_T values of each gene of interest, to obtain ΔC_t values of each gene of interest for each sample. For each gene, ΔC_t values in the control treatment (basal medium) were used to normalize ΔC_t values of each treatment to obtain $\Delta\Delta C_t$ and mRNA fold expression values [$2^{(-\Delta\Delta C_t)}$]. Standard deviation was determined from the replicate samples at each experimental condition.

2.3.6. Sequencing

2.3.6.1. Gel extraction of PCR products

PCR and gel electrophoresis were carried out as previously described (see sections 2.3.3 and 2.3.4 respectively). To maximise the amount of extracted PCR product, 50-55 cycles of PCR were done, and the PCR products were loaded in 3 wells per sample, to be combined after excision from the gels. Electrophoresis ran at 100V for 40 minutes to fully separate the bands. A picture of the gel was taken under UV conditions before extracting the PCR products from the gels.

The PCR products were extracted using the QIAquick Gel Extraction Kit (Qiagen). Selected DNA fragments were excised from the agarose gels using a scalpel and a UV transilluminator. The scalpel was cleaned between each sample by dipping the blade into 100% ethanol, then wiping the blade with tissue. The gel slices were weighed in 1.5 ml eppendorf tubes, and 3 volumes of Buffer QG were added to the gel slices (i.e. 300 μ l of Buffer QG to each 100 mg of gel). The maximum amount of gel slice was limited to 400 mg per sample as per supplier's instructions. The gel slices were incubated at 50°C for 10 minutes and vortexed every 2-3 minutes to help dissolve the agarose gel completely. After solubilising the agarose gels, the colour of the mixture was checked; if still yellow, indicating a pH \leq 7.5, no additional step was needed to adjust pH; if colour was orange or violet, 10 μ l of 3M sodium acetate, pH 5.0, were added. To increase the yield of < 500 bp DNA fragments, 1 volume of isopropanol was added to the samples, and the samples were mixed.

The samples were then applied to QIAquick spin columns and centrifuged for 1 minute at 13,000 rpm at room temperature. The flow-through was discarded. 0.5 ml of Buffer QG was added to the QIAquick columns and the samples were centrifuged for 1 minute at 13,000 rpm to remove all traces of agarose. The samples were then washed by adding 0.75 ml of Buffer PE, leaving the samples stand for 2-5 minutes and then centrifuging for 1 minute at 13,000 rpm. The flow-through was discarded and the samples were centrifuged for an additional 1 minute at 13,000 rpm to remove residual ethanol from Buffer PE.

QIAquick columns were transferred to clean microcentrifuge tubes. 30 μ l of Buffer EB were dispensed directly on the QIAquick columns membranes to elute bound DNA; to increase the DNA concentration, the columns were let to stand for 4 minutes before centrifuging for 1 minute at 13,000 rpm. The average eluate volume was 28 μ l. The DNA concentration of eluates was measured using a NanoDrop 2000

Spectrophotometer (Thermo Scientific), using Buffer EB as blank. The DNA samples were then frozen at -20°C.

2.3.6.2. Sanger sequencing

Sequencing of PCR products was carried out externally, via the LIGHTRUN sequencing service (Sanger sequencing, GATC Biotech) on an ABI 3730xl DNA Analyzer system. 5 µl of samples with a DNA concentration higher than 20 ng/µl were sent for sequencing in 1.5 ml tubes along with 5 µl of 5 µM appropriate primer pairs for a total volume of 10 µl.

2.3.6.3. Analysis of sequencing data

Sequencing data was provided by GATC Biotech as a set of three files per sample: a chromatogram (Ab1 Trace File) which contains the raw data (signal strength) of the sequence analysis and other ABI information alongside the graphically displayed individual bases; and two text files (FAS. and SEQ. files) which contain the sequence of the sample. The Phred basecaller calculates the respective quality value for each base using the peaks in the chromatogram (Phred score). Phred 20 means accuracy of 99%, meaning a read error probability of 1:100. In the text files, the notation of the bases is defined as follows: "N" is equivalent to quality value < Phred 10; a lower case letter, e.g. "a" is equivalent to a quality value of Phred 10-19; and an upper case letter, e.g. "A" is equivalent to a quality value of ≥ Phred 20.

For analysis, chromatograms were opened using the GATCViewer software (GATC Biotech), and PCR product sequences were manually copied in a text file. They were then compared with the gene sequence to identify which regions of the gene were present in both sequences, using Clustal Omega (EMBL-EBI) (Goujon *et al.*, 2010; Sievers *et al.*, 2011; McWilliam *et al.*, 2013).

2.3.7. Statistical analysis

Statistical analysis was performed as described in Figure 2.2 (McDonald, 2014; Mangiafico, 2015). The Shapiro-Wilk's test was used to assess the normality of distribution of investigated parameters (for each variable). The F test was used to assess the homogeneity of variances when there were two variables; the Bartlett test and the Levene's tests were used when there were more than two variables. Data were expressed as mean ± standard deviation; the number of repeat assays is indicated by "n" in each figure legend as appropriate. The values $P < 0.05$ were considered

statistically significant. Statistical analysis was done using the R software (<https://www.r-project.org/>, version 3.5.3). The Dunn test required the dunn.test package (<https://cran.r-project.org/web/packages/dunn.test/index.html>).

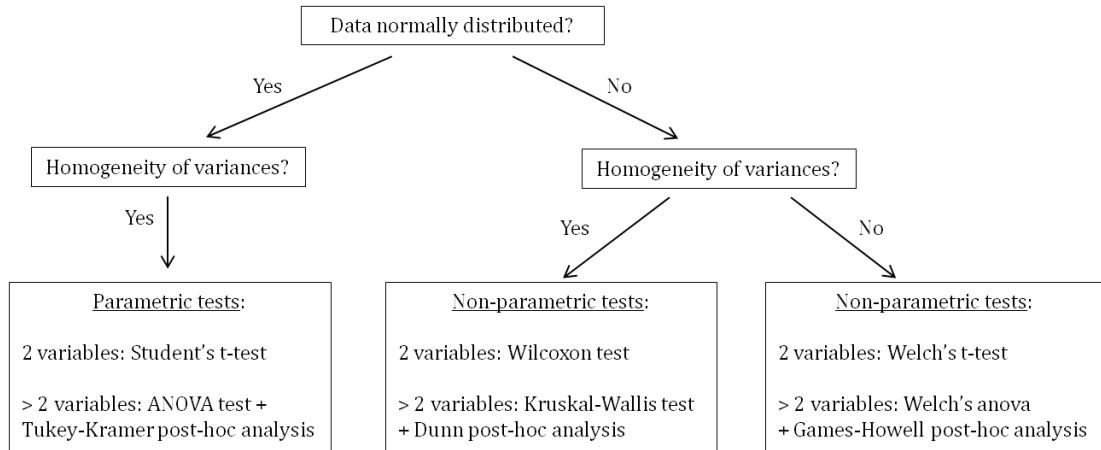


Figure 2.2: Statistical analysis of data

Normality of distribution and homogeneity of variances were assessed to choose the appropriate statistical test.

2.4. Electrophysiology

2.4.1. Physiological recording solution

All chemical components were obtained from Sigma and were prepared in distilled H₂O and stored at 2 – 8 °C. The volume of each solution (see table 2.6 for composition) was adjusted to 100 ml with distilled water. The pH of the Sodium “Locke” extracellular solution and that of the High K⁺ intracellular solution were adjusted to 7.4 and 7.2 respectively, with NaOH or HCl. The electrophysiological solutions were stored at 4°C up to 1 week; they were warmed to room temperature before use, and filtered through a non-sterile 0.2 µm PVDF-membrane 4 mm syringe filter (Whatman) to avoid crystals that could block the microelectrode tip, or attach to the cells and prevent giga seal formation.

Sodium “Locke” extracellular solution: 100 ml

Component	Quantity	Final concentration
NaCl	877 mg	150 mM
KCl	0.3 ml of 1 M stock	3 mM
CaCl ₂	0.2 ml of 1 M stock	2 mM
MgCl ₂	0.2 ml of 1 M stock	2 mM
HEPES	238 mg	10 mM
D-glucose	180 mg	10 mM

High K⁺ intracellular solution: 100 ml

Component	Quantity	Final concentration
NaCl	0.5 ml of 1 M stock	5 mM
KCl	1.045 g	140 mM
CaCl ₂	100 µl of 100 mM stock	30 nM free [Ca ²⁺]
MgCl ₂	0.1 ml of 1 M stock	1 mM
HEPES	238 mg	10 mM
EGTA	2.2 ml of 50 M stock	11 mM

Table 2.6: Composition of electrophysiological solutions

2.4.2. Electrode fabrication

Recording electrodes were pulled just before use from 1.5 mm outside-diameter, 0.86 mm inside-diameter borosilicate glass capillaries (Warner Instruments) by a Narishige PP-83 two-stage electrode puller set to produce two equal length electrodes with a resistance of 4 – 8 MΩ for single channel patch-clamping, and 1 – 2 MΩ. A silver/silver chloride wire was used as reference electrode.

2.4.3. Electrophysiology apparatus

An Ag-AgCl recording wire was connected to an I-V converter amplifying headstage (CV 203BU Headstage, Axon Instruments), which was mounted on a Scientifica three-dimensional mechanical micromanipulator. The micromanipulator, as well as the inverted microscope, the recording chamber and the cells from which signals were recorded, were placed within a Faraday cage surrounding an anti-vibration table in order to minimise electrical and vibrational interference. To further reduce electrical

noise, all metallic apparatus and electronic instruments in use were electrically earthed.

Signals were amplified by an Axopatch amplifier (Axopatch 200, Axon Instruments) with filter cut-off at 5 kHz, digitised at 20 kHz and transmitted to a computer through a NIDAQ-MX interface (National Instruments), and visualised on the Windows Whole-Cell Patch (WinWCP, for whole-cell patch-clamp, version v5.0.3) or Windows Electrophysiology Disk Recorder (WinEDR, for single-channel patch-clamp, version v3.6.0) software (Dr John Dempster, University of Strathclyde).

2.4.4. Patch-clamp methodology

2.4.4.1. Single-channel patch-clamp

Cells were cultured for 1-7 days on 16 mm circular glass coverslips at seeding densities of 3,000 cells. Cultures were inspected by microscope before use to check they were healthy-looking and not confluent. Coverslips were washed in filtered sodium “Locke” extracellular solution before being transferred to a recording chamber, using a small amount of petroleum jelly to hold them in place. A few drops of filtered sodium “Locke” solution were then gently added onto the coverslip to form a convex meniscus of solution. The recording chamber was then transferred to the stage of the microscope, and the reference electrode tip was placed into solution. At 200x magnification, a cell was chosen to patch-clamp that was phase-bright, agranular and preferably not in contact with another cell.

A recording electrode was backfilled using a Microfil 34G fused-silica syringe needle with filtered High K⁺ intracellular solution, then threaded over the Ag-AgCl wire and sealed into place. The electrode tip was advanced into the solution covering the cells using the micromanipulator, and positive pressure was applied inside the electrode to prevent the aggregation of debris on the tip. Junction potential was adjusted to zero using the pipette offset on the amplifier. A 20 mV DC oscillating square-wave pulse (seal test) was applied via the WinEDR software across the electrode tip to determine electrode resistance from the current amplitude measured by the amplifier. The recording electrode tip was then advanced gently towards the cell. The microscope light was then switched off to avoid creating background noise and contact between the recording electrode tip and the cell was seen by an increase in electrical resistance in the seal test. Positive pressure was removed and negative pressure was gently applied to form a seal. When seal resistance increased slowly, negative voltages (-20 mV to -60

mV) were applied to help with seal formation. Seals with electrical resistance in the giga-Ohm range (a giga-seal) were typically achieved in a few seconds or a few minutes. Recordings were begun soon after at room temperature (around 20°C). Coverslips were discarded after one or two hours because the cells began to look unhealthy (figure 2.2).

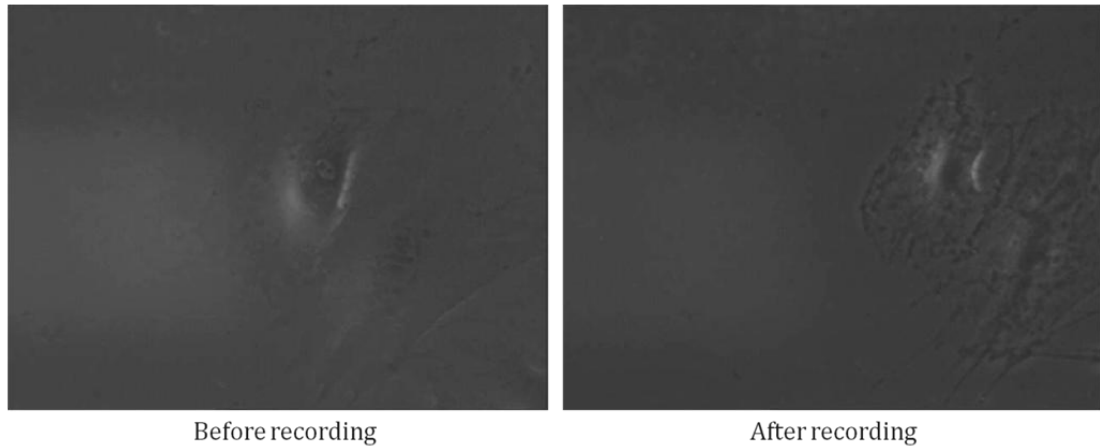


Figure 2.3: Example of 7F2 cells before and after recording

Cells began to look unhealthy after one or two hours of recording.

2.4.4.2. Perforated patch-clamp

The perforated patch-clamp technique was used to record from whole cells (Lippiat, 2009; Ishibashi *et al.*, 2012; Linley, 2013). A 40 mg/ml stock solution of Amphotericin B was prepared in distilled water and frozen up to 5 days; when used, it was kept on ice and away from light as Amphotericin B is light-sensitive (Lippiat, 2009). Cells were seeded on 16 mm circular glass coverslips and prepared for recording as described above.

The tip of the recording electrode was dipped into a High K⁺ intracellular solution to fill the very tip with solution free of Amphotericin, which can prevent seal formation. Then the electrode was backfilled with High K⁺ intracellular solution containing various concentrations of Amphotericin B (ranging from 200 to 400 µg/ml) and threaded over the Ag-AgCl wire. A giga-seal was formed as described above, except that a 5 mV instead of 20 mV DC oscillating square-wave pulse (seal test) was applied across the electrode tip (Linley, 2013) to determine to electrode resistance. Ideal electrode resistances were between 2 and 4 MΩ (Linley, 2013). After seal formation, a voltage of -70 mV was applied for 5 minutes to help get a perforated patch configuration (Linley, 2013).

2.4.5. Data acquisition and analysis

For cell-attached patches, recordings of thirty seconds and between ± 150 mV were made onto the hard-disk of a PC and saved as WCP or EDR files, using WinWCP (v5.0.3) or WinEDR (v3.6.0) softwares. Data were regularly saved to another PC for analysis and as back-up copies.

Chapter 3 – Protocol optimisation for the differentiation of murine 7F2 osteoblast-like cells into adipocytes

3.1. Introduction

3.1.1. *In vitro* differentiation into adipocytes

There are various published protocols to induce adipogenic differentiation *in vitro*. MSCs and preadipocytes can be differentiated into mature adipocytes when treated with a cocktail of adipogenic chemical stimuli such as dexamethasone, isobutylmethylxanthine (IBMX), insulin, indomethacin, or hydrocortisone (Scott *et al.*, 2011; Hemmingsen *et al.*, 2013). There is a lack of standardisation for *in vitro* adipogenic differentiation, even for established cell lines such as 3T3-L1 preadipocytes. To differentiate these preadipocytes, three ingredients are commonly used – dexamethasone, IBMX and insulin, but concentrations for each vary considerably (Scott *et al.*, 2011). These three components are also often used to differentiate mouse and human BMSCs, again with a great variety between the protocols; some of which only use one or two drugs to promote adipogenic differentiation (Scott *et al.*, 2011).

The 7F2 cell line was derived from the bone marrow of p53^{-/-} mice by Thompson *et al.* (1998). These cells are considered to be osteoblastic as they express ALP, secrete type I collagen and osteocalcin, and mineralise after 4-7 days of incubation with alpha modified essential medium (α -MEM) supplemented with 10 mM β -glycerophosphate and 50 μ g/ml ascorbic acid. However, these clones can be induced to differentiate into adipocytes when cultured with adipogenic medium. This is accompanied by the complete loss of expression of all osteoblastic markers except ALP. The adipogenic medium used by Thompson *et al.* was derived from a protocol originally published by Dorheim *et al.*, which contained 0.5 mM IBMX, 0.5 μ M hydrocortisone and 50 μ M indomethacin (Dorheim *et al.*, 1993); using instead 50 μ M indomethacin, 0.1 μ M dexamethasone and 50 μ g/ml ascorbic acid, which was found to accelerate the conversion to fat (Thompson *et al.*, 1998).

Indomethacin is a non-specific cyclooxygenase (COX) inhibitor and a non-steroidal anti-inflammatory drug (NSAID). NSAIDs, and in particular indomethacin, have been shown to promote adipogenesis and decrease osteogenesis. Styner *et al.* showed that indomethacin stimulated the adipogenic differentiation of both murine embryonic pluripotent cells and marrow-derived MSCs (Styner *et al.*, 2010): indomethacin induced adipocyte protein 2 (aP2) and adiponectin production, as well as the formation of lipid droplets; it promoted early adipogenesis, significantly upregulating PPAR γ 2 and C/EBP β expression. Indomethacin also suppressed prostaglandin E2 (PGE2), which is the principal product of COX2, and an anabolic agent that both promotes

Chapter 3 – Protocol optimisation for the differentiation of murine 7F2 osteoblast-like cells into adipocytes

osteoblastogenesis and decreases adipogenesis. However, it seemed that the effects of indomethacin were prostaglandin-independent, as adding PGE₂ did not reverse indomethacin-induced adipogenesis. This is in contrast with another study that showed that indomethacin increased the adipogenic differentiation of mouse embryonic fibroblasts, and that exogenous PGE₂ could reverse the effect of indomethacin (Inazumi *et al.*, 2011); PGE₂ signalling suppressed adipogenesis by inhibiting PPAR γ 2 expression in an autocrine manner.

Dexamethasone is an anti-inflammatory synthetic glucocorticoid, frequently used in the treatment of severe inflammatory diseases, such as rheumatoid arthritis or osteoarthritis (Shefrin and Goldman, 2009). Glucocorticoids signal via the glucocorticoid receptor which belongs to the steroid hormone receptor subclass of nuclear receptors. This receptor regulates gene expression as a dimer by binding to glucocorticoid responsive elements in the promoters of target genes, such as bone sialoprotein, osteocalcin, ALP, osteoprotegerin and type I collagen (Ogata *et al.*, 1995; Moutsatsou *et al.*, 2012). Many experimental and clinical studies report that glucocorticoids have many deleterious side effects in bone (Pereira *et al.*, 2002; Liu *et al.*, 2004; O'Brien *et al.*, 2004; Ohnaka *et al.*, 2005; Ton *et al.*, 2005; Wang *et al.*, 2005; Lane *et al.*, 2006; Swanson *et al.*, 2006; Ito *et al.*, 2007; Leclerc *et al.*, 2008; Koromila *et al.*, 2014; Briot and Roux, 2015). Dexamethasone has been shown to stimulate both osteogenic and adipogenic differentiation depending on the cell differentiation stage (Mikami *et al.*, 2011) and concentration of the drug (Ghali *et al.*, 2015). Several studies report that 10 nM dexamethasone inhibits proliferation of human MSCs, induces osteoblast commitment, maturation and extracellular matrix mineralisation (Cheng *et al.*, 1994; Siddappa *et al.*, 2007; Piek *et al.*, 2010); basal medium containing ascorbic acid and 10 nM dexamethasone increases ALP expression while decreasing BMP2 expression (Barradas *et al.*, 2012). On the contrary, others have shown that 10 nM dexamethasone stimulates adipogenesis in non-committed cells, but stimulates osteogenesis in cells already committed to the osteogenic lineage (Mikami *et al.*, 2011). When MSCs are exposed to dexamethasone for a prolonged period of time, or to an increased concentration of the drug (1 nM to 1 μ M), they yield higher numbers of adipocytes in cultures at the expense of osteoblasts (Yin *et al.*, 2006). Similarly, 100 nM – 1 μ M dexamethasone inhibits rat BMSC proliferation and promote adipogenesis and have time-dependent effects on osteoblastic marker expression, suppressing Runx2 and ALP expression in the early stage of differentiation, but increasing expression of ALP and osteopontin in the late stage (Song *et al.*, 2014). *In vivo*, administration of dexamethasone can induce osteoporosis in mice (Li *et al.*, 2013a; Zhang *et al.*, 2015). In

Chapter 3 – Protocol optimisation for the differentiation of murine 7F2 osteoblast-like cells into adipocytes

humans, it has been shown that long-term dexamethasone therapy is associated with bone loss, low BMD and increased fracture risk; dexamethasone-induced osteoporosis is accompanied by increased bone marrow adiposity (Staa *et al.*, 2002; Yao *et al.*, 2008; Weinstein, 2012).

In addition to the adipogenic medium components, other factors such as cell adhesion, cell shape or culture conditions also play an important role in regulating adipogenesis; for example, the number of passages and the cell seeding density are important parameters. Cell seeding density has been reported to affect several cell processes, such as proliferation and differentiation (Bitar *et al.*, 2008; Neuhuber *et al.*, 2008). For MSCs, higher densities enhance adipogenesis while lower densities favour osteogenesis under an adipogenic-osteogenic co-induction medium (McBeath *et al.*, 2004; Peng *et al.*, 2012). This may be due to the fact that cell spreading seems to promote osteogenesis; human MSCs cultured on larger islands of fibronectin differentiated along the osteogenic lineage, while human MSCs cultured on smaller islands differentiated into adipocytes (McBeath *et al.*, 2004). Ca^{2+} may play a role in regulating cell morphology; higher extracellular Ca^{2+} concentrations are associated with smaller nuclei and larger cytoskeletons, increasing the cell area and perimeter and promoting the osteogenic differentiation of human MSCs (Barradas *et al.*, 2012). Conventionally, cells are cultured to subconfluence before treatment with adipogenic medium, because this treatment inhibits cell proliferation (Murphy *et al.*, 2003; Mauney *et al.*, 2005); but it has also been reported that single-cell derived colonies of early passage human MSCs can differentiate into adipocytes (Sekiya *et al.*, 2004).

3.1.2. Chapter objectives and experimental strategies

The objective in this chapter was to optimise the protocol to differentiate 7F2 osteoblast-like cells into adipocytes, in order to test the effects of ghrelin or other pharmacological modulators on adipogenic differentiation in future experiments. Ideally, adipogenic differentiation should be efficient enough that a significant difference can be seen when comparing to 7F2 cells that were not induced to differentiate into adipocytes; but adipogenic differentiation should not be maximal, so that it will be possible in future experiments to detect a stimulatory effect of the tested pharmacological modulators (such as ghrelin) on adipogenesis.

7F2 cells were cultured with basal medium as a control, or with adipogenic medium to induce adipogenic differentiation. To optimise the protocol, the effects of several factors on adipogenesis were tested, including cell seeding density, length of treatment,

Chapter 3 – Protocol optimisation for the differentiation of murine 7F2 osteoblast-like cells into adipocytes

and addition of insulin to the adipogenic medium; the efficiency of adipogenic differentiation was assessed by Oil Red O staining, which stains lipids in red, to quantify the amount of lipid droplets inside the cells. To assess adipogenic differentiation in the final protocol, in addition to Oil Red O staining, RT-PCR and qRT-PCR analysis was used to investigate the expression of osteoblastic (Runx2, ALP and osteocalcin) and adipocytic (PPAR γ , C/EBP α , Glut4) markers.

3.2. Materials and Methods

3.2.1. Cell culture and adipogenic differentiation of 7F2 cells

7F2 cells were seeded and cultured as described in section 2.1. When testing the effects of the length of treatment on adipogenic differentiation, cells were seeded at a density of 5000 cells/cm². When testing the effects of insulin on adipogenic differentiation, 5 µg/ml insulin (Sigma) was added to adipogenic medium (described in section 2.1.2.1), and cells were seeded at a density of 5000 cells per cm².

3.2.2. Molecular biology

3.2.2.1. RNA extraction, DNase treatment and reverse transcription

See sections 2.3.1 and 2.3.2.

3.2.2.2. PCR

3.2.2.2.1. Oligonucleotide primers: house-keeping and differentiation marker genes

See sections 8.1.1 and 8.1.2.

3.2.2.2.2. PCR reaction compositions and conditions

The PCR reaction composition is described in section 2.3.3. The PCR reaction conditions were optimised and are detailed in table 3.1. Nuclease-free water was used as a negative control and three house-keeping genes, *Hprt1*, *Eef2* and *Gapdh*, were used as positive controls.

Chapter 3 – Protocol optimisation for the differentiation of murine 7F2 osteoblast-like cells into adipocytes

Hprt1, Pparg, and Gapdh primers:

Step	Temperature °C	Time	No. of cycles
Initial denaturation	95	1 min	1
Denaturation	95	30 s	
Annealing	58	30 s	30
Extension	68	30 s	
Final extension	68	5 min	1
Soak	4	Indefinite	

Eef2, Runx2, Alpl, and Cebpa primers:

Step	Temperature °C	Time	No. of cycles
Initial denaturation	95	1 min	1
Denaturation	95	30 s	
Annealing	58	30 s	35
Extension	68	30 s	
Final extension	68	5 min	1
Soak	4	Indefinite	

Glut4 primers:

Step	Temperature °C	Time	No. of cycles
Initial denaturation	95	1 min	1
Denaturation	95	30 s	
Annealing	56	30 s	40
Extension	68	30 s	
Final extension	68	5 min	1
Soak	4	Indefinite	

Osteocalcin primers (both sets):

Step	Temperature °C	Time	No. of cycles
Initial denaturation	95	1 min	1
Denaturation	95	30 s	
Annealing	58	30 s	40
Extension	68	30 s	
Final extension	68	5 min	1
Soak	4	Indefinite	

Table 3.1: PCR reaction conditions

3.2.2.3. Gel electrophoresis

See section 2.3.4.

3.2.2.4. Quantitative PCR

See section 2.3.5.

3.2.3. Statistical analysis

Statistical analysis was performed as described in section 2.3.7. Data were expressed as mean \pm standard deviation; the number of repeat assays is indicated by “n”. Two-sided Student’s t-tests (parametric), two-sided Wilcoxon tests and two-sided Welch’s t-tests (non-parametric) were used when basal medium was compared with adipogenic medium, i.e. when investigating the effects of the length of adipogenic treatment, the effects of seeding density (when comparing matching seeding densities), and when assessing the final adipogenic protocol (amount of Oil Red O stain and qRT-PCR analysis). Kruskal-Wallis tests (with Dunn post-hoc analysis) and Welch’s anova (with Games-Howell post-hoc analysis) were used when investigating the effects of seeding density (comparing the amount of Oil Red O between the various seeding densities in basal or adipogenic medium) and the effects of insulin. P values lower than 0.05 were considered as statistically significant. The calculations were performed using the R software (<https://www.r-project.org/>, version 3.5.3).

3.3. Results

3.3.1. Length of treatment

To determine the length of treatment that would allow a difference to be detected between cells cultured with basal medium and cells cultured with adipogenic medium, 7F2 cells were seeded on 12-well plates and cultured for 2, 4 or 7 days, then stained with Oil Red O. Photographs were taken daily at 200x magnification under a microscope; figure 3.1.A shows photographs of 7F2 cells after 2, 4 or 7 days, before and after Oil Red O staining. Oil Red O was extracted and quantified by measuring the absorbance at 490 nm with a spectrophotometer (figure 3.1.B). Lipid droplets were already visible after 2 days of culture with adipogenic medium but were too small to cause a significant difference in the amount of Oil Red O ($p = 0.661$; two-sided Student's t-test; $n = 1$ with 3 replicates per condition); the mean absorbance was quite high in both conditions (> 0.15) despite the absence of large lipid droplets, due to the presence of extracellular Oil Red O crystals. At 4 and 7 days, the amount of Oil Red O was higher in the wells of cells cultured with adipogenic medium compared with basal medium, although the difference was not statistically significant (day 4: $p = 0.114$ and day 7: $p = 0.058$; two-sided Student's t-test, $n = 1$ with 3 replicates per condition).

3.3.2. Seeding density has a strong effect on adipogenic trans-differentiation

7F2 cells were seeded at four different densities: 2500, 5000, 7500 or 10 000 cells/cm². Figure 3.2.A shows pictures of cells after 2, 4 and 7 days of adipogenic treatment. After 2 days of culture, multiple small lipid droplets could be seen in several cells in the wells with seeding densities of 7500 and 10 000 cells/cm² while being relatively rare in wells with seeding densities of 2500 and 5000 cells/cm². The amount and size of lipid droplets seemed to increase more rapidly in higher seeding densities, particularly at 7500 and 10 000 cells/cm², during the rest of the treatment. Oil Red O staining showed the presence of large lipid droplets inside the cells, particularly at higher densities (figure 3.2.B). There was no significant difference in the amount of Oil Red O in cells cultured with basal medium between the various seeding densities ($p = 0.3829$, $n = 2$, 3 replicates per condition, Kruskal-Wallis and Dunn tests). The amount of ORO increased with higher seeding density when the cells were cultured with adipogenic medium, but this increase was not statistically significant ($p = 0.2756$, $n = 2$, Kruskal-Wallis and Dunn tests) (figure 3.2.C). For identical cell seeding densities, the amount of Oil Red O was significantly higher in adipogenic medium compared with basal medium for 2500 cells/cm² ($p = 0.038$, $n = 2$, two-sided Student's t-test); 7500 cells/cm² ($p = 0.015$, $n = 2$,

Chapter 3 – Protocol optimisation for the differentiation of murine 7F2 osteoblast-like cells into adipocytes

two-sided Wilcoxon test); and 10000 cells/cm² ($p = 0.013$, $n = 2$, two-sided Wilcoxon test) (figure 3.2.D).

When the cells were not well distributed within the wells – thus creating areas of higher cell density and areas of lower cell density – the efficiency of adipogenic differentiation varied greatly (figure 3.2.E). In areas where cell density was higher from the beginning of the treatment, lipid droplets appeared sooner and increased in size and number more rapidly than in the rest of the well, regardless of the number of cells over the whole well.

3.3.3. Insulin failed to further stimulate adipogenic trans-differentiation

Among the various adipogenic cocktails that can be found in the literature, some contain insulin to help promote and maintain adipocyte proliferation and differentiation (Scott *et al.*, 2011). Therefore, the effect of insulin on adipogenic differentiation of 7F2 cells was tested. 7F2 cells were cultured with basal medium (BM), adipogenic medium (AM), or adipogenic medium with 5 µg/ml insulin (AM + Ins) (Molchadsky *et al.*, 2013; Zhang *et al.*, 2013; Bozec and Hannemann, 2016; Meyer *et al.*, 2016) (figure 3.3). Photographs were taken daily to monitor the emergence of lipid droplets at 200x magnification under a microscope; figure 3.3.A shows photographs taken after 3, 5 and 7 days of culture. Lipid droplets began to appear at day 2-3 of culture in the cells cultured with adipogenic medium in the presence and in the absence of insulin. The cells were stained using Oil Red O after 7 days of culture (figure 3.3.B). There was no visible difference in the size and number of lipid droplets in cells cultured with adipogenic medium in presence or in absence of insulin. The amount of Oil Red O was lower by 24% in cells cultured with adipogenic medium + insulin compared with adipogenic medium alone but the difference was not statistically significant ($p = 0.4$, $n = 6$, 2-3 replicates per condition, Kruskal-Wallis test and Dunn post-hoc analysis) (figures 3.3.C and D).

3.3.4. Adipogenic treatment: final protocol

3.3.4.1. Adipogenic treatment increases lipid content and decreases cell number

7F2 cells were seeded at 2500 cells/cm² and cultured for 7 days with basal or adipogenic medium. Figure 3.4.A shows photographs of 7F2 at days 2, 4 and 7 of culture. Adipogenic treatment induced the apparition of small lipid droplets after 2 days of culture; these droplets increased in size and number as the treatment continued. No lipid droplet was observed in cells cultured with basal medium. These observations were confirmed by Oil Red O staining (figure 3.4.B) and quantification of

Chapter 3 – Protocol optimisation for the differentiation of murine 7F2 osteoblast-like cells into adipocytes

staining (figure 3.4.C): the amount of Oil Red O staining was significantly higher in wells treated with adipogenic medium (0.17 ± 0.14) compared with basal medium (0.07 ± 0.05 ; $p = 0.02$, $n = 17$; two-sided Welch's t-test). This was also the case when Oil Red O quantification was normalised to basal medium for each repeat ($p = 0.0003$, $n = 17$; two-sided Welch's t-test): the amount of Oil Red O was 135% higher in cells cultured with adipogenic medium compared to cells cultured with basal medium. After 7 days of culture, the number of cells was 80% lower in wells cultured with adipogenic medium compared with basal medium ($p < 0.0001$, $n = 5$; two-sided Welch's t-test) (figure 3.4.D).

3.3.4.2. mRNA expression levels of adipogenic markers increase while mRNA expression levels of osteoblastic markers decrease

To confirm that 7F2 cells differentiated into adipocytes, the mRNA expression of several adipocytic markers – PPAR γ , C/EBP α , and Glut4, which is a target of C/EBP α (Moseti *et al.*, 2016) – as well as several osteoblastic markers – osteocalcin, Runx2, and ALP – were analysed by RT-PCR (figure 3.5.A). A band of the expected size was detected for each differentiation marker. When 7F2 cells were treated with adipogenic medium, the bands corresponding to the PCR products of two adipocytic markers, PPAR γ and C/EBP α , seemed to be more intense; Glut4 mRNA was barely detected in 7F2 cells cultured with basal medium but it was much more visible for cells treated with adipogenic medium. On the contrary, the band corresponding to the osteoblastic marker Runx2 PCR product seemed to be less intense for 7F2 cells cultured with adipogenic medium compared to cells cultured with basal medium. The bands corresponding to osteocalcin PCR products were faint (figure 3.5.A). The reverse primer of the first set of primers was located in intron 3, which can be retained in the mRNA (GenBank: BC069910.1) (Mammalian Gene Collection (MGC) Program Team, 2002). Another reverse primer located in exon 4 was designed (figure 3.5.B); the band corresponding to the expected size (178 bp, with no intron retention) was more intense in cells treated with basal medium compared with adipogenic medium. Another faint band of ~ 450 bp was observed; it seemed to correspond to the band that was detected using the first set of primers and that retains intron 3.

The mRNA expression of differentiation markers was also analysed by quantitative PCR (figures 3.5.C and D). PPAR γ mRNA expression was significantly higher in cells cultured with adipogenic medium (fold change = 5.46 ± 0.22) compared to cells cultured with basal medium ($p = 0.024$, $n = 2$, two-sided Welch's t-test). Similarly, C/EBP α mRNA

Chapter 3 – Protocol optimisation for the differentiation of murine 7F2 osteoblast-like cells into adipocytes

expression was higher in cells cultured with adipogenic medium (fold change = 25.3 ± 0.21) compared to cells cultured with basal medium ($p = 0.0048$, $n = 2$, two-sided Welch's t-test). The mRNA expression of the osteoblastic markers was not significantly lower in cells treated with adipogenic medium.

Figure 3.6 shows PCR data with no RT controls. No RT controls were not available for all samples. No band was observed in these gels, except very faint bands that correspond to probable dimers of primers (< 100 bp).

3.4. Discussion

3.4.1. Adipogenic differentiation of 7F2 cells

The aim of this chapter was to optimise the protocol to differentiate 7F2 cells into adipocytes, in a way that would allow detecting either a stimulatory or an inhibitory effect of ghrelin or other pharmacological modulators in future experiments. Culturing the cells for 7 days, with a seeding density of 2500 cells/cm² and changing the medium every 2-3 days, seemed to trigger a relatively efficient adipogenic differentiation, while still leaving room for a possible stimulatory effect of ghrelin or other pharmacological modulators. Adipogenic medium induced the apparition of lipid droplets inside the cells, significantly upregulated the mRNA expression of several adipocytic markers (PPAR γ and C/EBP α) but did not significantly downregulate osteoblastic markers. Altogether, these results indicated that our model, the 7F2 cell line, reliably differentiated into adipocytes when cultured with dexamethasone and indomethacin.

The adipogenic medium used here was similar to the one used by the team that isolated 7F2 cells from p53^{-/-} mice (Thompson *et al.*, 1998), since it contained indomethacin and dexamethasone. However, it was not supplemented with ascorbic acid, which was reported to accelerate conversion to fat: ascorbic acid was already present in basal medium, at the same concentration as the one used by Thompson *et al.* (1998).

Oil Red O staining, while allowing lipid droplets to be detected by staining them in red, did not seem to be an accurate technique to detect small differences in the amount of lipid droplets; there were often many Oil Red O crystals (precipitates) in the wells, which created a high background noise. These crystals proved impossible to get rid of despite several washings; and they tended to accumulate even more when there were many cells in the wells, particularly in wells containing basal medium in comparison with adipogenic medium. Filtering the solution twice instead of once helped a little but there did not seem to be enough staining left, as the color of the stained lipid droplets was closer to orange/pale red than to the bright red usually observed. The older the solution, the more Oil Red O crystals there were, so a fresh solution was prepared for each staining assay.

The osteoblastic markers osteocalcin, Runx2 and ALP were still expressed in the cells cultured with adipogenic medium. This is probably due to the fact that the cells did not all differentiate into adipocytes; there were still many osteoblast-like cells, which looked fibroblastic with no visible lipid droplets. ALP expression did not seem to be

Chapter 3 – Protocol optimisation for the differentiation of murine 7F2 osteoblast-like cells into adipocytes

affected by adipogenic medium, which is consistent with the observations of Thompson *et al.* that the 7F2 cell-derived adipocytes did not lose ALP expression (Thompson *et al.*, 1998). Interestingly, two of the tested adipocytic markers were expressed at the mRNA levels in 7F2 cells cultured with basal medium, the adipogenic transcription factors PPAR γ and C/EBP α . However, Glut4, which is a target of C/EBP α (Moseti *et al.*, 2016), was barely detected in 7F2 cells cultured with basal medium. C/EBP α , despite being expressed at the mRNA level in these cells, may not be expressed at the protein level, or not at a high enough level to activate the transcription of Glut4.

3.4.2. Chapter conclusions

The objective of this chapter was to optimise the protocol to differentiate 7F2 cells into adipocytes, in a way that would allow detecting either a stimulatory or an inhibitory effect of ghrelin or other pharmacological modulators in future experiments. Optimum conditions for adipogenic differentiation which met the criteria for my experiments were an adipogenic medium containing dexamethasone and indomethacin, but without insulin, at a seeding density of 2500 cells/cm². Having optimised the protocol to differentiate 7F2 cells into adipocytes, the next step was to investigate whether these cells expressed genes from ghrelin signalling.

Chapter 3 – Protocol optimisation for the differentiation of murine 7F2 osteoblast-like cells into adipocytes

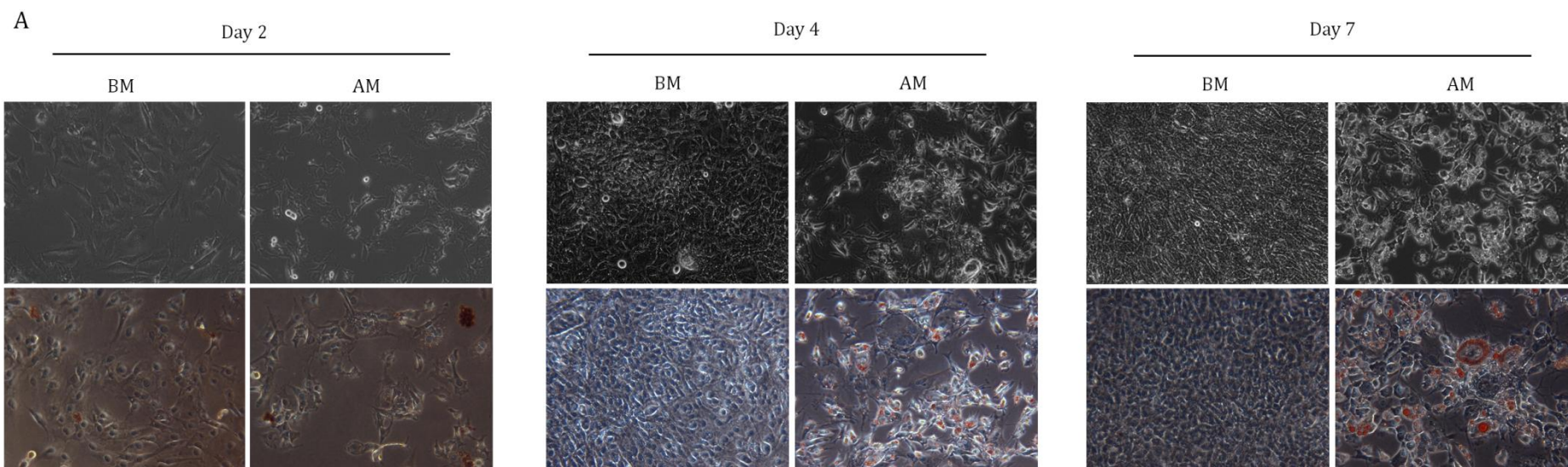


Figure 3.1: Oil Red O staining and quantification after 2, 4 and 7 days of treatment
(part 1)

7F2 cells were seeded on 12-well plates, cultured with basal (BM) or adipogenic medium (AM) for 2, 4 or 7 days, then stained with Oil Red O. A: Photographs taken before and after Oil Red O staining.

B

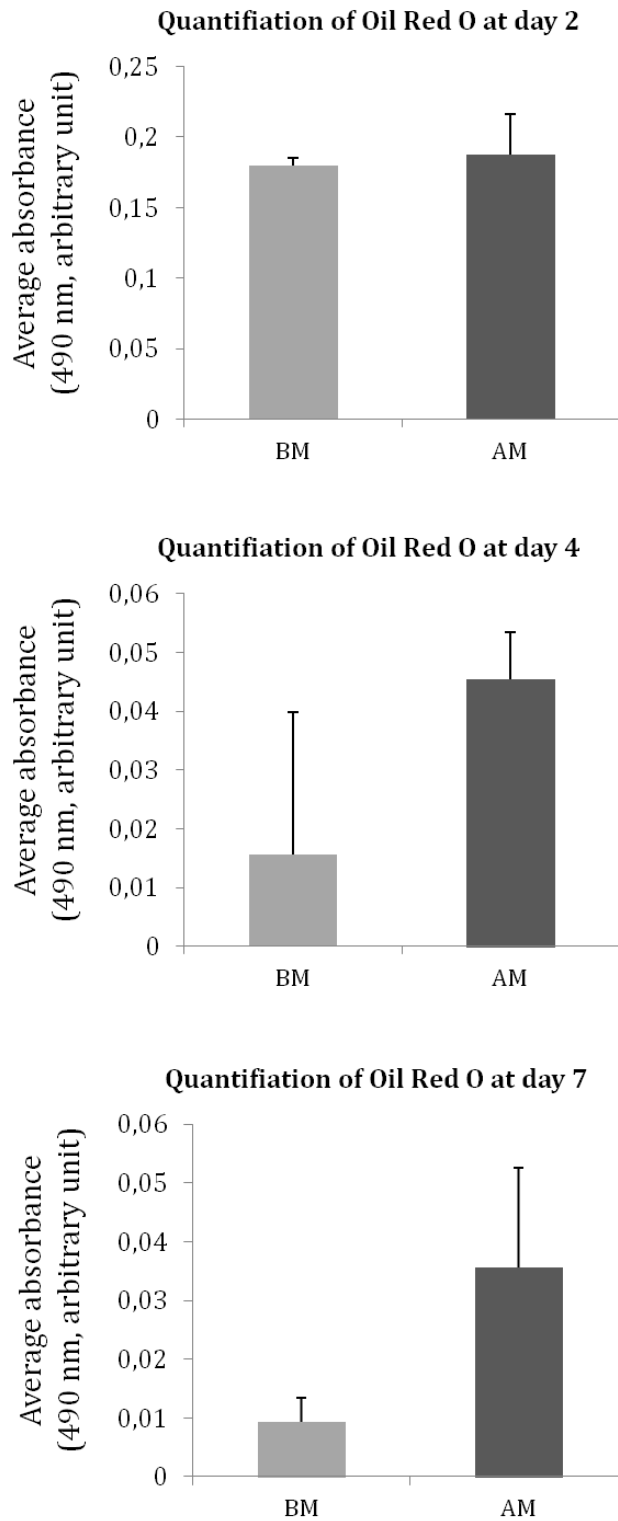


Figure 3.1: Oil Red O staining and quantification after 2, 4 and 7 days of treatment (part 2)

B: Quantification of Oil Red O by measuring the absorbance at 490 nm (n = 1 with 3 samples per condition; two-sided Student's t-tests); data are mean absorbance \pm SD.

Chapter 3 – Protocol optimisation for the differentiation of murine 7F2 osteoblast-like cells into adipocytes

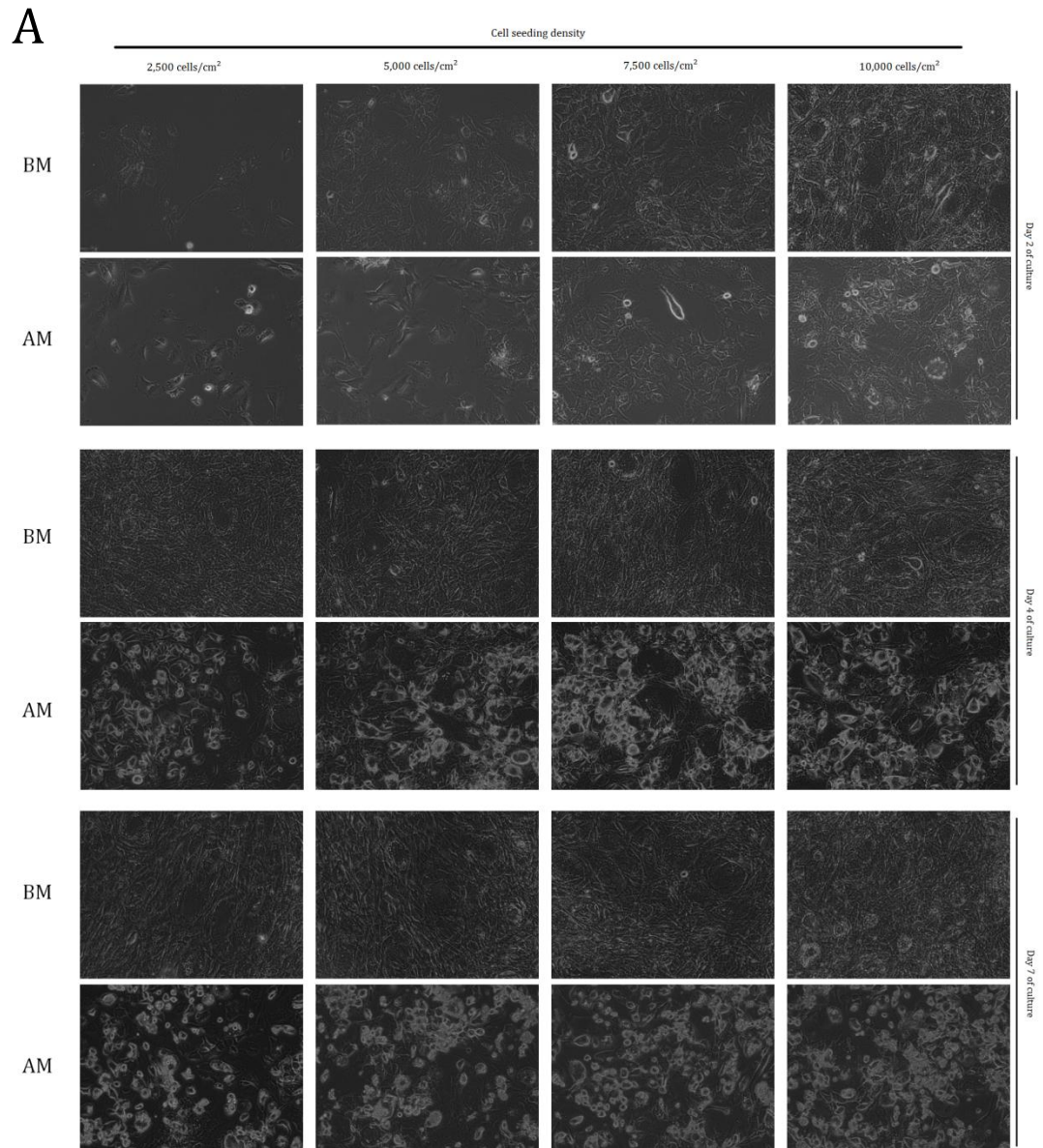


Figure 3.2: Effect of seeding density on the trans-differentiation of 7F2 cells (part 1)

7F2 cells were seeded at four different densities (2,500, 5,000, 7,500 and 10,000 cells/cm²) and cultured for 7 days with basal (BM) or adipogenic medium (AM). Photographs of the cells were taken daily at 200x magnification under a microscope; photographs after 2, 4 and 7 days are shown in A.

Chapter 3 – Protocol optimisation for the differentiation of murine 7F2 osteoblast-like cells into adipocytes

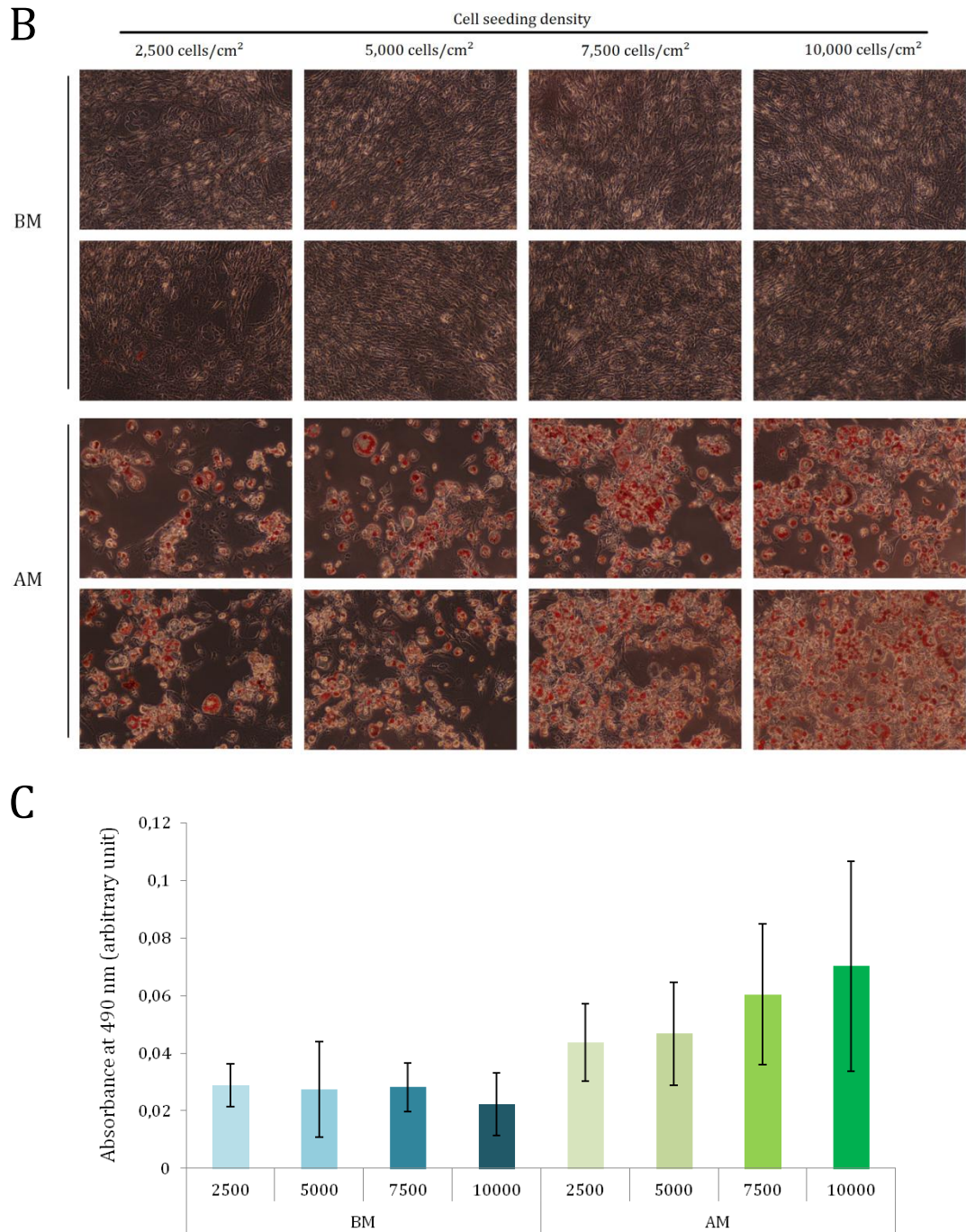


Figure 3.2: Effect of seeding density on the trans-differentiation of 7F2 cells (part 2)

B: Photographs of the cells stained with Oil Red O after 7 days of culture. C: Oil Red O was extracted and absorbance was measured with a spectrophotometer at 490 nm to quantify the amount of stain; the graph shows the mean absorbance for each culture media and seeding density \pm SD (n = 2, with 3 replicates per condition in each assay; Kruskal-Wallis tests and Dunn post-hoc analyses).

Chapter 3 – Protocol optimisation for the differentiation of murine 7F2 osteoblast-like cells into adipocytes

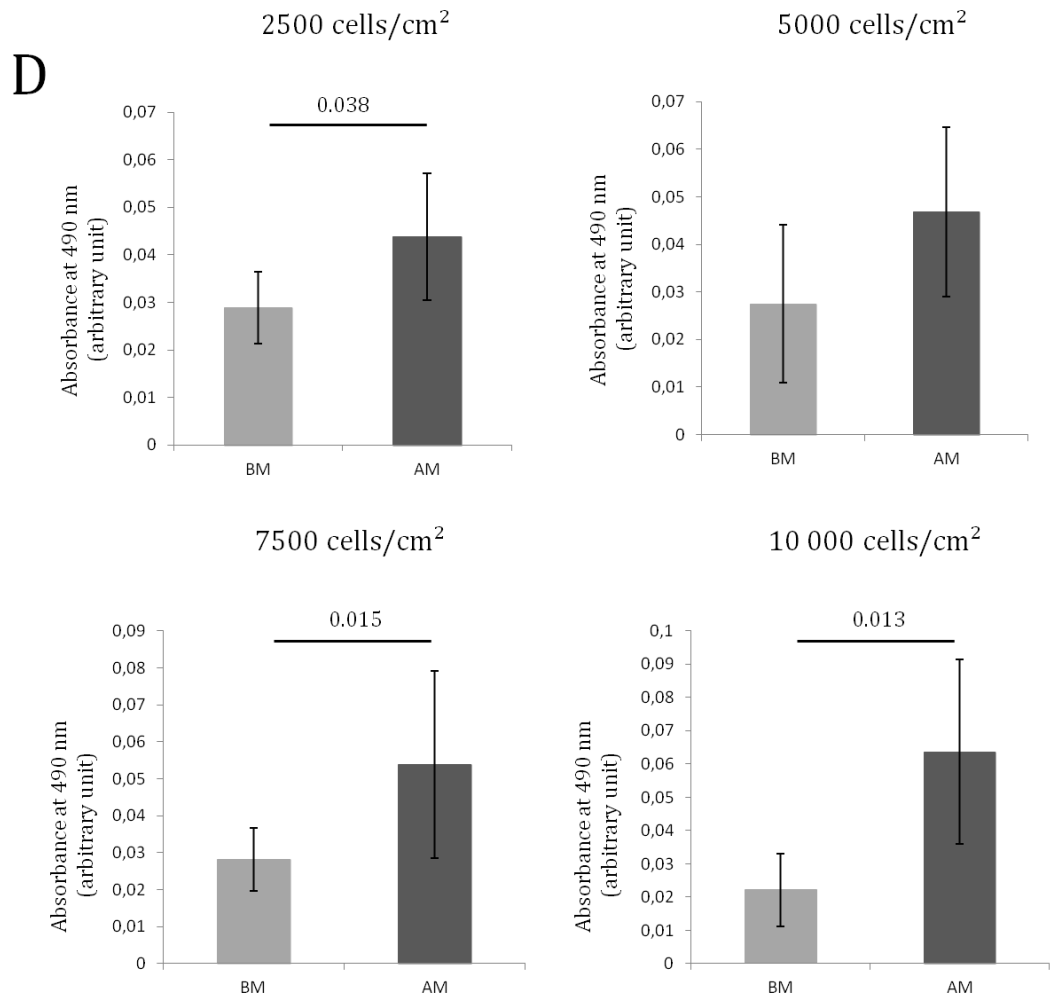


Figure 3.2: Effect of seeding density on the trans-differentiation of 7F2 cells (part 3)

D: Separate mean absorbance for each seeding density, comparing cells cultured with basal medium (BM) to cells cultured with adipogenic medium (AM) (n=2, with 3 replicates per condition in each assay; 2,500 cells/cm²: two-sided Student's t-test; 5,000 cells/cm², 7,500 cells/cm² and 10,000 cells/cm²: two-sided Wilcoxon tests).

Chapter 3 – Protocol optimisation for the differentiation of murine 7F2 osteoblast-like cells into adipocytes

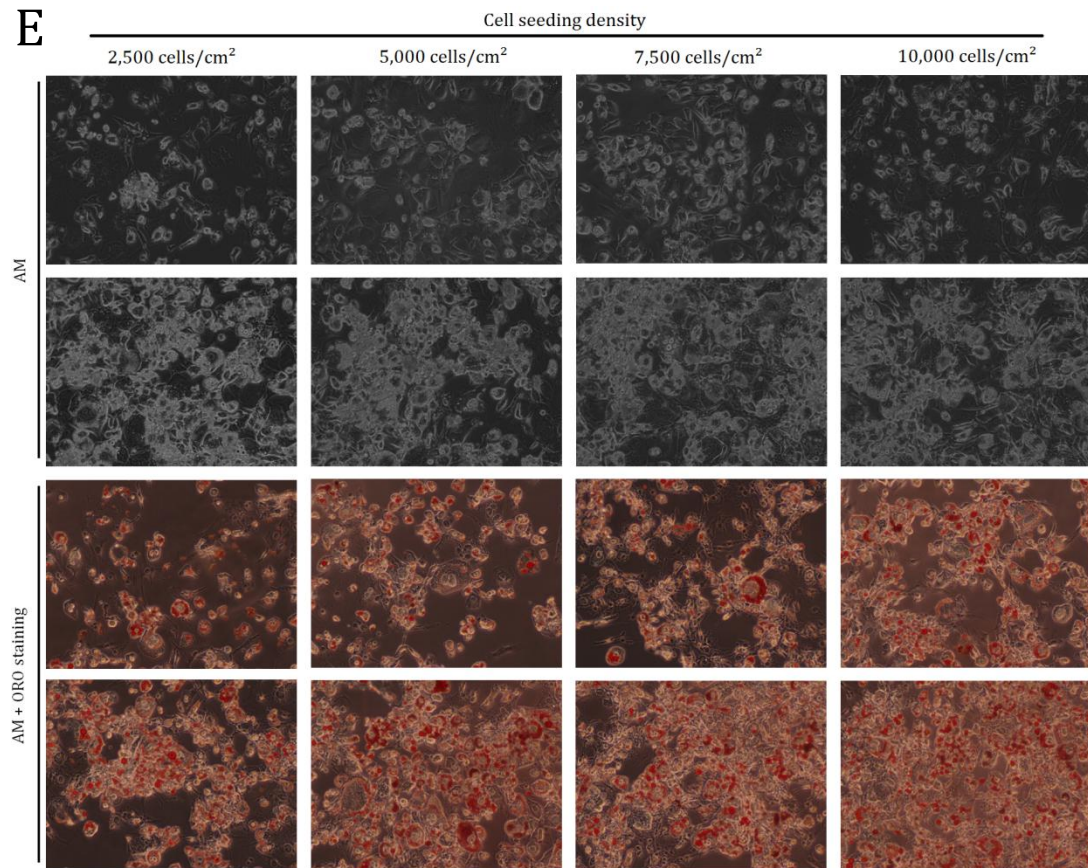


Figure 3.2: Effect of seeding density on the trans-differentiation of 7F2 cells (part 4)

E: Photographs showing the effect of local density within the wells, without and with Oil Red O staining. Cell density could vary greatly within the wells.

Chapter 3 – Protocol optimisation for the differentiation of murine 7F2 osteoblast-like cells into adipocytes

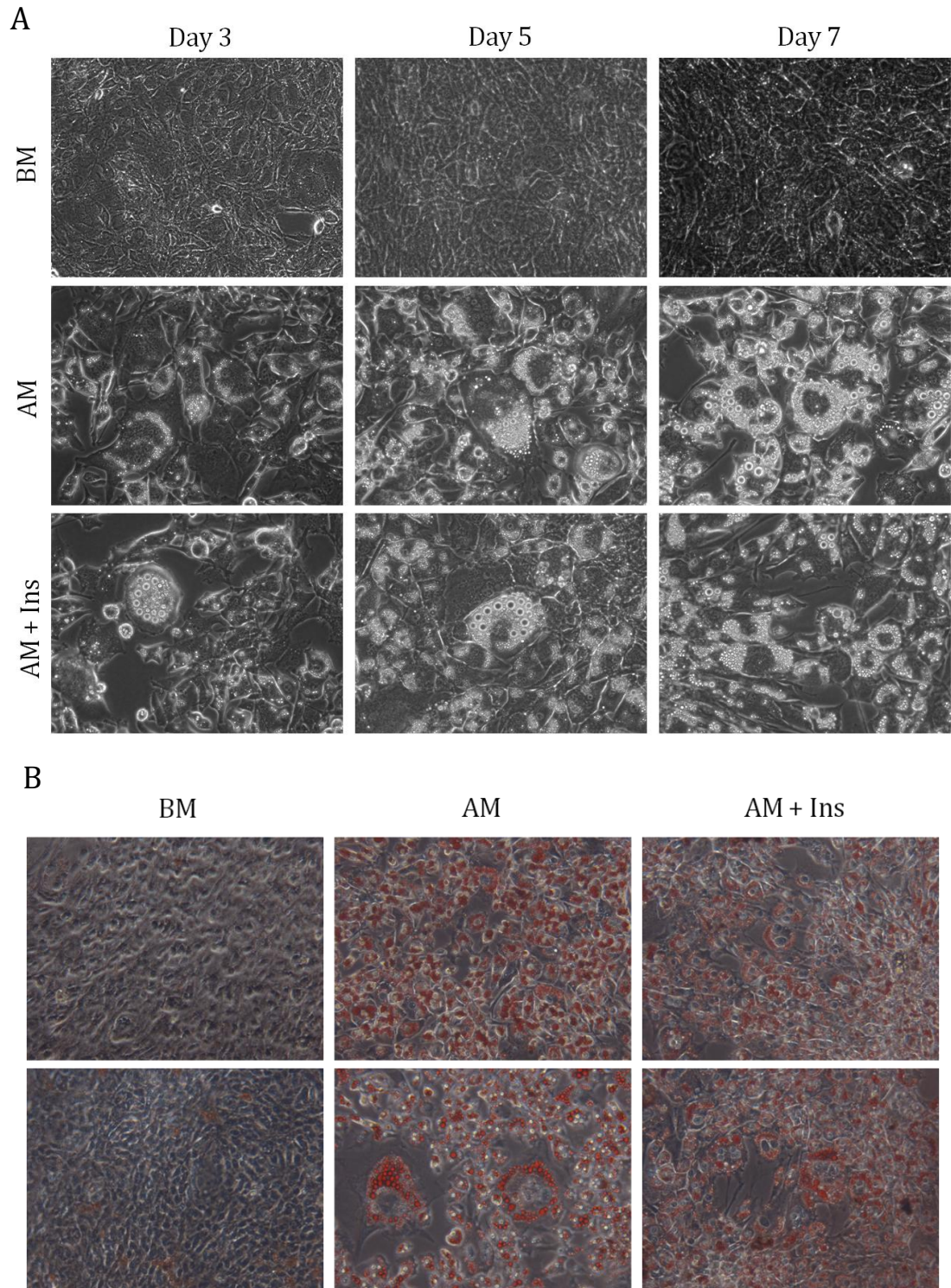


Figure 3.3: Effects of 5 $\mu\text{g}/\text{ml}$ insulin on adipogenic differentiation (part 1)

A: Photographs of 7F2 cells cultured with basal medium (BM), adipogenic medium (AM; containing dexamethasone and indomethacin), or adipogenic medium + 5 $\mu\text{g}/\text{ml}$ insulin (AM + Ins; containing dexamethasone, indomethacin and insulin), after 2, 4 and 7 days of culture. B: Photographs of 7F2 cells stained with Oil Red O after 7 days of culture with basal medium (BM), adipogenic medium (AM) or adipogenic medium + insulin (AM + Ins). Photographs were taken at 200x magnification.

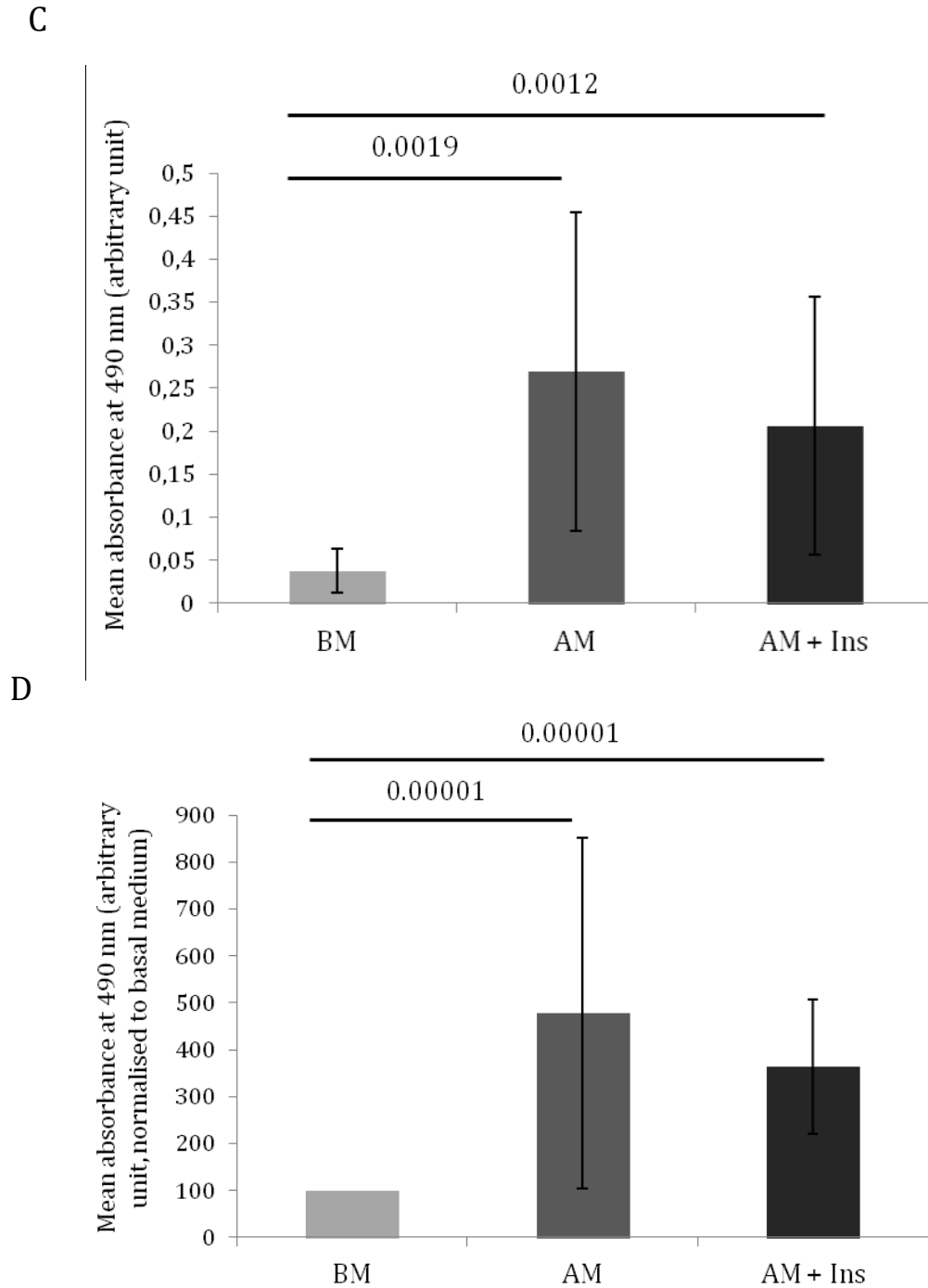


Figure 3.3: Effects of 5 $\mu\text{g}/\text{ml}$ insulin on adipogenic differentiation (part 2)

C: Quantification of Oil Red O staining by measuring the absorbance at 490 nm ($n = 6$; 2-3 replicate samples per condition for a total of 13 replicates per condition; Welch's anova and Games-Howell post-hoc analysis). D: Quantification of Oil Red O staining, normalised to basal medium ($n = 6$; 2-3 replicate samples per condition, for a total of 13 replicates per condition; Kruskal-Wallis test and Dunn post-hoc analysis). Data are mean absorbance \pm SD.

Chapter 3 – Protocol optimisation for the differentiation of murine 7F2 osteoblast-like cells into adipocytes

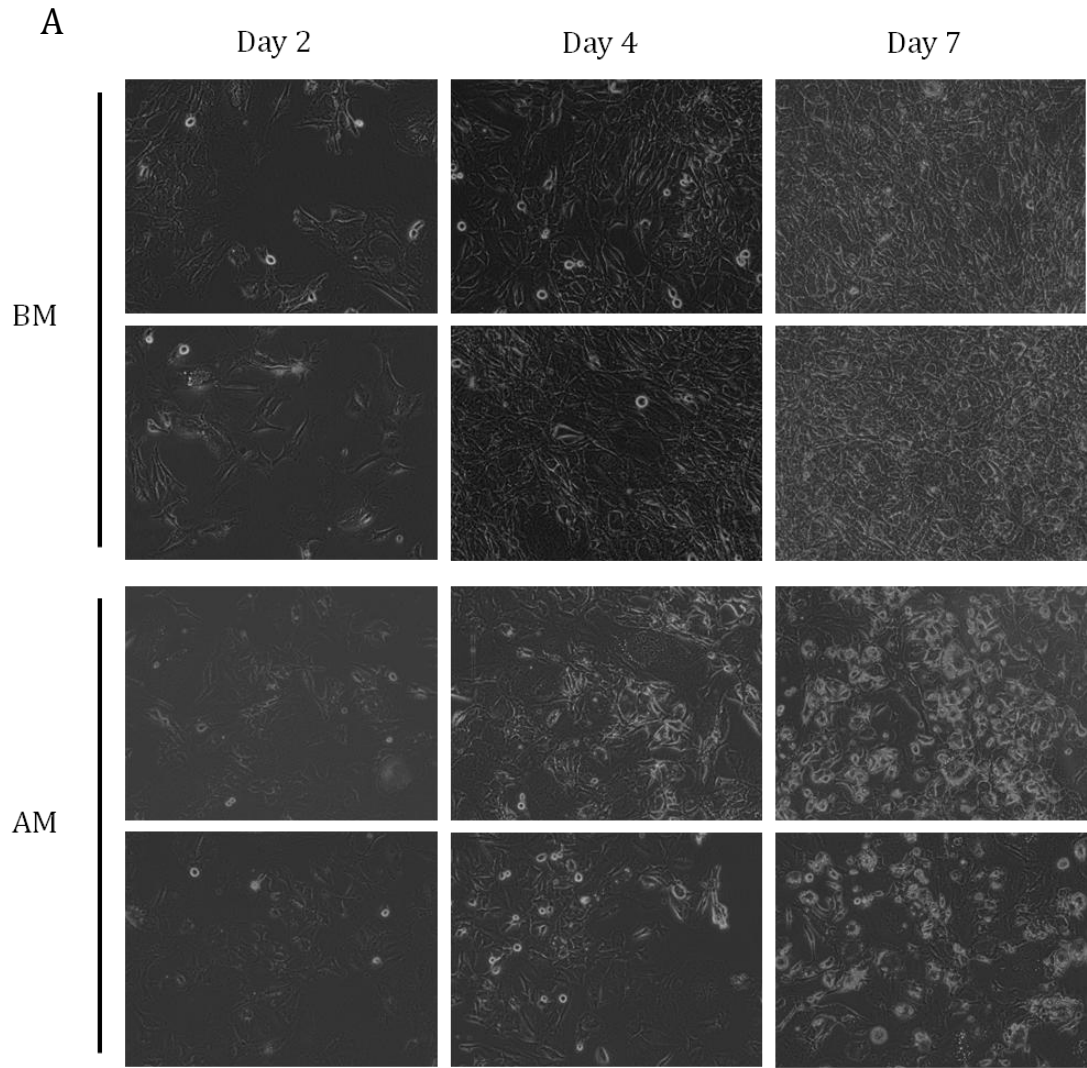
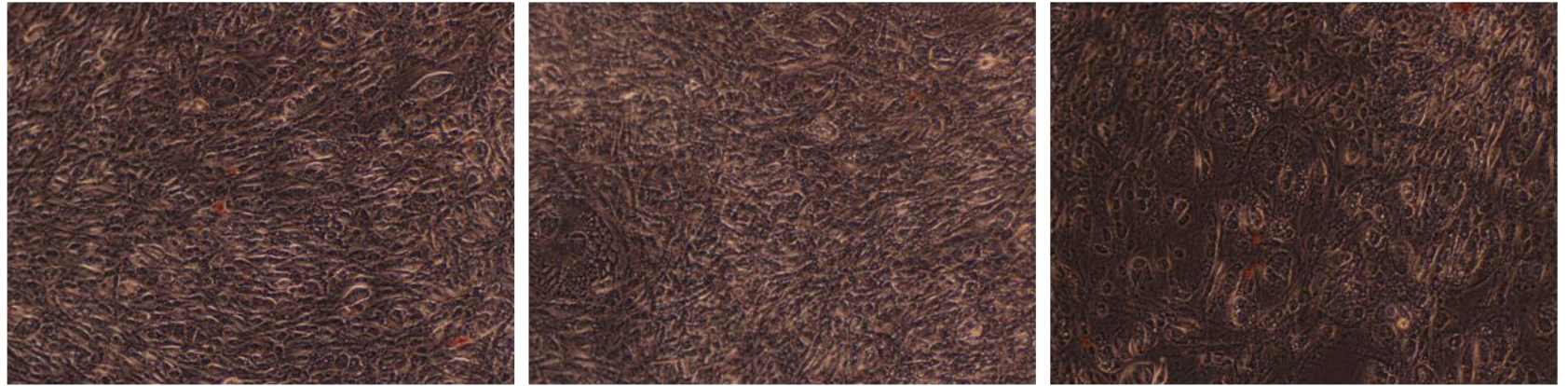


Figure 3.4: Effect of adipogenic treatment on 7F2 cell lipid content and cell number (part 1)

A: Photographs of 7F2 cells cultivated with basal medium (BM) or adipogenic medium (AM) at days 2, 4 and 7.

B

BM



AM

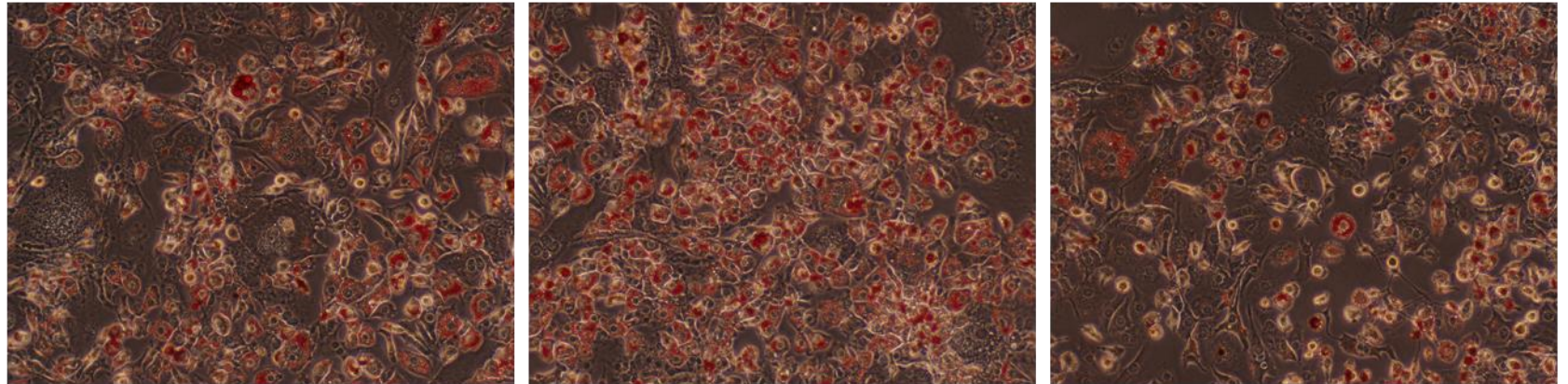


Figure 3.4: Effect of adipogenic treatment on 7F2 cell lipid content and cell number (part 2)

B: Photographs of 7F2 cells stained with Oil Red O after 7 days of culture with basal or adipogenic medium.

Chapter 3 – Protocol optimisation for the differentiation of murine 7F2 osteoblast-like cells into adipocytes

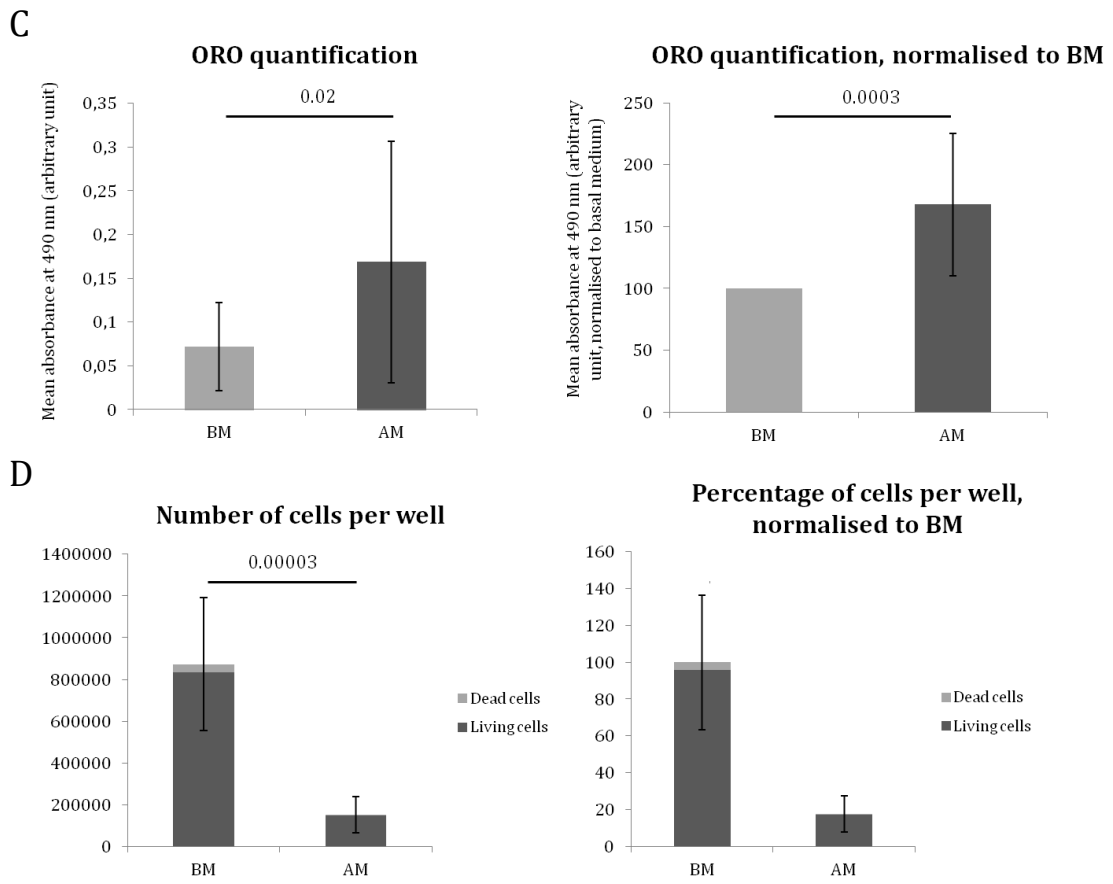


Figure 3.4: Effect of adipogenic treatment on 7F2 cell lipid content and cell number (part 3)

C: Quantification of Oil Red O staining by measuring the absorbance at 490 nm; raw data and data normalised to basal medium (n = 17, with 2-3 replicates per condition in each assay; two-sided Welch's t-tests). D: Number of cells cultivated with basal medium or adipogenic medium for 7 days; raw data and data normalised to basal medium (n = 5, with 1-2 replicate samples per condition in each assay; two-sided Welch's t-tests). Cells were counted using Trypan Blue. Data are mean absorbance or mean number of cells \pm SD.

Chapter 3 – Protocol optimisation for the differentiation of murine 7F2 osteoblast-like cells into adipocytes

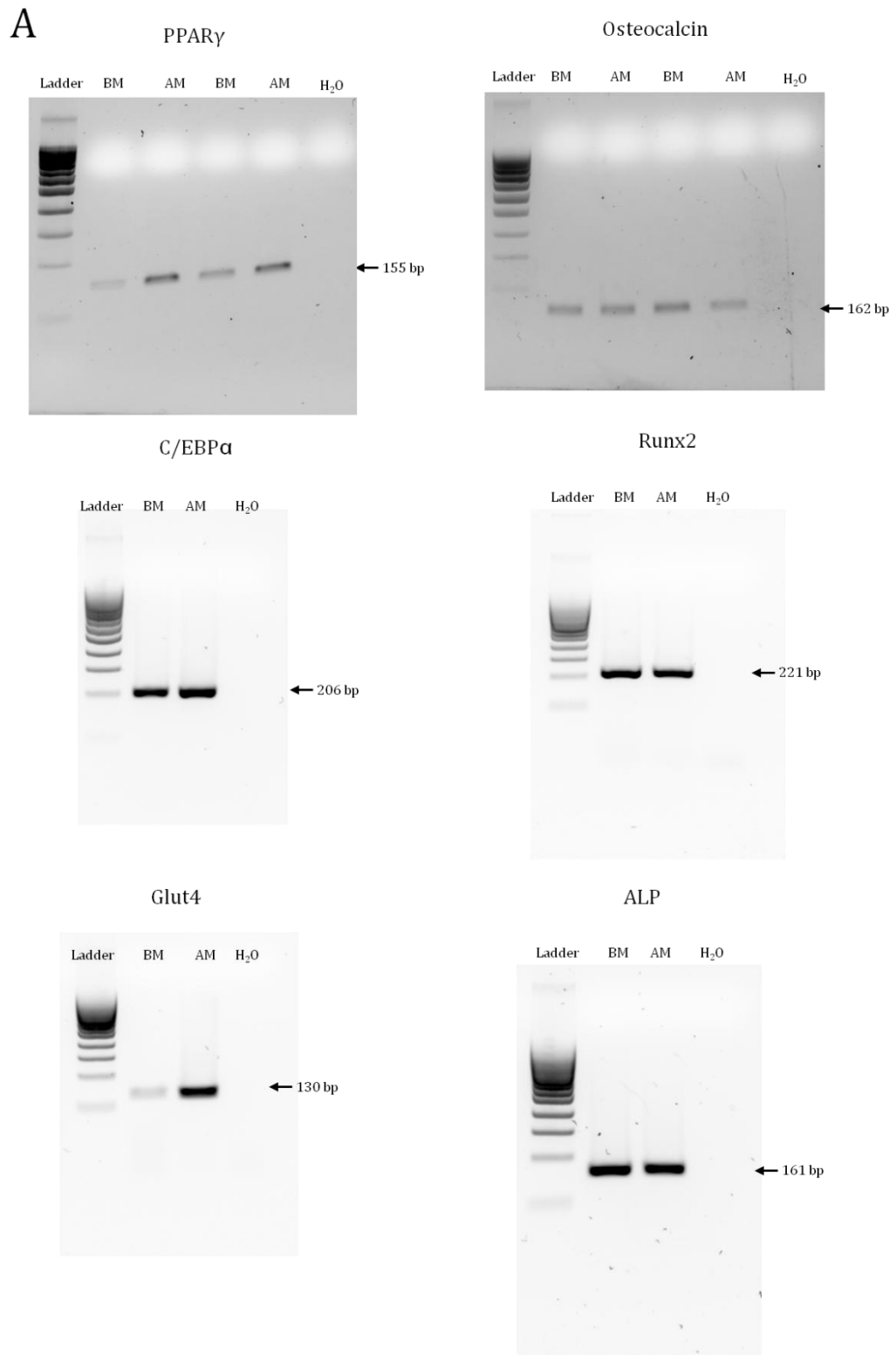


Figure 3.5: Effect of adipogenic medium on the mRNA expression of differentiation markers (part 1)

A: RT-PCR for PPAR γ , C/EBP α , Glut4 (adipocytic markers); osteocalcin (first set of primers), Runx2 and ALP (osteoblastic markers).

Chapter 3 – Protocol optimisation for the differentiation of murine 7F2 osteoblast-like cells into adipocytes

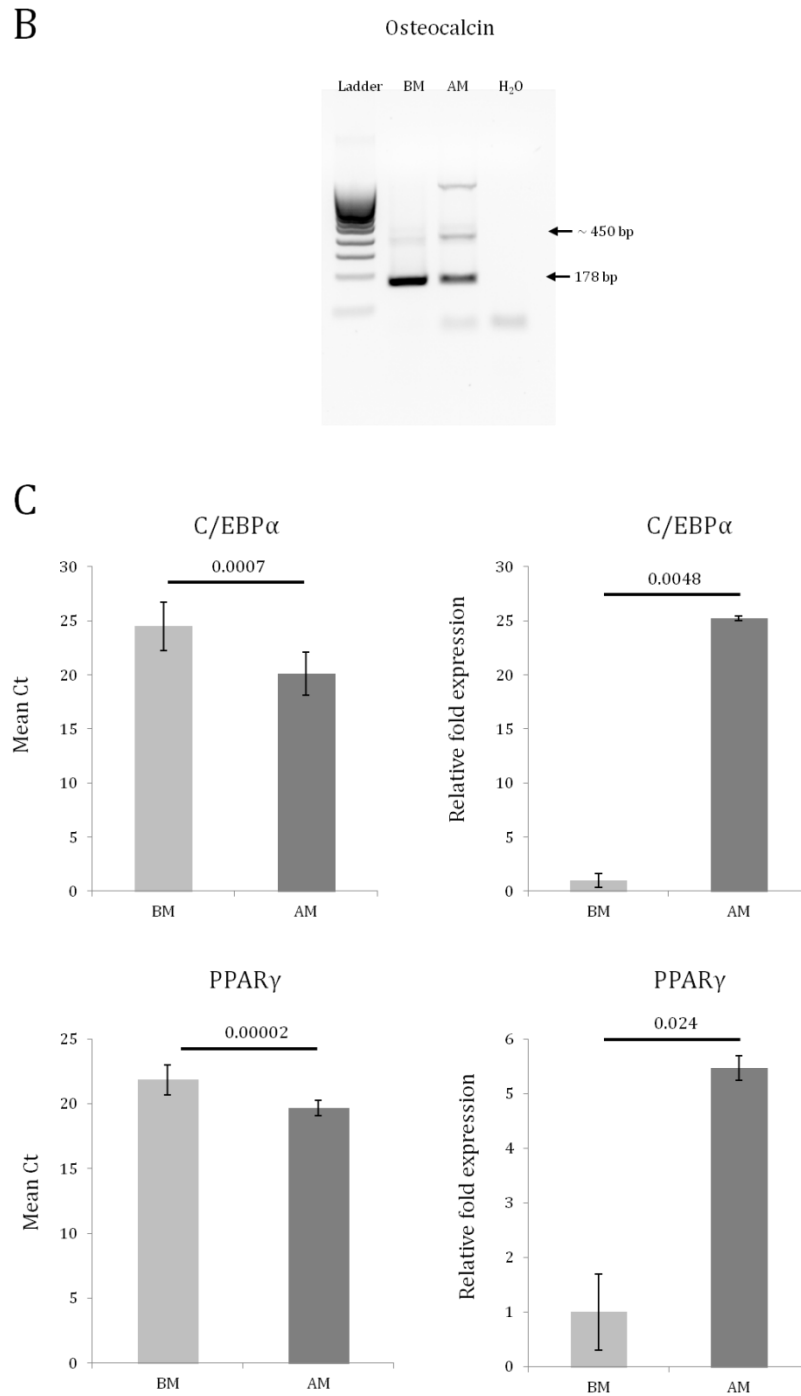


Figure 3.5: Effect of adipogenic medium on the mRNA expression of differentiation markers (part 2)

B: RT-PCR for osteocalcin (second set of primers). C: qRT-PCR data for C/EBP α and PPAR γ (n = 2, 3 replicate samples per condition in each assay; each sample was run in duplicate). Data are mean Ct \pm SD (left graphs; two-sided Wilcoxon test for C/EBP α ; two-sided Welch's t-test for PPAR γ), and fold change \pm SD (right graphs; two-sided Welch's t-tests); the relative fold expression was normalised by the reference gene EEF2. RNA was extracted from 7F2 cells cultured for 7 days with basal medium or with adipogenic medium.

Chapter 3 – Protocol optimisation for the differentiation of murine 7F2 osteoblast-like cells into adipocytes

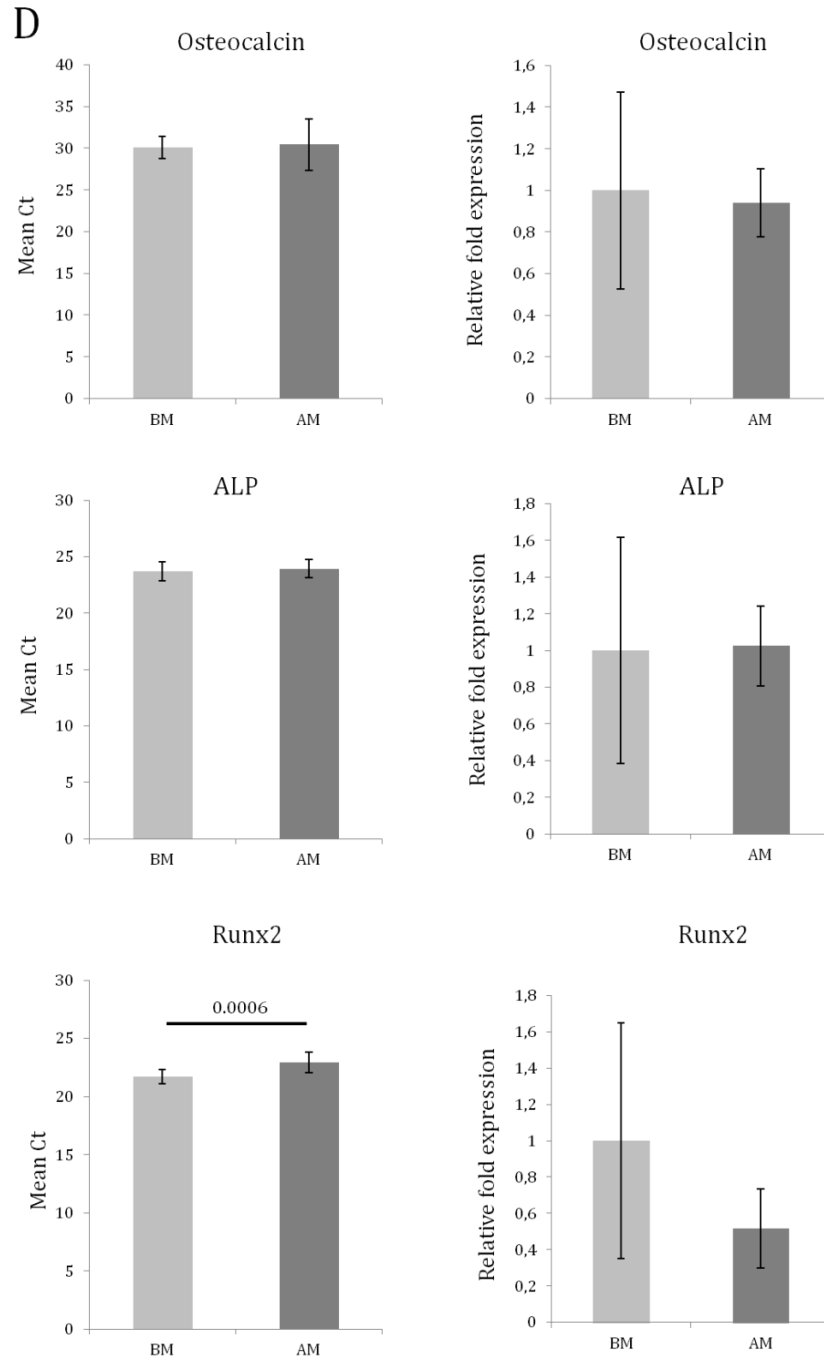


Figure 3.5: Effect of adipogenic medium on the mRNA expression of differentiation markers (part 3)

D: qRT-PCR for osteocalcin, Runx2 and ALP (n = 2, with 3 replicate samples per condition in each assay; each sample was run in duplicate). Data are mean Ct \pm SD in graphs on the left (two-sided Welch's t-test for osteocalcin, two-sided Student's t-test for Runx2 and two-sided Wilcoxon test for ALP), and fold change \pm SD in graphs on the right (two-sided Student's t-test for osteocalcin; two-sided Welch's t-tests for Runx2 and ALP); the relative fold expression was

Chapter 3 – Protocol optimisation for the differentiation of murine 7F2 osteoblast-like cells into adipocytes

normalised by the reference gene *EEF2*. RNA was extracted from 7F2 cells cultured for 7 days with basal medium or with adipogenic medium.

Chapter 3 – Protocol optimisation for the differentiation of murine 7F2 osteoblast-like cells into adipocytes

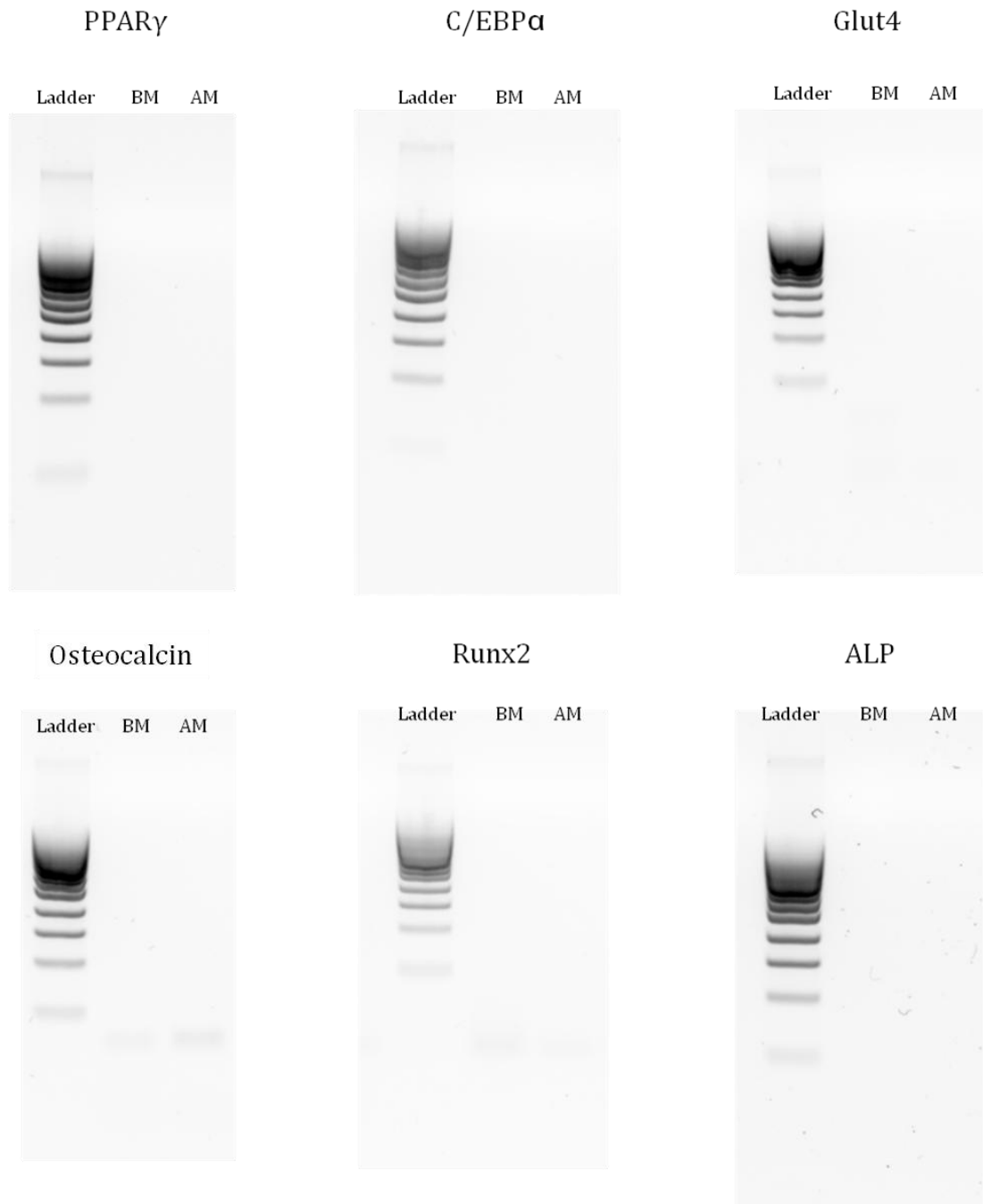


Figure 3.6: No RT controls for differentiation markers

RT-PCR for PPAR γ , C/EBP α , Glut4 (adipocytic markers); osteocalcin (first set of primers), Runx2 and ALP (osteoblastic markers) with no RT controls.

Chapter 4 – 7F2 osteoblast-like cells and 7F2 cell-derived adipocytes express *Ghsr*, *Mboat4* and several isoforms of *Ghrl*

4.1. Introduction

4.1.1. Ghrelin: one gene that encodes a variety of peptides

4.1.1.1. Structure of the ghrelin gene

The structure of the mouse ghrelin gene was described by Tanaka *et al.* (2001a) using ghrelin cDNA cloned from the stomach; it contains five exons (Ex1-Ex5) and four introns (In1-In4) (Tanaka *et al.*, 2001a). The first exon is short and contains only 19 bp, which encode part of the 5'UTR (untranslated region). Exons 2 to 5 encode preproghrelin which is 117 amino acid-long, which contains a 23-amino-acid signal peptide encoded by exon 2. The signal peptide is cleaved from preproghrelin, giving rise to proghrelin. Proghrelin is acylated, then transported to the Golgi (Zhu *et al.*, 2006), where it is cleaved to generate two peptides: 28-amino-acid mature ghrelin, encoded by exons 2 and 3; and 23-amino-acid obestatin, encoded by exon 4 and a few nucleotides from exon 5 (figure 4.1) (Kojima and Kangawa, 2005; Yang *et al.*, 2008). The enzyme PC1/3 (proprotein convertase, also called prohormone convertase) is required for the conversion of preproghrelin to mature ghrelin and obestatin; PC1/3 generates the C-terminus of mature ghrelin by cleaving after Arg28 of proghrelin (Zhu *et al.*, 2006). PC1/3 has been shown to be expressed in rats, in the pituitary, the hypothalamus (Nilni, 2007; Dong and Day, 2013) and the gastrointestinal tract (Macro *et al.*, 1996), which also produce ghrelin.

Ghrelin is extremely well conserved in mammals; ghrelin homologues have been identified in human, rhesus monkey, rat, mouse, Mongolian gerbil, cow, pig, sheep and dog. The sequences of the gene and its promoter are well conserved. In particular, the first 10 residues are identical in mammals, and the sequence of the mature peptide from rats and mice differs by two amino acids from human ghrelin (Davenport *et al.*, 2005; Kojima and Kangawa, 2005). The first five residues of mature ghrelin play a central role in the activity of the peptide, particularly the Ser3 residue which can be acylated; acylation is necessary for ghrelin to bind to its receptor GHSR1a in hypothalamus and pituitary, regulating GH secretion, food intake and energy stores (Kojima and Kangawa, 2005).

In humans, the ghrelin gene also contains five exons, named exon 0 to exon 4 (Ex0-Ex4), and four introns. The short first exon contains only 20 bp and encodes part of the 5'UTR. There are two different transcriptional initiation sites in the ghrelin gene; one at 80 bp and the other at 555 bp upstream of the ATG codon, giving rise to two distinct

Chapter 4 – 7F2 osteoblast-like cells and 7F2 cell-derived adipocytes express *Ghsr*, *Mboat4* and several isoforms of *Ghrl*

mRNA transcripts, transcript-A and transcript-B. Transcript-A, which is an alternative splicing product from exon 1 to exon 4, is the main form of human ghrelin mRNA *in vivo*; it is translated into 117-amino acid preproghrelin. 28-amino-acid ghrelin is encoded by exons 1 and 2. Exons 2, 3 and 4 encode for 66-amino-acid C-ghrelin (C-terminal peptide of ghrelin), which contains 23-amino-acid obestatin. Obestatin is entirely encoded by exon 3 (Seim *et al.*, 2007).

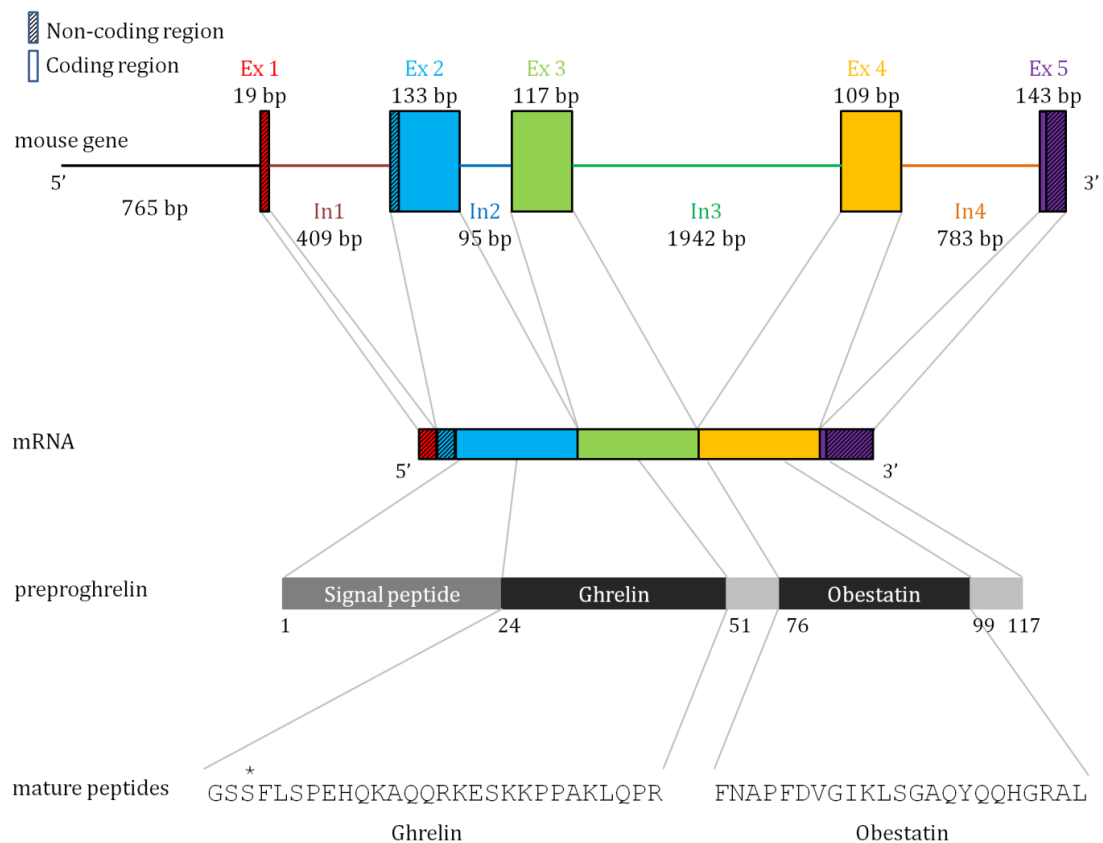


Figure 4.1: From the mouse ghrelin gene to mature peptide

Asterisk indicates the Ser3 residue acylated by Ghrelin *O*-acyltransferase (GOAT).

4.1.1.2. Alternative splicing of the ghrelin gene

Alternative splicing is a mechanism through which a single gene can give rise to multiple transcripts. It contributes significantly to protein diversity in humans and mice, generating multiple proteins that can play important roles in regulating physiological processes. Aberrant alternative splicing is often involved in pathophysiological processes, particularly in cancers, generating altered proteins that

promote carcinogenesis (Venables *et al.*, 2009; David and Manley, 2010; Pal *et al.*, 2012).

The ghrelin gene is complex and generates multiple peptides in addition to ghrelin and obestatin, by alternative splicing (Hosoda *et al.*, 2000b; Tanaka *et al.*, 2001a; Jeffery *et al.*, 2002; Kawamura *et al.*, 2003; Jeffery *et al.*, 2005a). A number of transcript variants have been identified in humans, sheep, rats and mice. Some of these variants are conserved between multiple species, suggesting the existence of mammalian-specific alternative splicing of the ghrelin gene and that these ghrelin gene-derived transcripts are functional (Seim *et al.*, 2016).

For example, In1-ghrelin is a variant that contains Ex0-1, In1, and Ex2 but lacks Ex3-4, which shifts the reading frame of this transcript. This variant has been identified in various human tissues (Genbank #GU942497) including thymus, testis, kidney, stomach, uterus, brain, and mammary tissues (Gahete *et al.*, 2011). It has also been identified in Olive baboons (Genbank #HM048926) (Gahete *et al.*, 2011). It may encode a propeptide that retains the first 36 amino acids of native preproghrelin, including the signal peptide and the first 12 amino acids of native ghrelin, but has a different C-terminal tail that does not produce obestatin. The Ser3 residue that can be acylated by GOAT in native ghrelin is retained in this variant sequence, and the expression level of In1-ghrelin mRNA seem to correlate strongly with those of GOAT, suggesting that it could be a substrate for this enzyme. In1-ghrelin may play a role in the pathophysiology of cancer (Gahete *et al.*, 2011).

Another variant, In2-ghrelin, has been identified in mice (Genbank #DQ993169). It has a completely different structure containing Ex2, In2, and Ex3; Ex1, Ex4 and Ex5 are absent from this variant. Interestingly, the sequence of In2 varied from that originally reported by Tanaka *et al.* (2001a) (Genbank #AB060078), with eight TG repeats in tandem in the middle of the In2, instead of seven. Since Ex1 is absent from this variant and has been identified as a 5'UTR, its exclusion would not modify the predicted start codon of In2-ghrelin. This transcript variant contains a putative peptide that retains the first 36 amino acids of native preproghrelin including the five first residues of native ghrelin (GSSFL), and a novel 19 amino-acid C-terminal tail encoded by In2 (VSQSVSLSPHIYPDLVCVCV). Since exons 4 and 5 are missing, obestatin is probably not produced.

In2-ghrelin mRNA was not detected in the stomach extracts but was expressed in the pituitary and hypothalamus, and seemed to be dependent on energy intake, suggesting

Chapter 4 – 7F2 osteoblast-like cells and 7F2 cell-derived adipocytes express *Ghsr*, *Mboat4* and several isoforms of *Ghrl*

that this transcript may encode a peptide that plays an important role in coordinating the neuroendocrine response to metabolic stress. This peptide may be acylated and bind GHSR1a as it retains the first five residues of native ghrelin, and pituitary GOAT expression seemed to parallele the changes on In2-ghrelin expression (Gahete *et al.*, 2010).

A number of other variants have been identified, such as ghrelin gene-derived transcript (GGDT) (Tanaka *et al.*, 2001b), Des-Gln14-ghrelin (Hosoda *et al.*, 2000b; Kojima and Kangawa, 2005), In2c-ghrelin (Seim *et al.*, 2013), exon 2-deleted preproghrelin (Seim *et al.*, 2016), or exon 3-deleted proghrelin (Jeffery *et al.*, 2002, 2005b; Yeh *et al.*, 2005).

4.1.2. Chapter hypothesis, objectives and experimental strategies

The chapter hypothesis is 1) that 7F2 osteoblast-like cells and 7F2 cell-derived adipocytes express the key genes from ghrelin signalling (presented in Chapter 1, section 1.4.1), i.e. *Ghrl*, *Ghsr* and *Mboat4*, at the mRNA level, and 2) that ghrelin treatment exerts some feedback on their expression levels.

The objectives of this chapter were to investigate the expression of *Ghrl*, *Ghsr* and *Mboat4* using RT-PCR analysis in 7F2 cells cultured with basal or adipogenic medium. qRT-PCR was used to quantify the expression levels of these three genes, and to assess the effects of ghrelin treatment on these, in 7F2 cells cultured with basal or adipogenic medium and treated with two different concentrations of ghrelin (20 nM and 200 nM). RT-PCR and sequencing were used to investigate the structure of *Ghrl* mRNA isoforms expressed in 7F2 osteoblast-like cells and 7F2 cell-derived adipocytes, using various sets of primers spanning the gene sequence.

4.2. Materials and Methods

4.2.1. Adipogenic differentiation and ghrelin treatment of 7F2 cells

7F2 cells were seeded at a density of 2500 cells/cm² and cultured with basal and adipogenic medium as described in section 2.1., and treated with 20 nM or 200 nM ghrelin (Cambridge Bioscience) for 7 days. After 7 days of culture, 7F2 cells were stained with Oil Red O as described in section 2.1.

4.2.2. Molecular biology

4.2.2.1. RNA extraction, DNase treatment and reverse transcription

See sections 2.3.1 and 2.3.2.

4.2.2.2. PCR

4.2.2.2.1. Oligonucleotide primers: house-keeping and ghrelin signalling genes

See sections 8.1.1., 8.1.3. and 8.1.4.

4.2.2.2.2. PCR reaction compositions and conditions

The PCR reaction composition is described in section 2.3.3. The PCR reaction conditions were optimised and are detailed in table 4.1. Nuclease-free water was used as a negative control and three house-keeping genes, *Hprt1*, *Eef2* and *Gapdh*, were used as positive controls.

***Hprt1* and *Gapdh* primers:**

Step	Temperature °C	Time	No. of cycles
Initial denaturation	95	1 min	1
Denaturation	95	30 s	
Annealing	58	30 s	30
Extension	68	30 s	
Final extension	68	5 min	1
Soak	4	Indefinite	

***Eef2*, Ex 1 – Ex 3, Ex 2 – In 2 (both sets of primers), and Ex 2 – Ex 3 primers:**

Step	Temperature °C	Time	No. of cycles
Initial denaturation	95	1 min	1
Denaturation	95	30 s	
Annealing	58	30 s	35
Extension	68	30 s	
Final extension	68	5 min	1
Soak	4	Indefinite	

Ex 3 – Ex 4 and Ex 4 – Ex 5 primers:

Step	Temperature °C	Time	No. of cycles
Initial denaturation	95	1 min	1
Denaturation	95	30 s	
Annealing	56	30 s	40
Extension	68	30 s	
Final extension	68	5 min	1
Soak	4	Indefinite	

Table 4.1: PCR reaction conditions

4.2.2.3. Gel electrophoresis

See section 2.3.4.

4.2.2.4. Gel extraction of PCR products and sequencing

See section 2.3.6. PCR reactions were performed as described above (section 4.2.2.2), but with 50-55 cycles instead of the usual 30-40 cycles, to increase the number of copies.

4.2.2.5. Quantitative PCR

See section 2.3.5.

4.2.3. Statistical analysis

Statistical analysis was performed as described in section 2.3.7. Data were expressed as mean \pm standard deviation; the number of repeat assays is indicated by “n”. In qRT-PCR experiments, ANOVA tests (with Tukey-Kramer post-hoc analysis), Kruskal-Wallis tests (with Dunn post-hoc analysis) and Welch’s anova (with Games-Howell post-hoc analysis) were used to compare the expression levels of the GOIs between the experimental conditions, using the raw C_T values and fold changes. P values lower than 0.05 were considered as statistically significant. The calculations were performed using the R software (<https://www.r-project.org/>, version 3.5.3).

4.3. Results

4.3.1. 7F2 cells express *Ghrl*, *Ghsr*, and *Mboat4*

mRNA was extracted from 7F2 cells cultured for 7 days with basal or adipogenic medium. RT-PCR analysis was performed for three genes: *Ghrl*, *Ghsr* and *Mboat4* (figure 4.2). A band of the expected size was detected for *Mboat4* (240 bp) and *Ghsr* (215 bp), both in 7F2 cells and 7F2 cells treated with adipogenic medium. However, for the ghrelin gene, only a faint band of the expected size (220 bp) could be observed; there was a much more intense band which was about 90 bp longer than the expected size (figure 4.2.A). Since the primers were located on exon 2 and exon 3, this longer band could retain intron 2, which has been reported to be 93 bp long (Tanaka *et al.*, 2001a), or 95 bp long (Kineman *et al.*, 2007). No band was observed for the no RT controls (figure 4.2.B), confirming that the cDNA samples were not contaminated with genomic DNA.

4.3.2. mRNA expression of ghrelin signalling system is responsive to adipogenic medium and exogenous ghrelin

mRNA was extracted from 7F2 cells cultured for 7 days with basal or adipogenic medium, with or without 20 nM or 200 nM ghrelin. qRT-PCR analysis was performed for three genes: *Ghrl* (figure 4.3), *Ghsr* (figure 4.4) and *Mboat4* (figure 4.5). Data were normalised to two house-keeping genes: HPRT1, which is commonly used for qPCR analysis, and EEF2, which has been shown to have similar expression levels in many tissues, including bone and fat tissues (Kouadjo *et al.*, 2007).

For *Ghrl*, the mean Ct was significantly lower in cells cultured with basal medium + 200 nM ghrelin (24.45 ± 0.49) compared to basal medium alone (26.95 ± 2.05 ; $p = 0.015$, $n = 2$, 3 replicates per condition, Welch's anova and Games-Howell post-hoc analysis). Similarly, the mean Ct was lower in cells cultured with adipogenic medium + 200 nM ghrelin (24.27 ± 0.69) compared with adipogenic medium alone (26.30 ± 1.78 ; $p = 0.032$, $n = 2$, 3 replicates per condition, Welch's anova and Games-Howell post-hoc analysis) (figure 4.3.B). In data normalised to HPRT1, *Ghrl* mRNA levels were higher in cells cultured with basal medium + 200 nM ghrelin (144.84 ± 0.58) compared with basal medium alone (1 ± 0.73 ; $p = 0.0102$, $n = 2$, Kruskal-Wallis test and Dunn post-hoc analysis) and compared with basal medium + 20 nM ghrelin (104.21 ± 0.23 ; $p = 0.0141$). Similarly, *Ghrl* mRNA levels were higher in cells cultured with adipogenic medium + 200 nM ghrelin (123.07 ± 0.33) compared with adipogenic medium alone

(0.79 ± 0.40 ; $p = 0.0089$) and compared with adipogenic medium + 20 nM ghrelin (111.04 ± 0.15 ; $p = 0.0152$). When data was normalised to *EEF2*, *Ghrl* mRNA levels were higher in cells cultured with basal medium + 200 nM ghrelin (15.07 ± 0.44) compared with basal medium alone (1 ± 0.65 ; $p = 0.0072$, $n = 2$, Kruskal-Wallis test and Dunn post-hoc analysis), and they were also higher in adipogenic medium + 200 nM ghrelin (18.79 ± 0.47) compared with adipogenic medium alone (1.91 ± 0.20 ; $p = 0.0161$). However, there was no significant difference between basal medium + 20 nM ghrelin and basal medium + 200 nM ghrelin, or between adipogenic medium + 20 nM and adipogenic medium + 200 nM ghrelin.

Ct values were high (> 30) for *Ghsr* and *Mboat4*, indicating that their mRNA expression levels were low (figures 4.4.A, 4.4.B, 4.5.A and 4.5.B). There was no significant difference in their expression levels between basal and adipogenic medium alone (figures 4.4.C and 4.5.C). However, when treating the cells with 20 nM or 200 nM ghrelin, the results were contradictory depending on which house-keeping gene expression was normalised to. There was no significant difference in the fold changes for both *Ghsr* (normalised to HPRT1: $p = 0.09$; normalised to *EEF2*: $p = 0.075$, Welch's anova tests) and *Mboat4* (normalised to HPRT1: $p = 0.054$, ANOVA test; normalised to *EEF2*: $p = 0.087$, Kruskal-Wallis test).

4.3.3. Identification of ghrelin variant expressed in 7F2 cells

4.3.3.1. Ghrelin mRNA retains several introns in 7F2 cells

Since 7F2 osteoblast-like cells and 7F2 cell-derived adipocytes express a variant isoform of ghrelin, the next stage of this study consisted of characterising the structure of this variant, using RT-PCR analysis with several combinations of primers spanning the various exons of *Ghrl*. Figure 4.6 shows the agarose gels corresponding to various combinations of primers.

RT-PCR with primers located on exon 1 and exon 3 (*Ghrl*30_E1f - *Ghrl*753_E3r) revealed the presence of 4 bands; 3 of these bands were present in all the treatments, while the fourth was only visible when the cells were treated with ghrelin. The smaller band corresponded to 199 bp, which may contain exon 1, intron 2 and exon 3. The larger bands corresponded to 648 bp, which may contain exon 1, intron 1, exon 2 and exon 3; and 741 bp, which may contain exon 1, intron 1, exon 2, intron 2 and exon 3. The fourth band, which was ~400 bp long, may contain exon 1, exon 2, intron 2 and exon 3, although in theory this PCR product should be 332 bp long. The 199 bp and 741

bp bands were more intense when the cells were treated with 200 nM ghrelin compared with cells cultured with basal or adipogenic medium alone.

RT-PCR with primers located on exon 2 and exon 3 (Ghrl458_E2f - Ghrl753_E3r) showed two bands, as in previous experiments. The smaller bands corresponded to exon 2 and exon 3 (220 bp) while the longer bands retained intron 2. The longer band was much more intense in 7F2 cells treated with 200 nM ghrelin compared with cells cultured with basal or adipogenic medium alone. On the contrary, the smaller band was fainter in cells treated with 200 nM ghrelin.

RT-PCR with primers located on exons 3 and 4 (Ghrl698_E3f - Ghrl2752_E4r) did not detect any band for 7F2 cells cultured with basal or adipogenic medium; but a very faint band corresponding to the expected size (126 bp) was detected for 7F2 cells treated with 200 nM ghrelin. Using a forward primer spanning the end of exon 3 and the beginning of exon 4, coupled with a reverse primer on exon 5, showed the presence of 2 bands; the small one corresponded to 146 bp, which may contain exons 3, 4 and 5; and the longer band corresponded to 2088 bp, which may retain intron 3.

A set of primers was used to detect a PCR product containing exon 2 and intron 2 (Ghrl458_E2f - Ghrl607_In2r), with a reverse primer located at the beginning of intron 2. A band corresponding to the expected size (169 bp) was detected. Similarly to the other gels, in the presence of 200 nM ghrelin, the band was more intense than in the absence of ghrelin treatment. An additional band was detected but it is not known what it could correspond to.

RT-PCR with primers located on exons 4 and 5 (Ghrl2751_E4f - Ghrl3657_E5r) showed the presence of a 141 bp-long band, which corresponds to exon 4 and exon 5, without intron 4, for 7F2 cells cultured with basal and adipogenic medium alone. An additional, a faint band was detected for cells treated with 200 nM ghrelin; this band corresponded to 924 bp and may contain exon 4, intron 4 and exon 5. Finally, RT-PCR with primers located on exons 1 and 4, and exons 1 and 5, did not show any band.

No band was observed for the no RT controls (figure 4.7).

To summarise, the presence of exon 1, intron 1, exon 2, intron 2, exon 3, exon 4, intron 4 and exon 5 were detected at the mRNA level and 7F2 cells and 7F2-cell derived adipocytes expressed several variant isoforms of ghrelin. The expression levels of the variant isoform(s) were not affected by adipogenic medium, but were upregulated by treatment with 200 nM ghrelin in both basal and adipogenic medium.

4.3.3.2. Sequencing data

PCR products were sequenced to confirm the presence of the various exons and introns detected by RT-PCR analysis (see Appendix, section 8.2.).

The first sequenced PCR product (24BA88) was obtained with primers located on exons 1 and 3; sequencing and sequence alignment with the mouse ghrelin gene confirmed the presence of intron 1, exon 2, intron 2, and the beginning of exon 3. Here, intron 2 contained 8 TG repeats instead of 7, and was 95 bp long. The second sequenced PCR product (24BA89) was obtained with primers located on exons 2 and 3; sequencing and sequence alignment confirmed the presence of exon 2, intron 2 and exon 3. The third sequenced PCR product (24BA90) was obtained with primers located on exons 4 and 5; sequencing and sequence alignment confirmed the presence of exon 4, intron 4 and exon 5. Finally, the fourth sequence PCR product (24BA45) was obtained with a forward primer located on the junction between exons 3 and 4, and a reverse primer on exon 5; sequencing and sequence alignment also confirmed the retention of intron 4. For all the PCR products, the sequencing reaction did not seem to be very efficient in the area flanking the primers.

4.3.4.3. Prediction of protein structure

The prediction of the protein structure was done on a hypothetical sequence containing exon 1, intron 1, exon 2, intron 2, exon 3, exon 4 and exon 5, based on the RT-PCR and sequencing data presented in the previous sections. The ExPASy tool predicted four open reading frames (ORFs).

Two ORFs are short, encoding peptides that contain only 15 and 28 amino acids; BLAST against existing proteins in mice do not show any significant alignment with existing sequences.

Another ORF encodes a putative 55 amino acid peptide, which retains the signal peptide (MLSSGTICSLLLLSMLWMDMAMA) and the first 12 amino acids of native ghrelin (GSSFLSPEHQKA) with a novel C-terminal sequence (QVSQSVSLSPHIYPDLCVCV). It is encoded by exon 2 and part of intron 2, which introduces a new stop codon.

The last ORF encodes a 46 amino acid putative peptide that would be encoded by exons 4 and 5 (MLPSMLASSCQELSISSMAGPWGSFFRISSGKRSKRRQLTSNHGQA); this

Chapter 4 – 7F2 osteoblast-like cells and 7F2 cell-derived adipocytes express *Ghsr*,
Mboat4 and several isoforms of *Ghrl*

sequence does not align significantly with existing peptides; the ProP 1.0 Server tool does not predict any signal peptide, but predicts a cleavage site at Arg36.

4.4. Discussion

The aim of this chapter was to verify if 7F2 osteoblast-like cells and 7F2 cell-derived adipocytes expressed the key genes from ghrelin signalling, i.e. *Ghrl*, *Ghsr*, and *Mboat4*, at the mRNA level, and to study the effects of ghrelin treatment on the expression levels of these genes.

4.4.1. 7F2 cells express *Ghsr*, *Mboat4*, and variant isoforms of *Ghrl*

RT-PCR analysis showed that *Ghsr*, *Mboat4* and *Ghrl* were expressed both in 7F2 osteoblast-like cells and in 7F2 cell-derived adipocytes. Interestingly, two bands were detected for *Ghrl*, one that was the expected size (220 bp) but was faint, and a much more intense band that was about 90 bp longer, suggesting that these cells expressed a variant isoform of ghrelin.

To characterise this variant isoform, RT-PCR analysis was performed with several primer sets (Kineman *et al.*, 2007) located on the various exons of the mouse ghrelin gene and PCR products were sequenced. Among the various PCR products obtained with the primer sets spanning the mouse ghrelin gene, only a few could be sent for sequencing; despite 50-55 cycles of PCR, most of the bands that were detected with RT-PCR analysis were too faint and did not contain enough PCR products for the sequencing reaction to work. Sequences are attributed a quality score (Phred score) to each base of the sequence. Phred20 means that the base was identified with 99% accuracy (error probability of 1:100). Among the PCR products with a high enough concentration that were sent for sequencing, only a few had a high overall Phred score. N bases correspond to Phred < 10. There are several possible causes for the low Phred score. There could have been mutations in the PCR products due to the high number of PCR cycles; also, DNA molecules could have been cross-linked due to the use of U.V. light during gel extraction, even though the duration of exposure was limited.

RT-PCR with primers located on exons 1 and 3 showed several bands. The sequence obtained for the longer band (741 bp) had a high Phred score overall (> 20 for almost all bases) and had a strong identity to the mouse ghrelin gene sequence, so the sequencing data seemed reliable. It confirmed the full retention of introns 1 and 2. For the PCR product with primers located on exons 2 and 3, the overall Phred score was lower, but the sequence still aligned relatively well with the mouse ghrelin gene, further confirming the retention of intron 2. Exon 4, intron 4 and exon 5 were also detected by RT-PCR analysis. Also, RT-PCR with primers located on exons 3 and 4 did

not seem to detect any band. However, results with other primer sets confirmed the presence of exons 3 and 4, so intron 3 may be retained, but was too long for the PCR reaction to work, as intron 3 is 1972 bp long in the mouse ghrelin gene. Similarly, PCR with primers located on exons 1 and 5 did not show any band; this too may be due to the fact that the PCR products would have been too long due to the retention of introns, especially intron 3. Overall, the data indicate that 7F2 osteoblast-like cells and 7F2 cell-derived adipocytes expressed several isoforms of ghrelin, one of which contains exon 1, intron 1, exon 2, intron 2, exon 3, and may contain exons 4 and 5 as well. Since the PCR reaction with primers on exons 1 and 5 did not work, it is difficult to conclude on the exact number and structures of variants expressed by these cells.

Ghrelin is ubiquitously expressed; the highest levels of expression are detected in the stomach and intestine (Gnanapavan *et al.*, 2002), but local concentrations in other tissues that produce ghrelin may be relatively high. GHSR expression may be more restricted, although data on GHSR expression are contradicting; Gnanapavan *et al.* (2002) reported that the highest levels of expression were detected in the pituitary and brain, while other tissues such as the stomach, the small intestine, or the liver, had low expression levels. Others have reported a wider tissue distribution: GHSR mRNA was detected in many organs such as the heart, lung, liver, kidney, pancreas, and adipose tissue, indicating that ghrelin may have multiple functions in these tissues (Kojima and Kangawa, 2005). Very low GHSR expression levels have been detected in white adipose tissue and brown adipose tissue (Sun *et al.*, 2007; Davies *et al.*, 2009; Lin *et al.*, 2011).

The fact that 7F2 cells and 7F2 cell-derived adipocytes express *Ghrl*, *Ghsr* and *Mboat4* at the mRNA level suggests that they may produce acylated ghrelin, and that this hormone may have auto- and/or paracrine effects. This is consistent with previous studies that demonstrated that ghrelin, apart from its role in regulating GH release, food intake, energy balance and glucose metabolism, also has functions in bone, stimulating osteoblast proliferation and differentiation in rats, mice, and humans (Choi *et al.*, 2003; Kim *et al.*, 2005; Maccarinelli *et al.*, 2005; Delhanty *et al.*, 2006). *Ghrl* and *Mboat4* mRNA expression has been demonstrated in mice by others (Delhanty *et al.*, 2014a; Hopkins *et al.*, 2017). Although some studies did not detect GHSR1a mRNA in bone cells from human (Delhanty *et al.*, 2006), rat and mouse (Costa *et al.*, 2011), others have detected GHSR1a mRNA in osteoblasts from mice (Kim *et al.*, 2005; Delhanty *et al.*, 2014b), rats (Fukushima *et al.*, 2005) and humans (Costa *et al.*, 2011). Interestingly, in humans, GHSR was only found to be expressed in 25-30% of bone marrow and osteoblasts samples (Costa *et al.*, 2011); *Ghsr* may be expressed by a subpopulation of cells, or

expression varies among individuals, which could explain why some studies do not detect *Ghsr* mRNA while others do. Also, acylated ghrelin and unacylated ghrelin were shown to induce proliferation of osteoblasts even when GHSR1a expression was not detected, suggesting the existence of another receptor (Delhanty *et al.*, 2006). Here, *Ghsr* expression was detected at the mRNA level but the bands were relatively faint in comparison to ghrelin, suggesting it may not be highly expressed. This was confirmed by qRT-PCR analysis. If ghrelin has an effect on 7F2 cells, it may be mediated by another receptor. Finally, of the variant isoforms of ghrelin expressed by 7F2 cells may encode for a peptide that retains the first 12 amino acids of native ghrelin, including the third serine residue that can be acylated by GOAT; hence, this variant, if expressed at the protein level, may be acylated, bind GHSR1a or another receptor, and exert biological functions in 7F2 cells.

Several studies report GHSR-independent effects of acylated ghrelin in various tissues, including fat and bone (Thompson *et al.*, 2004; Delhanty *et al.*, 2006; Costa *et al.*, 2011; Parsons *et al.*, 2015). Ghrelin is very likely to have other receptors. Unacylated ghrelin, which is almost inactive at GHSR1a, has been reported to mimic the effects of acylated ghrelin in several tissues, even in the absence of GHSR1a, and acylated ghrelin binding seems to be competitively reduced by unacylated ghrelin. Unacylated ghrelin may also have specific receptors at which acylated ghrelin is inactive (Callaghan and Furness, 2014). In addition, GHSR1a and GHSR1b form heterodimers with other GPCRs, which have different pharmacological properties and mediate effects on various processes such as lipid accumulation, myoblast differentiation, osteoblast proliferation, insulin secretion, cardioprotection, and tumour cell proliferation (Callaghan and Furness, 2014).

4.4.2. Ghrelin treatment promotes ghrelin mRNA expression

The aim of this chapter was also to study whether ghrelin treatment affected the mRNA expression levels of the key genes from ghrelin signalling, i.e. *Ghsr*, *Ghrl*, and *Mboat4*. qRT-PCR analysis showed no effect of 20 nM ghrelin on the expression levels of *Ghsr* and *Mboat4*, which were relatively low. On the contrary, 20 nM and 200 nM ghrelin clearly upregulated the expression of *Ghrl*, in particular the isoforms that retained Intron 2, suggesting a positive feedback loop and that this variant isoform of ghrelin may play an important role in bone metabolism.

Recently, it has been demonstrated that the ghrelin gene is very complex and gives rise to many transcripts, notably in mice and humans; some retain introns, and some exons

are deleted in other variants (Kineman *et al.*, 2007; Seim *et al.*, 2007, 2016; Gahete *et al.*, 2011). Some of these variant isoforms of ghrelin can have biological functions. For example, In1-ghrelin is upregulated in various types of cancers, and promotes cancer progression (Hormaechea-Agulla *et al.*, 2017). One of the variants expressed by 7F2 cells contains exon 1, intron 1, exon 2, intron 2 and exon 3, and may also contain exons 4 and 5. Prediction of protein sequence from a transcript containing exon 1, intron 1, exon 2, intron 2, exon 3, exon 4 and exon 5 would contain four ORFs; two of them would encode short novel peptides of 15 and 28 amino acids. Another ORF would give rise to a peptide that is encoded by exon 2 and part of intron 2; this peptide would retain the signal peptide, as well as the first 12 amino acids of native ghrelin. This putative peptide has been predicted in another study that identified an In2-ghrelin variant (Kineman *et al.*, 2007), which contains exon 2, intron 2 and exon 3, but lacks exons 1, 4 and 5. However, the putative peptide encoded by this variant has yet to be identified at the protein level. The fourth ORF predicted in the 7F2 cells transcript would give rise to a 46 amino acid peptide that is encoded by exons 4 and 5; this putative peptide sequence does not align significantly with any known peptide in mice. Despite being encoded by exons 4 and 5, it does not correspond to obestatin sequence due to a translational frameshift. If one or several of these ORFs encode a peptide, this novel isoform of ghrelin could have osteoblast-specific effects, and could be involved in the effects of ghrelin in bone.

4.4.3. Chapter conclusions

The hypothesis that 7F2 osteoblast-like cells and 7F2 cell-derived adipocytes expressed the three genes from ghrelin signalling, i.e. *Ghrl*, *Ghsr* and *Mboat4*, at the mRNA level was verified. It was shown in this section of work that 7F2 cells and 7F2 cell-derived adipocytes express *Ghsr*, *Mboat4* and *Ghrl* mRNA, although *Ghsr* and *Mboat4* expression levels were low. This suggests that, if ghrelin has any effect on 7F2 cells, these effects may be mediated by a receptor other than GHSR1a. The hypothesis that ghrelin treatment exerted some feedback on their expression levels was also verified, as treatment with 200 nM ghrelin significantly increased *Ghrl* mRNA expression in both 7F2 cells and 7F2-cell derived adipocytes.

In addition, this study shows for the first time that 7F2 cells and 7F2 cell-derived adipocytes express several variant isoforms of ghrelin, one of which contains exon 1, intron 1, exon 2, intron 2 and exon 3, and may contain exons 4 and 5. This previously un-reported isoform was more highly expressed than native ghrelin. Ghrelin treatment

Chapter 4 – 7F2 osteoblast-like cells and 7F2 cell-derived adipocytes express *Ghsr*, *Mboat4* and several isoforms of *Ghrl*

increased the mRNA expression of *Ghrl*, especially that of the variant isoform retaining intron 2. This suggests that this variant isoform may play an important role in 7F2 cells. However, it was only detected at the mRNA level, and it would be interesting to study whether this variant isoform is expressed at the protein level, and whether it is acylated by GOAT, like native ghrelin.

Having identified that 7F2 cells and 7F2-cell derived adipocytes expressed genes from ghrelin signalling, the next stage was to test whether ghrelin had any effect on the proliferation and adipogenic differentiation of 7F2 cells.

Chapter 4 – 7F2 osteoblast-like cells and 7F2 cell-derived adipocytes express *Ghsr*, *Mboat4* and several isoforms of *Ghrl*

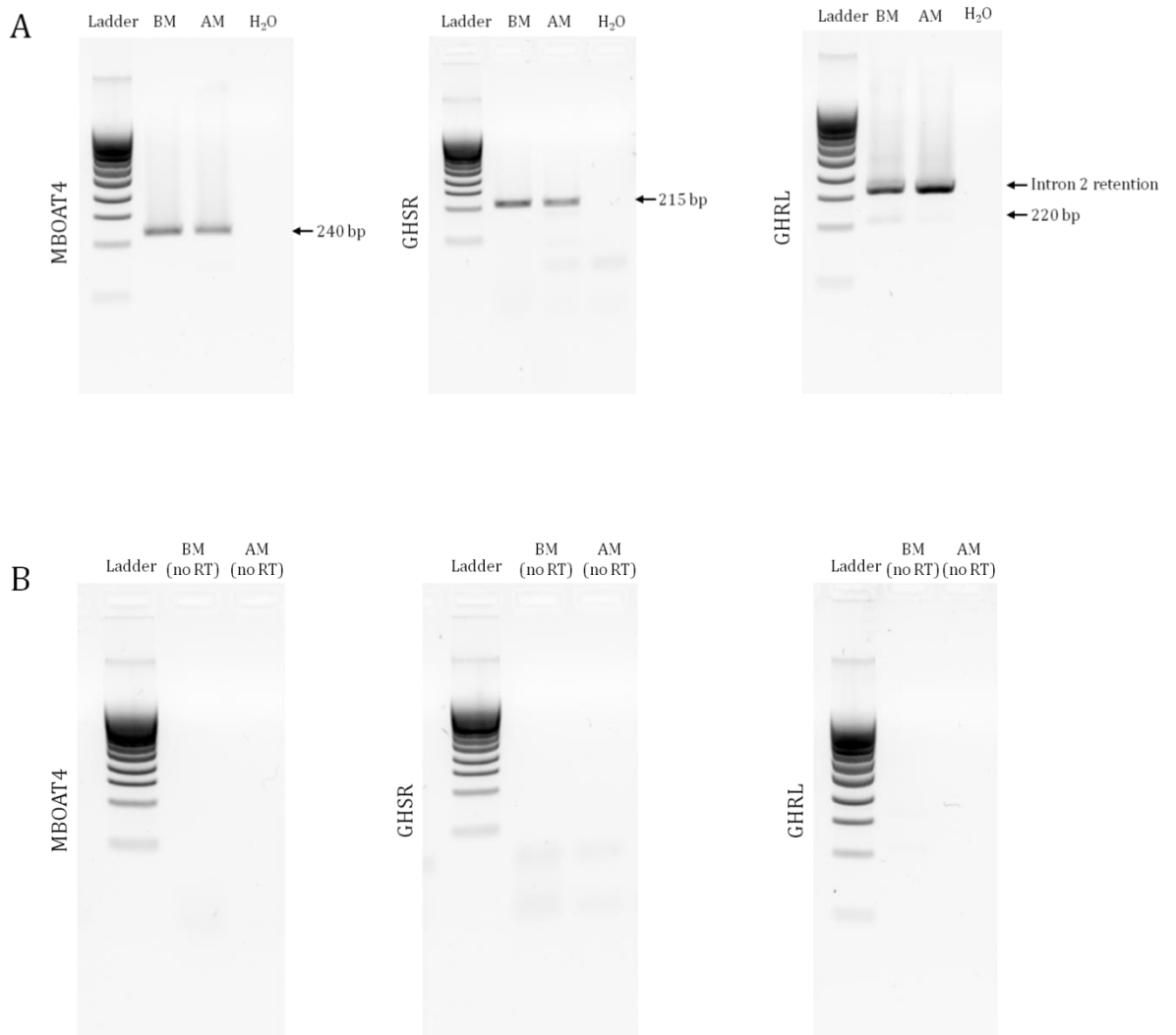


Figure 4.2: RT-PCR for the genes from ghrelin signalling

mRNA was extracted from 7F2 cells cultured with basal (BM) or adipogenic medium (AM) for 7 days. A: PCR with cDNA samples. B: PCR with corresponding no RT controls.

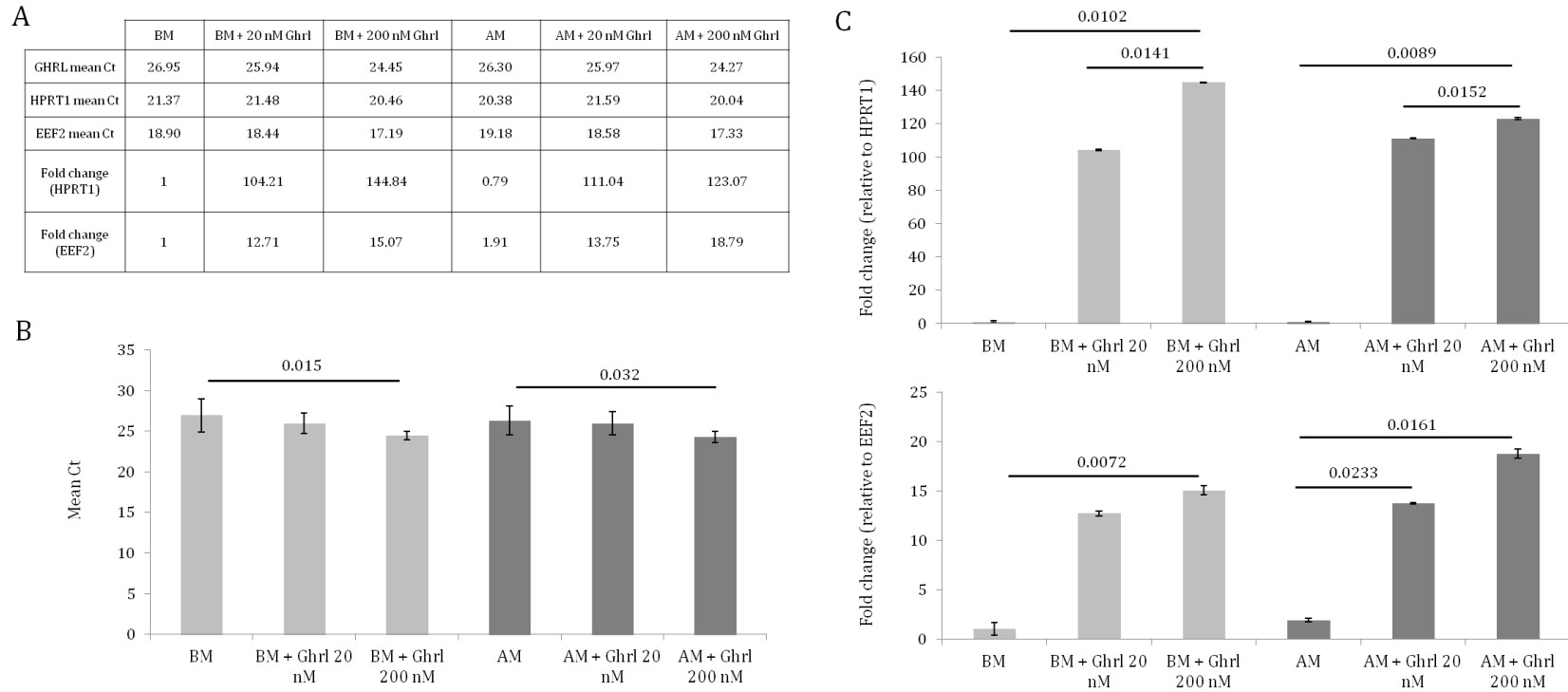


Figure 4.3: qRT-PCR analysis of *Ghrl* expression in 7F2 cells treated with ghrelin

7F2 cells were cultured for 7 days with basal (BM) or adipogenic medium (AM), with or without 20 nM or 200 nM ghrelin. After 7 days of culture, RNA was extracted and gene expression was analysed using qRT-PCR. A: Raw Ct values and fold changes. B: Graph showing mean Ct values \pm SD for each condition ($n = 2$; 3 replicate samples per condition; each sample was run in duplicate; Welch's anova and Games-Howell post-hoc analysis). C: Expression of *Ghrl* normalised to HPRT1 (top) and to EEF2 (bottom). Data are fold change \pm SD; numbers above the horizontal lines are p values ($n = 2$; 3 replicate samples per condition, each sample was run in duplicate; Kruskal-Wallis + Dunn tests).

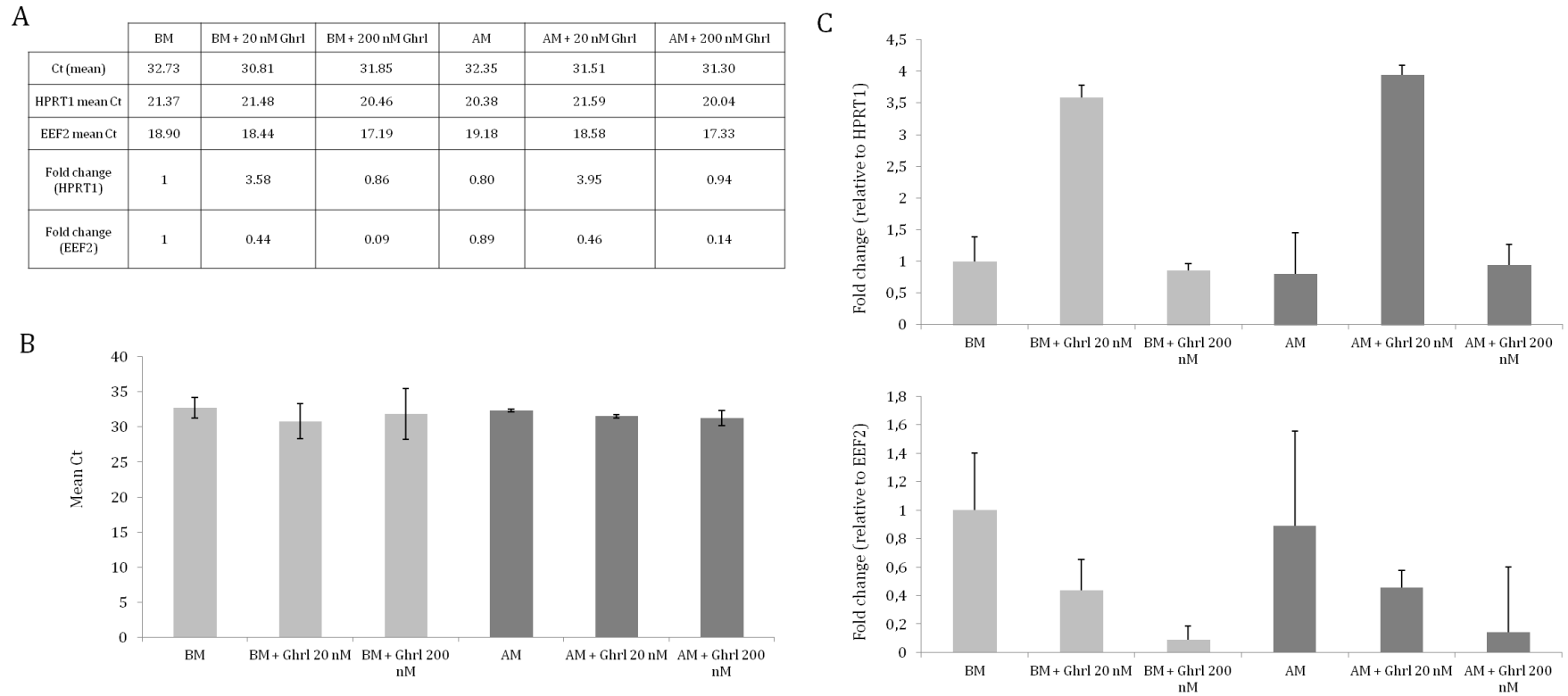


Figure 4.4: qRT-PCR analysis of *Ghsr* expression in 7F2 cells treated with ghrelin

7F2 cells were cultured for 7 days with basal (BM) or adipogenic medium (AM), with or without 20 nM or 200 nM ghrelin. After 7 days of culture, RNA was extracted and gene expression was analysed using qRT-PCR. A: Raw Ct values and fold changes. B: Graph showing mean Ct values \pm SD for each condition ($n = 1$; 3 replicate samples per condition, each sample was run in duplicate; Kruskal-Wallis test). C: Expression of *Ghsr* normalised to HPRT1 (top) and to EEF2 (bottom). Data are fold change \pm SD ($n = 1$; 3 replicate samples per condition, each samples was run in duplicate; Welch's anova).

Chapter 4 – 7F2 osteoblast-like cells and 7F2 cell-derived adipocytes express *Ghsr*, *Mboat4* and several isoforms of *Ghrl*

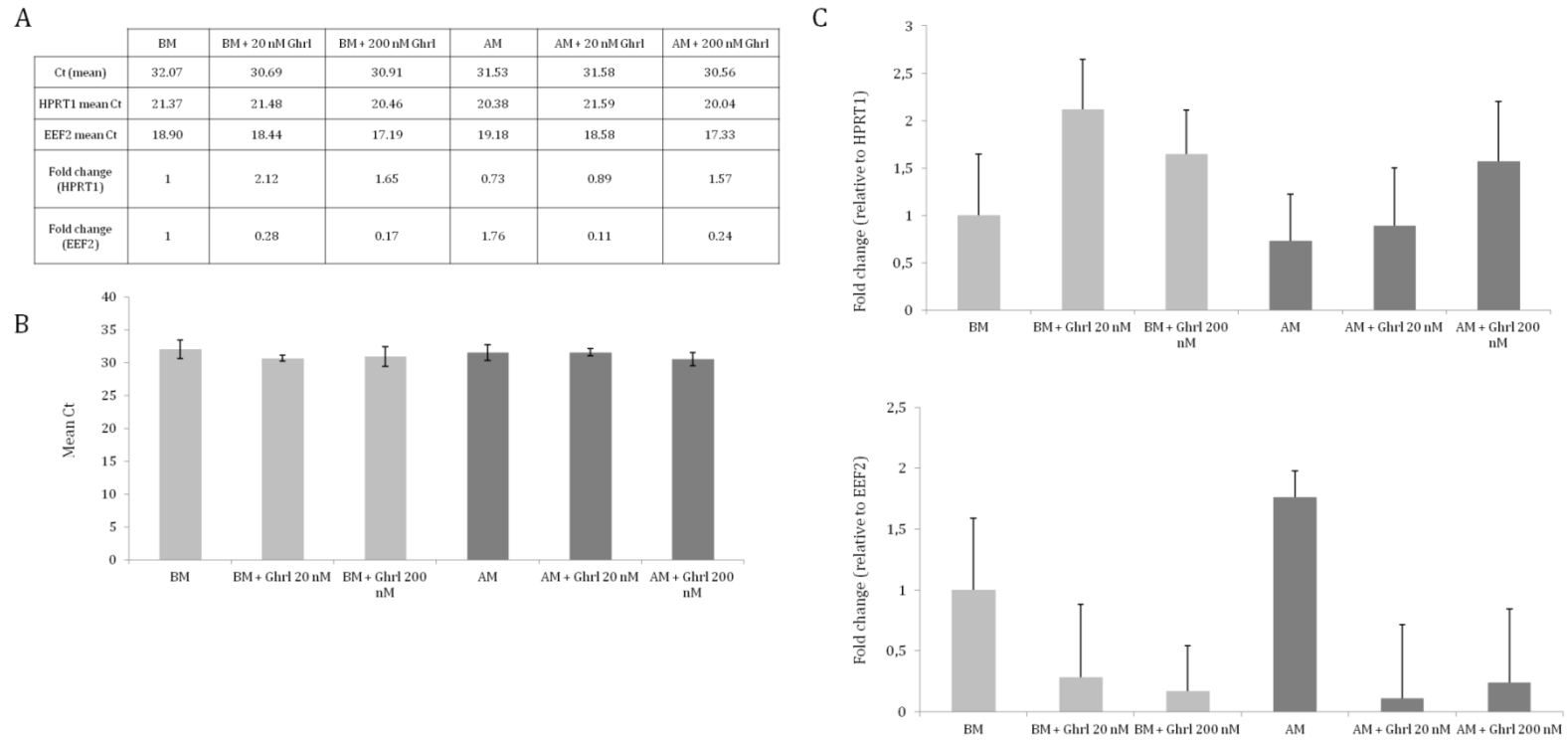
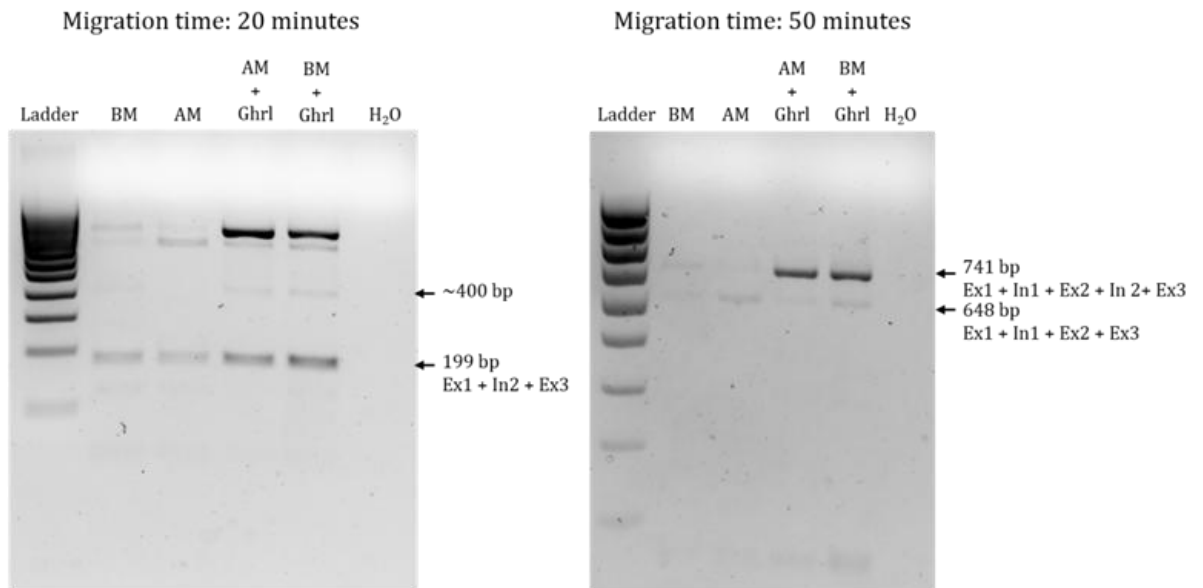


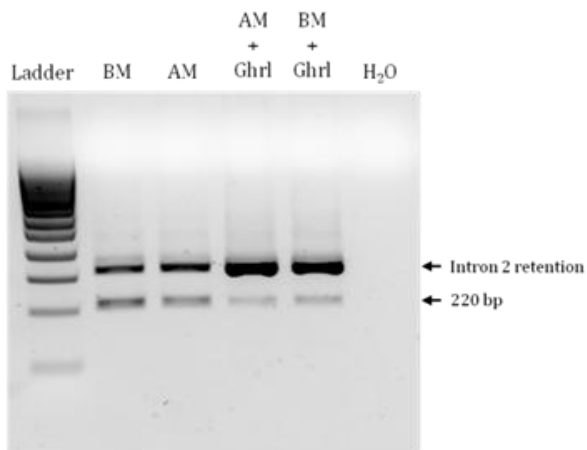
Figure 4.5: qRT-PCR analysis of *Mboat4* expression in 7F2 cells treated with ghrelin

7F2 cells were cultured for 7 days with basal (BM) or adipogenic medium (AM), with or without 20 nM or 200 nM ghrelin. After 7 days of culture, RNA was extracted and gene expression was analysed using qRT-PCR. A: Raw Ct values and fold changes. B: Graph showing mean Ct values \pm SD for each condition ($n = 1$; 3 replicate samples per condition, each sample was run in duplicate; Kruskal-Wallis test). C: Expression of *Mboat4* normalised to HPRT1 (top) and to EEF2 (bottom). Data are fold change \pm SD ($n = 1$; 3 replicate samples per condition, each samples was run in duplicate; ANOVA test for data normalised to HPRT1; Kruskal-Wallis test for data normalised to EEF2).

GHRL: Ex 1 - Ex 3



GHRL: Ex 2 - Ex 3



GHRL: Ex 3 - Ex 4

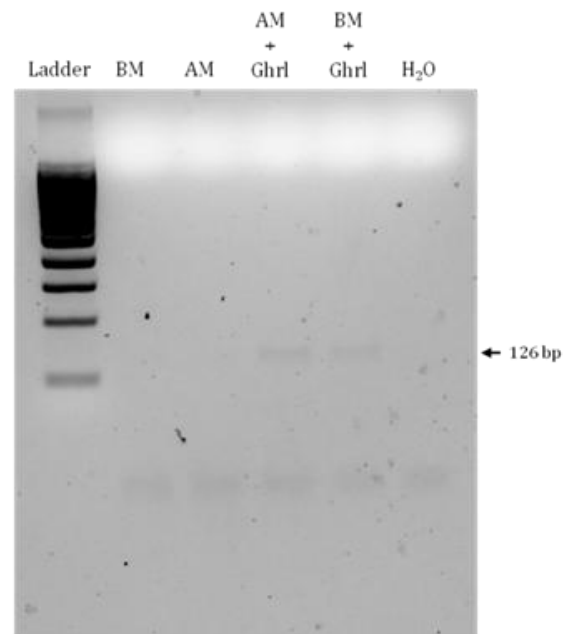
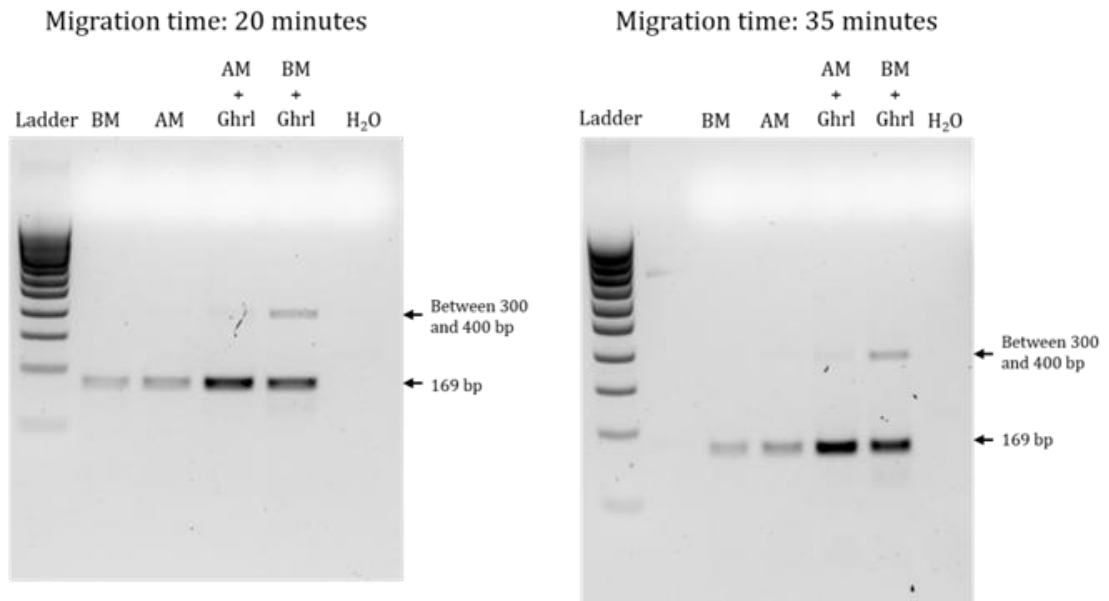


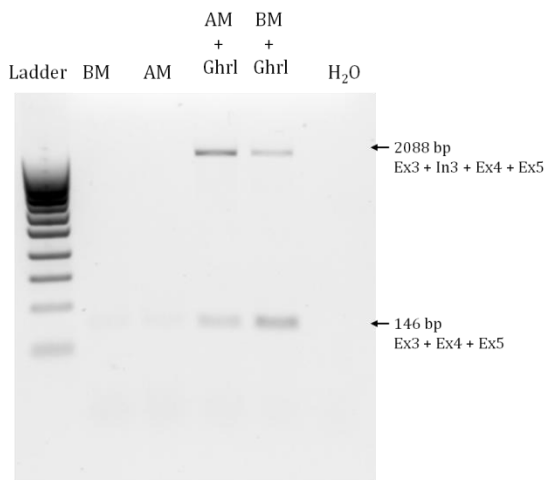
Figure 4.6: Characterisation of the ghrelin variant expressed in 7F2 cells by RT-PCR analysis (part 1)

7F2 cells were cultured for 7 days with basal (BM) or adipogenic (AM) medium, with or without 200 nM ghrelin. After 7 days, RNA was extracted and RT-PCR analysis was performed with various sets of primers spanning the ghrelin gene.

GHRL: Ex 2 – In2



GHRL: Ex 3/4 – Ex 5



GHRL: Ex 4 – Ex 5

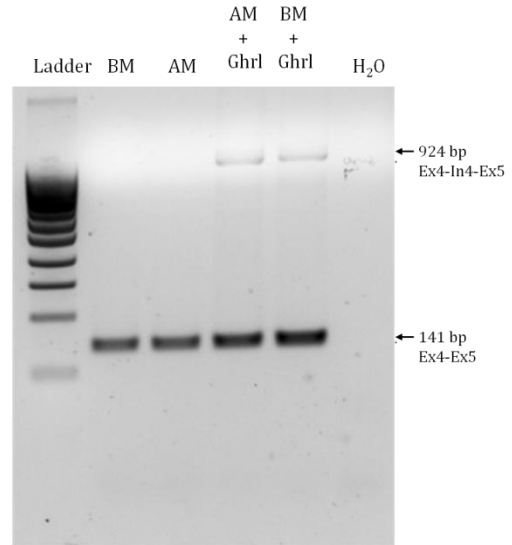
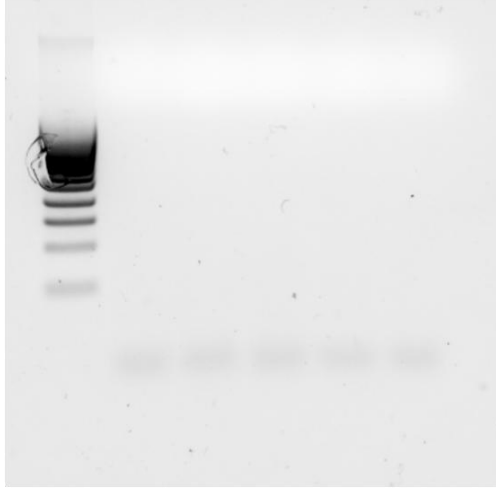


Figure 4.6: Characterisation of the ghrelin variant expressed in 7F2 cells by RT-PCR analysis (part 2)

7F2 cells were cultured for 7 days with basal (BM) or adipogenic (AM) medium, with or without 200 nM ghrelin. After 7 days, RNA was extracted and RT-PCR analysis was performed with various sets of primers spanning the ghrelin gene.

GHRL: Ex 1 – Ex 4

			AM	BM	
			+	+	
Ladder	BM	AM	Ghrl	Ghrl	H ₂ O



GHRL: Ex 1 – Ex 5

			AM	BM	
			+	+	
Ladder	BM	AM	Ghrl	Ghrl	H ₂ O

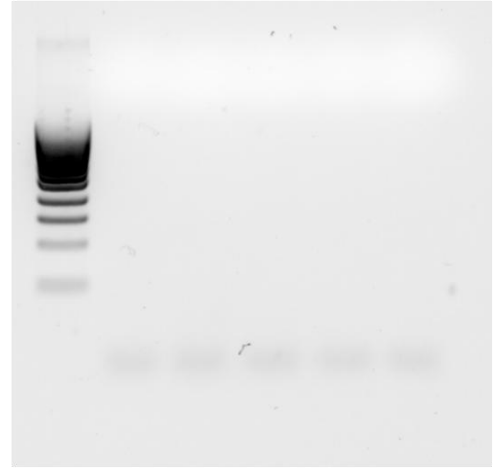


Figure 4.6: Characterisation of the ghrelin variant expressed in 7F2 cells by RT-PCR analysis (part 3)

7F2 cells were cultured for 7 days with basal (BM) or adipogenic (AM) medium, with or without 200 nM ghrelin. After 7 days, RNA was extracted and RT-PCR analysis was performed with various sets of primers spanning the ghrelin gene.

Chapter 4 – 7F2 osteoblast-like cells and 7F2 cell-derived adipocytes express *Ghsr*, *Mboat4* and several isoforms of *Ghrl*

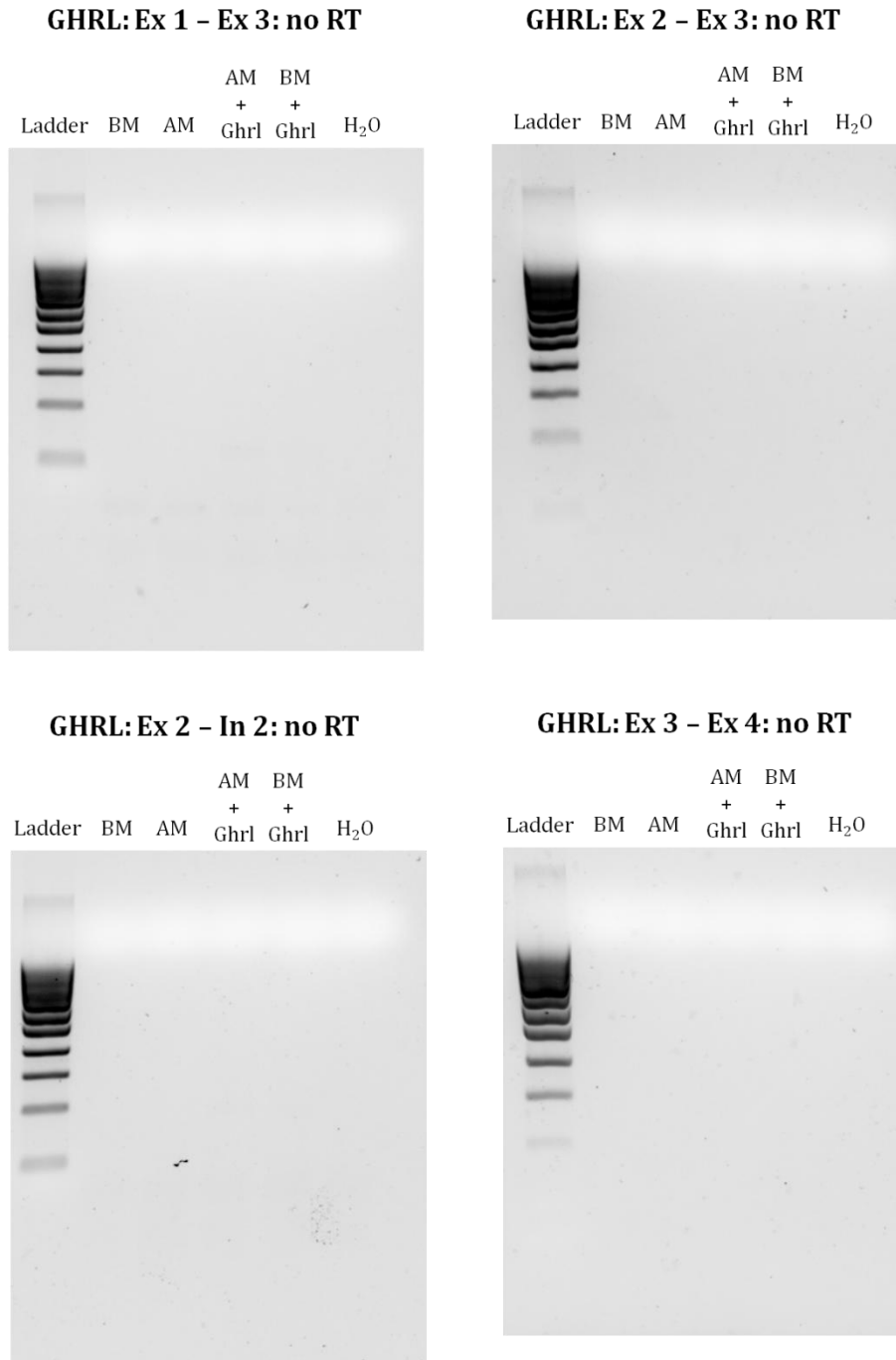


Figure 4.7: No RT controls for the ghrelin variants (part 1)

7F2 cells were cultured for 7 days with basal (BM) or adipogenic (AM) medium, with or without 200 nM ghrelin. After 7 days, RNA was extracted and RT-PCR analysis was performed for the no RT controls, with various sets of primers spanning the ghrelin gene.

GHRL: Ex 4 – Ex 5: no RT

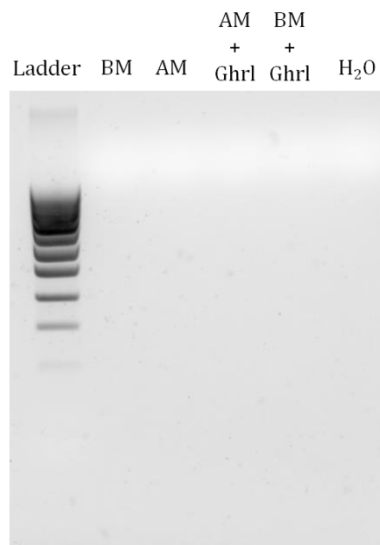


Figure 4.7: No RT controls for the ghrelin variants (part 2)

7F2 cells were cultured for 7 days with basal (BM) or adipogenic (AM) medium, with or without 200 nM ghrelin. After 7 days, RNA was extracted and RT-PCR analysis was performed for the no RT controls, with various sets of primers spanning the ghrelin gene.

Chapter 5 – The influence of ghrelin and K⁺ channel ligands on adipogenic differentiation of 7F2 cells

5.1. Introduction

5.1.1. K_{ATP} channels

K_{ATP} channels are a subfamily of inwardly-rectifying potassium (Kir) channels (Hibino *et al.*, 2010). The property of inward rectification refers to the current-voltage relationship of these channels; when the current flowing through the channel is plotted against membrane potential, the inward (negative) current is much larger than the outward (positive) current. In other words, these channels conduct larger inward currents at membrane voltage negative to the potassium equilibrium potential, than outward currents at more positive voltages. Inward rectification is not an inherent property of the protein itself which forms the channel (Lopatin *et al.*, 1994); rather, it is caused by intracellular cations (such as Mg²⁺) and polyamines, which block the outward flow of potassium ions in a voltage-dependent manner by binding to the inner ion-conducting vestibule of the channel.

K_{ATP} channels are “weak” rectifiers, as they can carry a measureable outward K⁺ current, while “strong” rectifiers cannot. K_{ATP} channels open spontaneously in inside-out membrane patch, and they control the resting membrane potential. They are sensitive to changes in [ATP]; their opening is inhibited by intracellular ATP and activated by intracellular nucleoside-diphosphates (NDP), such as ADP (Hibino *et al.*, 2010). They are composed of 4 Kir6.x subunits (Kir6.1 or Kir6.2), and 4 sulfonylurea receptor (SUR) subunits (SUR1, SUR2A and SUR2B). The Kir subunits have two transmembrane domains, which are the pore-forming subunits and contain the ATP-binding site, which is located at the interface between the N- and C-termini (Hibino *et al.*, 2010); Kir6.1 is encoded by *Kcnj8* and Kir6.2 is encoded by *Kcnj11*. The SUR subunits are regulatory and are encoded by two genes: *Abcc8* (SUR1) and *Abcc9*, which has several isoforms, including SUR2A and SUR2B; they possess two binding domains for nucleotides (figure 5.1) (Hibino *et al.*, 2010).

K_{ATP} channels can be subcategorised into smaller conductance Kir6.1 channels (35 – 40 pS) or larger conductance Kir6.2 channels (65 – 80 pS), according to their subunit composition and their pharmacology. It is possible to construct Kir6.1/6.2 heteromers *in vitro* (Pountney *et al.*, 2001); but the presence of such heteromeric channels *in vivo* remains controversial (Hibino *et al.*, 2010). K_{ATP} channels are voltage-independent; they are inwardly-rectifying at depolarising potentials, due to blockage by Mg²⁺ ions in the pore (Lopatin *et al.*, 1994). The accessory SUR subunits are targets for drugs that

Chapter 5 – The influence of ghrelin and K⁺ channel ligands on adipogenic differentiation of 7F2 cells

can open or block K_{ATP} channels; K_{ATP} channels are all sensitive to inhibition by sulphonylurea drugs such as glibenclamide and tolbutamide; but they do not respond to the same K_{ATP} channel openers. For example, pinacidil activates channels built with SUR2 but not SUR1, and the effect is greater for SUR2B than for SUR2A (Babenko *et al.*, 2000); diazoxide activates both SUR1 and SUR2B (Gribble Fiona M. *et al.*, 1997; Shyng *et al.*, 1997). Hence, different combinations of Kir6.x and SUR subunits lead to tissue-specific K_{ATP} channels with particular physiological and pharmacological properties (Inagaki *et al.*, 1996; Seino *et al.*, 2000).

K_{ATP} channels are present in many cells and regulate a variety of cellular functions by coupling cell metabolism with membrane potential. For example, they play an important role in glucose-mediated insulin secretion (Ashcroft, 2005; Diehlmann *et al.*, 2011; Rorsman and Ashcroft, 2018); genetic modification of Kir6.2 or SUR1 leads to various phenotypes of glucose homeostasis disorders (Hibino *et al.*, 2010), and a mutation activating Kir6.2 causes permanent neonatal diabetes (Gloyn *et al.*, 2004). K_{ATP} channels are expressed in osteoblasts, osteoclasts, and adipocytes (Hibino *et al.*, 2010), where they have roles in cell proliferation, secretion, and metabolism. A study showed that human MSCs expressed Kir6.1, Kir6.2 and SUR2A; upon adipogenic differentiation, Kir6.1 and SUR2A were downregulated; upon osteogenic differentiation, Kir6.2 was strongly upregulated (Diehlmann *et al.*, 2011). Changes of K_{ATP} channel expression suggest that these channels may contribute to *in vitro* differentiation of MSCs. Another study showed that Kir6.1 and SUR2B were expressed in human adipose tissue, but not SUR1, SUR2A or Kir6.2 (Gabrielsson *et al.*, 2004). K_{ATP} channels are involved in mediating ghrelin signalling: in pancreatic β-cells, K_{ATP} channels composed of Kir6.2 and SUR1 subunits, mediate the inhibition of insulin secretion by ghrelin (MacDonald and Wheeler, 2003; Dezaki *et al.*, 2007).

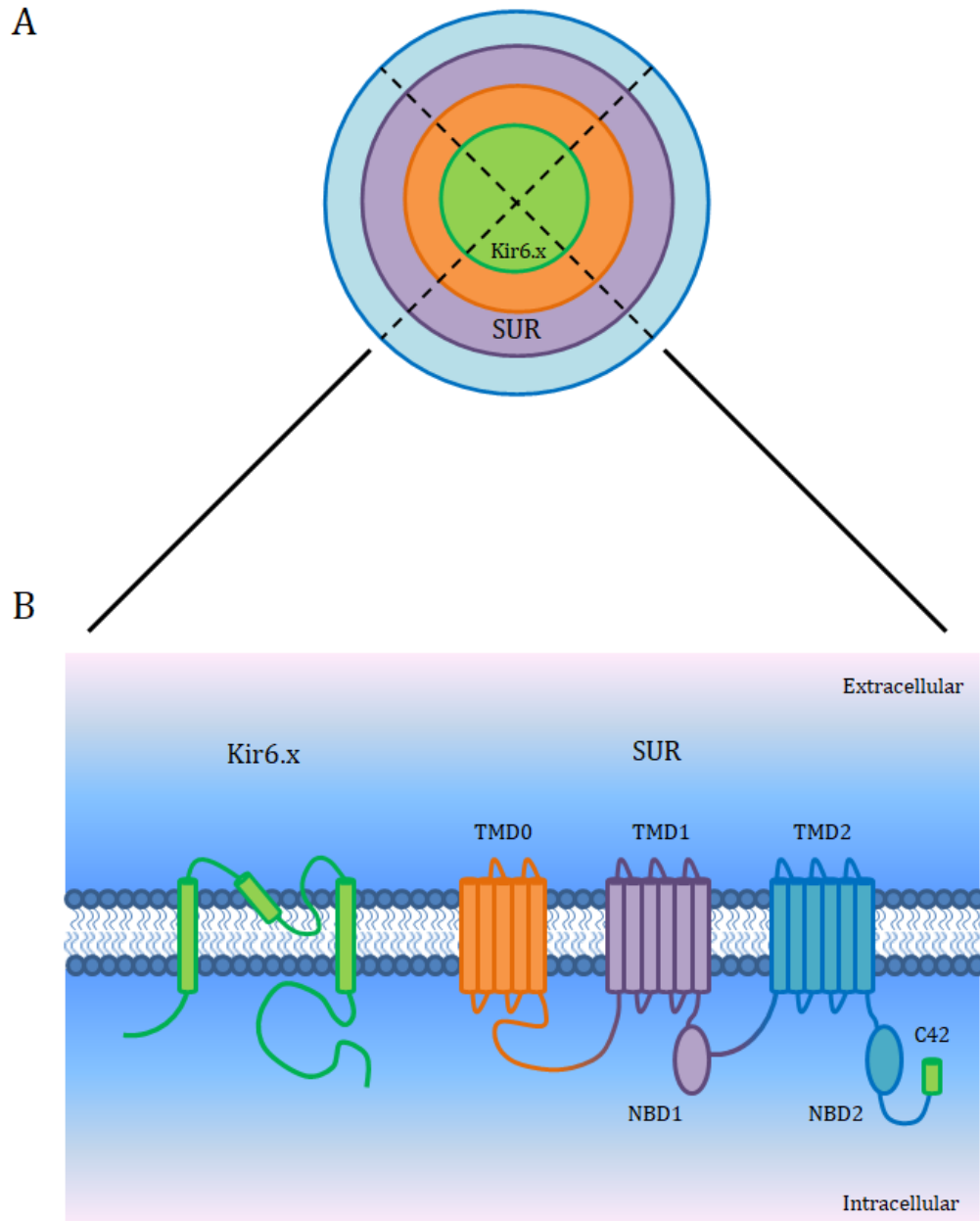


Figure 5.1: K_{ATP} channel structure

A: Top view of a functional K_{ATP} channel. K_{ATP} channels are heterooctamers composed of 4 Kir6.x subunits and 4 SUR subunits. B: Molecular constituents of K_{ATP} channels. Each SUR unit has 2 nucleotide-binding domains (NBD). SUR2A and SUR2B differ in the COOH-terminal 42 amino acids (C42). TMD: transmembrane domain. Adapted from (Hibino *et al.*, 2010).

5.1.2. BK channels

Also called K_{Ca}1.1, Big K channels, or maxi-K channels, BK channels are large conductance calcium-activated and voltage-sensitive potassium channels: they are activated by micromolar increases in intracellular Ca²⁺ concentration, sensitive to changes in membrane potential (depolarisation), and are responsible for negative feedback of Ca²⁺ entry (Lee and Cui, 2010). They are formed by 4 α -subunits, which are pore-forming and encoded by *Kcnma1*; and 4 auxiliary, regulatory β -subunits, encoded by *Kcnmb1* to *Kcnmb4* (see figure 5.2). The α -subunits are structurally similar to those of the voltage-dependent K⁺ channels; they are composed of 7 transmembrane domains (S0 – S6) and have an extracellular N-terminus, contrary to other K_{Ca} channels. S4 contains positively charged arginine and lysine residues which are responsible for the voltage sensitivity of the channel, and S5 – S6 contain the pore-forming loop and the K⁺ selective region. The four β -subunits can be homotetrameric or heterotetrameric, which modulates the activity of the ion channel, particularly the sensitivity to activating or inhibitory ligands.

BK channels are expressed in many cell types (Ge *et al.*, 2014). Alternative splicing and the various patterns of expression of the regulatory subunits give rise to many subtypes of BK channels, allowing them to have different biophysiological properties in different tissues and modifying the susceptibility to various channel modulators (Li, 2012; Kyle and Braun, 2014). BK channels have conductances in the range 150 – 300 pS, although typically > 200 pS. They are sensitive to inhibition by the scorpion peptides charybdotoxin, which blocks BK channels and other types of voltage-gated potassium channels, and iberiotoxin, which is a specific blocker of most BK channels (Wang *et al.*, 2014; Yu *et al.*, 2016). They are also sensitive to the non-specific K⁺ channel blocker tetraethylammonium (TEA) (Henney, 2008).

The pore-forming subunit KCNMA1 is widely expressed in most cells and tissues, including neuronal cells, vascular smooth muscle cells, endothelial cells, and bone cells (Henney *et al.*, 2009; Zhang *et al.*, 2014). BK channels are also expressed in human preadipocytes and osteoblasts (Wann *et al.*, 2004; Hirukawa *et al.*, 2008) and in human MSCs (Li *et al.*, 2005). BK channels are involved in human bone marrow-derived MSC proliferation and differentiation (Zhang *et al.*, 2014): silencing BK channels significantly reduces adipogenic differentiation, with decrease of lipid accumulation and expression of adipocytic marker PPAR γ . Zhang *et al.* (2014) also showed that silencing BK channels decreases osteogenic differentiation with reduction of mineralisation and osteocalcin

Chapter 5 – The influence of ghrelin and K⁺ channel ligands on adipogenic differentiation of 7F2 cells

secretion. Other studies showed that BK channels regulate preadipocyte proliferation (Hu *et al.*, 2009), osteoblast and osteoblast-like cell proliferation, osteoblast differentiation and mineralisation (Henney *et al.*, 2009; Li, 2012), and osteocalcin secretion (Moreau *et al.*, 1997; Henney, 2008). This indicates that BK channels play an important role in maintaining bone marrow physiological function and bone homeostasis (Zhang *et al.*, 2014).

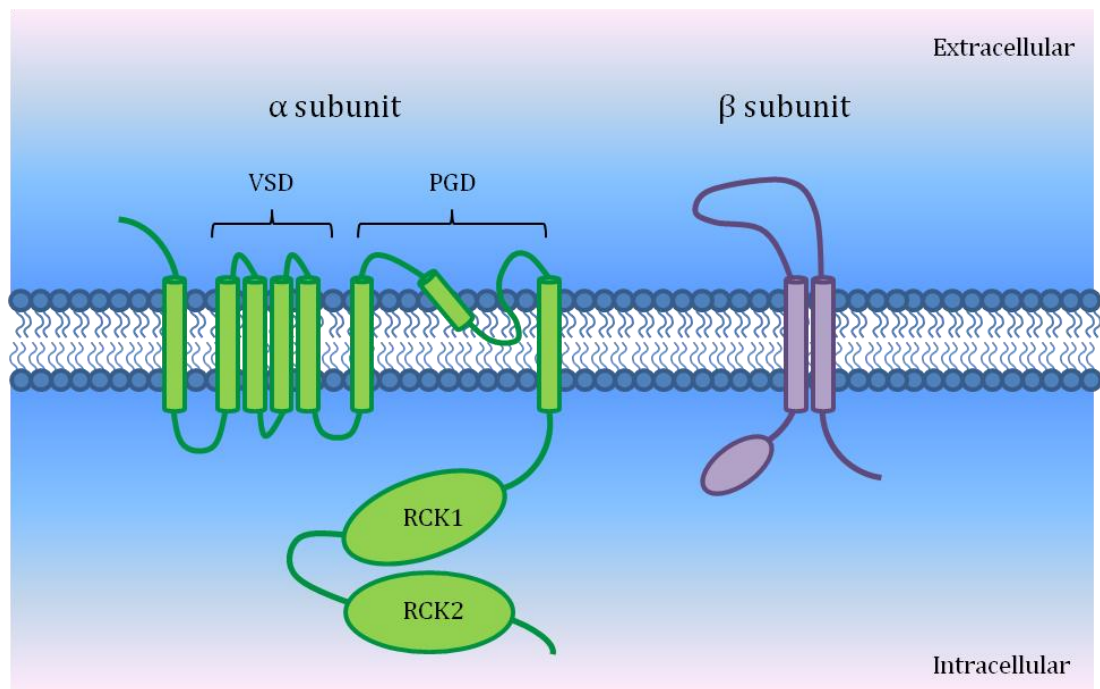


Figure 5.2: BK channel structure

Molecular constituents of BK channels, which are composed of 4 α -subunits and 4 β -subunits. VSD: voltage-sensor domain; PGD: pore-gate domain; RCK: regulator of K⁺ conductance. Adapted from (Li and Yan, 2016).

5.1.3. Chapter hypothesis, objectives and experimental strategy

As mentioned in the main introduction (chapter 1, section 1.4.2), ghrelin is an essential player of bone homeostasis, affecting both osteoblastogenesis and bone marrow adipogenesis, and ion channels are also involved in regulating cell proliferation and differentiation, including in bone. Do ghrelin and potassium channels play a role in 7F2 cell proliferation and adipogenic trans-differentiation?

The objective of this chapter was to investigate whether ghrelin and potassium channel ligands can influence 7F2 cell numbers and adipogenic differentiation, using cell

Chapter 5 – The influence of ghrelin and K⁺ channel ligands on adipogenic differentiation of 7F2 cells

counting, Oil Red O staining and RT-PCR and qRT-PCR tools. The effects of ghrelin treatment on cell numbers, lipid content and mRNA expression of differentiation markers were analysed; the hypothesis was that ghrelin could inhibit 7F2 cell adipogenic differentiation. The mRNA expression of several potassium channel subunits was investigated using RT-PCR, and the effects of potassium channel ligands on lipid content and cell numbers were tested. The hypothesis was that potassium channel blockers could inhibit 7F2 cell adipogenic differentiation and that potassium channel openers could promote 7F2 cell adipogenic differentiation.

5.2. Materials and Methods

5.2.1. Cell culture

5.2.1.1. Adipogenic differentiation and ghrelin treatment of 7F2 cells

7F2 cells were seeded at a density of 2500 cells/cm² and cultured with basal and adipogenic medium as described in section 2.1, and treated with 20 nM or 200 nM ghrelin (Cambridge Bioscience) for 7 days. After 7 days of culture, 7F2 cells were stained with Oil Red O as described in section 2.1.

5.2.1.2. Cell counting

See section 2.2.

5.2.1.3. Inhibition of GHSR

7F2 cells were cultured with basal and adipogenic medium as described previously, and treated with 20 nM ghrelin with or without 1mM of the GHSR blocker D-[Lys3] GHRP-6 (DLS, from Sigma). After 7 days of culture, mRNA was extracted and analysed by RT-PCR and qRT-PCR.

5.2.1.4. Treatment with tetraethylammonium (TEA)

A 3 mM stock solution of TEA was prepared by dissolving 24.855 mg of TEA in 45 ml of α -MEM. Medium was then filtered, then supplemented with 5 ml FBS (final concentration 10%). 7F2 cells were plated into 12-well tissue culture plates (Fisher Scientific) at a density of 2500 cells/cm² in basal or adipogenic medium with or without TEA at various concentrations (0.3 mM, 1 mM and 3 mM). Cells were incubated as usual for 7 days with medium replacement every 2-3 days. Pictures were taken daily under a microscope at a 200x magnification, except on week-ends. After 7 days, the cells were stained with Oil Red O as described in section 2.1.2.2. Cells were counted as described in section 2.2.

5.2.1.5. Treatment with diazoxide

A 40 mM stock solution of diazoxide was prepared by dissolving 92 mg of diazoxide in 1 ml of DMSO. 7F2 cells were plated into 12-well tissue culture plates (Fisher Scientific) at a density of 2500 cells/cm² in basal or adipogenic medium alone for 3 days; then the cells were cultured with basal or adipogenic medium with or without diazoxide at

Chapter 5 – The influence of ghrelin and K⁺ channel ligands on adipogenic differentiation of 7F2 cells

various concentrations (1 μ M, 10 μ M and 100 μ M), or with DMSO alone (0.25%), for the last 4 days of culture. After 7 days of culture, the cells were stained with Oil Red O as described in section 2.1.2.2.

5.2.2. Molecular biology

5.2.2.1. RNA extraction, DNase treatment and reverse transcription

See sections 2.3.1 and 2.3.2.

5.2.2.2. PCR

5.2.2.2.1. Oligonucleotide primers

See sections 8.1.1 and 8.1.5.

5.2.2.2.2. PCR reaction compositions and conditions

The PCR reaction composition is described in section 2.3.3. The PCR reaction conditions were optimised and are detailed in table 5.1. Nuclease-free water was used as a negative control and three house-keeping genes, *Hprt1*, *Eef2* and *Gapdh*, were used as positive controls.

Chapter 5 – The influence of ghrelin and K⁺ channel ligands on adipogenic differentiation of 7F2 cells

***Hprt1* and *Gapdh* primers:**

Step	Temperature °C	Time	No. of cycles
Initial denaturation	95	1 min	1
Denaturation	95	30 s	
Annealing	58	30 s	30
Extension	68	30 s	
Final extension	68	5 min	1
Soak	4	Indefinite	

***Eef2*, *Runx2*, *Alpl*, and *Cebpa* primers:**

Step	Temperature °C	Time	No. of cycles
Initial denaturation	95	1 min	1
Denaturation	95	30 s	
Annealing	58	30 s	35
Extension	68	30 s	
Final extension	68	5 min	1
Soak	4	Indefinite	

***Osteocalcin* primers (both sets):**

Step	Temperature °C	Time	No. of cycles
Initial denaturation	95	1 min	1
Denaturation	95	30 s	
Annealing	58	30 s	40
Extension	68	30 s	
Final extension	68	5 min	1
Soak	4	Indefinite	

***Glut4*, *Kcnj8*, *Kcnj11*, *Kcnd2*, *Kcnma1*, *Kcnmb1*, *Kcnmb2*, *Kcnmb3* and *Kcnmb4* primers:**

Step	Temperature °C	Time	No. of cycles
Initial denaturation	95	1 min	1
Denaturation	95	30 s	
Annealing	56	30 s	40
Extension	68	30 s	
Final extension	68	5 min	1
Soak	4	Indefinite	

Table 5.1: PCR reaction conditions

5.2.2.2.4. Gel electrophoresis

See section 2.3.4.

5.2.2.3. Quantitative PCR

See section 2.3.5.

5.2.3. Statistical analysis

Statistical analysis was performed as described in section 2.3.7. Data were expressed as mean ± standard deviation; the number of repeat assays is indicated by “n”. Differences were tested by ANOVA tests (with Tukey-Kramer post-hoc analysis), Kruskal-Wallis tests (with Dunn post-hoc analysis) and Welch’s anova (with Games-Howell post-hoc analysis). In qRT-PCR experiments, the statistical analyses were performed using raw C_T values and fold changes. P values lower than 0.05 were considered as statistically significant. The calculations were performed using the R software (<https://www.r-project.org/>, version 3.5.3).

5.3. Results

5.3.1. Effects of ghrelin on 7F2 cells and 7F2 cell-derived adipocytes

5.3.1.1. Effects of ghrelin on cell number

7F2 cells were cultured with basal or adipogenic medium, with or without 20 nM ghrelin, for 7 days; after 7 days of culture, cells were counted using a haemocytometer (figure 5.3). As observed previously, after 7 days of culture, the number of cells was significantly lower in wells cultured with adipogenic medium compared with basal medium ($p < 0.0001$; $n = 9$, 3 replicates per condition; Kruskal-Wallis and Dunn tests). Adding ghrelin to basal or adipogenic medium did not seem to affect cell numbers compared to basal or adipogenic medium alone, respectively.

5.3.1.2. Effects of ghrelin on adipogenic differentiation

5.3.1.2.1. Effect on lipid content

7F2 cells were cultured with basal or adipogenic medium, with or without 20 nM ghrelin, for 7 days and pictures were taken daily, except on week-ends. Figure 5.4.A shows pictures of cells taken at days 2, 4 and 7 of culture. Similarly to previous experiments, lipid droplets began to appear in cells at day 2 and continued growing over the length of the treatment in 7F2 cells cultured with adipogenic medium. Similarly, in 7F2 cells cultured with adipogenic medium + 20 nM ghrelin, lipid droplets began to form at day 2 of culture and became larger over time. No difference was observed between 7F2 cells cultured with basal medium alone or with basal medium + 20 nM ghrelin. After 7 days of culture, the cells were stained with Oil Red O (figure 5.4.B). Again, no difference was observed between 7F2 cells treated with ghrelin, and cells cultured in the absence of ghrelin. This was confirmed by extracting and quantifying the Oil Red O stain by measuring the absorbance at 490 nm (figure 5.4.C); there was no difference between adipogenic medium alone and adipogenic medium + 20 nM ghrelin ($p = 0.3198$, $n = 11$, 3 replicates per condition, Kruskal-Wallis test and Dunn post-hoc analysis), and no difference between basal medium alone and basal medium + 20 nM ghrelin ($p = 0.2015$, $n = 11$, 3 replicates per condition; Kruskal-Wallis test and Dunn post-hoc analysis). Similar results were obtained when treating the cells with 200 nM ghrelin (figure 5.5) ($n = 1$, 3 replicates per condition; ANOVA test and Tukey-Kramer post-hoc analysis).

5.3.1.2.2. Effect on differentiation marker mRNA expression

To further assess the effects of ghrelin treatment on the adipogenic differentiation of 7F2 cells, the mRNA expression of several osteoblastic and adipogenic differentiation markers was analysed using RT-PCR and qRT-PCR. 7F2 cells were cultured for 7 days with basal or adipogenic medium, with or without 20 nM or 200 nM ghrelin. Figure 5.6 shows pictures of agarose gels for two osteoblastic markers, Runx2 and ALP, and two adipocytic markers, PPAR γ and C/EBP α . The bands corresponding to Runx2 and ALP appeared less intense when the cells were cultured with adipogenic medium; whereas the band corresponding to ALP was more intense in cells cultured with basal medium containing ghrelin compared to cells cultured with basal medium alone. On the contrary, PPAR γ and C/EBP α mRNA expression was upregulated in cells cultured with adipogenic medium compared with basal medium; this effect was attenuated in 7F2 cells cultured with adipogenic medium + 20 nM ghrelin.

The mRNA expressions of osteoblastic and adipogenic markers were also analysed using qRT-PCR (n=2, 3 replicate samples per condition; each sample was run in duplicate in each assay) (figure 5.7). 7F2 cells were treated with 20 nM or 200 nM ghrelin. Osteocalcin mRNA expression was higher in 7F2 cells treated with 20 nM and 200 nM ghrelin in both basal medium and adipogenic medium, but the differences were not significant (p = 0.23, Kruskal-Wallis test). Similarly, 20 nM and 200 nM ghrelin did not significantly affect ALP mRNA expression (p = 0.11, Kruskal-Wallis test). Runx2 mRNA expression was significantly lower in 7F2 cells cultured with adipogenic medium (0.21 ± 0.49) compared to cells cultured with basal medium (1 ± 0.73 ; p = 0.0073, Kruskal-Wallis test and Dunn post-hoc analysis), but 20 nM and 200 nM ghrelin had no significant effect on Runx2 mRNA expression levels (figure 5.7. B). The mRNA expression of C/EBP α was higher in 7F2 cells cultured with adipogenic medium alone (10.47 ± 0.48) compared to cells cultured with basal medium alone (1 ± 0.74 ; p = 0.0003, Kruskal-Wallis test and Dunn post-hoc analysis); C/EBP α expression was also higher in cells cultured with adipogenic medium + 20 nM ghrelin (39.56 ± 0.10) compared to cells cultured basal medium + 20 nM ghrelin (1.36 ± 0.46 ; p = 0.0005, Kruskal-Wallis and Dunn tests) and higher in cells cultured with adipogenic medium + 200 nM ghrelin (13.95 ± 0.19) compared to cells cultured with basal medium + 200 nM ghrelin (1.02 ± 0.55 ; p = 0.0052, Kruskal-Wallis and Dunn tests), respectively (figure 5.7.D). However, 20 nM and 200 nM ghrelin had no significant effect on C/EBP α expression compared to basal or adipogenic medium alone. Similar results were obtained for PPAR γ expression (figure 5.7.D).

5.3.1.2.3. The effects of ghrelin in 7F2 cells may be mediated by GHSR

To test whether the effects of ghrelin on the mRNA expression of differentiation markers were mediated by GHSR, a blocker of GHSR, D-[Lys3] GHRP-6 (DLS, 1 mM) was added to basal medium and adipogenic medium containing 20 nM ghrelin. 7F2 cells were cultured for 7 days and RNA was extracted and analysed using RT-PCR and qRT-PCR. These experiments were only performed once. mRNA expression of differentiation markers was analysed using RT-PCR and photographs of agarose gels are shown in figure 5.8. When 7F2 cells were treated with adipogenic medium, the bands corresponding to osteoblastic markers osteocalcin, Runx2 and ALP PCR products appeared fainter, while the bands corresponding to adipocytic markers PPAR γ , C/EBP α and Glut4 PCR products appeared more intense. In cells cultured with adipogenic medium + 20 nM ghrelin, the bands corresponding to osteoblastic markers appeared even fainter, except for ALP. However, in the presence of 1 mM DLS, these bands appeared more intense, except for ALP. Similarly, in cells cultured with adipogenic medium + 20 nM ghrelin, the bands corresponding to adipocytic markers appeared slightly more intense, except for PPAR γ , but were fainter when the cells were cultured in the presence of 1 mM DLS. No RT controls are shown in figure 5.10; no PCR product was observed for any of the differentiation markers.

qRT-PCR analysis on differentiation markers was also performed to test the effects of 1 mM DLS on mRNA expression levels (figure 5.9). Adipogenic medium decreased the expression levels of Runx2 and ALP by 80% and 60% respectively, while the expression of C/EBP α and PPAR γ were respectively ten times and two times higher, compared to basal medium. When the cells were cultured with adipogenic medium + 20 nM ghrelin, the expression levels of both osteoblastic and adipocytic markers were increased compared to the expression levels in cells cultured with adipogenic medium alone. However, in cells cultured with adipogenic medium + 20 nM ghrelin + 1 mM DLS, the expression levels of all markers were decreased compared to cells cultured with adipogenic medium + 20 nM ghrelin, without DLS. Expression levels of all tested markers were lower in cells cultured with basal medium + 20 nM ghrelin + 1 mM DLS compared to cells cultured with basal medium + 20 nM ghrelin, without DLS.

5.3.1.3. Ionic mechanisms in 7F2 cells and 7F2 cell derived adipocytes, and the effects of ghrelin on these

5.3.1.3.1. K_{ATP} channels

mRNA was extracted from 7F2 cells cultured for 7 days with basal or adipogenic medium, with or without 20 nM ghrelin. RT-PCR analysis was performed for the K_{ATP} channel subunits (figure 5.11): the two pore-forming subunits Kir6.1 (*Kcnj8*) and Kir6.2 (*Kcnj11*) (figure 5.11.A); and the regulatory subunits SUR1 (*Abcc8*), and SUR2 (*Abcc9*), which has several isoforms (figure 5.11.B). Two sets of primers were used for SUR2 (*Abcc9*): the first one detected SUR2 mRNA for all isoforms, while the second one allowed to distinguish between the two isoforms SUR2A and SUR2B, with PCR product expected sizes of 397 bp and 221 bp, respectively. *Kcnj8* was detected at the mRNA level (figure 5.11.A), but the results were inconsistent: on some repeats, no PCR product could be detected, while on other repeats, one or several bands were detected, one of which corresponded to the expected size (155 bp). *Kcnj11* mRNA expression was not detected on the various repeats (n = 6) in cells cultured with basal or adipogenic medium alone in the early stage of this study, so it was not tested in cells treated with ghrelin. The regulatory subunit SUR1 (*Abcc8*) was also not detected at the mRNA level (figure 5.11.B). SUR2 (*Abcc9*) mRNA expression was detected; RT-PCR analysis with the second set of primers showed a band at 221 bp, which was the expected size for the SUR2B subunit.

qPCR analysis was performed for the K_{ATP} channel subunits that were detected at the mRNA level: Kir6.1 (*Kcnj8*) and SUR2 (*Abcc9*), with the first set of primers only, which detects all SUR2 isoforms at the mRNA level (figure 5.12). qPCR data confirmed that *Kcnj8* mRNA expression was low, with mean Cts of 29.52 for 7F2 cells cultured with basal medium, 30.85 for 7F2 cells cultured with adipogenic medium, 28.63 for 7F2 cells cultured with adipogenic medium + 20 nM ghrelin, and 32.20 for 7F2 cells cultured with basal medium + 20 nM ghrelin (n = 1, 3 replicate samples per condition; each replicate sample was run in duplicate) (figure 12.A). *Abcc9* expression levels were significantly higher in 7F2 cells cultured with adipogenic medium + 20 nM ghrelin (166.96 ± 0.13) compared to cells cultured with basal medium + 20 nM ghrelin (31.13 ± 0.14; p = 0.0248; Kruskal Wallis and Dunn tests; n = 1, 3 replicate samples per condition; each replicate sample was run in duplicate), and higher in cells cultured with adipogenic medium + 200 nM ghrelin (202.48 ± 0.31) compared to cells cultured with

Chapter 5 – The influence of ghrelin and K⁺ channel ligands on adipogenic differentiation of 7F2 cells

basal medium + 200 nM ghrelin (32.94 ± 0.27 ; $p = 0.0163$, Kruskal-Wallis and Dunn tests) (figure 12.B).

5.3.1.3.2. BK channel

mRNA was extracted from 7F2 cells cultured for 7 days with basal or adipogenic medium. RT-PCR analysis was performed for the BK channel subunits (figure 5.13): the pore-forming α subunit encoded by *Kcnma1* and the four regulatory β 1-4 subunits encoded by *Kcnmb1* to *Kcnmb4*. A band of 167 bp was observed in most repeats for *Kcnma1*; it appeared fainter for 7F2 cells cultured with adipogenic medium compared with basal medium. No band was detected for *Kcnmb1*, *Kcnmb3* and *Kcnmb4*. A faint band corresponding to 155 bp was observed for *Kcnmb2*.

qPCR analysis was performed for the BK channel subunit *Kcnma1* ($n = 1, 3$ replicate samples per condition; each replicate sample was run in duplicate) (figure 5.14). The mean Cts were relatively high, indicating that the *Kcnma1* mRNA expression level was low. *Kcnma1* mRNA expression was lower in adipogenic medium (0.18 ± 0.21) compared with basal medium (1 ± 0.49 ; $p = 0.04$, ANOVA test and Tukey-Kramer post-hoc analysis), which is consistent with the RT-PCR data, but it was restored when the cells were cultured with adipogenic medium containing 20 nM ghrelin (0.99 ± 0.30). *Kcnma1* mRNA expression was upregulated in cells cultured with basal medium + 20 nM compared with basal medium alone.

5.3.2. Pharmacological modulation of K⁺ channels: effect on adipogenesis

Having detected the expression of various ion channel subunits by RT-PCR, the next step was to investigate whether drugs which modify the activity of these ion channels could affect cell processes such as proliferation and differentiation, using tetraethylammonium (TEA), which is a generic blocker of voltage-dependent and Ca²⁺-activated K⁺ channels, and diazoxide, which is a K_{ATP} channel opener.

5.3.2.1. Effects of TEA

5.3.2.1.1. TEA decreases the amount of lipids in 7F2-cell derived adipocytes

7F2 cells were cultured with basal or adipogenic medium, with or without TEA at various concentrations (0.3 mM, 1 mM and 3 mM), for 7 days. Figure 5.15.A, B and C show pictures of the cells at days 2, 4 and 7 of culture. In 7F2 cells treated with adipogenic medium, lipid droplets began to appear around day 2 of treatment and grew

Chapter 5 – The influence of ghrelin and K⁺ channel ligands on adipogenic differentiation of 7F2 cells

in size and number over the rest of the treatment. Treating 7F2 cells with TEA did not prevent the apparition of lipid droplets; however TEA seemed to limit the size of these lipid droplets. This effect was concentration-dependent and was particularly visible in cells cultured with adipogenic medium containing 3 mM TEA. This was confirmed by Oil Red O staining after 7 days of treatment; the cells cultured with adipogenic medium containing TEA possessed smaller lipid droplets than the cells cultured with adipogenic medium alone (figure 5.15.D). The Oil Red O stain was extracted and quantified by measuring the absorbance at 490 nm; data are presented in figure 5.15.E (n = 4, with 2-3 replicates per condition); data were normalised to basal medium in figure 5.15.F. The absorbance value was relatively high (> 0.11) in cells cultured with basal medium due to the presence of many Oil Red O crystals in the wells despite repeated washings. Quantification of Oil Red O stain did not show any significant difference between the cells treated with the various concentrations of TEA (p = 0.64, Kruskal-Wallis test), but a trend could be seen, especially for cells cultured with adipogenic medium + TEA: the amount of Oil Red O stain decreased with increasing concentrations of TEA.

5.3.2.1.2. TEA decreases cell proliferation

7F2 cells were cultured for 7 days with basal or adipogenic medium, with or without various concentrations of TEA, for 7 days. Figure 5.15.A shows pictures of the cells at days 2, 4 and 7 of culture. TEA decreased cell proliferation in a dose-dependent manner. This was confirmed by counting the cells, using a haemocytometer, although the differences in cell numbers were not statistically significant (p = 0.06, Kruskal-Wallis test, n = 1, with 2 replicates per condition) (figure 5.16).

5.3.2.2. Effects of diazoxide on 7F2 cell adipogenic differentiation

The K_{ATP} channel opener diazoxide was tested at various concentrations against the adipogenic differentiation of 7F2 cells over a period of 7 days. 7F2 cells were cultured with basal or adipogenic medium for 3 days; then, culture medium was replaced with basal or adipogenic medium containing various concentrations of diazoxide (1 μM, 10 μM and 100 μM) for the last 4 days of culture. Figure 5.17.A shows pictures of the cells at day 7 of culture, and figure 5.17.B shows pictures of cells stained with Oil Red O after 7 days of culture. Diazoxide did not seem to affect the development and growth of lipid droplets. Diazoxide did not seem to affect cell number either; however, cell morphology was modified in the presence of diazoxide, especially at 100 μM. This may be due to the presence of DMSO, as the cells presented similar morphologies in the wells with basal or adipogenic medium + DMSO.

Chapter 5 – The influence of ghrelin and K⁺ channel ligands on adipogenic differentiation of 7F2 cells

The Oil Red O stain was extracted and quantified by measuring the absorbance at 490 nm; data are presented in figure 5.17.C (n = 3, with 3-4 replicates per condition in each repeat); data were normalised to basal medium in figure 5.17.D. Similarly to experiments with TEA, the absorbance was high (> 0.21) in wells of cells cultured with basal medium and adipogenic medium, due to the many Oil Red O crystals in the wells. Quantification of Oil Red O stain did not show any significant difference basal and adipogenic medium, and between the various concentrations of diazoxide (p = 0.85, Kruskal-Wallis test). However, a trend could be seen for cells cultured with adipogenic medium + diazoxide: the amount of Oil Red O stain decreased with increasing concentrations of diazoxide.

5.4. Discussion

This section of work aimed to study the effects of ghrelin treatment and potassium channel ligands on the proliferation and adipogenic differentiation of 7F2 cells.

5.4.1. Ghrelin treatment affects 7F2 cell differentiation, but not proliferation

Overall, 20 nM ghrelin treatment had no effect on 7F2 cells numbers, suggesting that it did not stimulate nor suppress cell proliferation, at least within the timeframe used (7 days). 20 nM and 200 nM ghrelin had no effect on lipid content: lipid droplets appeared at the same time as in cells cultured with adipogenic medium alone; Oil Red O staining showed no visible difference in the size or abundance of lipid droplets, which was confirmed by quantification of Oil Red O stain. qRT-PCR analysis showed that treatment with 20 nM and 200 nM ghrelin did not significantly alter the expression levels of both osteoblastic and adipocytic markers, although their expression levels were higher in the presence of 20 nM ghrelin compared to basal or adipogenic medium alone. The effects of 20 nM ghrelin on mRNA expression was attenuated by the addition of 1 mM DLS, which is a GHSR antagonist, suggesting that ghrelin signalling was mediated via GHSR. However, the effect of DLS was only tested once and further studies on this aspect of the work would be advised to gain confidence in the results.

Adipose tissue is a major endocrine organ, secreting various hormones and cytokines, called adipokines, in the circulation. These adipokines play crucial roles in regulation of various physiologic and pathologic processes, including metabolism and metabolic disorders; they affect various tissues, particularly bone. Leptin is one of the most abundant adipokines and is involved in the regulation of glucose metabolism; it is highly expressed in bone marrow adipocytes and has been shown to inhibit osteoblast function and bone formation (Rodeheffer and Horowitz, 2016; Yue *et al.*, 2016). Interestingly, ghrelin and leptin antagonise each other in the regulating energy balance, and these hormones have been shown to interact in regulation of bone metabolism, sensing the availability of nutrients and regulating directly and indirectly bone formation via paracrine and endocrine mechanisms (Delhanty *et al.*, 2014a). Consistent with this, ghrelin has been shown by multiple studies to stimulate bone formation and osteoblast proliferation and differentiation, both *in vivo* and *in vitro* (Kim *et al.*, 2005; Choi *et al.*, 2013). On the other hand, *in vivo* experiments also show that ghrelin increases bone marrow adiposity (Thompson *et al.*, 2004); *in vitro*, some studies have shown that preadipocyte proliferation and differentiation was directly stimulated by

Chapter 5 – The influence of ghrelin and K⁺ channel ligands on adipogenic differentiation of 7F2 cells

ghrelin, but others have reported that overexpression of ghrelin inhibited adipogenesis (Zhang *et al.*, 2004). Ghrelin is very likely to have tissue- and cell type-specific actions; in bone, it is unclear whether ghrelin alters MSC differentiation, or whether ghrelin stimulates the differentiation of cells already committed to the osteoblastic or adipocytic lineages.

It is difficult to say whether ghrelin promoted or suppressed the adipogenic differentiation of 7F2 cells in this study. The effects on lipid content were inconsistent; no effect was detected when observing the cells stained with Oil Red O under the microscope, and when analysing the Oil Red O stain quantification data, from one repeat to another, ghrelin either increased, decreased, or had no visible effect on lipid content, suggesting that there was a great variability from one repeat to another. Several factors may have contributed to this variability; Oil Red O crystals formed even though the staining solution was filtered. These crystals attached to the cells, despite repeated washings, and they were not homogenous between the wells and between the repeats. Also, as shown in Chapter 3, local cell density has an influence on lipid content, with higher densities increasing lipid content of the cells. Overall, ghrelin did not seem to have a stimulatory or inhibitory effect on lipid content. In addition, treatment with 20 nM ghrelin promoted the mRNA expression of both osteoblastic and adipocytic markers, but these changes in expression levels were not statistically significant. This may be due to the fact that there was a great variability between qRT-PCR repeats, and that few repeat assays were performed.

The absence of a clear effect of ghrelin treatment may be due to several factors. First, here 7F2 cells were treated with human ghrelin instead of mouse ghrelin. Ghrelin is highly conserved, especially in mammals; mouse ghrelin differs from human ghrelin by 2 amino acids, and the region that can be acylated and that is involved in GHSR binding is conserved (Kojima and Kangawa, 2005), but treating 7F2 cells with mouse ghrelin may have a stronger, clearer effect on adipogenic differentiation. In addition, ghrelin has a very short half-life in cell culture (Zhang *et al.*, 2004); overexpressing ghrelin or replacing ghrelin more frequently in the culture medium may have a stronger effect on 7F2 cell adipogenic differentiation. Ghrelin at nanomolar concentrations can activate GHSR1a *in vitro* (Kojima *et al.*, 1999) and circulating levels of ghrelin are in the range 0.1 to 0.5 nM (Callaghan and Furness, 2014). However, since many tissues express ghrelin, local concentrations in those tissues may be higher; consistent with this, assays that detect bound peptide measure higher levels of ghrelin (3-4 nM) (Callaghan and Furness, 2014). Here, concentrations of 20 nM and 200 nM were used, but a wider

range of concentrations may be used in future investigations. Moreover, 7F2 cells express a ghrelin variant retaining intron 2, and mRNA of this variant is much more abundant than that of native ghrelin. If this variant is expressed at the protein level, it would be interesting to investigate whether it can affect cell proliferation or adipogenic differentiation of 7F2 cells.

5.4.2. Potassium channel ligands modulate proliferation and adipogenic differentiation of 7F2 cells

The expression of various potassium channel subunits was analysed by RT-PCR and qRT-PCR. Several ion channel subunits were detected in both 7F2 cells and 7F2 cell-derived adipocytes, in particular the K_{ATP} subunits KCNJ8 (Kir6.1) and SUR2B, and the BK channel subunits KCNMA1 (KCa1.1) and KCNMB2; however KCNJ8 and KCNMA1 expression levels were low. SUR2B was slightly upregulated in 7F2 cell-derived adipocytes compared to 7F2 cells cultured with basal medium, and strongly upregulated when the cells were treated with 20 nM and 200 nM ghrelin.

BK channels are expressed in several human osteoblastic cells, including primary human HOB-c osteoblasts, MG63 and SaOS-2 human osteoblast-like cell lines. MG63 cells and primary osteoblasts express the α subunit and all four associated β subunits, and functional BK channels could be readily recorded in single-channel patch clamp experiments, suggesting that these channels are abundant (Henney, 2008) and that BK channels play an important role in human osteoblasts. In the present study however, BK channel α subunit expression was relatively low and only a very low expression of β 2 could be detected by RT-PCR analysis. In addition, the α subunit was downregulated in 7F2 cell-derived adipocytes compared to 7F2 osteoblastic cells. This suggests that this family of channel may not play a central role in 7F2 cells, which are murine osteoblast-like cells; in this cell type, BK channels may be an artefact from cell culture. Ion channel expression patterns, and particularly potassium channel expression patterns, seem to be species-specific. For example, mouse BMSCs highly express intermediate-conductance Ca²⁺-activated K⁺ channels (Tao *et al.*, 2007), whereas it is not detected in human BMSCs, which rather express BK channels (Heubach *et al.*, 2004; Li *et al.*, 2005).

As the expression of several potassium channel subunits was detected in 7F2 cells, the role of potassium channels in regulating proliferation and adipogenic differentiation was tested by modulating ion channel activity via two types of pharmacological agents: TEA, which is a blocker of voltage-dependent and Ca²⁺-activated K⁺ channels, and

Chapter 5 – The influence of ghrelin and K⁺ channel ligands on adipogenic differentiation of 7F2 cells

diazoxide, which is a K_{ATP} opener. The effects of TEA and diazoxide on adipogenic differentiation were assessed by Oil Red O staining of lipid droplets and quantification of stain; the effects of TEA and diazoxide on the mRNA expression levels of differentiation markers could not be tested due to lack of time.

Diazoxide has an inhibitory effect on rat preadipocyte proliferation and differentiation (50 μM, 100 μM and 150 μM diazoxide) (Wang *et al.*, 2007) and 100 μM diazoxide was shown to activate K_{ATP} channels in electrophysiology experiments (Larsson *et al.*, 1993), although diazoxide is more effective when applied to the intracellular rather than the extracellular side of the membrane (Kozlowski *et al.*, 1989). Here, diazoxide (1 μM, 10 μM and 100 μM) did not have any significant effect on 7F2 cell numbers or lipid content, suggesting that K_{ATP} channels may not play a role in 7F2 cell proliferation or adipogenic differentiation. However, a mistake was made when preparing the culture medium containing diazoxide: the concentration of DMSO was not adjusted between the various doses of diazoxide tested, which very likely biased the results. Hence, 1 μM diazoxide contained 0.0025% DMSO, 10 μM diazoxide contained 0.025% DMSO, and 100 μM diazoxide contained 0.25% DMSO. The concentration of the DMSO control was adjusted to match that of 100 μM diazoxide (0.25% DMSO). Repeating this experiment with correct preparation of the the medium containing diazoxide may provide more exploitable data. Also, only one K_{ATP} channel opener was tested; using other K_{ATP} channel openers or channel blockers may provide useful data on the role of K_{ATP} channels in 7F2 cells. Besides, K_{ATP} channels regulate osteocalcin secretion in osteoblasts (Moreau *et al.*, 1997) as well as secretion of other hormones such as insulin (Seino *et al.*, 2000; Ashcroft, 2005) and leptin (Standridge *et al.*, 2000). K_{ATP} channels may regulate osteocalcin secretion from 7F2 cells and adipokine secretion for 7F2 cell-derived adipocytes, which was not tested here.

Contrary to diazoxide, TEA (0.3 mM, 1 mM and 3 mM) decreased cell number and limited the size of lipid droplets inside 7F2 cell-derived adipocytes in a concentration-dependent manner. This range of concentrations was chosen based on concentrations used in other studies: 3mM TEA increased MG63 cell numbers without increasing the number of dead cells, whereas 10-30 mM TEA caused cell death (Li, 2012). In electrophysiology experiments using mouse neuroblastoma cells, the concentration for half maximal block of voltage-dependent potassium channels by external TEA was 80 μM in excised membrane patches (Im and Quandt, 1992), and 0.6 mM TEA blocked delayed rectifier potassium channels in whole-cell configuration when applied to the external solution (Quandt and Im, 1992). The fact that TEA limited the size of lipid

Chapter 5 – The influence of ghrelin and K⁺ channel ligands on adipogenic differentiation of 7F2 cells

droplets suggests that K⁺ channels may be involved in the regulation of the adipogenic differentiation of 7F2 cells. K⁺ channels, and particularly voltage-dependent and Ca²⁺-activated K⁺ channels, are involved in regulating proliferation and adipogenic differentiation of MSCs and preadipocytes. For example, the intermediate conductance Ca²⁺-activated K⁺ channels K_{Ca}3.1 participate in regulating cell proliferation in mouse preadipocytes (Zhang *et al.*, 2012).

5.4.2. Chapter conclusions

The hypothesis that ghrelin could stimulate 7F2 cell proliferation was not verified. There was no experimental evidence that ghrelin inhibits adipogenic differentiation either; 20 nM ghrelin did not affect lipid content, but increased the expression levels of both osteoblastic and adipocytic markers, although this effect was not statistically significant. However, only two concentrations of ghrelin were tested (20 nM and 200 nM), and the ghrelin used here was human; testing other concentrations, and using mouse ghrelin may be interesting in future work. In addition, the effects of 20 nM ghrelin on the expression of differentiation markers were attenuated in the presence of a GHSR blocker, DLS, suggesting that the effects of ghrelin are mediated by this receptor.

Expression of several K⁺ channel subunit was detected in 7F2 cells and adipocytes, including K_{ATP} channel subunits (Kir6.1 and SUR2B) and BK channel subunits (α and β 2); Kir6.1 and SUR2B were upregulated by 20 nM ghrelin. TEA, but not diazoxide, decreased cell proliferation and adipogenic differentiation in 7F2 cells, suggesting a role for K⁺ channels in these processes.

Since K⁺ channels may play a role in regulating 7F2 cell proliferation and adipogenic differentiation, the next stage of this study was to identify the ion channels present in 7F2 cells, using electrophysiology techniques.

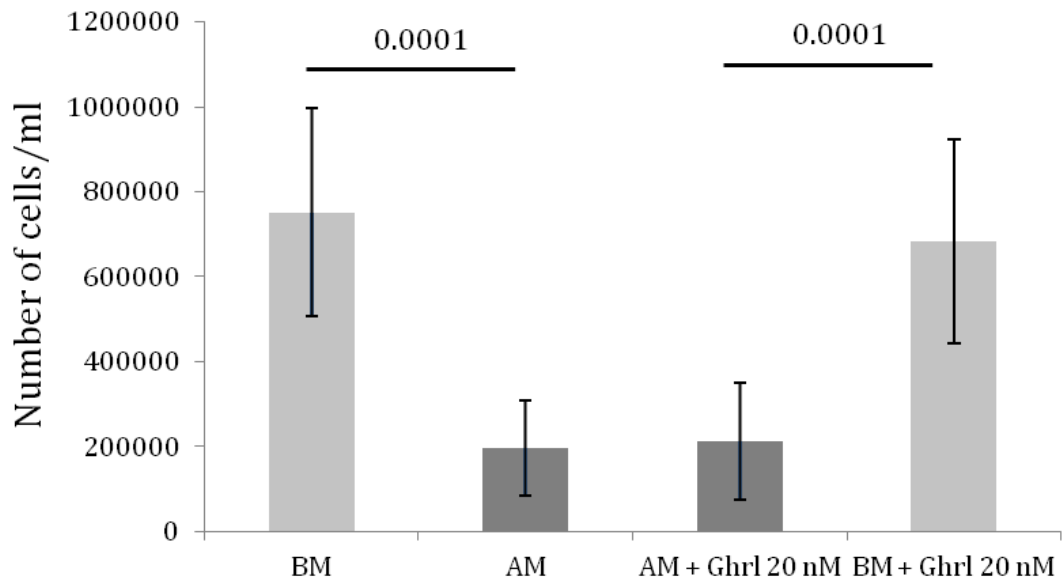


Figure 5.3: Effects of 20 nM ghrelin on cell numbers

7F2 cells were cultured with basal (BM) or adipogenic medium (AM) with or without 20 nM ghrelin for 7 days. After 7 days of culture, cells were counted. Data are mean \pm SD (n=9, 3 replicates per condition in each assay; Kruskal-Wallis and Dunn tests).

Chapter 5 – The influence of ghrelin and K⁺ channel ligands on adipogenic differentiation of 7F2 cells

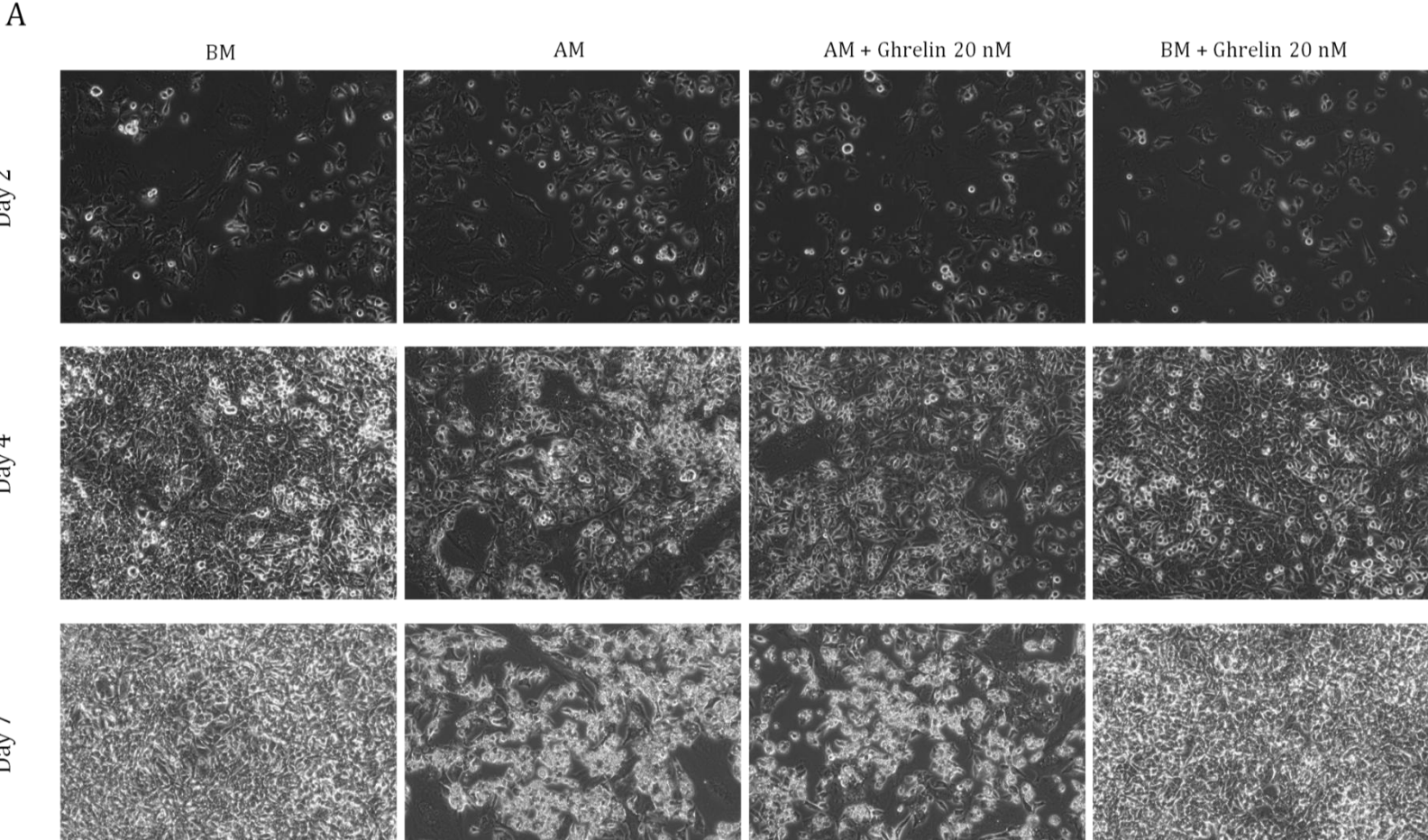


Figure 5.4: Effects of 20 nM ghrelin on the lipid content (part 1)

7F2 cells were cultured for 7 days with basal (BM) or adipogenic medium (AM), with or without 20 nM ghrelin. A: Pictures of cells at days 2, 4 and 7 of culture.

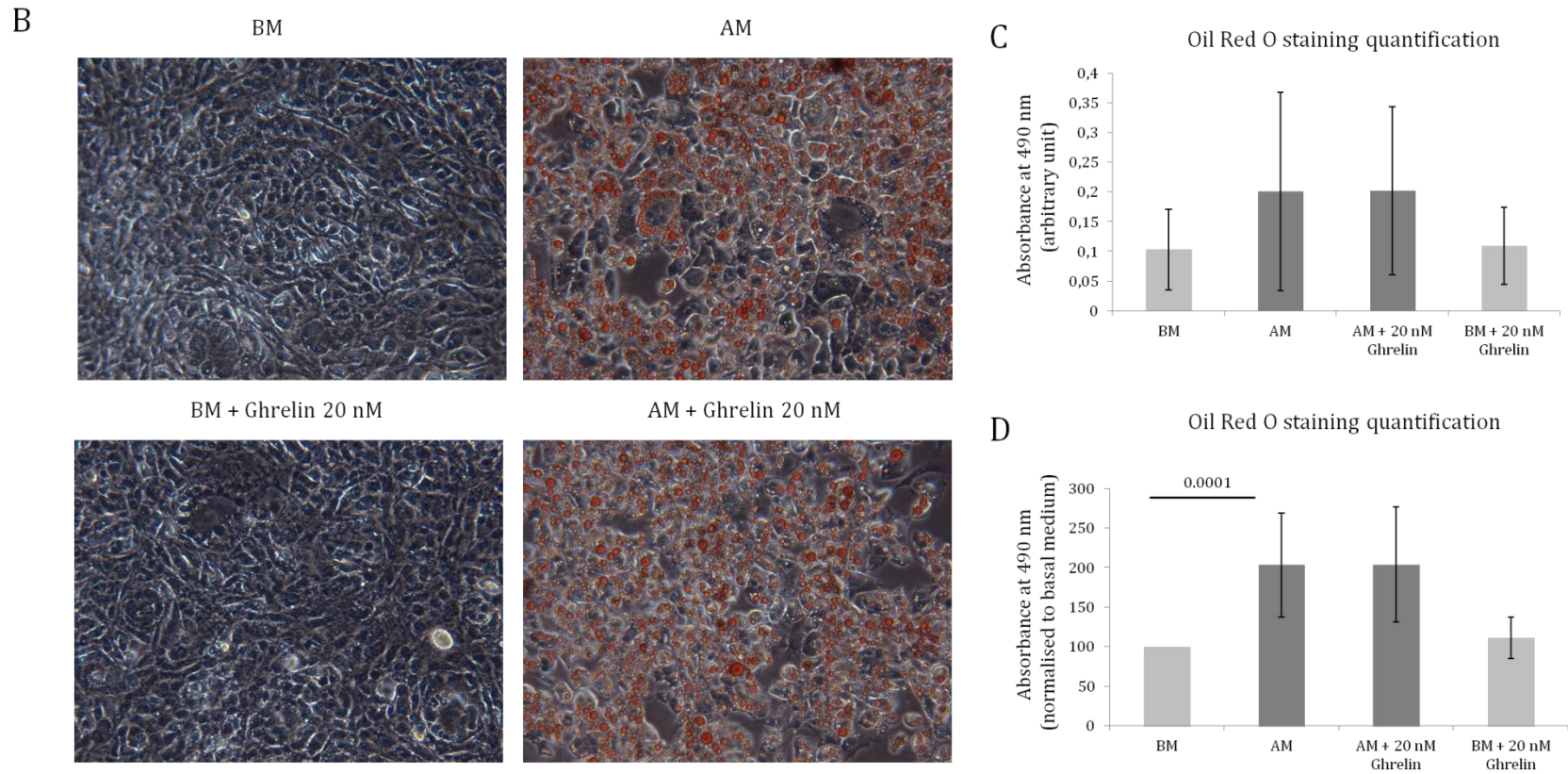


Figure 5.4: Effects of 20 nM ghrelin on the lipid content (part 2)

B: Pictures of 7F2 cells stained with Oil Red O. C and D: Quantification of Oil Red O by measuring the absorbance at 490 nm; (C) represents raw data, and (D) represents data normalised to basal medium. Data are mean \pm SD (n = 11, 3 replicates per condition in each assay; Kruskal-Wallis tests and Dunn post-hoc analyses).

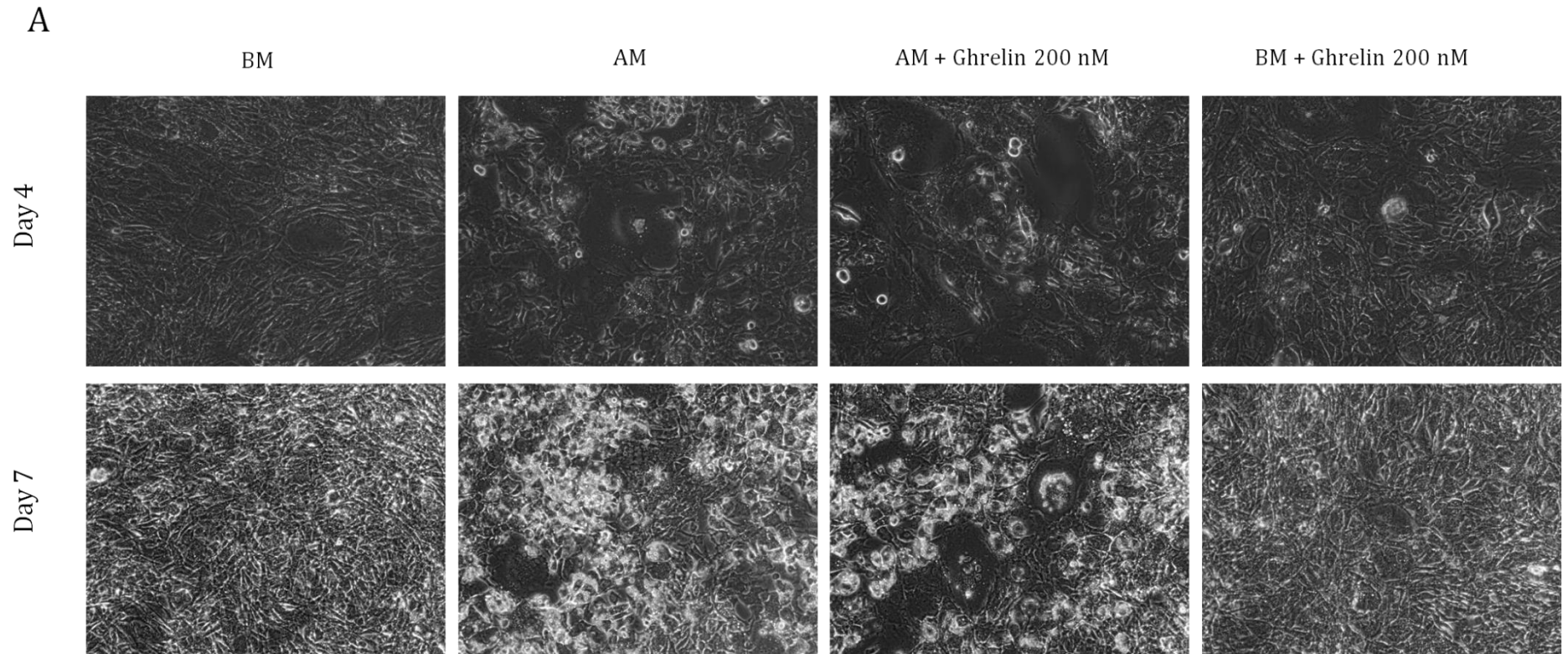
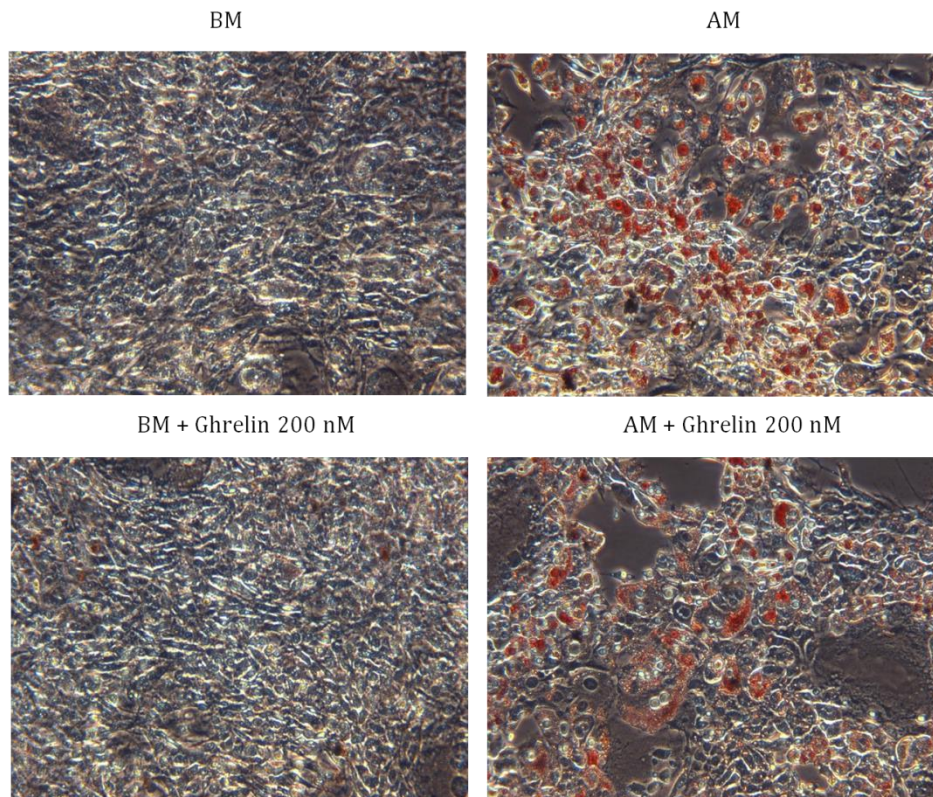


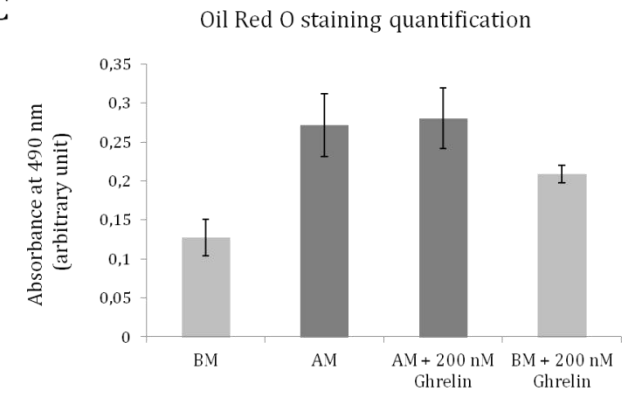
Figure 5.5: Effects of 200 nM ghrelin on lipid content (part 1)

7F2 cells were cultured for 7 days with basal (BM) or adipogenic medium (AM), with or without 200 nM ghrelin. A: Pictures of cells at days 2, 4 and 7 of culture.

B



C



D

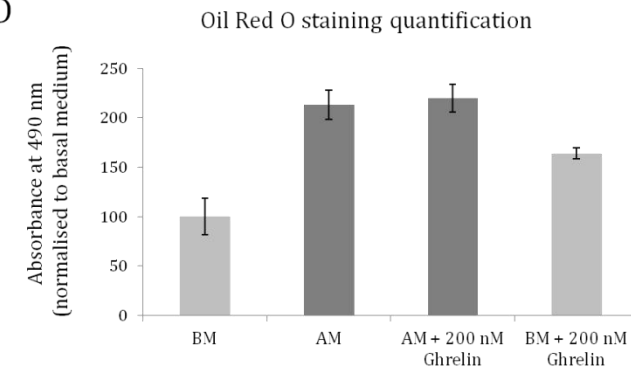


Figure 5.5: Effects of 200 nM ghrelin on lipid content (part 2)

B: Pictures of 7F2 cells stained with Oil Red O. C and D: Quantification of Oil Red O by measuring the absorbance at 490 nm; (C) represents raw data, and (D) represents data normalised to basal medium. Data are mean \pm SD (n = 1, 3 replicates per condition; raw data: ANOVA test; normalised data: Kruskal-Wallis test and Dunn post-hoc analysis).

Chapter 5 – The influence of ghrelin and K⁺ channel ligands on adipogenic differentiation of 7F2 cells

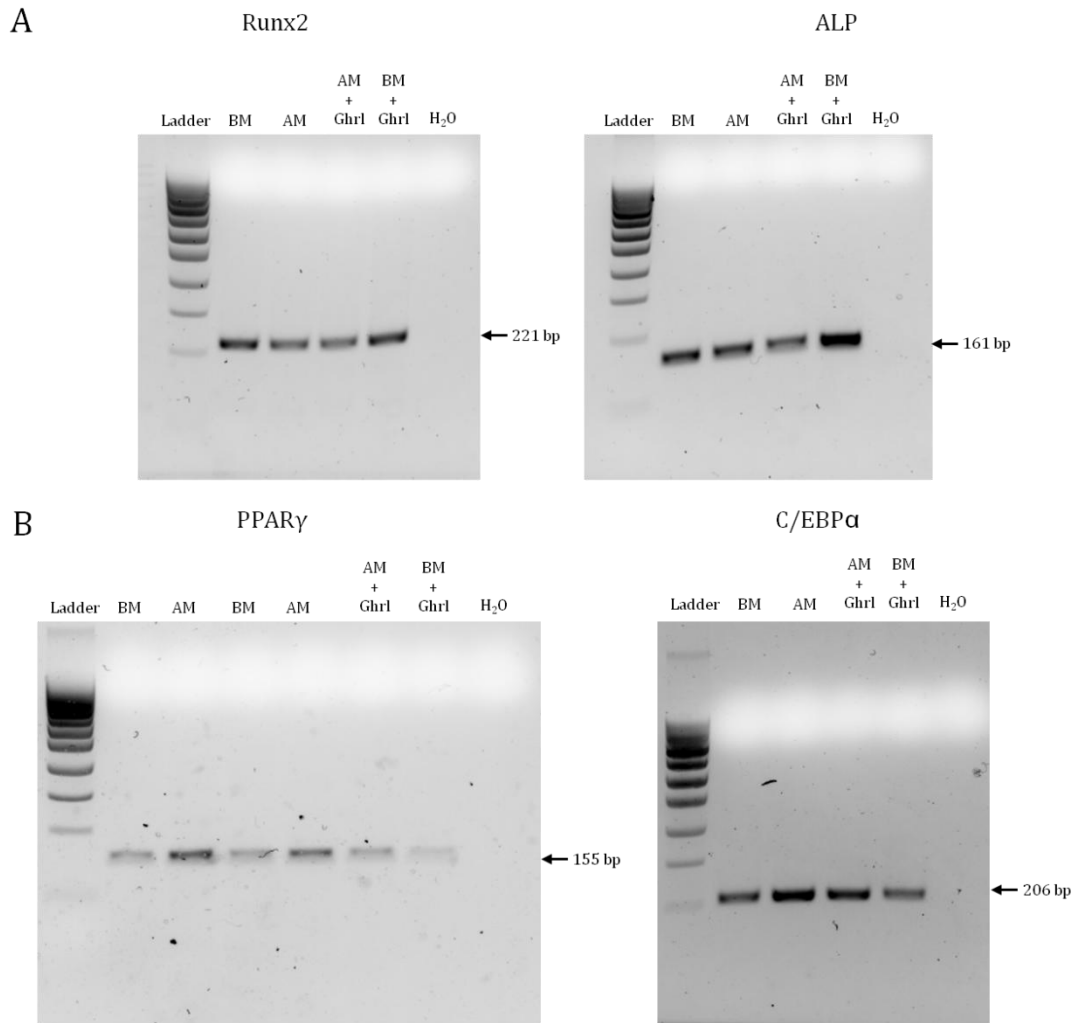


Figure 5.6: RT-PCR analysis of differentiation markers in 7F2 cells treated with 20 nM ghrelin

7F2 cells were cultured for 7 days with basal (BM) or adipogenic medium (AM), with or without 20 nM ghrelin. After 7 days of culture, RNA was extracted and gene expression was analysed using RT-PCR. A: RT-PCR for two osteoblastic markers, Runx2 and ALP. B: RT-PCR analysis of two adipocytic markers, PPAR γ and C/EBP α .

Chapter 5 – The influence of ghrelin and K⁺ channel ligands on adipogenic differentiation of 7F2 cells

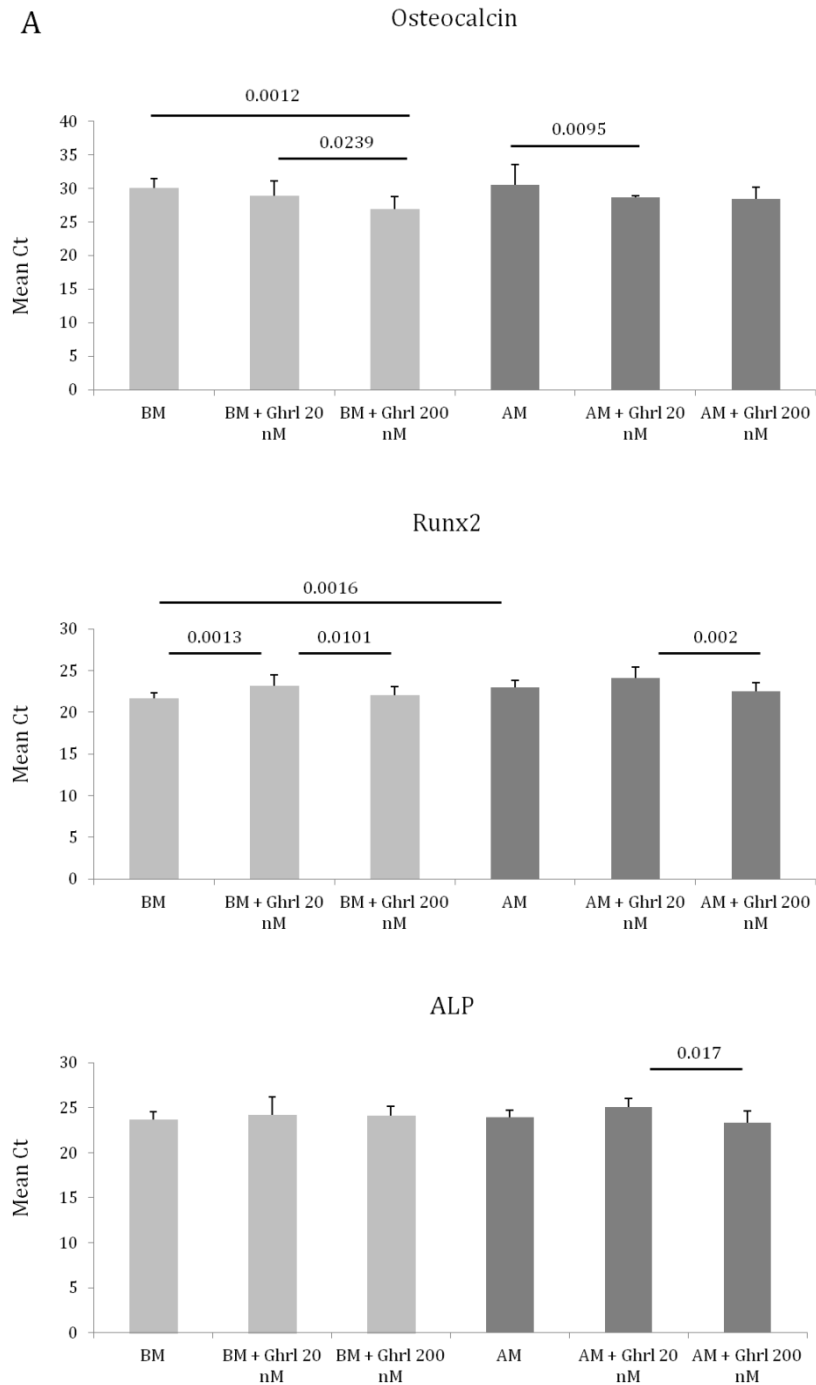


Figure 5.7: qRT-PCR analysis of differentiation markers in 7F2 cells treated with 20 nM and 200 nM ghrelin (part 1)

7F2 cells were cultured for 7 days with basal (BM) or adipogenic medium (AM), with or without 20 nM or 200 nM ghrelin. After 7 days of culture, RNA was extracted and gene expression was analysed using RT-PCR. A: qRT-PCR analysis for the osteoblastic markers osteocalcin, Runx2, and ALP. Data are mean Ct + SD (n = 2, with 3 replicate samples per condition in each assay; each sample was run in duplicates; Kruskal-Wallis tests and Dunn post-hoc analysis for osteocalcin and Runx2; Welch's anova and Games-Howell post-hoc analysis for ALP).

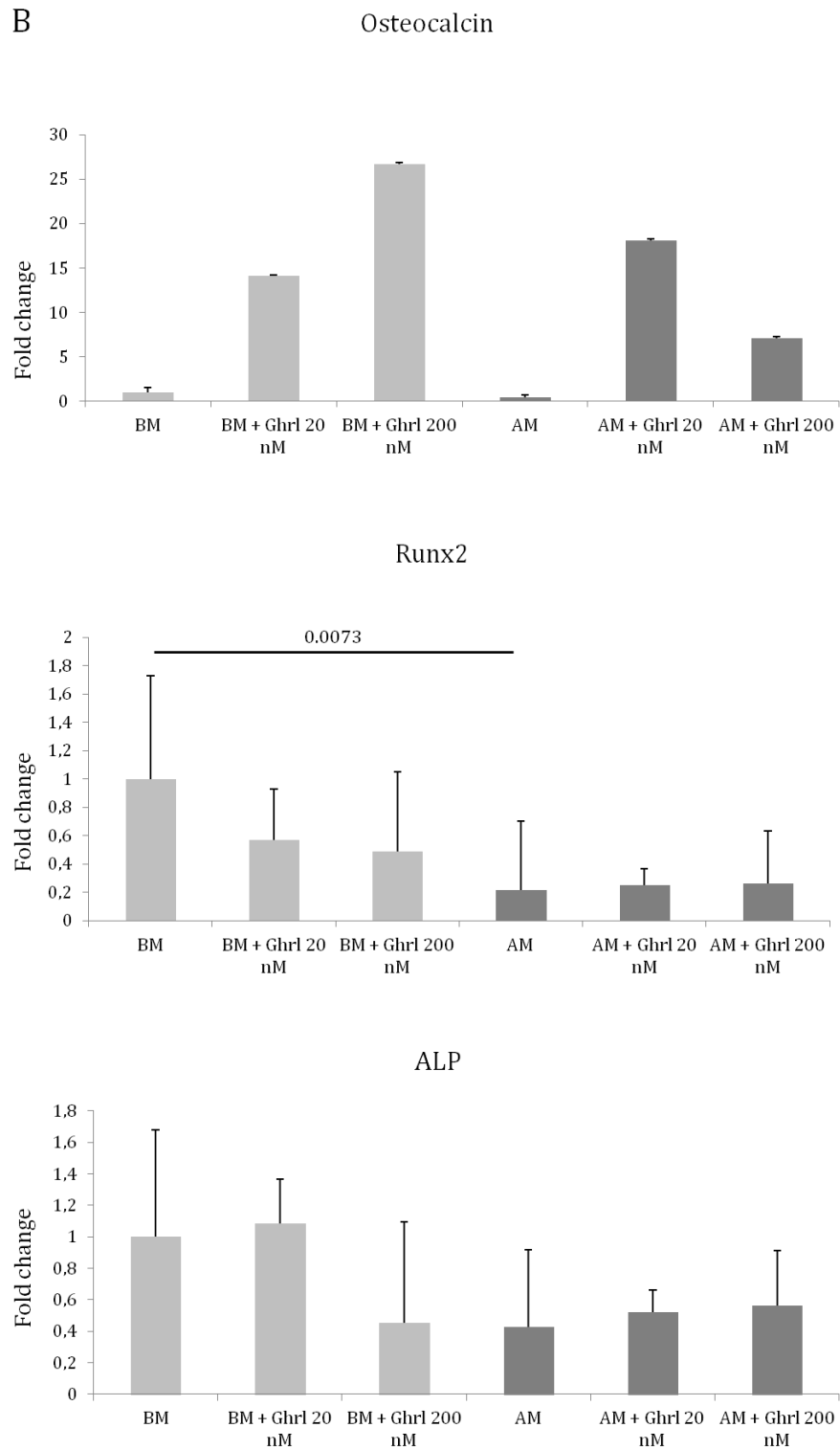


Figure 5.7: qRT-PCR analysis of differentiation markers in 7F2 cells treated with 20 nM and 200 nM ghrelin (part 2)

B: qRT-PCR analysis for the osteoblastic markers osteocalcin, Runx2, and ALP. Data are fold change + SD, normalised to HPRT1 expression (n = 2, 3 replicate samples per condition in each assay; each sample was run in duplicate; Kruskal-Wallis tests and Dunn post-hoc analysis).

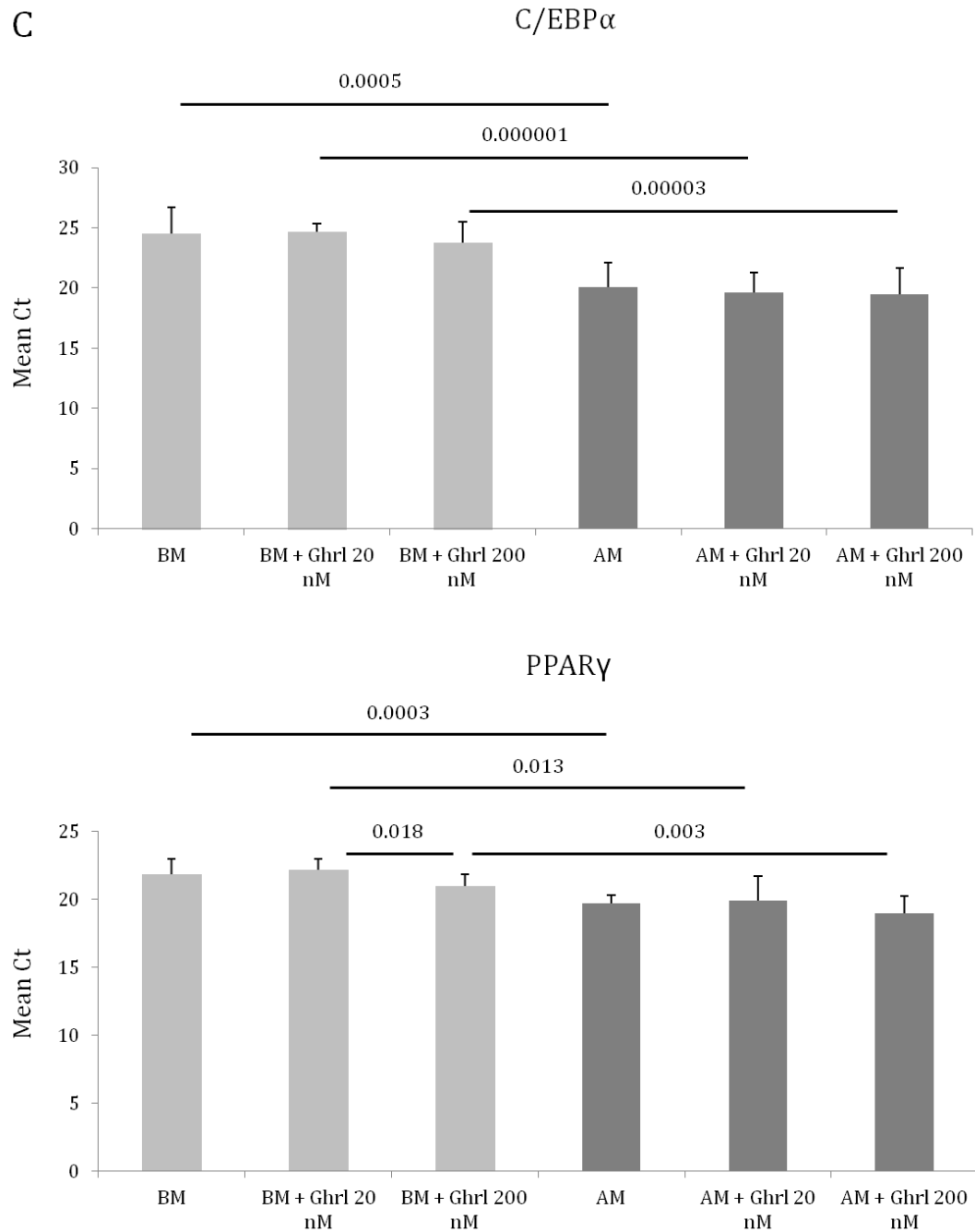


Figure 5.7: qRT-PCR analysis of differentiation markers in 7F2 cells treated with 20 nM and 200 nM ghrelin (part 3)

C: qRT-PCR analysis for the adipocytic markers PPAR γ and C/EBP α . Data are mean Ct + SD (n = 2, 3 replicate samples per condition in each assay; each sample was run in duplicate; Welch's anova and Games-Howell post-hoc analyses).

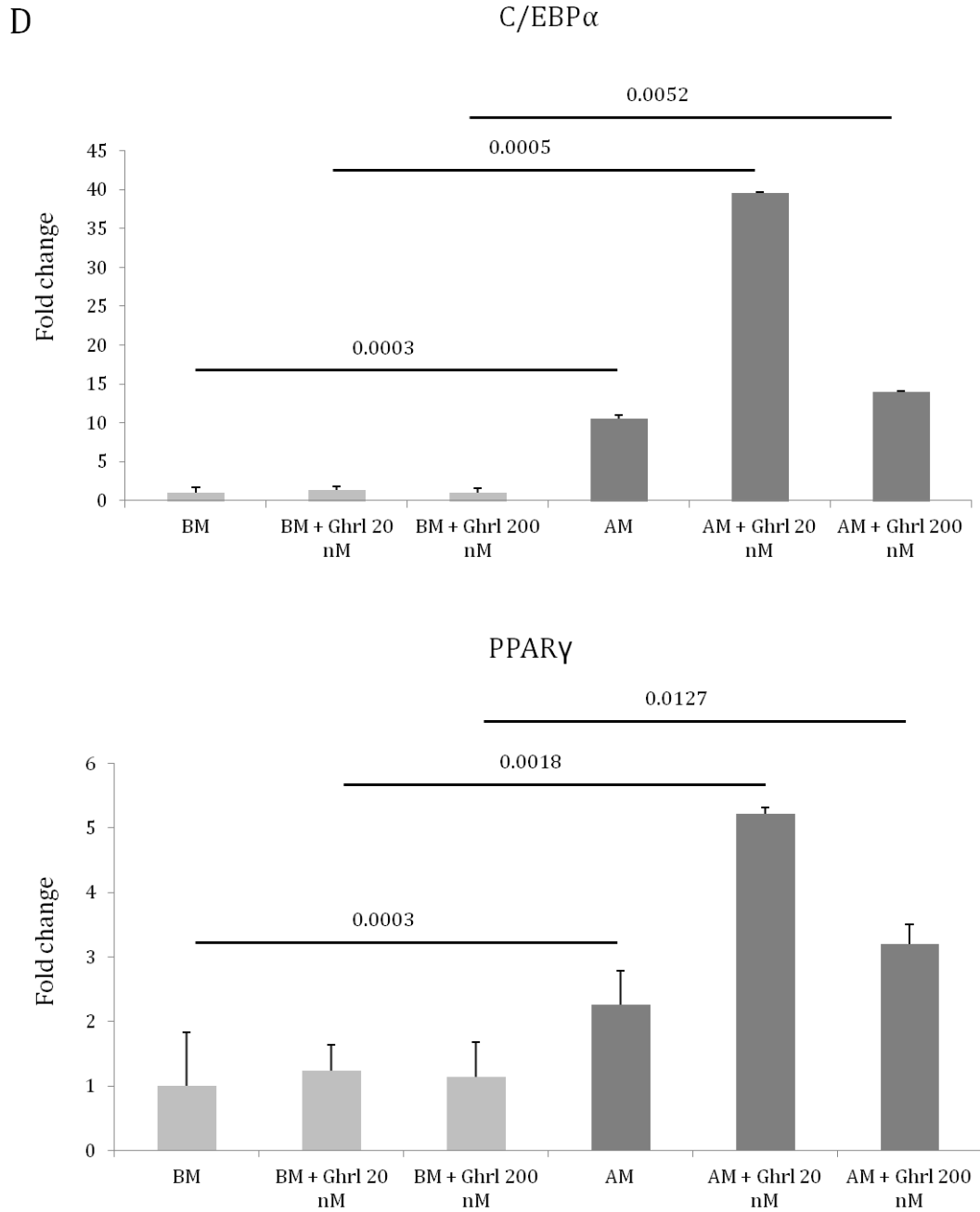


Figure 5.7: qRT-PCR analysis of differentiation markers in 7F2 cells treated with 20 nM and 200 nM ghrelin (part 4)

D: qRT-PCR analysis for the adipocytic markers PPAR γ and C/EBP α . Data are fold change + SD, normalised to HRPT1 expression (n = 2, 3 replicate samples per condition in each assay; each sample was run in duplicate; Kruskal-Wallis tests and Dunn post-hoc analyses).

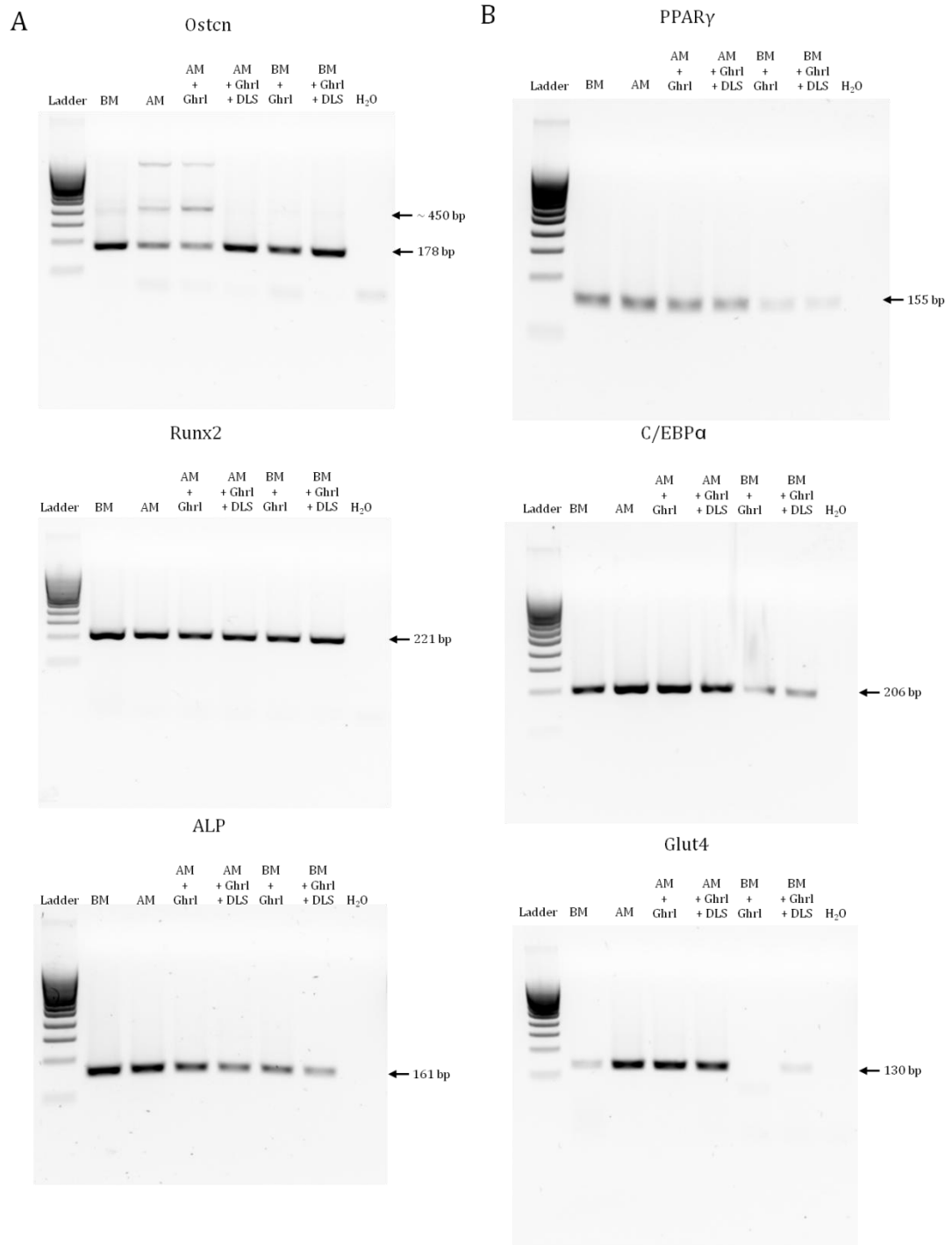


Figure 5.8: Role of GHSR in the effects of ghrelin on the adipogenic differentiation of 7F2 cells: RT-PCR analysis

7F2 cells were cultured for 7 days with basal (BM) or adipogenic medium (AM), with or without 20 nM ghrelin, and with or without GHSR blocker DLS. A; RT-PCR analysis of the osteoblastic markers osteocalcin, Runx2 and ALP. B: RT-PCR analysis of the adipogenic markers PPAR γ , C/EBP α and Glut4 (n=1).

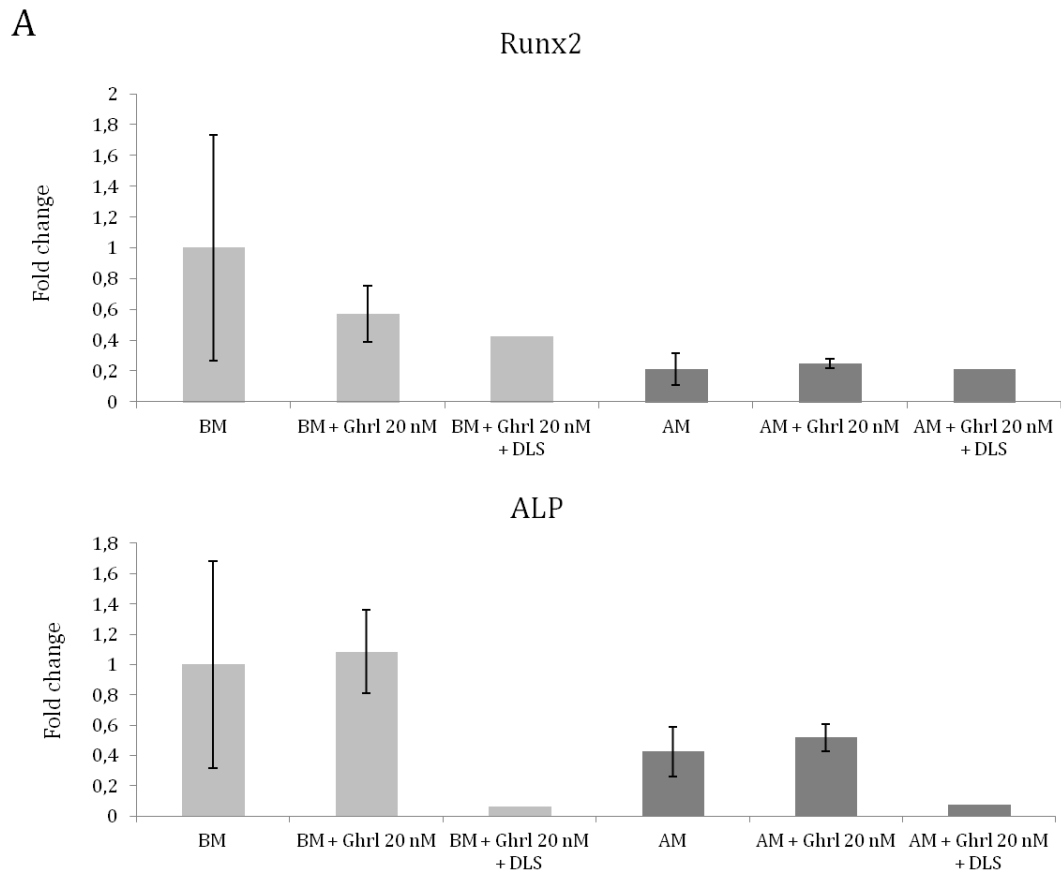


Figure 5.9: Role of GHSR in the effects of ghrelin on the adipogenic differentiation of 7F2 cells: qRT-PCR analysis (part 1)

7F2 cells were cultured for 7 days with basal (BM) or adipogenic medium (AM), with or without 20 nM ghrelin, and with or without GHSR blocker DLS. After 7 days of culture, RNA was extracted and gene expression was analysed using RT-PCR. A; qRT-PCR analysis of the osteoblastic markers Runx2 and ALP. Data are fold change \pm SD ($n = 2, 3$ replicate samples per condition in each assay, except for AM + Ghrl 20 nM + DLS and BM + Ghrl 20 nM + DLS, where the experiment was only performed once ($n = 1$), with only one sample per condition; each sample was run in duplicate). Expression was normalised to HPRT1.

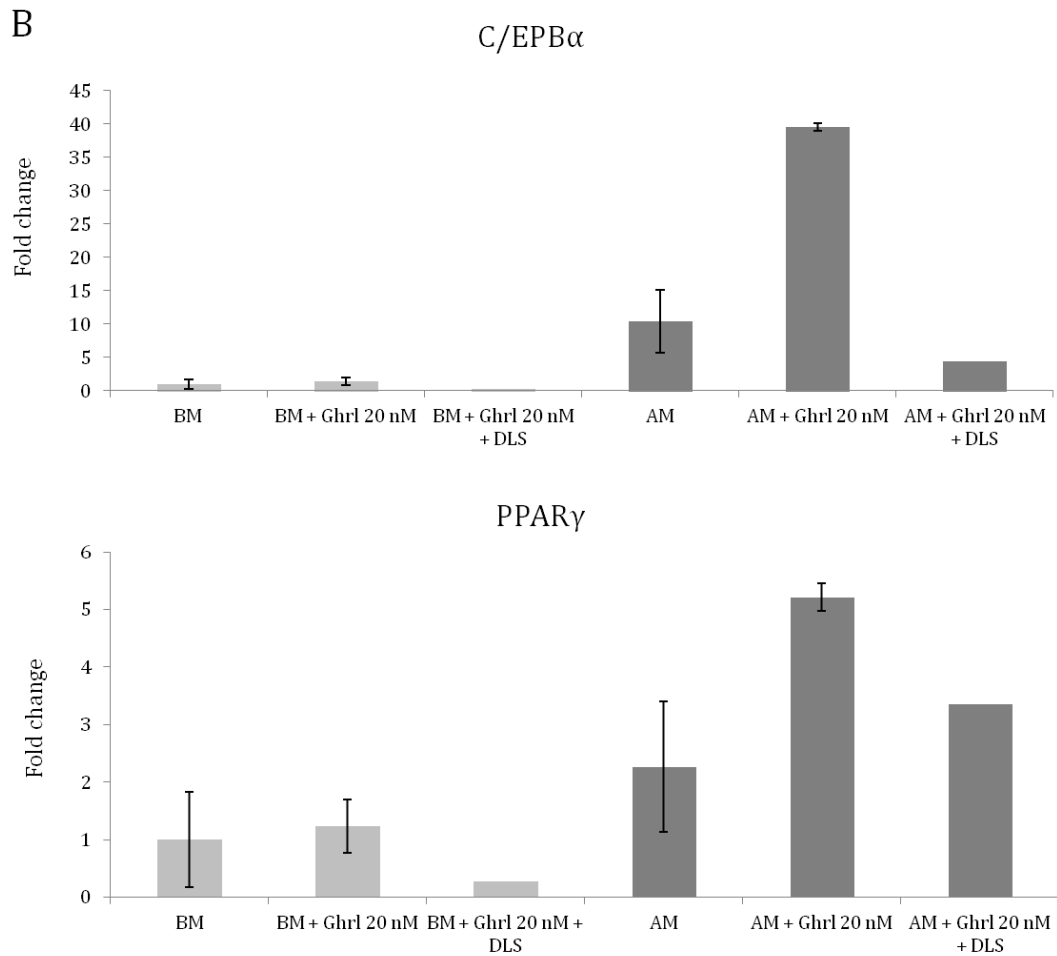


Figure 5.9: Role of GHSR in the effects of ghrelin on the adipogenic differentiation of 7F2 cells: qRT-PCR analysis (part 2)

B: qRT-PCR analysis of the adipogenic markers *C/EBP α* and *PPAR γ* . Data are fold change \pm SD ($n = 2, 3$ replicate samples per condition in each assay, except for AM + Ghrl 20 nM + DLS and BM + Ghrl 20 nM + DLS, where the experiment was only performed once ($n = 1$), with only one sample per condition; each sample was run in duplicate). Expression was normalised to *HPRT1*.

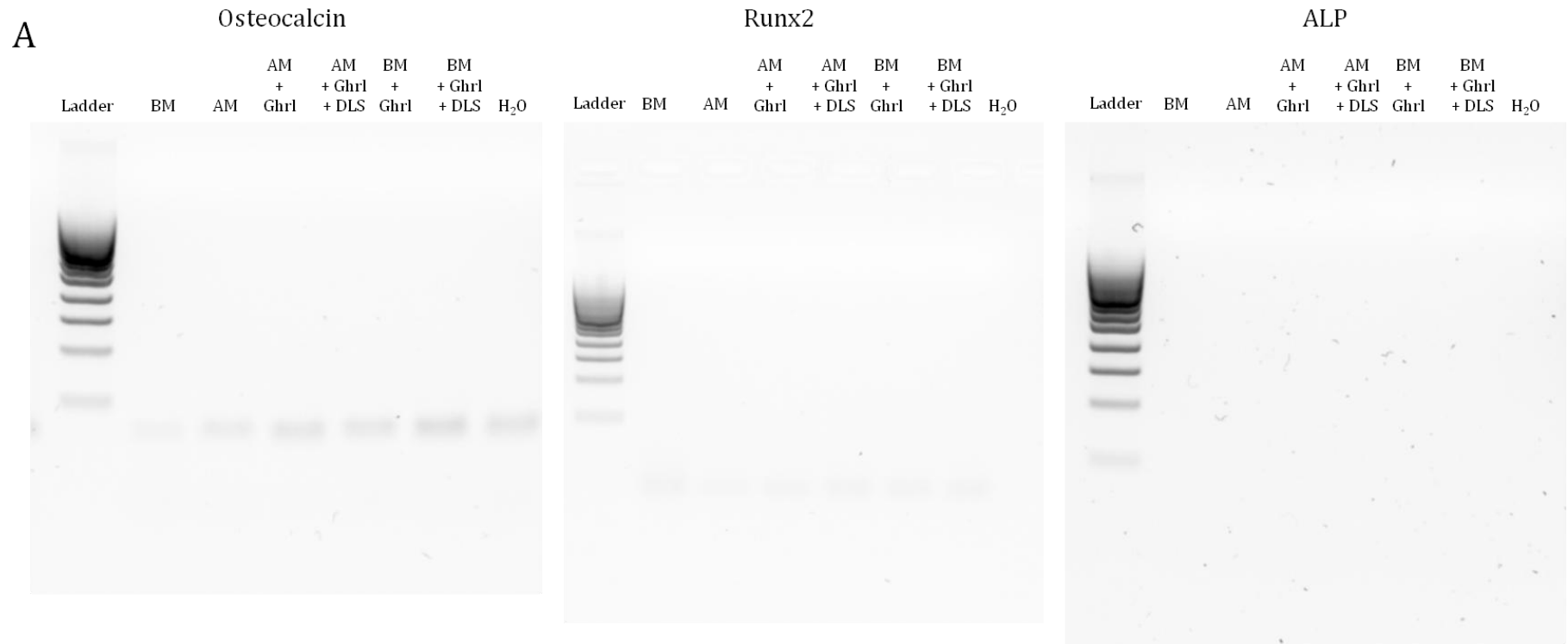


Figure 5.10: No RT controls for the differentiation markers (part 1)

7F2 cells were cultured for 7 days with basal (BM) or adipogenic medium (AM), with or without 20 nM ghrelin, and with or without GHSR blocker DLS. A; No RT controls of the RT-PCR analysis of the osteoblastic markers osteocalcin, Runx2 and ALP.

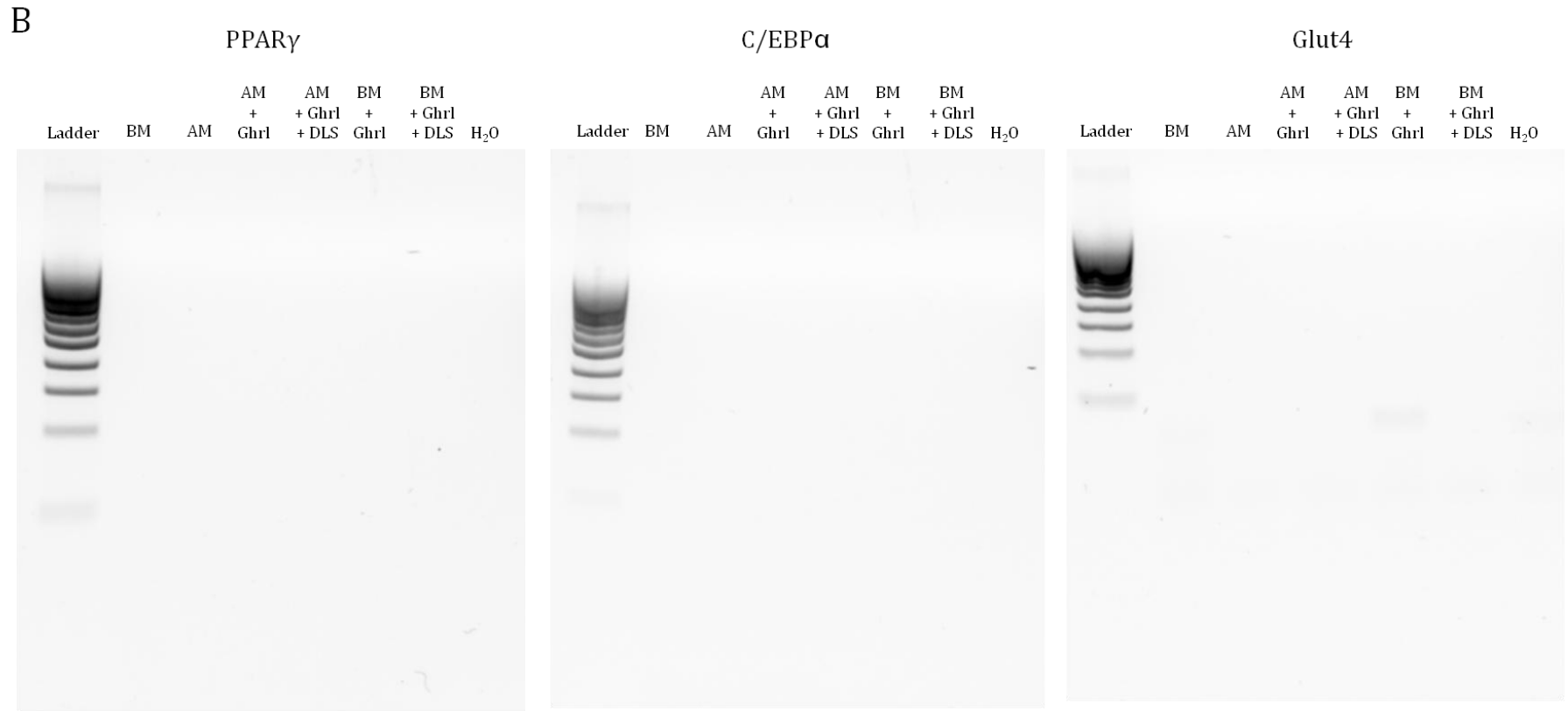


Figure 5.10: No RT controls for the differentiation markers (part 2)

7F2 cells were cultured for 7 days with basal or adipogenic medium, with or without 20 nM ghrelin, and with or without GHSR blocker DLS. B: No RT controls of the RT-PCR analysis of the adipogenic markers PPAR γ , C/EBP α and Glut4.

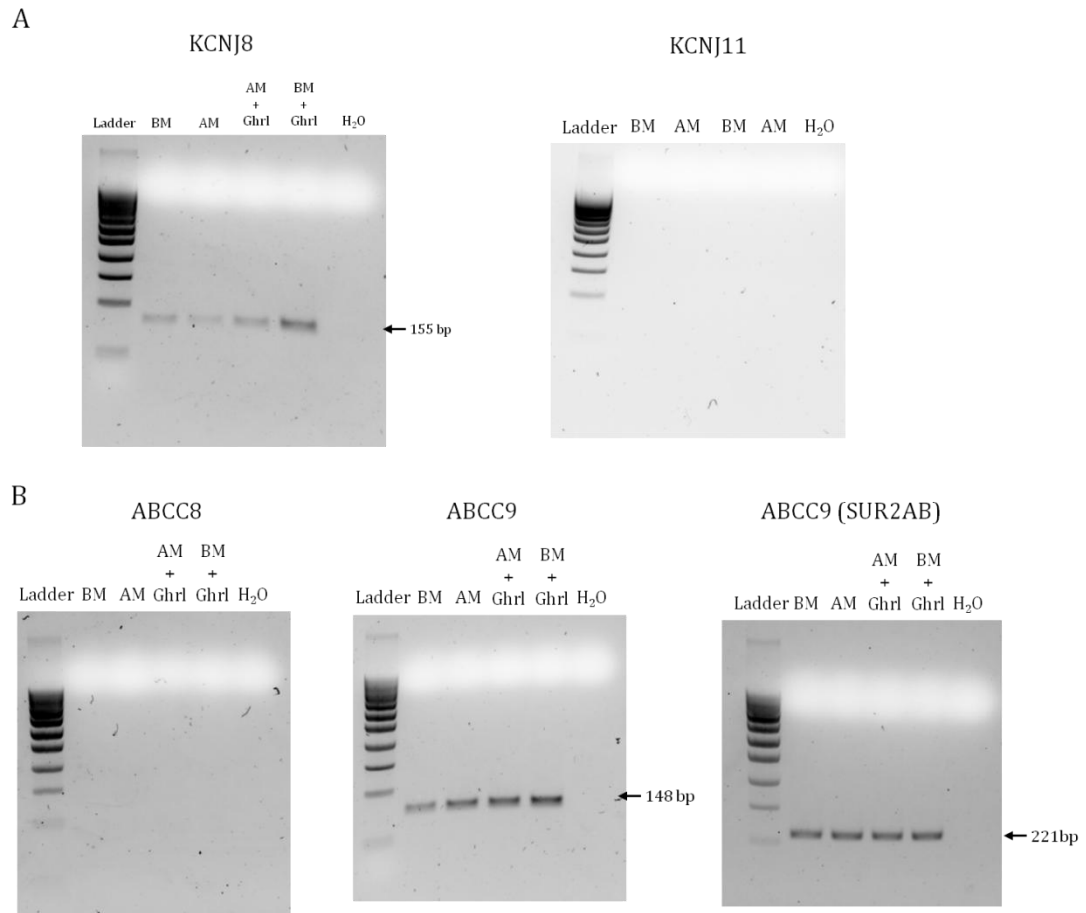


Figure 5.11: RT-PCR analysis for the K_{ATP} channel subunits

mRNA was extracted from 7F2 cells cultured for 7 days with basal (BM) or adipogenic medium (AM) with or without 20 nM ghrelin, except for KCNJ11, which was only tested in cells cultured with basal or adipogenic medium alone. RT-PCR was performed for the two pore-forming K_{ATP} channel subunits: Kir6.1 (KCNJ8) and Kir6.2 (KCNJ11) (A), and the accessory subunits SUR1 (ABCC8) and SUR2 (ABCC9) (B). For ABCC9, two sets of primers were used; the first set detected mRNA expression of all known ABCC9 isoforms, while the second set (SUR2AB) could distinguish between the two isoforms SUR2A and SUR2B.

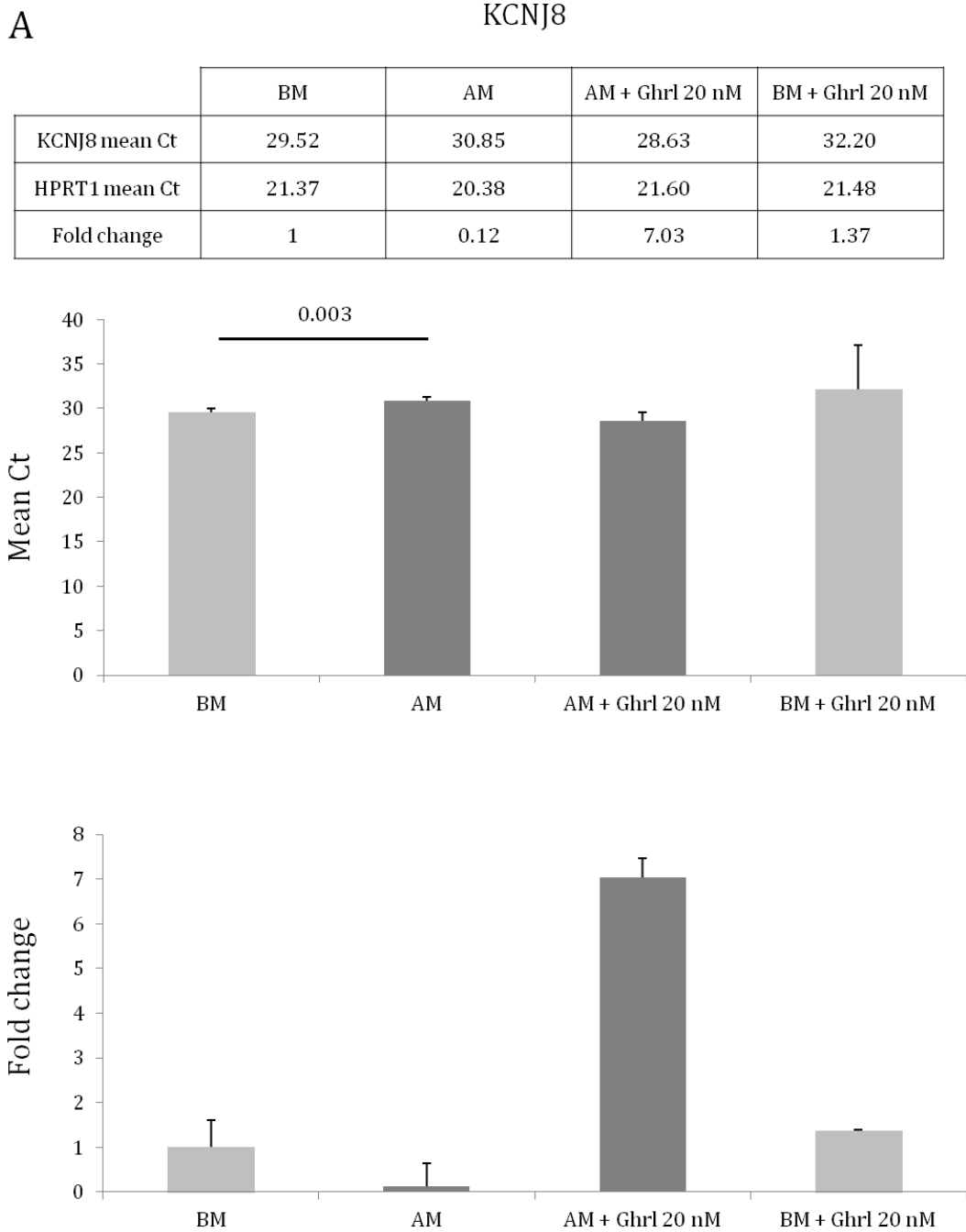


Figure 5.12: qPCR analysis for K_{ATP} channel subunits (part 1)

mRNA was extracted from 7F2 cells cultured for 7 days with basal (BM) or adipogenic medium (AM), with or without 20 nM ghrelin. A: qPCR analysis for Kir6.1 (*KCNJ8*) ($n = 1, 3$ replicate samples per condition; each sample was run in duplicate). Data are mean Ct \pm SD (top graph; Welch's anova and Games-Howell post-hoc analysis) and mean fold change \pm SD (bottom graph; ANOVA test); the relative fold expression was normalised by the reference gene *EEF2*.

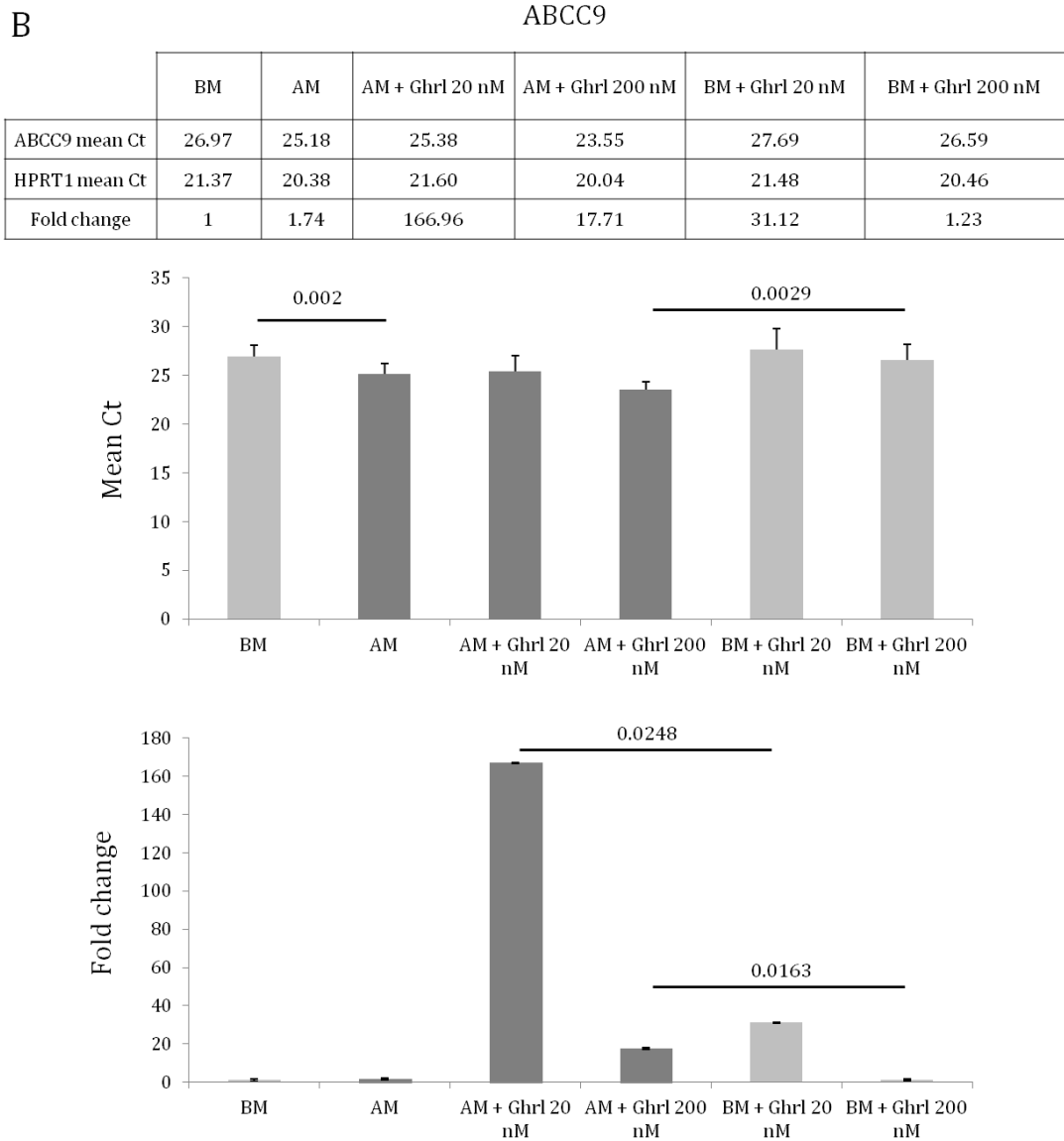


Figure 5.12: qPCR analysis for K_{ATP} channel subunits (part 2)

B: qPCR analysis for SUR2 (*Abcc9*) ($n = 1, 3$ replicate samples per condition; each sample was run in duplicate). Data are mean Ct \pm SD (top graph; Kruskal-Wallis test and Dunn post-hoc analysis) and mean fold change \pm SD (bottom graph; Kruskal-Wallis test and Dunn post-hoc analysis); the relative fold expression was normalised by the reference gene *EEF2*.

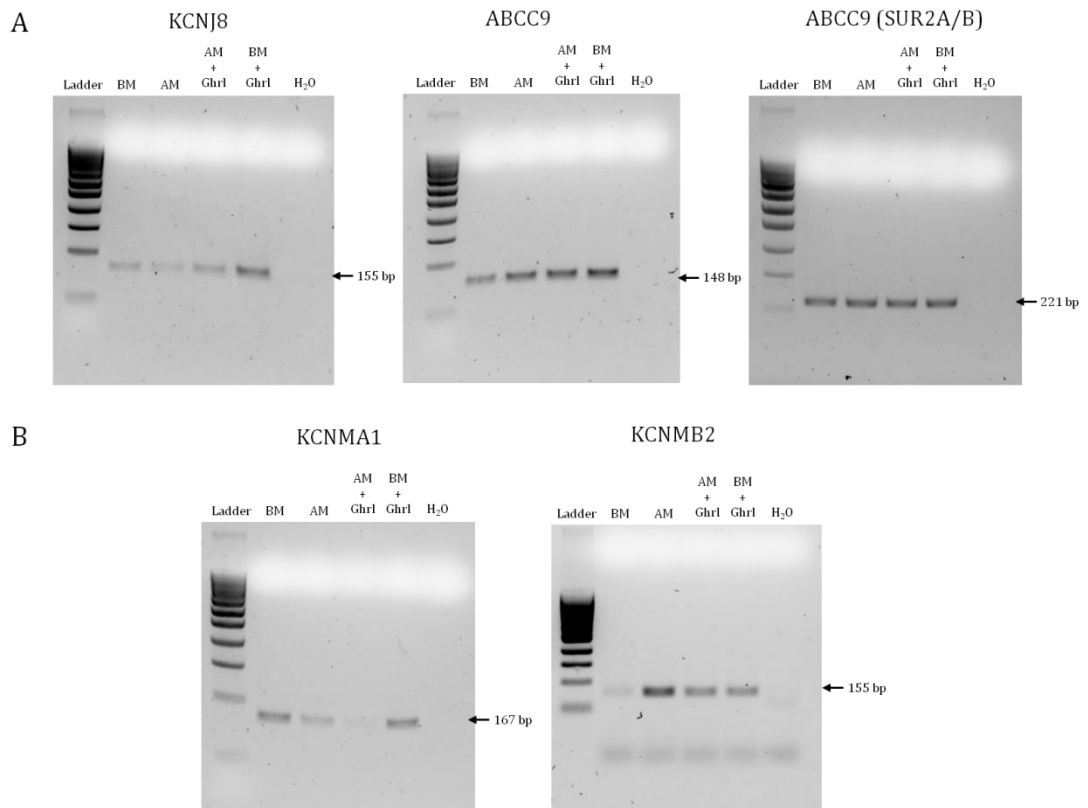
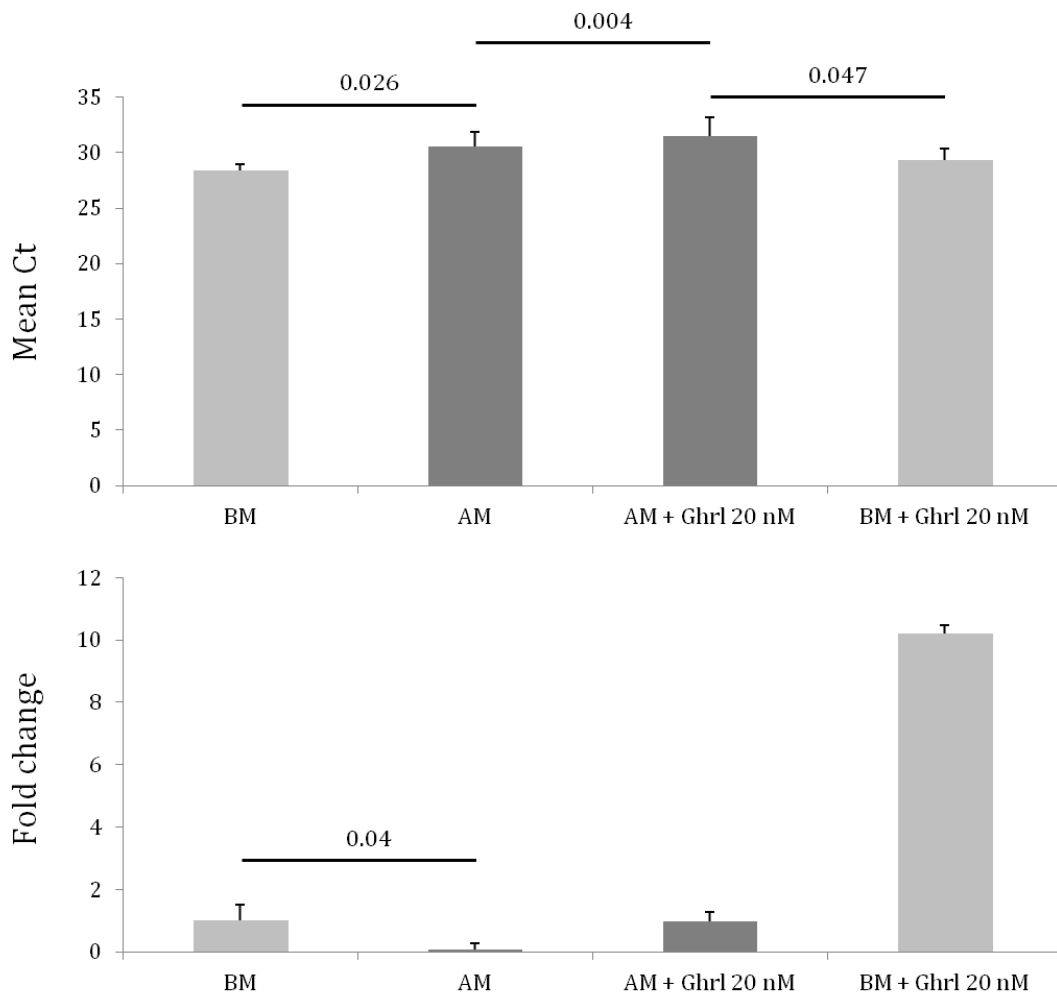


Figure 5.13: RT-PCR analysis for the BK channel subunits

mRNA was extracted from 7F2 cells cultured for 7 days with basal (BM) or adipogenic (AM) medium, with or without 20 nM ghrelin. RT-PCR was performed for the pore-forming subunit KCNMA1, and for the four regulatory subunits KCNMB1 to KCNMB4.

KCNMA1

	BM	AM	AM + Ghrl 20 nM	BM + Ghrl 20 nM
Ct (mean)	28.42	30.54	31.46	29.30
HPRT1 mean Ct	21.37	20.38	21.60	21.48
Fold change	1	0.07	0.99	10.22

Figure 5.14: qPCR analysis for *Kcnma1*

mRNA was extracted from 7F2 cells cultured for 7 days with basal (BM) or adipogenic (AM) medium, with or without 20 nM ghrelin. qPCR analysis was performed for *Kcnma1* ($n = 1, 3$ replicate samples per condition; each sample was run in duplicate). Data are mean Ct \pm SD (top graph; ANOVA test and Tukey-Kramer post-hoc analysis) and fold change \pm SD (bottom graph; ANOVA test and Tukey-Kramer post-hoc analysis); the relative fold expression was normalised by the reference gene *EEF2*.

A

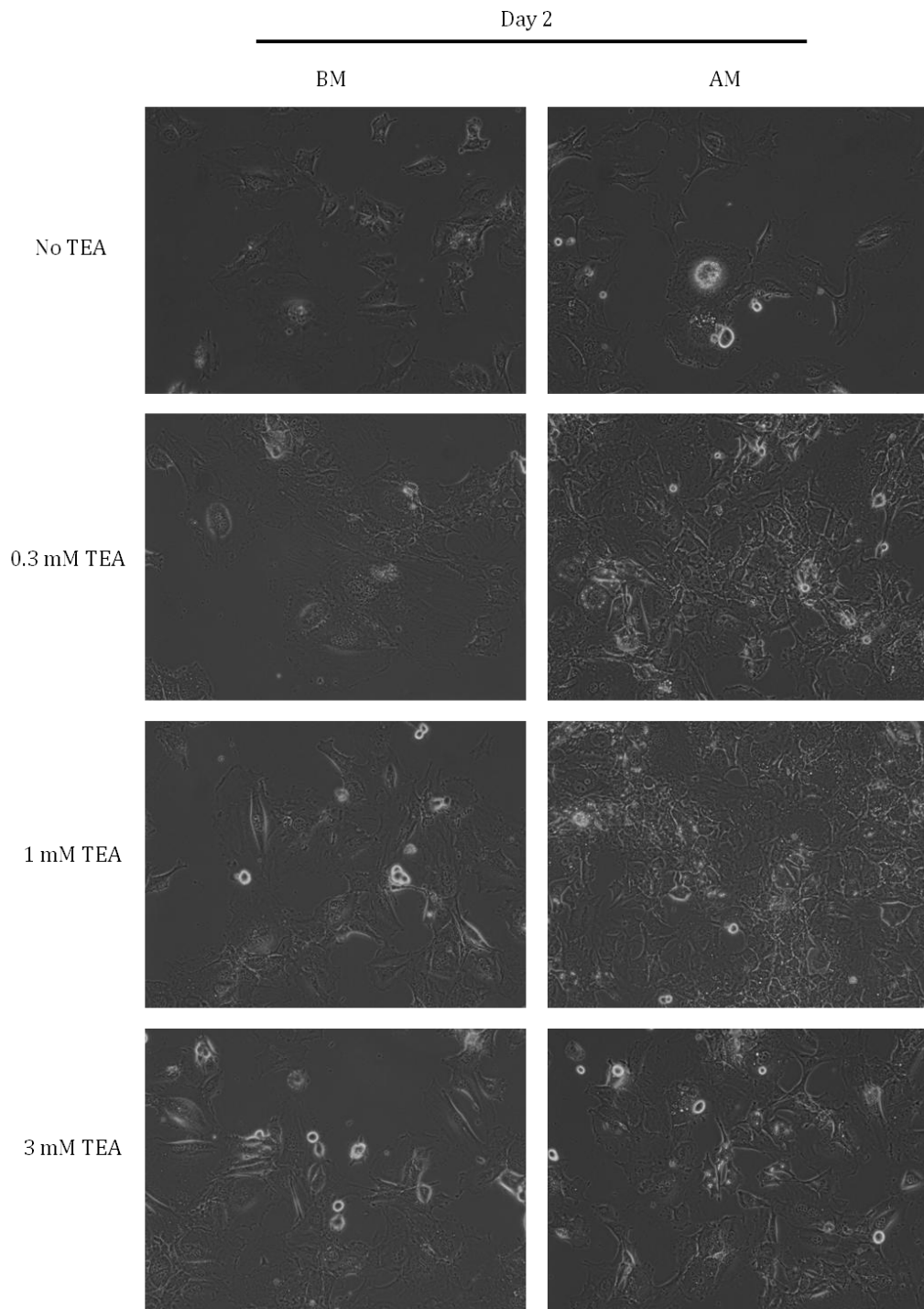


Figure 5.15: Effects of TEA on 7F2 cell adipogenic differentiation (part 1)

7F2 cells were cultured for 7 days with basal (BM) or adipogenic medium (AM), with or without various concentrations of TEA (0.3 mM, 1 mM, and 3 mM) (n=4, with 2 or 3 replicates per repeat). A: Pictures of 7F2 cells at day 2.

B

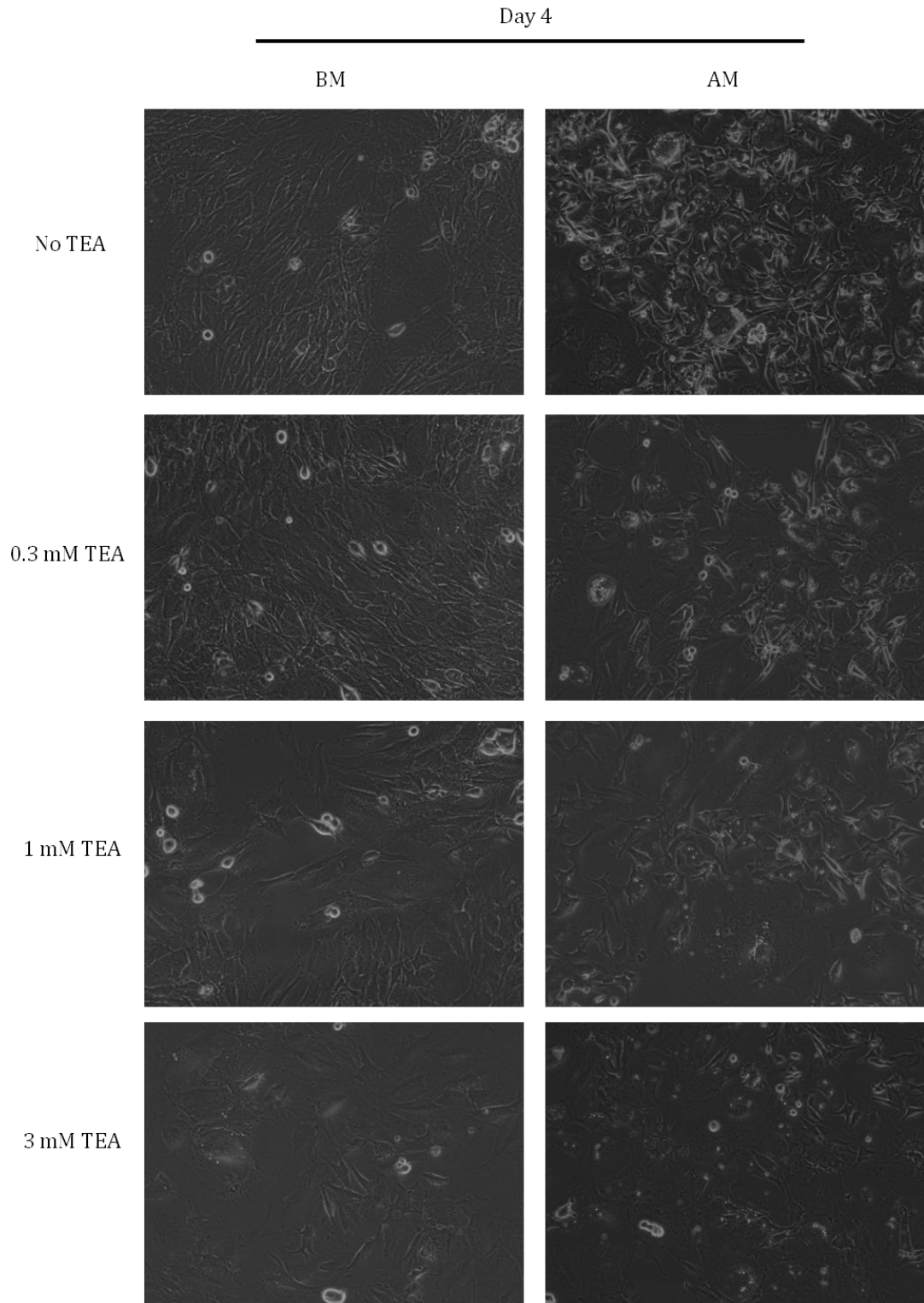


Figure 5.15: Effects of TEA on 7F2 cell adipogenic differentiation (part 2)

B: Pictures of 7F2 cells at day 4.

C

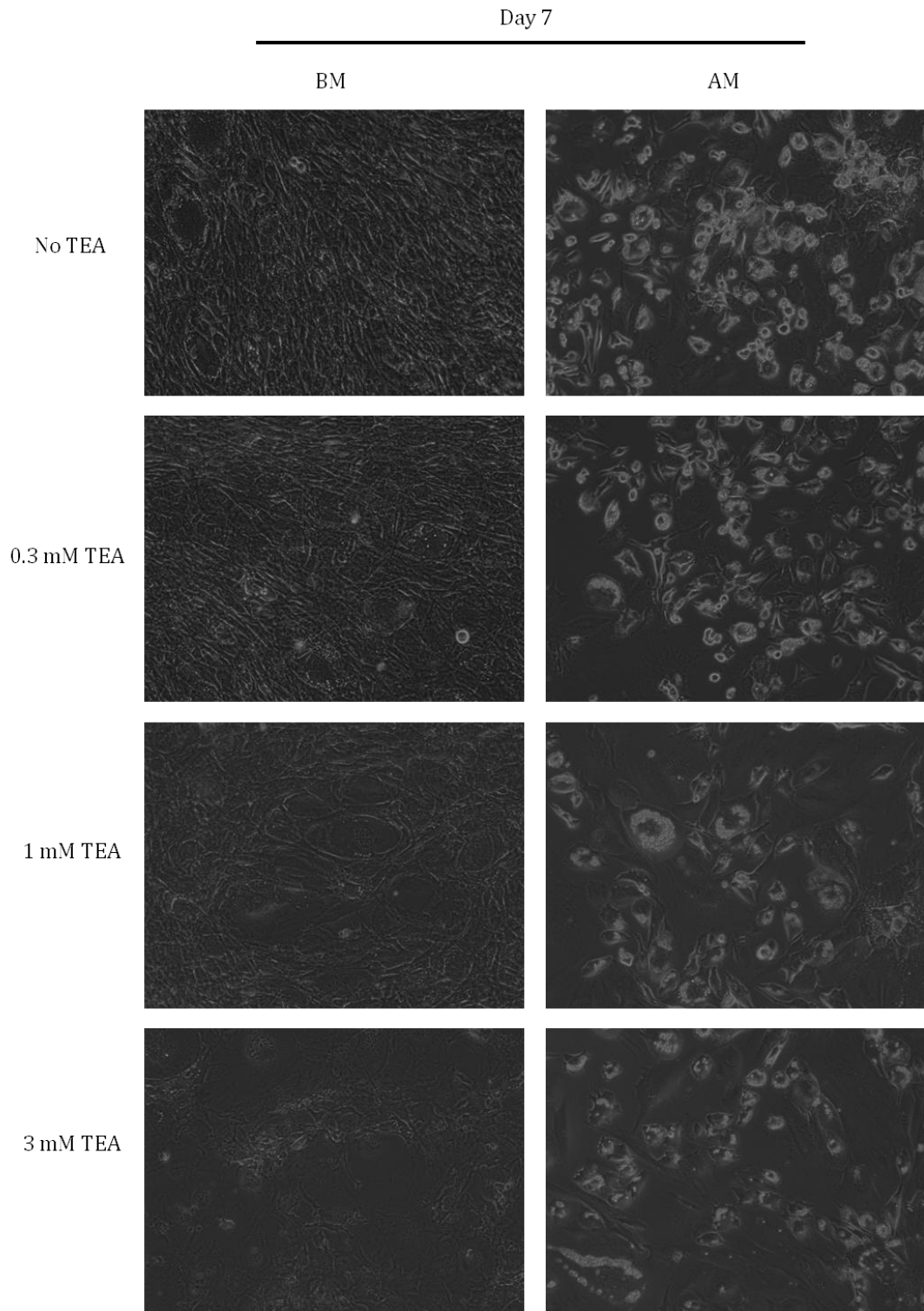


Figure 5.15: Effects of TEA on 7F2 cell adipogenic differentiation (part 3)

C: Pictures of 7F2 cells at day 7.

D

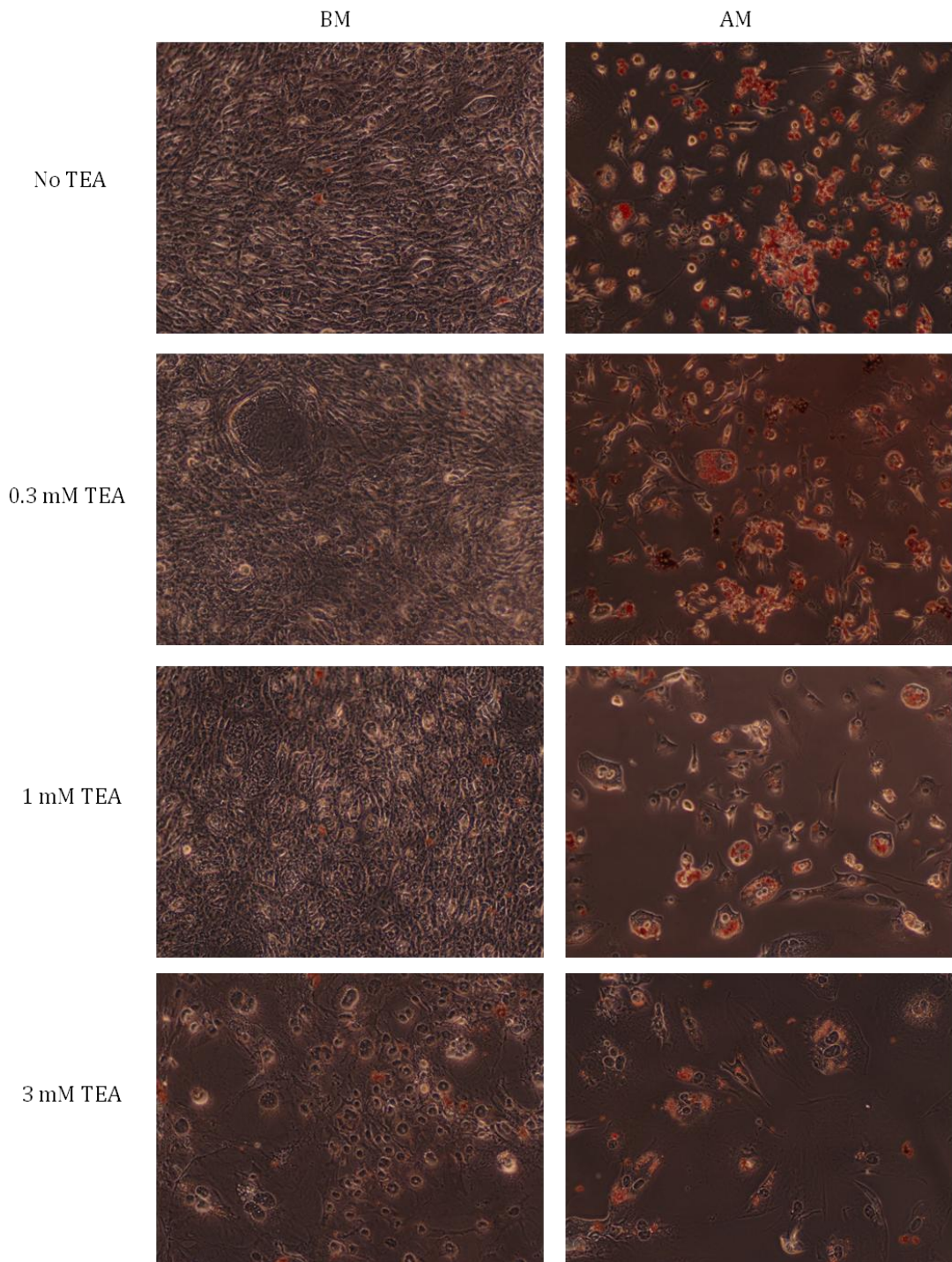
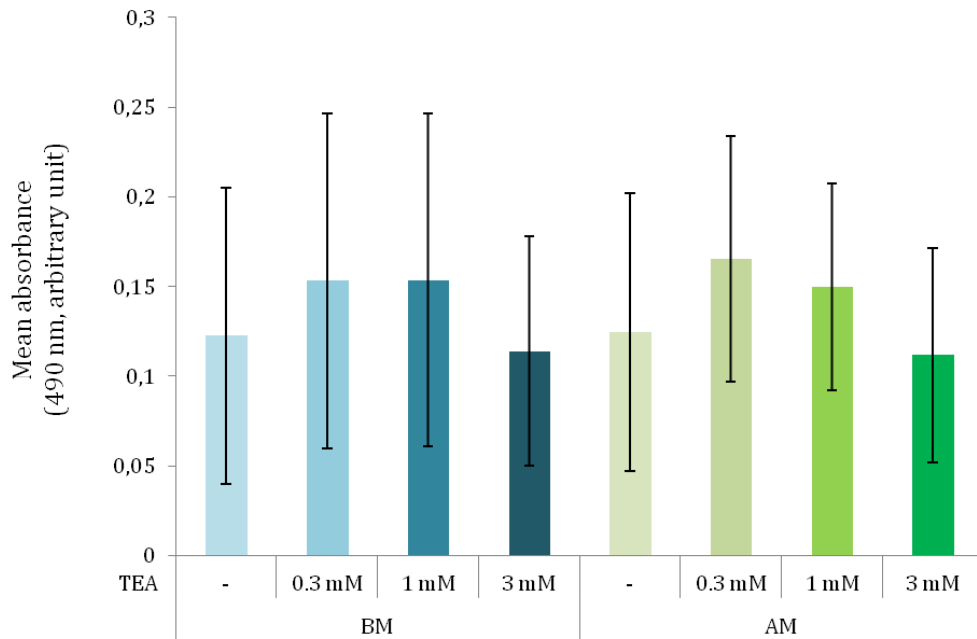


Figure 5.15: Effects of TEA on 7F2 cell adipogenic differentiation (part 4)

D: Pictures of 7F2 cells stained with Oil Red O after 7 days of culture.

E



F

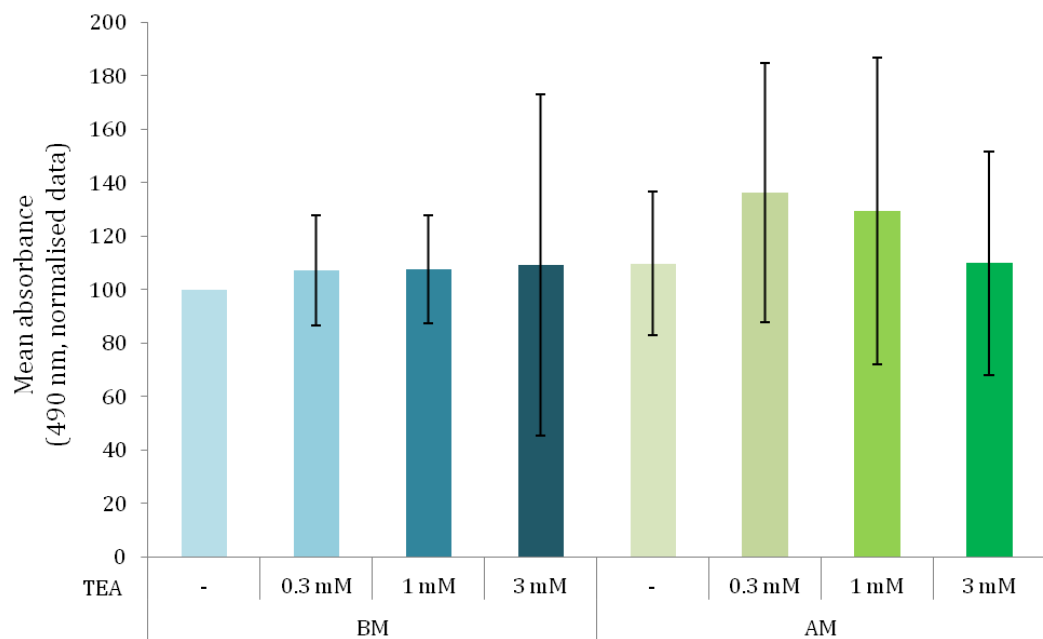


Figure 5.15: Effects of TEA on 7F2 cell adipogenic differentiation (part 5)

E: Oil Red O stain was extracted and quantified by measuring the absorbance at 490 nm. F: Quantification data was normalised to basal medium. Data are mean absorbance \pm SD ($n = 4$; 2-3 replicates per condition in each assay for a total of 10 replicates; Kruskal-Wallis tests).

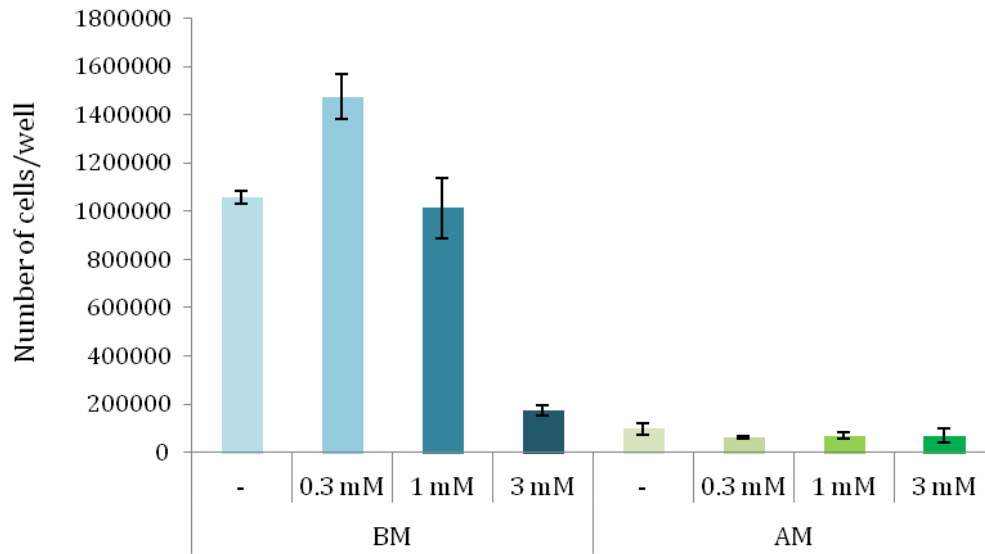


Figure 5.16: Effects of TEA of cell numbers

7F2 cells were cultured with basal (BM) or adipogenic medium (AM), with or without TEA in various concentrations (0.3 mM, 1 mM and 3 mM). Cells were counted after 7 days of culture (n = 1, 2 replicates per condition; Kruskal-Wallis test).

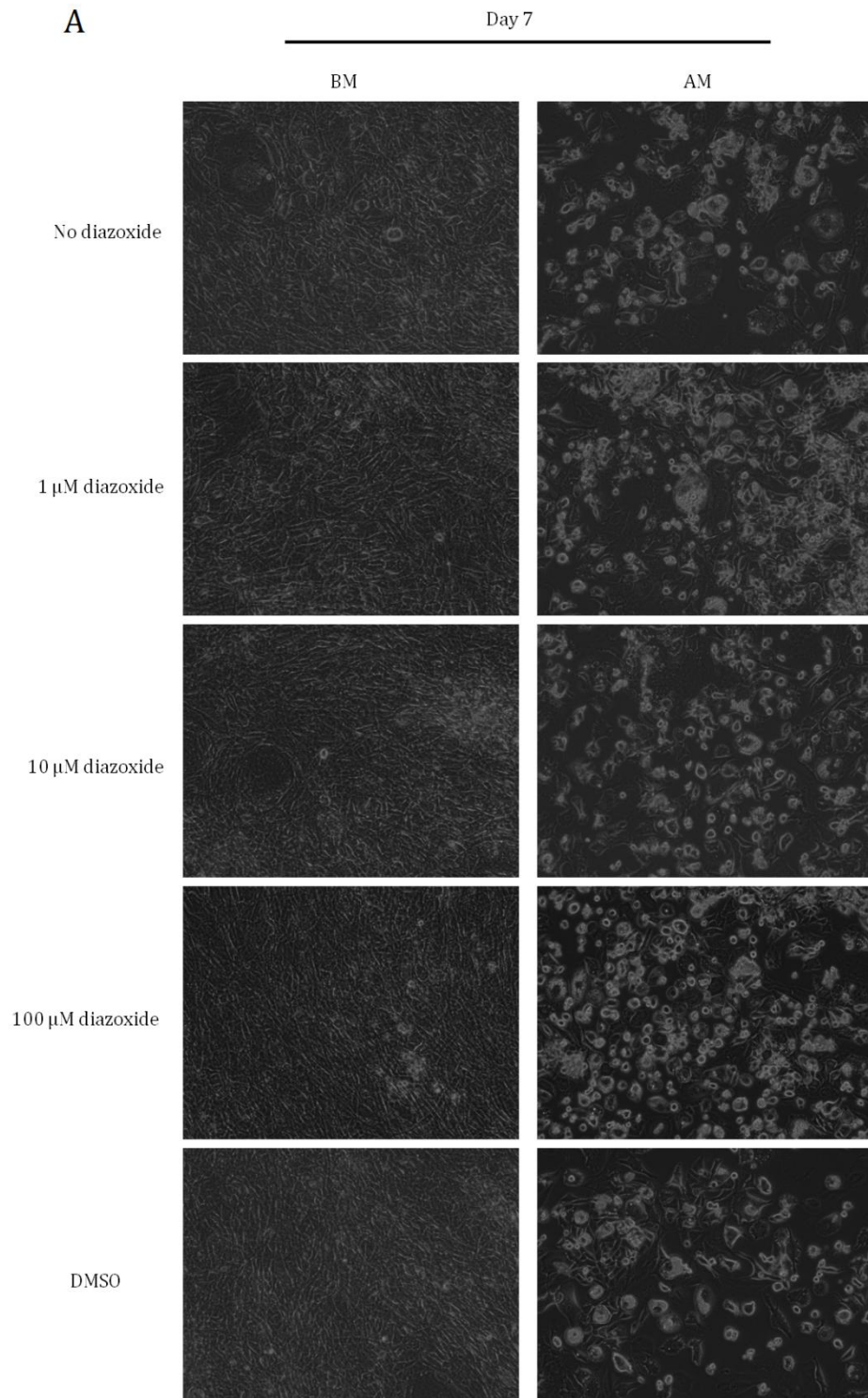


Figure 5.17: Effects of diazoxide on the adipogenic differentiation of 7F2 cells (part 1)

7F2 cells were cultured for 7 days with basal (BM) or adipogenic medium (AM) for 3 days, then culture medium was replaced with medium containing various concentrations of diazoxide (1 μ M, 10 μ M and 100 μ M) (n=3, with 3 or 4 replicates per repeat). A; Pictures of 7F2 cells at day 7 of culture.

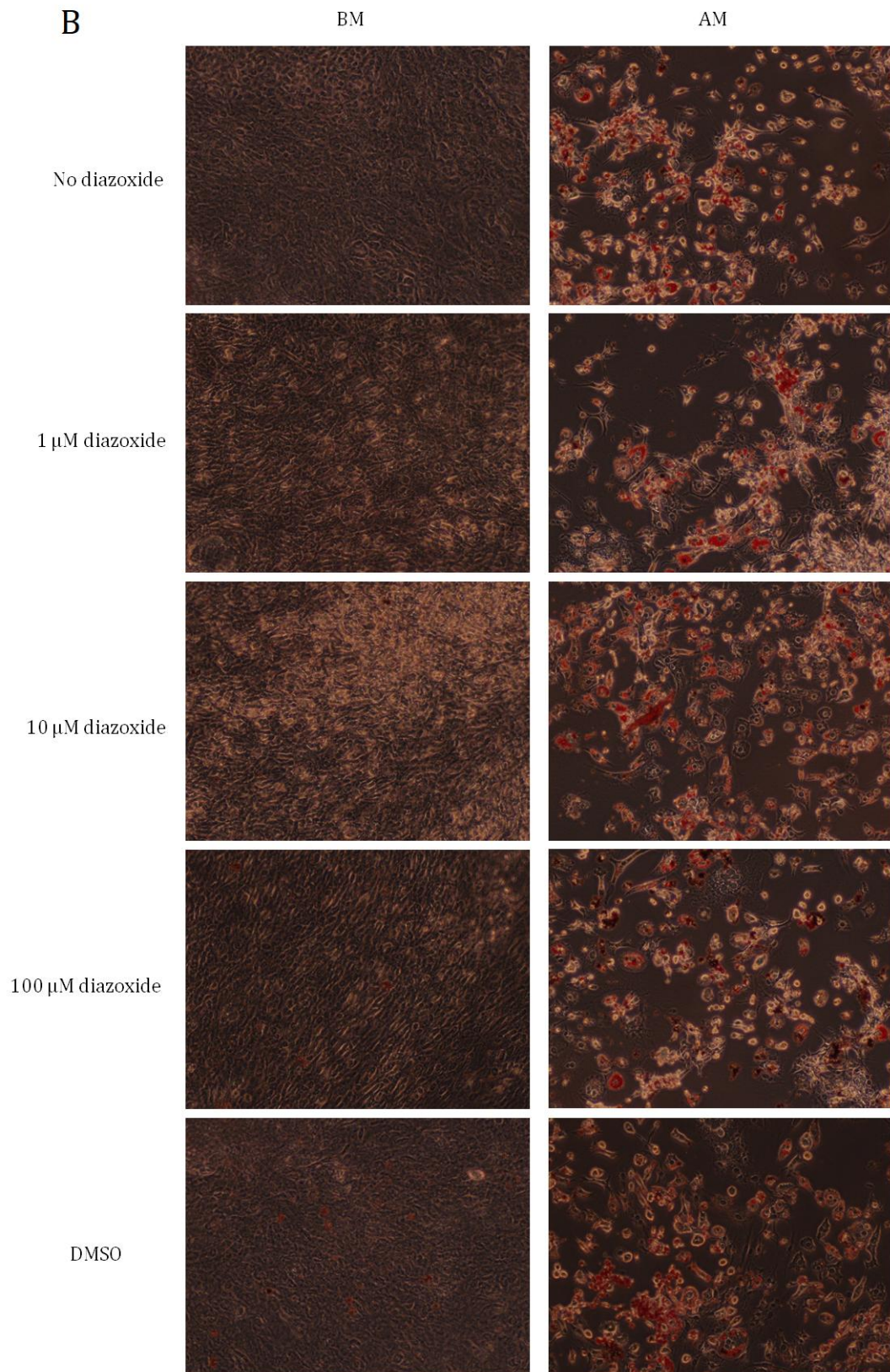


Figure 5.17: Effects of diazoxide on the adipogenic differentiation of 7F2 cells (part 2)

B: Pictures of 7F2 cells stained with Oil Red O after 7 days of cultures.

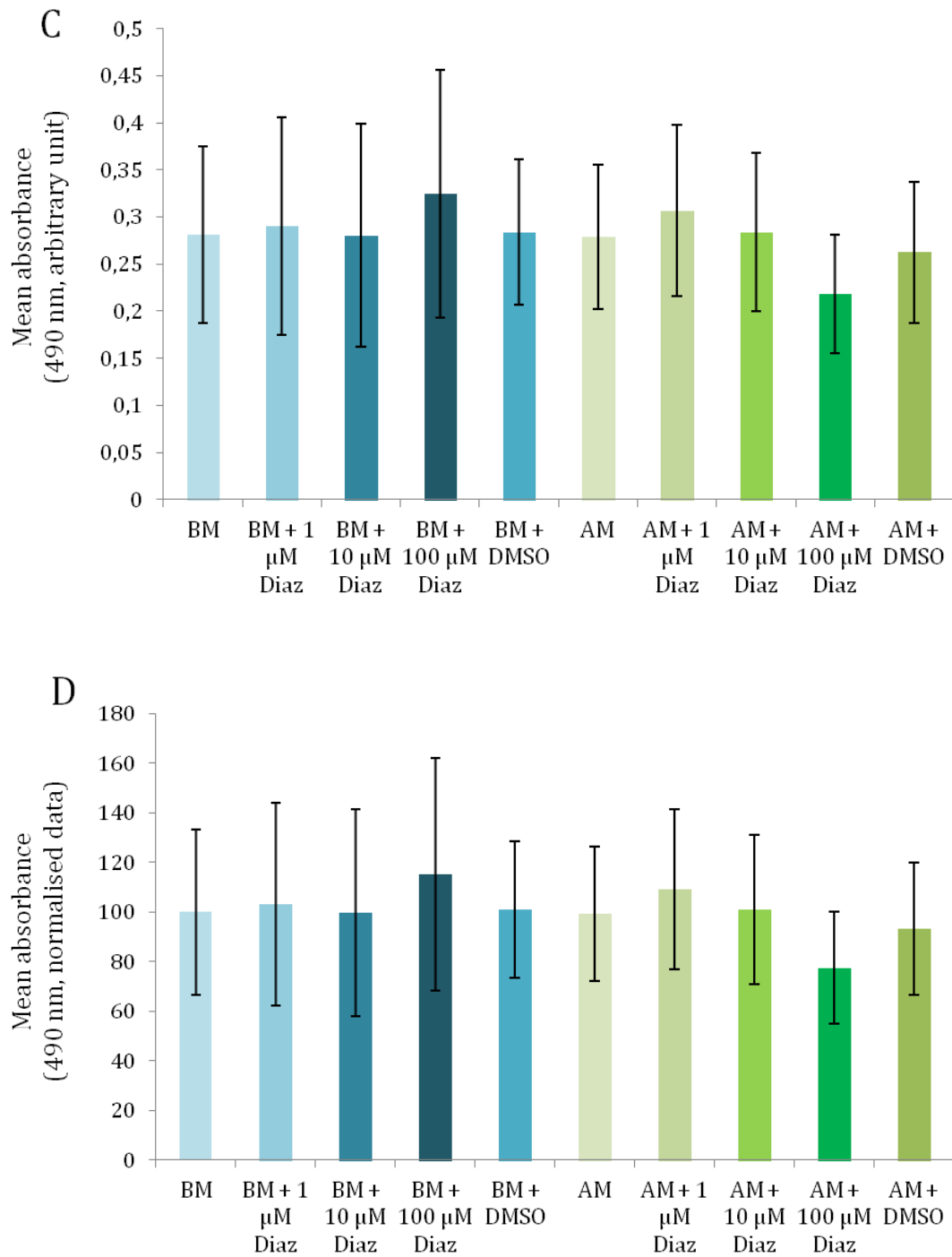


Figure 5.17: Effects of diazoxide on the adipogenic differentiation of 7F2 cells (part 3)

C: Oil Red O stain was extracted and quantified by measuring the absorbance at 490 nm. D: Quantification data was normalised to basal medium (n = 3, 3-4 replicates per condition in each assay for a total of 10 replicates; Kruskal-Wallis tests).

Chapter 6 - A comparison of the electrophysiological characteristics of osteoblasts and adipocytes, and the effects of ghrelin on these

6.1. Introduction

As established in the main introduction (see chapter 1), ion channels, and particularly potassium channels, are involved in regulating major cell processes such as proliferation and differentiation, particularly in bone. Ion channels have also been involved in mediating ghrelin signalling in various tissues.

6.1.1. Ionic mechanisms in ghrelin signalling

Ion channels, particularly calcium and potassium channels, are involved in mediating the effects of ghrelin signalling in various cell types. GHSR is a GPCR and GHSR activation can in turn activate ion channels via various G proteins. In the brain, GHSR1a is coupled to phospholipase C and inositol phosphate production through the G proteins $G\alpha_q/G\alpha_{11}$, triggering Ca^{2+} entry from intracellular stores (Holst *et al.*, 2003; Alexander SPH *et al.*, 2011b). Activation of phospholipase C may also lead to tyrosine phosphorylation of potassium channels, which inhibits these channels and causes membrane depolarisation, activating L-type voltage-gated calcium channels and stimulating GH secretion (Petersenn *et al.*, 2001). In neurons of the arcuate nucleus, GHSR1a has been reported to activate the G protein $G\alpha_s$, leading to activation of protein kinase A (PKA) and increased cytoplasmic Ca^{2+} via opening of N-type Ca^{2+} channels (Kohno *et al.*, 2003). In addition, the orexigenic actions of ghrelin in the nodose ganglia are mediated by K_{ATP} channels containing the Kir6.2 subunit (Grabauskas *et al.*, 2015).

Ghrelin signalling is also mediated by ion channels in other organs. Ghrelin has been shown to increase T-type Ca^{2+} channel expression and inhibit proliferation in PC-3 human prostate carcinoma cells (Díaz-Lezama *et al.*, 2010). Ghrelin and des-acyl ghrelin exert vasodilator effects in rat mesenteric vascular bed via activation of small- and intermediate-conductance Ca^{2+} -activated K^+ channels, inwardly-rectifying K^+ channels and the Na^+/K^+ ATPase pump (Moazed *et al.*, 2009). In the pancreas, ghrelin attenuates glucose-induced insulin secretion from pancreatic beta cells via its receptor GHSR1a, the G protein $G\alpha_{i2}$ and the activation of delayed outward voltage-gated K^+ channels Kv2.1 (Dezaki *et al.*, 2007; Yada *et al.*, 2014). Ghrelin binding to GHSR1a activates the G protein $G\alpha_{i2}$, decreasing cAMP production and activating voltage-gated potassium channels, which attenuates membrane excitability and suppresses glucose-induced Ca^{2+} entry into the cytosol, suppressing insulin release (figure 6.1). This effect is diminished in the presence of TEA, which blocks voltage-dependent potassium channels (Im and Quandt, 1992; Quandt and Im, 1992; Dezaki *et al.*, 2004); 30 mM TEA has been reported to block K^+ currents through Kv2.1 by 87% (Ikeda and Korn, 1995).

Chapter 6 – A comparison of the electrophysiological characteristics of osteoblasts and adipocytes, and the effects of ghrelin on these

In addition, perforated-patch clamp experiments in rat pancreatic beta cells indicate that ghrelin increases the amplitude of K_v currents in a reversible manner at potentials positive to -30 mV. This effect is not blocked by tolbutamide, which is a blocker of K_{ATP} channels, but is suppressed in the presence of TEA and stromatoxin, which is a specific blocker of Kv2.1 (Dezaki *et al.*, 2007).

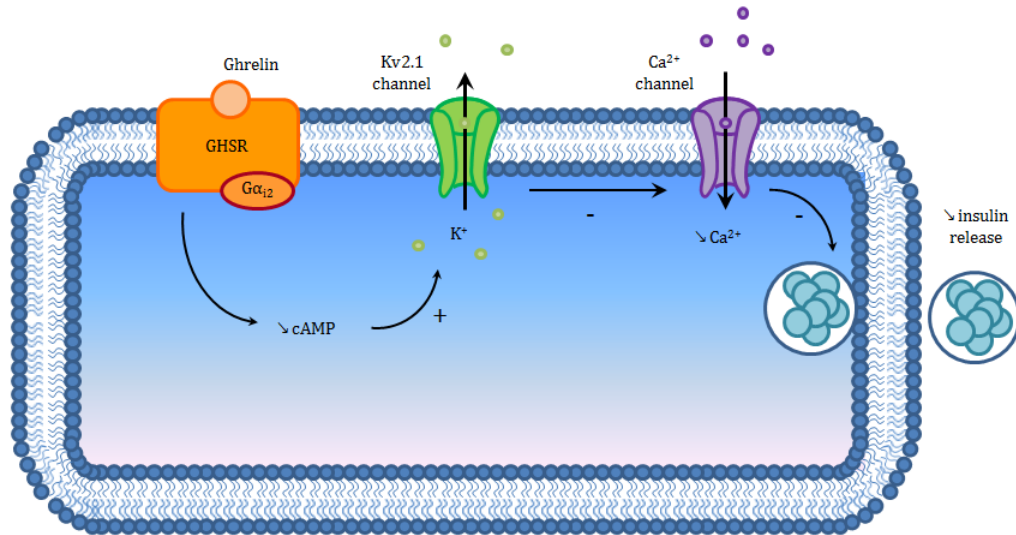


Figure 6.1: Ghrelin inhibits insulin secretion via activation of Kv2.1

Ghrelin binds and activates GHSR1a, which in turn activates $G\alpha_{i2}$, leading to decreased cAMP production and activation of Kv2.1 channels. Activation of Kv2.1 channels reduces membrane excitability, inhibiting voltage-dependent Ca^{2+} channels and blocking the entry of Ca^{2+} in the cytosol, which suppresses insulin release. Adapted from (Alamri *et al.*, 2016).

6.1.2. Chapter objectives and hypothesis

As ion channels are known to be involved in regulating cell proliferation and differentiation, and in mediating ghrelin signalling, the objective of this chapter was to investigate and compare the electrophysiological properties of 7F2 osteoblast-like cells and 7F2 cell-derived adipocytes, and the effects of ghrelin treatment on these, using electrophysiology techniques. Ion channel activity was recorded in single-channel patch clamping experiments. The hypothesis was that adipogenic differentiation and ghrelin treatment would modify the electrophysiological properties of 7F2 osteoblast-like cells.

6.2. Materials and Methods

6.2.1. Adipogenic differentiation and ghrelin treatment of 7F2 cells

7F2 cells were cultured for 1-7 days on 16 mm circular glass coverslips at seeding densities of 3,000 cells with basal or adipogenic medium and, where indicated, treated with 20 nM ghrelin (Cambridge Bioscience) for 3 to 7 days.

6.2.2. Electrophysiology

See section 2.4.

6.3. Results

The number of successful patches was 38 for 7F2 cells cultured with BM (success rate: 46.9 %), 30 successful patches for 7F2 cells cultured with AM (71.4%), 53 successful patches for 7F2 cells cultured with AM + Ghrl (74.6%) and 21 successful patches for 7F2 cells cultured with BM + Ghrl (48.8 %) (table 6.1). When 7F2 cells were cultured with adipogenic medium, only cells containing lipid droplets were selected for electrophysiological study. Cell-attached patches were disrupted and spontaneously excised to inside-out configuration patches very readily, especially in cells cultured with adipogenic medium, but a few patches remained cell-attached (table 6.1). Patch configurations are illustrated in figure 6.2.

Analysis of single channel data indicated the presence of several currents: 22 currents were detected in 7F2 cells cultured with BM, 12 currents were detected in 7F2 cells cultured with AM, 19 currents were detected in 7F2 cells cultured with AM + Ghrl and 12 currents in 7F2 cells cultured with BM + Ghrl (table 6.2). Some of these currents were similar, and a few patches presented several types of currents. Other potential currents were detected but too little data were obtained through infrequent appearances in recordings, which prevented reliable characterisation of these currents. The various currents detected in patch-clamp experiments were categorised according to their electrophysiological characteristics (summarised in table 6.3), including mean conductance and similarities in current amplitudes and voltage range of activation. Conductance (γ) was calculated according to $\gamma = V/I$, by linear regression over the linear portions of the current-voltage plots.

Chapter 6 – A comparison of the electrophysiological characteristics of osteoblasts and adipocytes, and the effects of ghrelin on these

	BM	AM	AM + Ghrl	BM + Ghrl
Number of attempts	81	42	71	43
Number of successful patches	38	30	53	21
Number of currents detected	22	12	19	12
Cell-attached patches	7	4	3	8
Excised inside-out patches	3	5	12	3
Undetermined patch configuration	12	3	4	1

Table 6.1: Summary of electrophysiology recordings

Current/Mean conductance	BM	AM	AM + Ghrl	BM + Ghrl
Current 1: 6.2 ± 3 pS			✓	✓
Current 2: 6.5 ± 4.1 pS			✓	✓
Current 3: 28.5 ± 2 pS	✓		✓	✓
Current 4: 34.1 ± 1 pS	✓			
Current 5: 42.1 ± 5.4 pS	✓	✓	✓	
Current 6: 67.5 ± 2.1 pS			✓	
Current 7: 80.8 pS				✓
Current 8: 158.4 pS	✓			
Current 9: 200.1 pS				✓
Current 10: 6.3 pS from -70 to +60 mV; 65,9 pS from +60 to +150 mV	✓		✓	
Current 11: 1,3 pS from -150 mV to -40 mV; 28,7 pS from -40 mV to +80 mV		✓		
Current 12: 14.6 pS from +20 to +100 mV and 233.3 pS from +110 to +140 mV			✓	

Table 6.2: List of the currents detected

Chapter 6 – A comparison of the electrophysiological characteristics of osteoblasts and adipocytes, and the effects of ghrelin on these

Conductance	Reversal potential	Voltage-sensitive?	Voltage-dependent?	Rectifying?
6.2 ± 3 pS		Yes	Yes	Yes
6.5 ± 4.1 pS			Yes	
28.5 ± 2 pS	Cell-attached: -69.2 ± 10.5 mV (-109 mV for AM + Ghrl; -81 mV for BM + Ghrl); Excised-inside out: -55 mV	Yes	Yes	No
34.1 ± 1 pS	Unknown patch configuration: -22.5 ± 0.7 mV	Yes	No	Weakly rectifying
42.1 ± 5.4 pS	Cell-attached: -2.4 ± 9.1 mV Excised inside-out: -24 ± 8.5 mV	Yes	No	Weakly rectifying
67.5 ± 2.1 pS	Excised inside-out: -36 mV	Weakly	No	No
80.8 pS	Excised inside-out: -60 mV		Yes	
158.4 pS		Yes	Yes	
200.1 pS	Cell-attached: -24 mV		Yes	Weakly rectifying
6.3 pS from -70 to +60 mV; 65,9 pS from +60 to +150 mV		Yes	No	Yes
1,3 pS from -150 mV to -40 mV; 28,7 pS from -40 mV to +80 mV	Cell-attached: -16 mV; Excised inside-out: -17 mV			Yes
14.6 pS from +20 to +100 mV; 233.3 pS from +110 to +140 mV			Yes	

Table 6.3: Summary of the characteristics of the currents detected

6.3.1. Small conductance currents

6.3.1.1. Current 1

This current was detected in 26% (n = 5) of successful patches of 7F2 cells cultured with adipogenic medium + 20 nM ghrelin in excised inside-out configurations, and 25% (n = 3) of successful patches of 7F2 cultured with basal medium + ghrelin in cell-attached configurations. Representative current tracings of this channel activity and the corresponding I/V relationship are shown in figures 6.3 and 6.4. It was an inward current that increased linearly with increasing pipette voltage and had a mean conductance of 6.2 ± 3 pS in 7F2 cells cultured with adipogenic medium + ghrelin, and $2.3 \text{ pS} \pm 6.7$ pS in 7F2 cells cultured with basal medium + ghrelin. No outward current was detected in these patches.

6.3.1.2. Current 2

This current was detected in 11% (n = 2) of successful patches of 7F2 cells cultured with adipogenic medium + 20 nM ghrelin (excised inside-out configurations), and in one successful patch of 7F2 cultured with basal medium + ghrelin; it is not known whether it was in cell-attached or in excised inside-out configuration. Representative current tracings of this channel activity and the corresponding I/V relationship are shown in figures 6.5 and 6.6. It was an outward current that increased linearly with increasing pipette voltage; it has a mean conductance of 6.5 ± 4.1 pS in 7F2 cells cultured with adipogenic medium + ghrelin, and 13.9 pS in 7F2 cells cultured with basal medium + ghrelin.

6.3.1.3. Current 3

This channel was detected in 13% (n=5) of successful patches of 7F2 cells cultured with basal medium (cell-attached configurations) and in 25% (n = 3) of successful patches of 7F2 cultured with basal medium + ghrelin (cell-attached configurations). It was also detected in 21% (n=4) successful patches of 7F2 cells cultured with adipogenic medium + 20 nM ghrelin; one was in cell-attached configuration, and three were in excised inside-out configurations. Representative current tracings of this channel activity and the corresponding I/V relationship are shown in figures 6.7, 6.8, 6.9 and 6.10. The current increased linearly with increasing electrode voltage and had a mean conductance of 28.5 ± 2 pS in 7F2 cells cultured with basal medium, 24.6 ± 4.1 pS in 7F2 cells cultured with adipogenic medium + ghrelin, and 28.6 ± 3.7 pS in 7F2 cells cultured with basal medium + ghrelin.

6.3.1.4. Current 4

This channel was detected in 5% (n=2) of successful patches of 7F2 cells cultured with basal medium. It was not possible to determine if the cell was still attached, or if the patch was in excised inside-out configuration. Representative current tracings of this channel activity and the corresponding I/V relationship are shown in figure 6.11. The current increased linearly with increasing pipette voltage, displayed inward rectification, and had a mean conductance of 34.1 ± 1 pS.

6.3.1.5. Current 5

This channel was detected in 13% (n=5) of successful patches of 7F2 cells cultured with basal medium (cell-attached configurations), 10% (n=3) of successful patches from 7F2 cell-derived adipocytes (excised inside-out configurations), and 11% (n=2) of successful patches of 7F2 cells cultured with adipogenic medium + 20 nM ghrelin (undetermined patch configurations). Representative current tracings of this channel activity and the corresponding I/V relationship are shown in figures 6.12, 6.13 and 6.14. The current increased linearly with increasing electrode voltage, displayed inward rectification, and had a mean conductance of 42.1 ± 5.4 pS in 7F2 cells cultured with basal medium, 39.9 ± 0.8 pS in 7F2 cells cultured with adipogenic medium, and 43.3 ± 0.6 pS in 7F2 cells cultured with adipogenic medium + ghrelin.

6.3.2. Intermediate conductance currents

6.3.2.1. Current 6

This current was detected in 11% (n=2) of successful patches of 7F2 cells cultured with adipogenic medium + 20 nM ghrelin in excised inside-out configurations. Representative current tracings of this channel activity and the corresponding I/V relationship are shown in figure 6.15. The current increased with increasing pipette voltage and had a mean conductance of 67.5 ± 2.1 pS.

6.3.2.2. Current 7

This current was detected in one successful patch of 7F2 cells cultured with basal medium + 20 nM ghrelin in excised inside-out configuration. Representative current tracings of this channel activity and the corresponding I/V relationship are shown in

figure 6.16. The current increased linearly with increasing pipette voltages and had a conductance of 80.8 pS.

6.3.3. Large conductance currents

6.3.3.1. Current 8

This current was detected in 8% (n = 3) of patched 7F2 cells cultured in basal medium; two of these patches were in cell-attached configuration and one was in excised inside-out configuration. This channel was not active spontaneously at 0 mV holding potential; it became active when voltages of ≥ 100 mV were applied several times, and then remained active over a large range of voltages (0 mV to +150 mV). In one of the cell-attached patch and in the excised inside-out patch, only partial data could be recorded. Figure 6.17 shows data records corresponding to the cell-attached patch where the BK channel could be recorded over a full range of voltages (0 mV to +150 mV); the current increased linearly with increasing pipette voltage and had a conductance of 158.4 pS. Figure 6.18 shows the recording data for the large conductance channels detected in 7F2 cells cultured in basal medium in excised inside-out configuration, although there is little data. The current had a conductance of 244.1 pS.

6.3.3.2. Current 9

This current was detected in one successful patch of 7F2 cells cultured with basal medium + 20 nM ghrelin in excised inside-out configuration. Representative current tracings of this channel activity and the corresponding I/V relationship are shown in figure 6.19. The current increased linearly with increasing pipette voltages and had a conductance of 200.1 pS.

6.3.4. Rectifying currents

3 types of rectifying currents were recorded. The first one (current 10) was detected in one cell-attached patch of 7F2 cells cultured with basal medium, and one excised inside-out patch of 7F2 cells cultured with adipogenic medium + 20 nM ghrelin. Representative current tracings of this channel activity and the corresponding I/V relationship are shown in figures 6.20 and 6.21. In 7F2 cells cultured with basal medium, this current had a 6.3 pS conductance from -70 mV to +60 mV and a

Chapter 6 – A comparison of the electrophysiological characteristics of osteoblasts and adipocytes, and the effects of ghrelin on these

conductance of 65.9 pS from +60 mV to +150 mV. In 7F2 cells cultured with adipogenic medium + ghrelin, the conductance was 4 pS from -120 mV to 80 mV and 269.5 pS from 80 to 100 mV.

The second one (current 11) was detected in 6.7% (n = 2) of 7F2 cells cultured with adipogenic medium, one in a cell-attached configuration, and one in an excised inside-out configuration. Both had very similar characteristics, with similar conductances and zero-current potentials. Representative current tracings of this channel activity and the corresponding I/V relationship are shown in figure 6.22. The current in the cell-attached patch had a conductance of 1.3 pS from -150 mV to -40 mV and a conductance of 28.7 pS from -40 mV to +80 mV; in the excised inside-out patch, it had a conductance of 3.2 pS from -140 mV to -70 mV and a conductance of 30.9 pS from -60 mV to +70 mV.

The third one (current 12) was detected in one excised patch from a 7F2 cell cultured with adipogenic medium + ghrelin (figure 6.23). It had a conductance of 14.6 pS from 20 mV to 100 mV and 233.3 pS from 110 mV to 140 mV.

6.4. Discussion

6.4.1. Problems encountered while recording electrophysiological data

Several difficulties were met during electrophysiological experiments; in particular, at times recordings contained a lot of electrical noise, which interfered with the characterisation of very small currents (< 2 pA) during analysis, especially at early stage experiments. Although this was filtered carefully, both during recording at 5 kHz and digitally afterwards at 20 kHz, it was impossible to separate the electrical noise from the signal sufficiently which prevented the analysis of ion channel kinetics such as dwell times, and probably artificially increased open probability.

Attempts were made to further study the electrophysiological properties of 7F2 cells and adipocytes by whole-cell patch clamp experiments (fig. 6.2), which may have overcome many of the signal-to-noise ratio problems that occurred. This technique also allows testing various channel openers or blockers to characterise functional ion channels present in a cell, more easily than the single-channel patch clamp technique, which allows characterising a single ion channel, by calculating its conductance and investigating its kinetics. However, despite a very large number of attempts ($n = 92$) over many months of experimental time, the whole-cell configuration could not be obtained with 7F2 cells and 7F2 cell-derived adipocytes. Part of the problem was the difficulty in achieving high resistance seals (> 1 G Ω), as the whole-cell patch clamp methods require larger microelectrode tips (1-3 M Ω resistance instead of 4-8 M Ω for single-channel patch clamp); this may be due to the fact that cell membranes are not smooth, which was more likely to interfere with seal formation. Another part of the problem may have been membrane fragility: cell-attached patches were disrupted and spontaneously excised to inside-out configuration patches very readily, preventing whole-cell patch configurations.

Attempts with an alternative technique, the perforated patch-clamp technique (fig. 6.2), were also made, to no avail ($n = 22$). This technique uses an antibiotic such as amphotericin B to create pores in the patch of membrane within the tip of the microelectrode. In the case of amphotericin B, these pores are permeable to the small monovalent ions (Na⁺, K⁺ and Cl⁻), allowing recording the currents carried by these ions, but present a physical barrier to impermeable ions (e.g. Ca²⁺) and molecules with a molecular weight above approximately 200 g/mol such as ATP. Amphotericin B usually acts within 15 minutes of entering in contact with the membrane, but in this study, it did not seem to work no matter how long the substance was left to act (> 30 min), or

Chapter 6 – A comparison of the electrophysiological characteristics of osteoblasts and adipocytes, and the effects of ghrelin on these

what concentration was used (Lippiat, 2009; Ishibashi *et al.*, 2012; Linley, 2013). Amphotericin B concentrations were between 200 and 400 $\mu\text{g/ml}$; concentrations could not be too high, as amphotericin B tends to prevent initial seal formation. In addition, the tip of the microelectrode was dipped in amphotericin B-free High K^+ solution for 5-15 seconds, as advised in protocols, so that amphotericin B would need to diffuse to the tip before it could create pores in the membrane, and would not interfere with seal formation. Also, amphotericin B is light-sensitive, so the stock powder was stored wrapped in aluminium foil, as was the solution as soon as it was prepared, so the exposure to light would be limited. The inefficiency of this technique may also be due to the fact that cell-attached patches spontaneously excised to inside-out configuration patches.

In single-channel patch clamp experiments, cell-attached patches were disrupted very readily, especially in cells cultured with adipogenic medium, suggesting that cell membrane was fragile. After recording, the patch configuration was verified by checking seal resistance before and after moving the microelectrode away from the cell. If seal resistance suddenly changed (for example, dropping from $> 2 \text{ G}\Omega$ to below $1 \text{ G}\Omega$), then the patch was considered as cell-attached during recording; on the contrary, if seal resistance did not change when the microelectrode was moved away, then the patch was considered as excised during recording. It was assumed that the cell-attached patches spontaneously excised to inside-out configuration, not outside-out, due to the fact that outside-out configuration is usually obtained from a whole-cell configuration, which was found to be very difficult to achieve in this study, with 7F2 cells.

With the available single-channel data, it was possible to calculate the unitary conductance and measure the open probability of several of the currents detected in 7F2 osteoblastic and adipocytic cells; however, these data are not sufficient to identify the corresponding ion channels. That being said, candidates can be proposed for many of these currents.

6.4.2. Ion channel candidates

Some of the electrophysiological properties of 7F2 cells and 7F2 cell-derived adipocytes have been previously investigated in other studies (Henney, 2008; Li, 2012), but not extensively. Interestingly, these studies showed the presence of a number of different membrane currents in 7F2 cells, but no current was detected in 7F2 cell-derived adipocytes. In particular, 7F2 osteoblastic cells possess a voltage-independent, small conductance ($31 \pm 7 \text{ pS}$) channel, a voltage-dependent, large conductance ($154 \pm$

11 pS) K⁺ channel, and TRPV1 channels. The latter may be involved in regulation of differentiation into adipocytes (Henney, 2008). The present study reports the presence of 12 types of functional ion channels in both 7F2 cells and 7F2 cell-derived adipocytes, treated or not with ghrelin. 2 of the channels detected in previous studies, the voltage-independent, small conductance (31 ± 7 pS) channel and the voltage-dependent, large conductance (154 ± 11 pS) K⁺ channel, may correspond to the 34.1 ± 1 pS channel and the 158.4 pS channel, respectively: they have similar characteristics and were present in 7F2 cells cultured with basal medium, but not adipogenic medium. The other 10 currents detected in this study have not been reported in 7F2 cells before; hence, this thesis brings new information about ionic mechanisms in 7F2 osteoblasts and 7F2-cell derived adipocytes. It is likely that some of these currents are carried by ions other than potassium, in particular calcium and chloride ions.

6.4.2.1. Currents detected only in 7F2 osteoblast-like cells

Some of the currents were detected in 7F2 osteoblast-like cells only (with or without ghrelin), and may be osteoblast-like-specific, such as the 34.1 ± 1 pS and the large conductance channels which are mentioned in the previous section. The 34.1 ± 1 pS channel may correspond to ClC-Ka; this channel, when co-expressed with the accessory beta-subunit barttin, is constitutively active, has a conductance of 34-40 pS, and has voltage-independent open probability (Fischer *et al.*, 2010; L'Hoste *et al.*, 2013). Alternatively, the 34.1 pS conductance channel may correspond to the two P domain K⁺ channel K_{2p1.1}. This family of channels mediate many of the background K⁺ currents and activate over the physiological voltage-range (Alexander Stephen PH *et al.*, 2017); they are expressed in human osteoblasts and are involved in regulating bone remodelling (Hughes *et al.*, 2006). The K_{2p1.1} current-voltage relationship is nearly linear in symmetrical 140 mM K⁺ across the membrane and the channel has a conductance of 32 ± 2.2 pS with a reversal potential of 0 mV (Rajan *et al.*, 2005). Here however, the 34.1 pS conductance channel had a reversal potential of -22.5 ± 0.7 mV.

The large conductance channel had a unitary conductance of 158.4 pS in cell-attached configuration, and 244.1 pS in excised inside-out configuration. This channel seemed to behave like the BK channel: it gave rise to large currents (> 20 pA at > 100 mV), was voltage-sensitive and was not spontaneously active, but instead required the membrane to be depolarised/hyperpolarised several times to open, after which it remained active. The conductance was a little low in cell-attached configuration but still in the very broad window of conductance values for this channel type (150 - 300

pS). The fact that this channel was only detected in 3 patches is consistent with the RT-PCR and qRT-PCR data for the BK channel subunits (see Chapter 5), which indicated low expression levels, and further suggests that BK channels do not play a central role in 7F2 cells.

6.4.2.2. Currents detected only in 7F2 cells treated with ghrelin

Some currents were only detected when 7F2 cells were cultured with 20 nM ghrelin; in particular, the inward, 6.2 ± 3 pS current and the outward, 6.5 ± 4.1 pS current. In addition, no intermediate conductance current was recorded in the absence of ghrelin treatment, whereas a 67.5 ± 2.1 pS conductance current was detected in 7F2 cells cultured with adipogenic medium + ghrelin, and a 80.8 pS conductance current was detected in 7F2 cells cultured with basal medium + ghrelin. Ghrelin treatment may have promoted the expression of the corresponding ion channels.

The inward, 6.2 ± 3 pS conductance channel was voltage-dependent, as it was not activated at voltages > 0 mV. It was also clearly voltage-sensitive, as open probability decreased with increasing pipette voltage (toward depolarising voltages). It may correspond to two inwardly rectifying potassium channels, Kir2.4 or Kir2.3, although the conductance was lower than what was reported for these two channels (Alexander Stephen PH *et al.*, 2017). Alternatively, these ion channels may belong to another family, such as calcium channels; the T-type Ca^{2+} channel (Cav3.1) has a conductance of 7 pS (Monteil *et al.*, 2000).

The 6.5 pS conductance, outward current may correspond to various ion channels. Voltage-dependency could not be determined as open probability could not be analysed for these channels, due to the presence of several types of currents in the recordings. However, various voltage-gated potassium channels give rise to outward currents with similar conductances, such as Kv1.1, Kv1.3, Kv1.4, Kv1.5, Kv1.6 or Kv2.1 (Alexander Stephen PH *et al.*, 2017). Interestingly, Kv2.1 has been associated with ghrelin and leptin signalling in several studies. Indeed, Kv2.1 is involved in ghrelin regulation of insulin release in pancreatic beta cells; ghrelin has been shown to increase Kv2.1 current amplitudes, inhibiting membrane excitability and insulin secretion (Dezaki *et al.*, 2007; Yada *et al.*, 2014). Leptin has been shown to increase Kv2.1 and K_{ATP} channel densities in the same cell type, which may also inhibit membrane excitability and insulin secretion (Wu *et al.*, 2015). Kv2.1 expression has been identified in human primary osteoblasts (Pangalos *et al.*, 2011; Li *et al.*, 2013b); it is also expressed in adipocytes derived from human bone MSCs and is involved in regulating adipogenic

Chapter 6 – A comparison of the electrophysiological characteristics of osteoblasts and adipocytes, and the effects of ghrelin on these

differentiation (You *et al.*, 2013). RT-PCR and qRT-PCR analysis should be performed to verify if 7F2 cells express this ion channel, and whether it is upregulated when 7F2 cells are treated with ghrelin. Also, using specific Kv2.1 blockers such as stromatoxin or guangxitoxin in electrophysiology experiments would confirm that this channel is present and functional.

Two intermediate conductance channels were detected in 7F2 cells treated with 20 nM ghrelin. The 67.5 pS conductance channel was voltage-independent; this channel may correspond to the Ca²⁺-activated intermediate conductance K⁺ channel (KCa3.1) (Alexander Stephen PH *et al.*, 2017). It could also have been a K_{ATP} channel containing Kir6.2, encoded by *Kcnj11*; however, this subunit was not detected by RT-PCR analysis (see Chapter 5). The other intermediate conductance current was detected in 7F2 cells cultured with basal medium + 20 nM ghrelin; it was a 80.8 pS conductance, outward current and it may correspond to K_{2P}2.1, which has been reported to have a conductance of 85 pS in rats (Alexander Stephen PH *et al.*, 2017).

6.4.2.13. Currents detected in 7F2 cells both in absence and in presence of ghrelin

Several currents were detected 7F2 cells both in absence and in presence of ghrelin treatment. In particular, the 28.5 pS conductance current, was one of the most frequently observed currents. It was identified in 13% of patches from 7F2 cells cultured with basal medium (n = 5), 21% of patches from 7F2 cells cultured with adipogenic medium + ghrelin (n = 4) and 25% of patches from 7F2 cells cultured with basal medium + ghrelin (n = 3). This channel was activated by depolarising voltages. In cells cultured with basal medium with or without ghrelin, open probability seemed to decrease very slightly with increasing pipette voltage. However, electrical noise certainly artificially increased open probability at lower voltages (0 mV to +20 mV), suggesting that open probability was not affected by changes in pipette voltage, and that this ion channel was voltage-independent. However, in cells cultured with adipogenic medium + ghrelin, open probability increased with increasing pipette voltage between 0 mV and +60 mV, then plateaued between +60 mV and +140 mV, indicating that the ion channel was voltage-sensitive. This ion channel may correspond to the voltage-gated K⁺ channel Kv3.1, which has been reported to have a conductance of 27.0 pS in mouse and is present in unexcitable cells (Yasuda *et al.*, 2013; Alexander Stephen PH *et al.*, 2017).

Another ion channel, the 43.3 pS conductance channel, was present in 13% (n=5) of cells cultured with basal medium, 10% (n=3) of cells cultured with adipogenic medium,

Chapter 6 – A comparison of the electrophysiological characteristics of osteoblasts and adipocytes, and the effects of ghrelin on these

and in 11% (n=2) of 7F2 cells cultured with adipogenic medium + 20 nM ghrelin. Similarly to the 28.5 pS conductance channel, open probability decreased with increasing pipette voltage in patches from 7F2 cells cultured with basal or adipogenic medium alone, suggesting that the ion channel was voltage-sensitive, but when 7F2 cells were cultured with adipogenic medium + ghrelin, open probability increased with depolarising voltages. The channel displayed inward rectification and may correspond to two ion channels: Kir6.1/SUR2B and Kir1.1/SUR2B. Kir6.1/SUR2B has a conductance of 32.9-50 pS (Alexander Stephen PH *et al.*, 2017); a study reported that Kir6.1/SUR2B had a conductance of 32.9 pS both in cell-attached and excised inside-out patches, with a microelectrode containing 145 mM K⁺ (Yamada *et al.*, 1997). Here, microelectrodes contained 140 mM K⁺. In addition, 7F2 cells express both Kir6.1 and SUR2B subunits. Alternatively, the inward rectifier channel Kir1.1 can also associate with SUR2B and has a conductance of 39.0 pS in rats; this channel is a very weak inward rectifier: it gives rise to outward currents, while strong inward rectifiers only give rise to inward currents. Kir1.1/SUR2B is regulated by ATP (Ho *et al.*, 1993; Alexander Stephen PH *et al.*, 2017).

Finally, several currents with two conductances were recorded in this study. 7F2 cells cultured with basal medium alone and with adipogenic medium + ghrelin possessed an outward current that had a conductance of 6.3 pS from - 70 to + 60 mV, and a conductance of 65.9 pS from + 60 to + 150 mV. Another channel that gave rise to outward currents with two conductances was recorded in 7F2 cells cultured with adipogenic medium + ghrelin; it had a conductance of 14.6 pS from + 20 to + 100 mV, and a conductance of 233.3 pS from + 100 mV to + 140 mV. These channels may correspond to ion channels other than potassium channels, such as calcium or chloride channels.

7F2 cells cultured with adipogenic medium possessed a current displaying outward rectification, with a conductance of 1.3 pS from - 150 to - 40 mV, and a conductance of 28.7 pS from - 40 to + 80 mV. The current-voltage plots were similar to that of the two P domain potassium channel K_{2P}4.1 in the presence of 150 nM Na⁺; however, in the present study, this current was recorded in the presence of symmetric 140 mM K⁺ (Leonoudakis *et al.*, 1998; Alexander Stephen PH *et al.*, 2017). Alternatively, this channel may correspond to various chloride (Cl⁻) channels, such as the volume-regulated anion channel (VRAC) or ClC-3. VRAC has a conductance of 10-20 pS at negative potentials, and 50-90 pS at positive potentials (Alexander Stephen PH *et al.*, 2017), although here the conductance at positive potentials was much lower (28.7 pS).

Chapter 6 – A comparison of the electrophysiological characteristics of osteoblasts and adipocytes, and the effects of ghrelin on these

This channel displays outward rectification and has been reported to play a role in regulating membrane excitability, cell proliferation (Hoffmann *et al.*, 2014) and insulin release from pancreatic β cells (Best *et al.*, 2010). The ClC-3 channel has an inward conductance of 12.8 ± 1.8 pS and an outward conductance of 39.7 ± 0.6 pS (Duan *et al.*, 1997), which is closer to the current recorded in this study.

6.4.3. Chapter conclusions

Due to a lack of consistent evidence, it is difficult to make any firm conclusions about the identity of the ion channels recorded in this study; further work with pharmacological agents (specific channel blockers or openers) and RT-PCR analysis would be useful to confirm the identity of these channels. Subunits corresponding to BK channels and K_{ATP} channels were detected by RT-PCR analysis (Chapter 5), and currents that may correspond to these channels were recorded, suggesting that they are expressed at the protein level and functional; but the identity of the other ion channels detected in this study remains to be elucidated. Hence, it is difficult to accept or reject the hypothesis that adipogenic differentiation modified the electrophysiological properties of 7F2 osteoblast-like cells.

However, the hypothesis that ghrelin had an impact on the electrophysiological properties of 7F2 cells was accepted. Overall, ghrelin seemed to have two effects on 7F2 cell electrophysiological properties: some currents were only detected in 7F2 cells cultured with ghrelin, and ghrelin modified the open probabilities of some currents that were detected in 7F2 cells both in presence and in absence of ghrelin. Future work may investigate whether the currents detected in 7F2 cells treated with ghrelin are carried by ion channels whose expression is induced by ghrelin.

Chapter 6 – A comparison of the electrophysiological characteristics of osteoblasts and adipocytes, and the effects of ghrelin on these

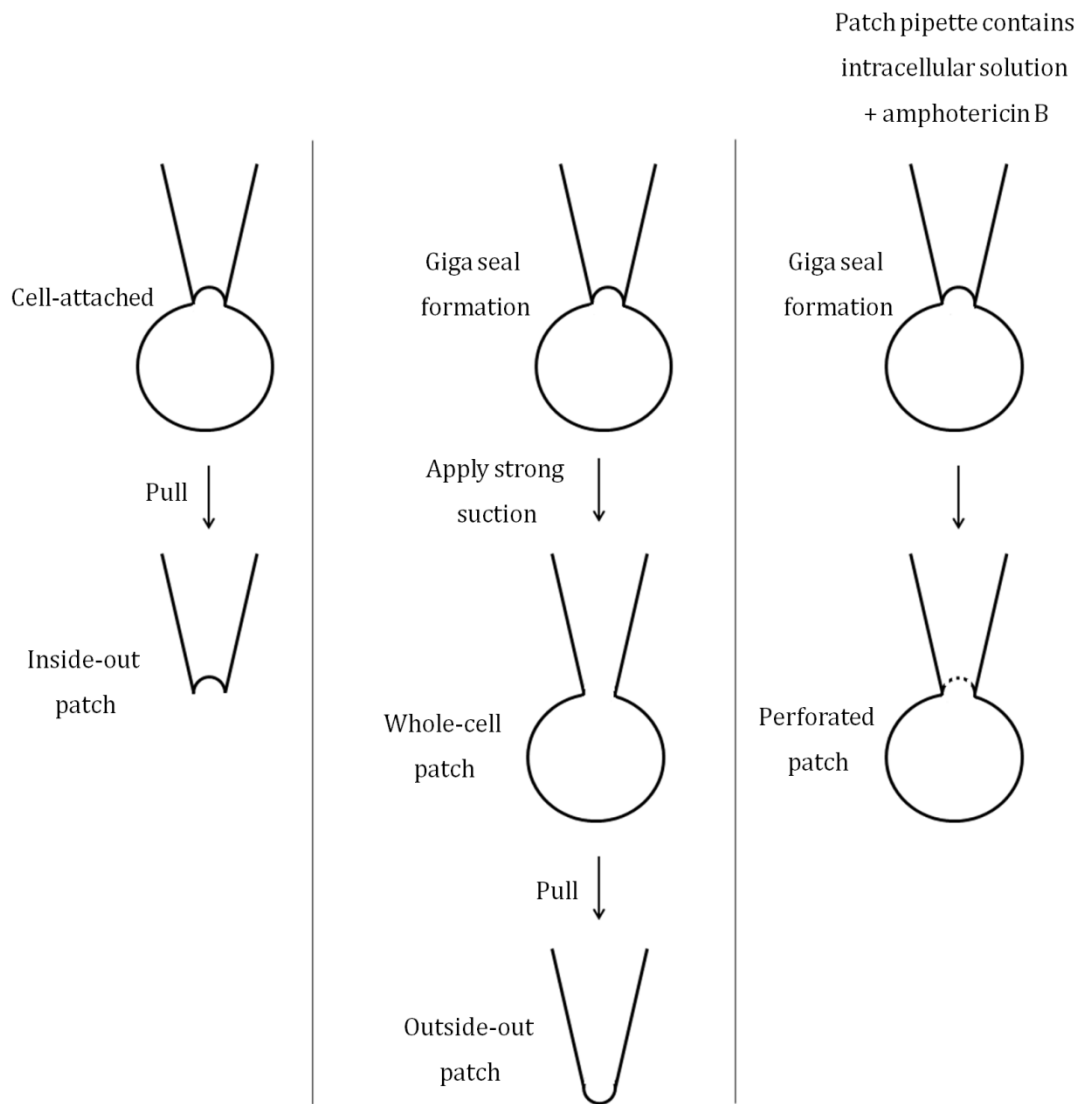


Figure 6.2: Patch configurations for electrophysiological recording.

In the perforated-patch clamping technique, the recording microelectrode contains an antibiotic in addition to intracellular solution; here it contained High K^+ solution and amphotericin B. Adapted from (Ogden and Stanfield, 1994)

Chapter 6 – A comparison of the electrophysiological characteristics of osteoblasts and adipocytes, and the effects of ghrelin on these

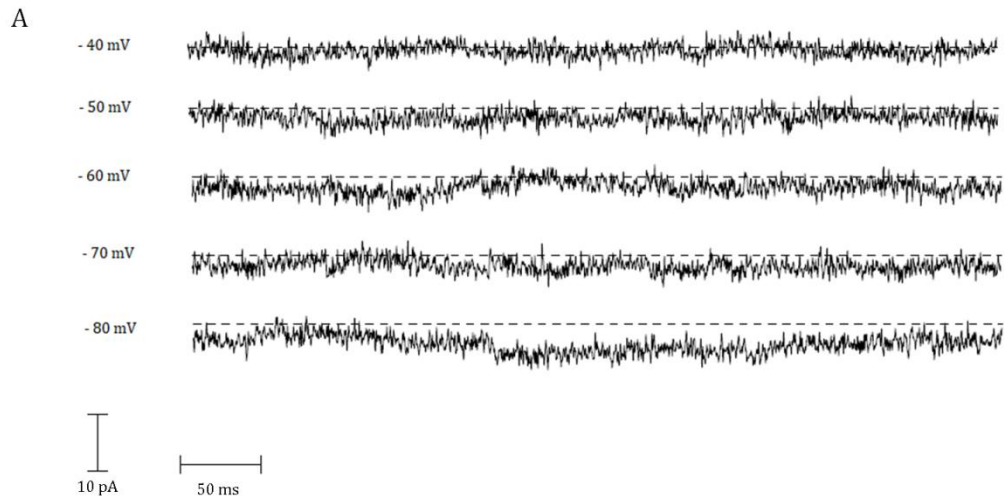


Figure 6.3: Current 1 in 7F2 cells cultured with adipogenic medium + 20 nM ghrelin
(part 1)

A: Typical recordings of current 1 in cell-attached patch configuration. Bath solution was Na⁺ Locke and pipette solution was high-K⁺ medium. Downward deflections represent ion channel opening.

Chapter 6 – A comparison of the electrophysiological characteristics of osteoblasts and adipocytes, and the effects of ghrelin on these

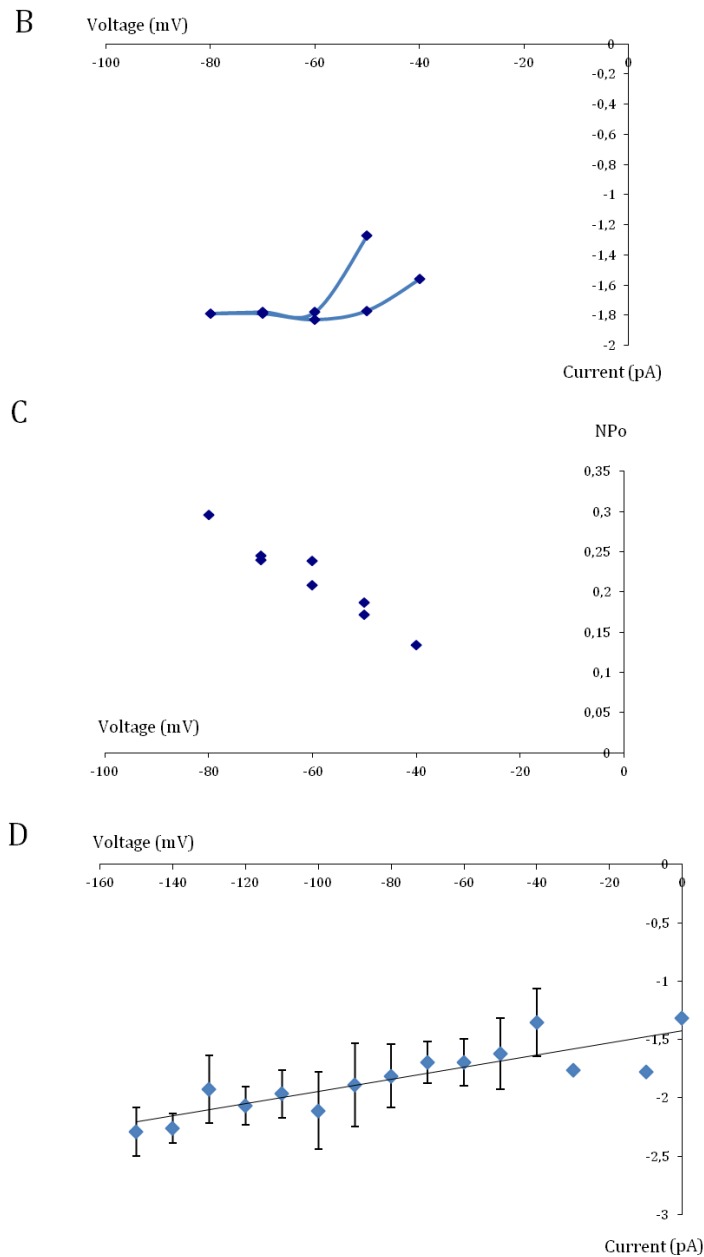


Figure 6.3: Current 1 in 7F2 cells cultured with adipogenic medium + 20 nM ghrelin (part 2)

B: Corresponding current-voltage data plot. Data points were derived from fitting amplitude histograms at each membrane potential. Lines of best fit yielded a conductance of 8.3 pS. C: Corresponding open probability plot. NPo ($P_o/3$) was used as a measure of open probability, as there were at least 3 currents of the same type in this patch; NPo decreased with increasing pipette voltage, indicating that this channel is voltage-sensitive. D: Current-voltage relationship for current 1 in cell-attached patches from 7F2 cells cultured with adipogenic medium + 20 nM ghrelin; each data point represents the average channel current calculated from amplitude histograms (mean \pm SD of 5 patches from different cells).

Chapter 6 – A comparison of the electrophysiological characteristics of osteoblasts and adipocytes, and the effects of ghrelin on these

A

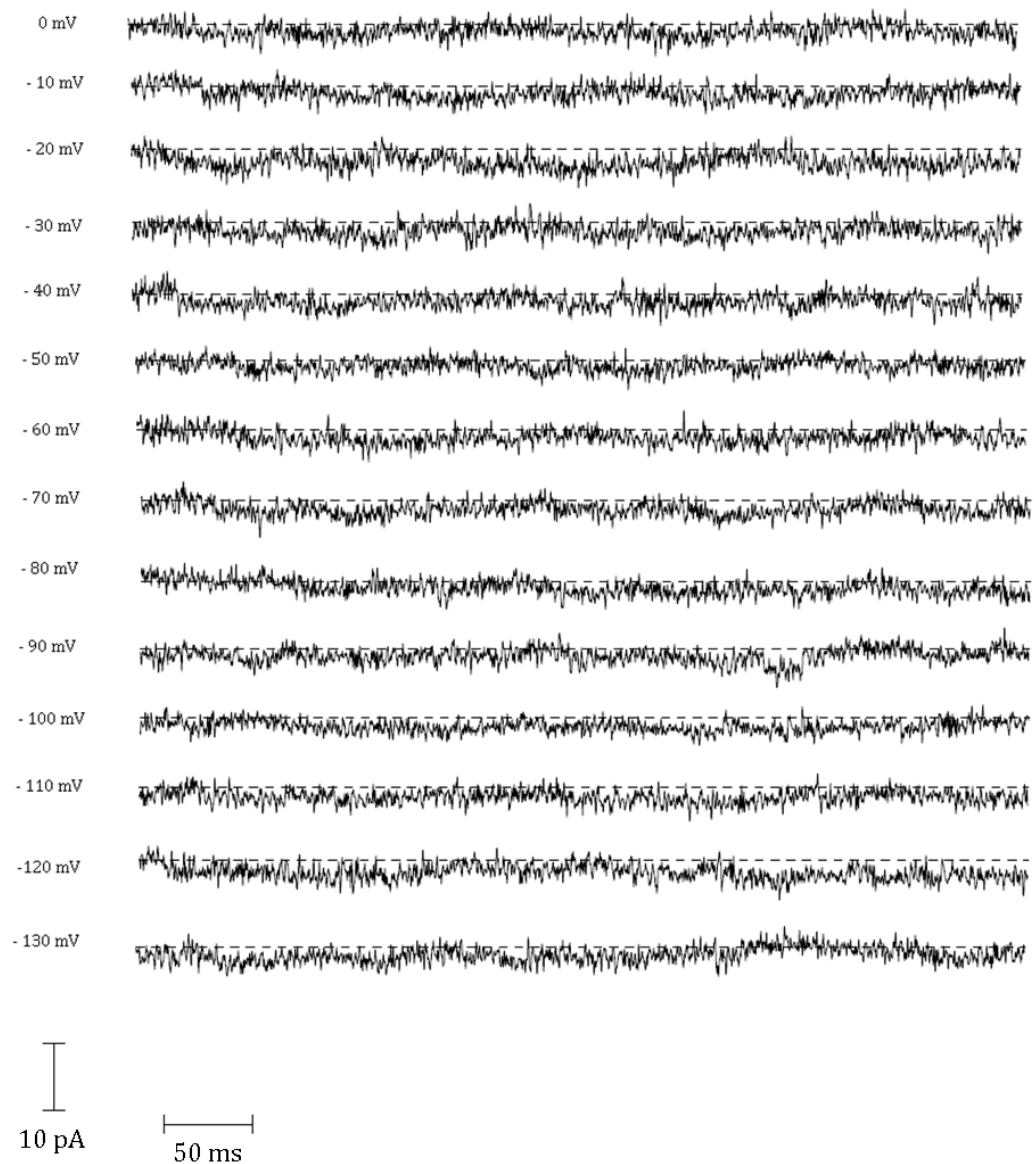


Figure 6.4: Current 1 in 7F2 cells cultured with basal medium + 20 nM ghrelin (part 1)

A: Typical recordings of current 1 in cell-attached patch configuration. Bath solution was Na⁺ Locke and pipette solution was high-K⁺ medium. Downward deflections represent ion channel opening.

Chapter 6 – A comparison of the electrophysiological characteristics of osteoblasts and adipocytes, and the effects of ghrelin on these

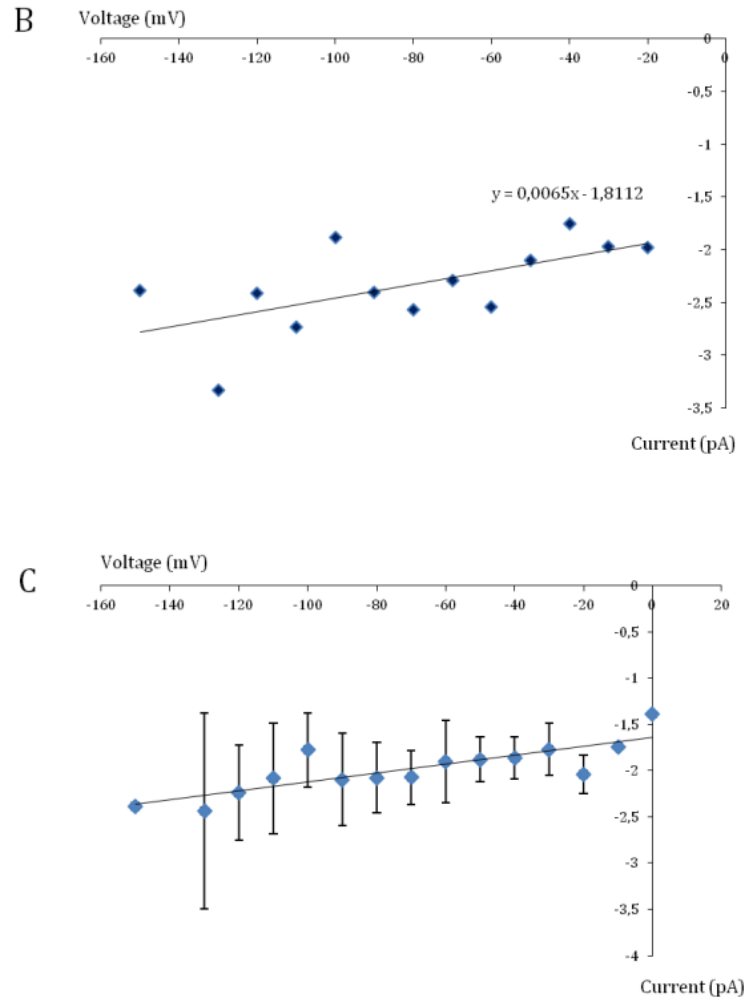


Figure 6.4: Current 1 in 7F2 cells cultured with basal medium + 20 nM ghrelin (part 2)

B: Corresponding current-voltage data plot. Lines of best fit yielded a conductance of 6.5 pS. Data points were derived from fitting amplitude histograms at each membrane potential. Probability of opening could not be analysed as all these patches exhibited several types of currents. C: Current-voltage relationship for current 1 in cell-attached patches from 7F2 cells cultured with basal medium; each data point represents the average channel current calculated from amplitude histograms (mean \pm SD of 3 patches from different cells).

Chapter 6 – A comparison of the electrophysiological characteristics of osteoblasts and adipocytes, and the effects of ghrelin on these

A

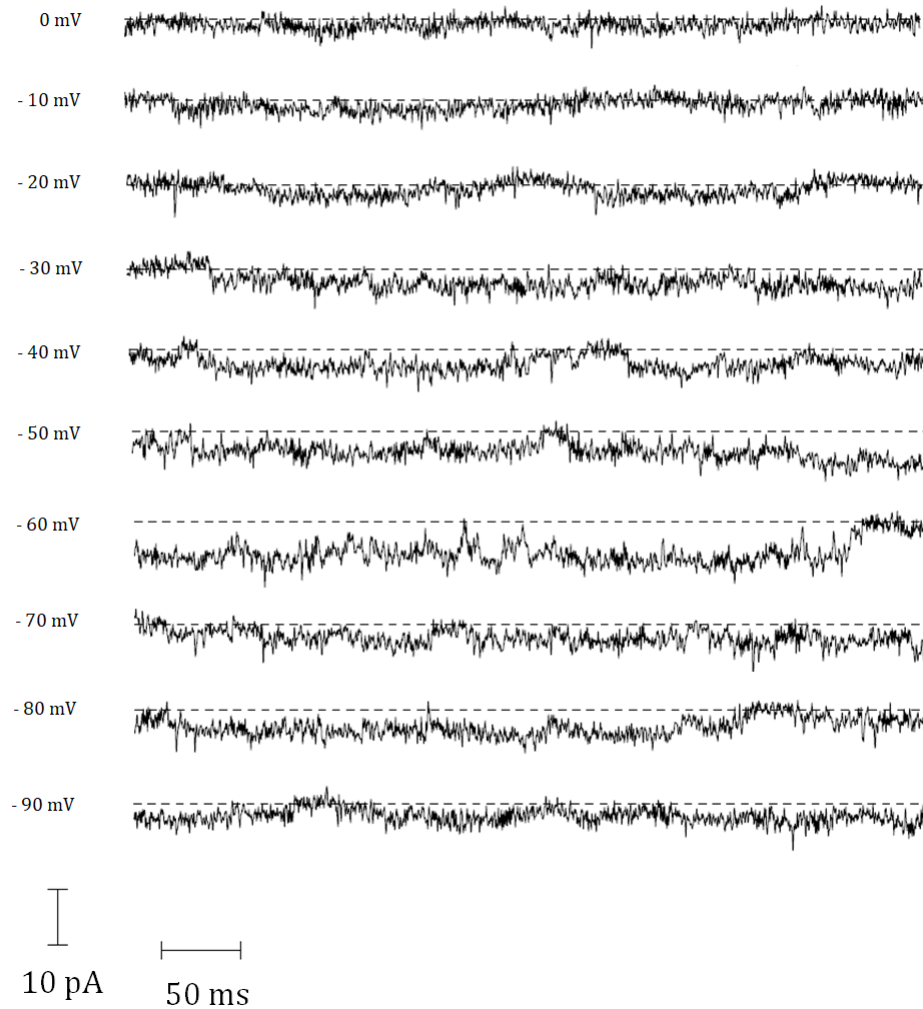


Figure 6.5: Current 2 in 7F2 cells cultured with adipogenic medium + 20 nM ghrelin (part 1)

A: Typical recordings of the current 2 in excised inside-out patch configuration. Bath solution was Na⁺ Locke and pipette solution was high-K⁺ medium. Downward deflections represent ion channel opening.

Chapter 6 – A comparison of the electrophysiological characteristics of osteoblasts and adipocytes, and the effects of ghrelin on these

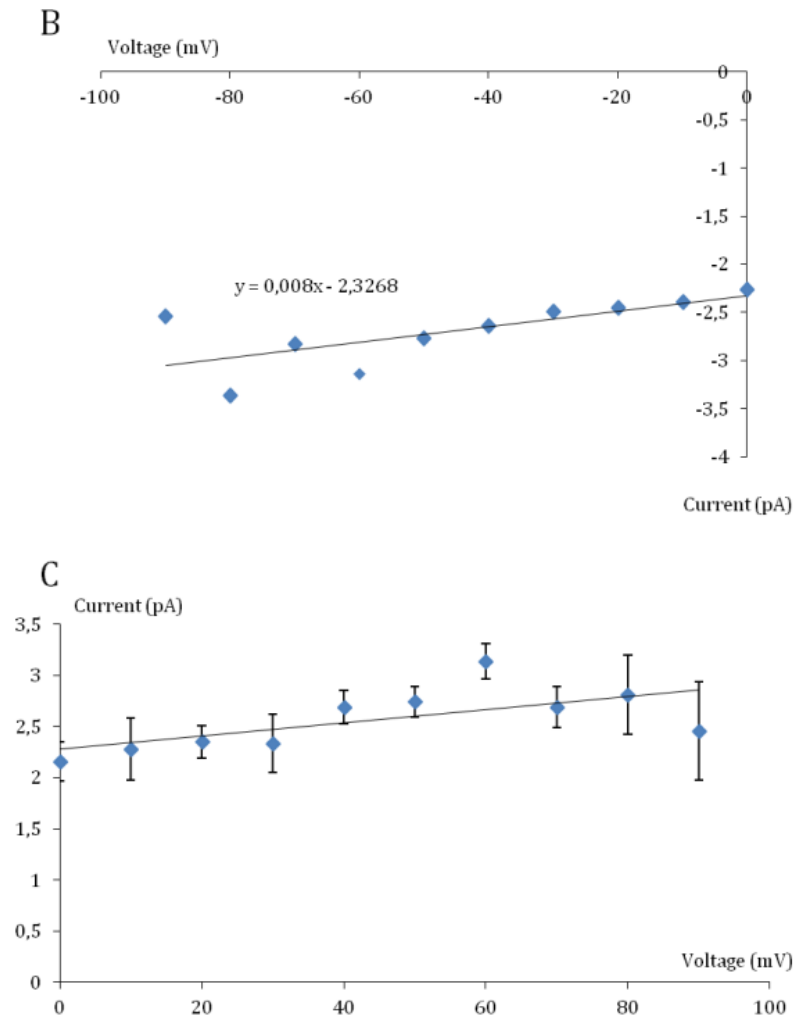


Figure 6.5: Current 2 in 7F2 cells cultured with adipogenic medium + 20 nM ghrelin (part 2)

B: Corresponding current-voltage data plot. Lines of best fit yielded a conductance of 8.0 pS. Data points were derived from fitting amplitude histograms at each membrane potential. C: Current-voltage relationship for current 2 in cell-attached patches from 7F2 cells cultured with adipogenic medium + 20 nM ghrelin; each data point represents the average channel current calculated from amplitude histograms (mean \pm SD of 2 patches from different cells). Probability of opening could not be analysed as all these patches exhibited several types of currents.

Chapter 6 – A comparison of the electrophysiological characteristics of osteoblasts and adipocytes, and the effects of ghrelin on these

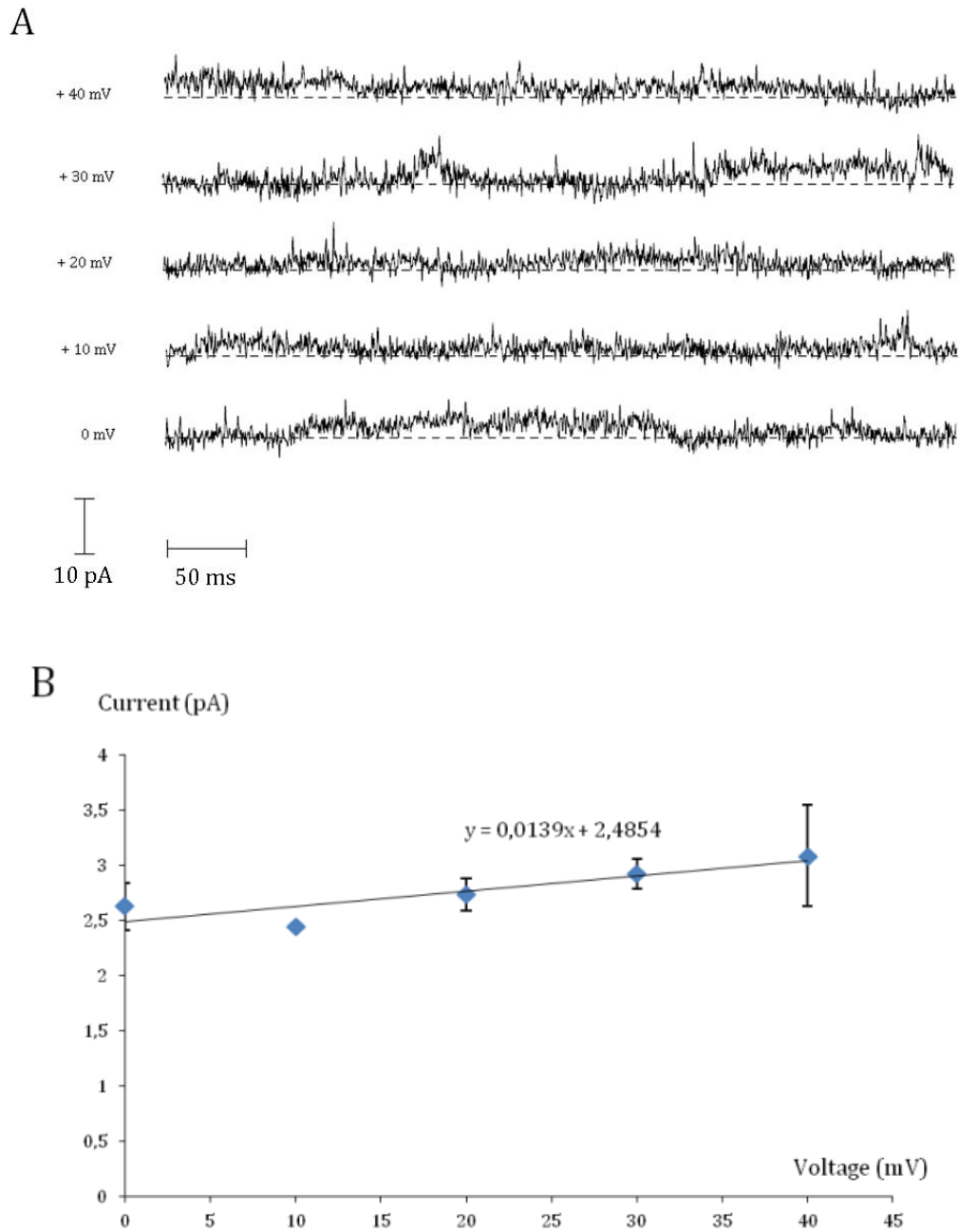


Figure 6.6: Current 2 in 7F2 cells cultured with basal medium + 20 nM ghrelin

A: Typical recordings of the 6.5 pS conductance channel current. Bath solution was Na⁺ Locke and pipette solution was high-K⁺ medium. Upward deflections represent ion channel opening. B: Corresponding current-voltage data plot. Lines of best fit yielded a conductance of 13.9 pS. Data points were derived from fitting amplitude histograms at each membrane potential. Probability of opening could not be analysed as this patch exhibited several types of currents.

Chapter 6 – A comparison of the electrophysiological characteristics of osteoblasts and adipocytes, and the effects of ghrelin on these

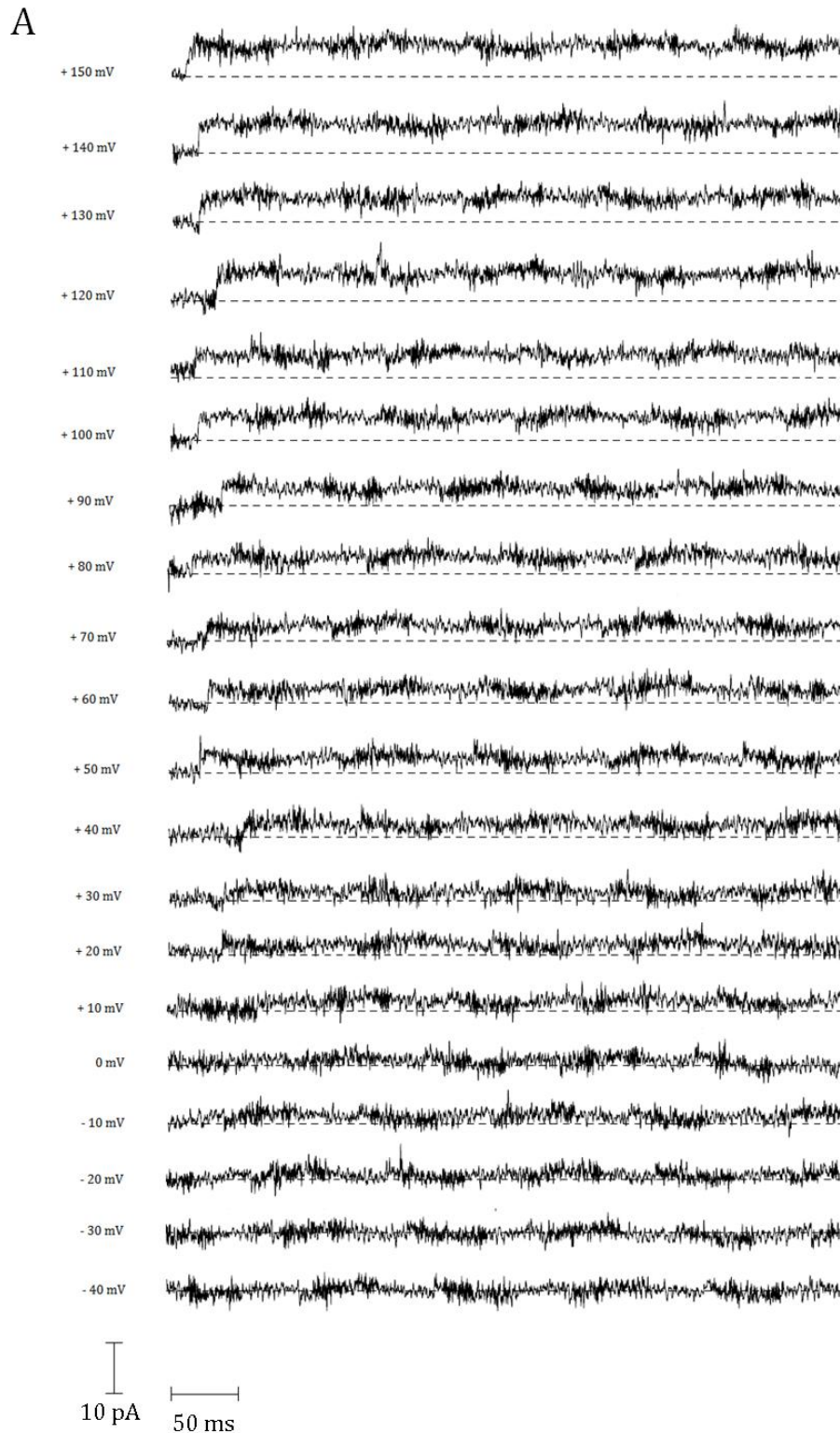


Figure 6.7: Current 3 in 7F2 cells cultured with basal medium (part 1)

A: Typical recordings of the current 3 in cell-attached patch configuration. Bath solution was Na⁺ Locke and pipette solution was high-K⁺ medium. Upward deflections represent ion channel open-state currents.

Chapter 6 – A comparison of the electrophysiological characteristics of osteoblasts and adipocytes, and the effects of ghrelin on these

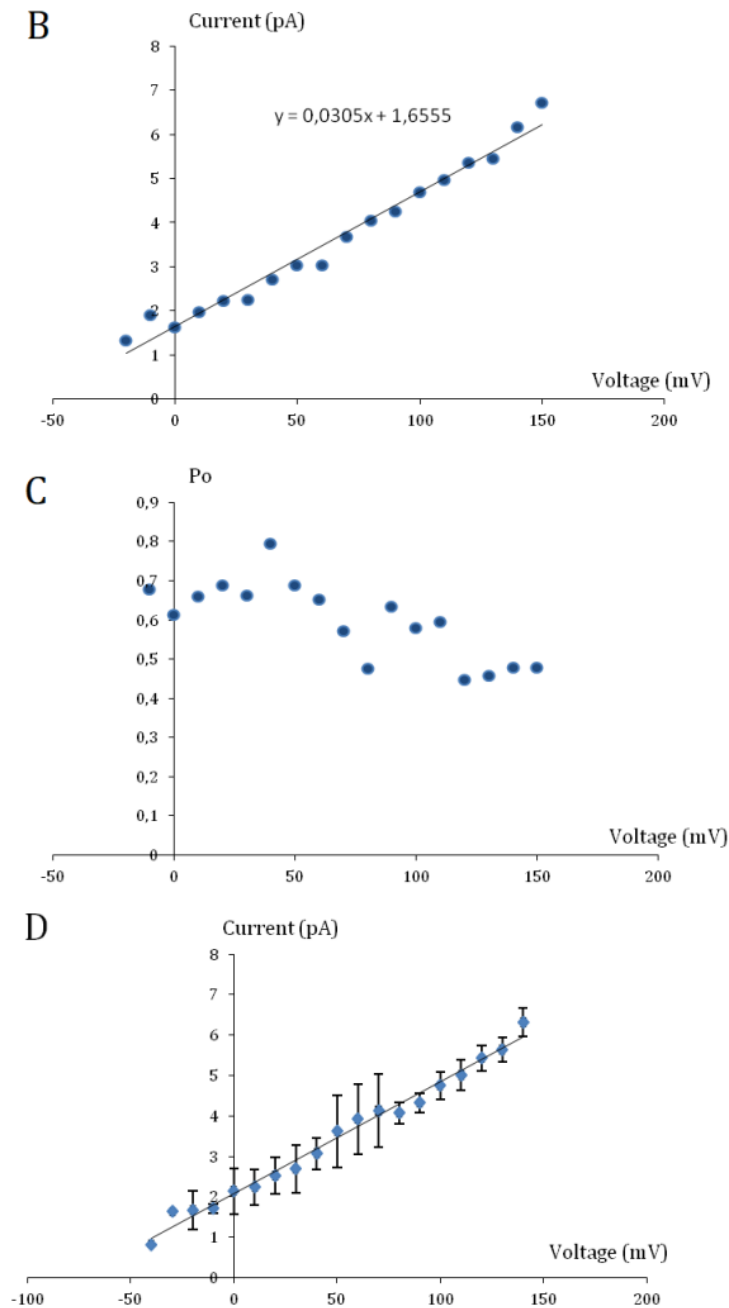


Figure 6.7: Current 3 in 7F2 cells cultured with basal medium (part 2)

B: Corresponding current-voltage data plot ($n = 1$). Line of best fit yielded a conductance of 30.7 pS. Data points were derived from fitting amplitude histograms at each membrane potential. C: Corresponding P_{open} plot. P_o decreased slightly with increasing pipette voltage. D: Current-voltage relationship for the current 3 in cell-attached patches from 7F2 cells cultured with basal medium; each data point represents the average channel current calculated from amplitude histograms (mean \pm SD of 5 patches from different cells). Reversal potential was -69.2 ± 10.5 mV.

Chapter 6 – A comparison of the electrophysiological characteristics of osteoblasts and adipocytes, and the effects of ghrelin on these

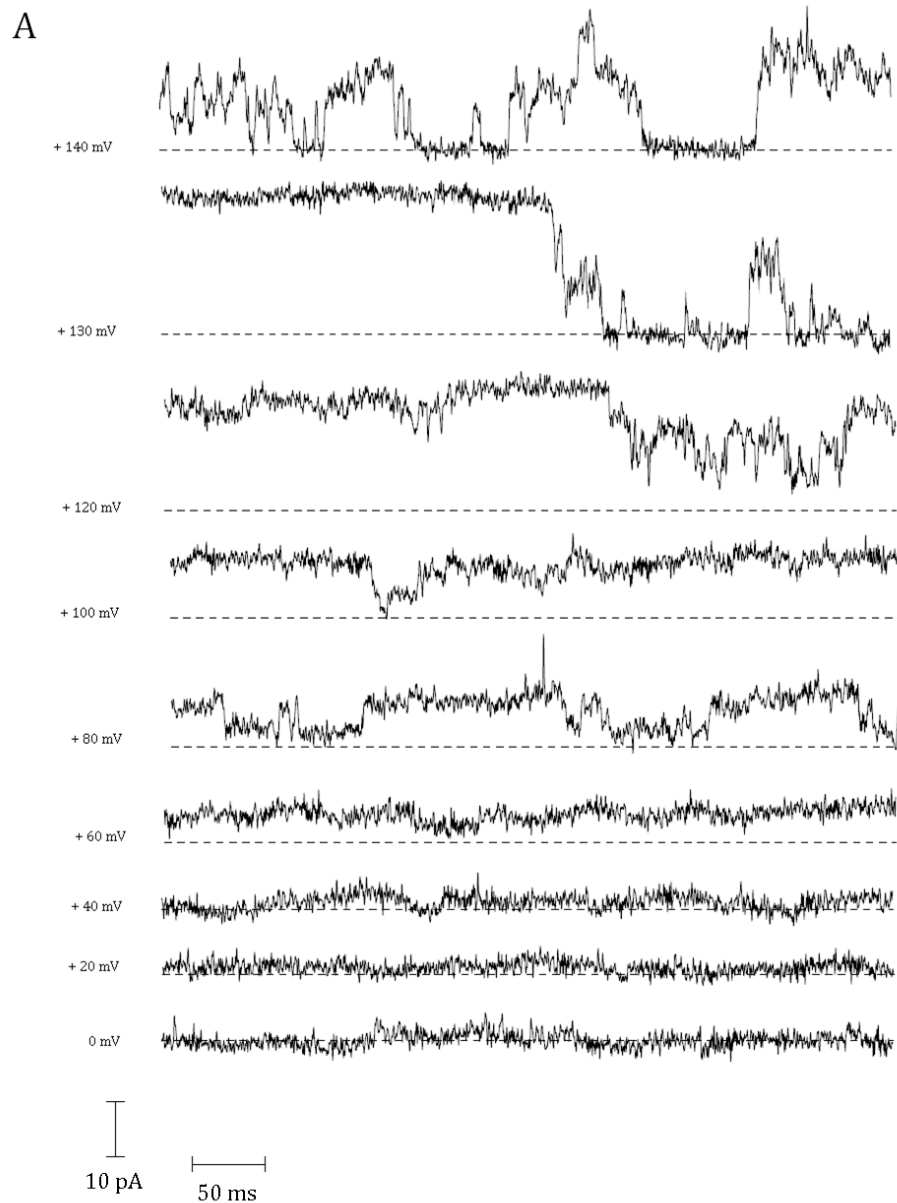


Figure 6.8: Current 3 in 7F2 cells cultured with adipogenic medium + ghrelin (cell-attached) (part 1)

A: Typical recordings of the current 3 in cell-attached patch configuration. Bath solution was Na⁺ Locke and pipette solution was high-K⁺ medium. Upward deflections represent ion channel opening.

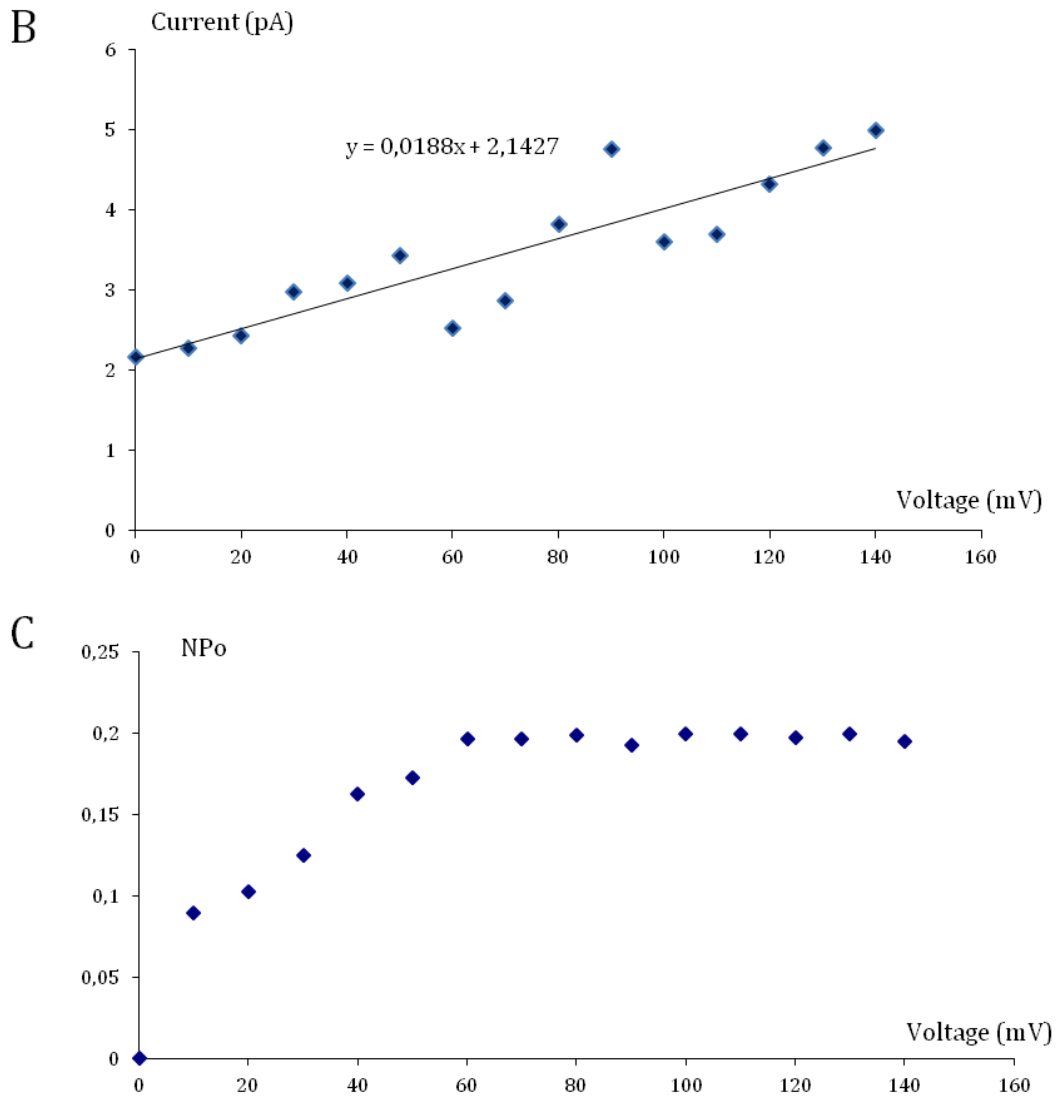


Figure 6.8: Current 3 in 7F2 cells cultured with adipogenic medium + ghrelin (cell-attached) (part 2)

B: Corresponding current-voltage data plot. Lines of best fit yielded a conductance of 18.8 pS. Data points were derived from fitting amplitude histograms at each membrane potential. C: Corresponding open probability plot. NPo ($P_o/5$) was used as a measure of open probability, as there were at least 5 currents of the same type in this patch; NPo increased with increasing pipette voltages from 0 mV to +60 mV, then plateaued at ~0.2. Reversal potential was -109 mV.

Chapter 6 – A comparison of the electrophysiological characteristics of osteoblasts and adipocytes, and the effects of ghrelin on these

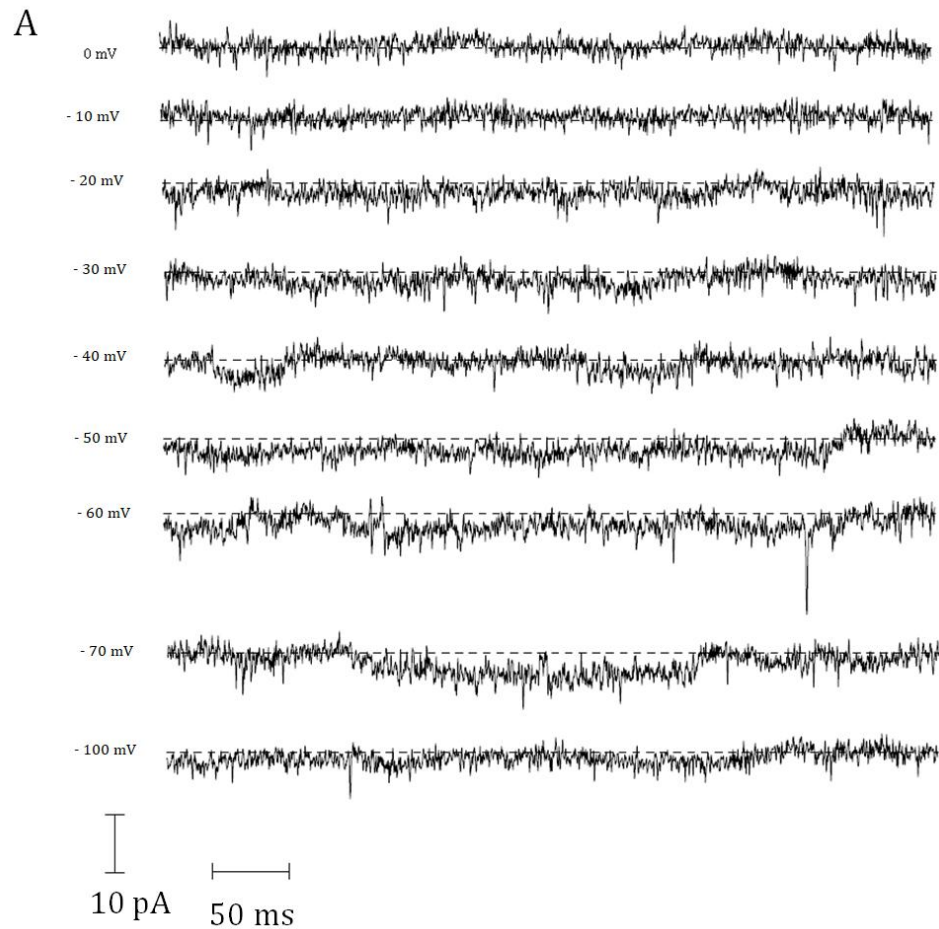


Figure 6.9: Current 3 in 7F2 cells cultured with adipogenic medium + ghrelin (excised inside-out) (part 1)

A: Typical recordings of the current 3 in excised inside-out patch configuration. Bath solution was Na⁺ Locke and pipette solution was high-K⁺ medium. Downward deflections represent ion channel opening.

Chapter 6 – A comparison of the electrophysiological characteristics of osteoblasts and adipocytes, and the effects of ghrelin on these

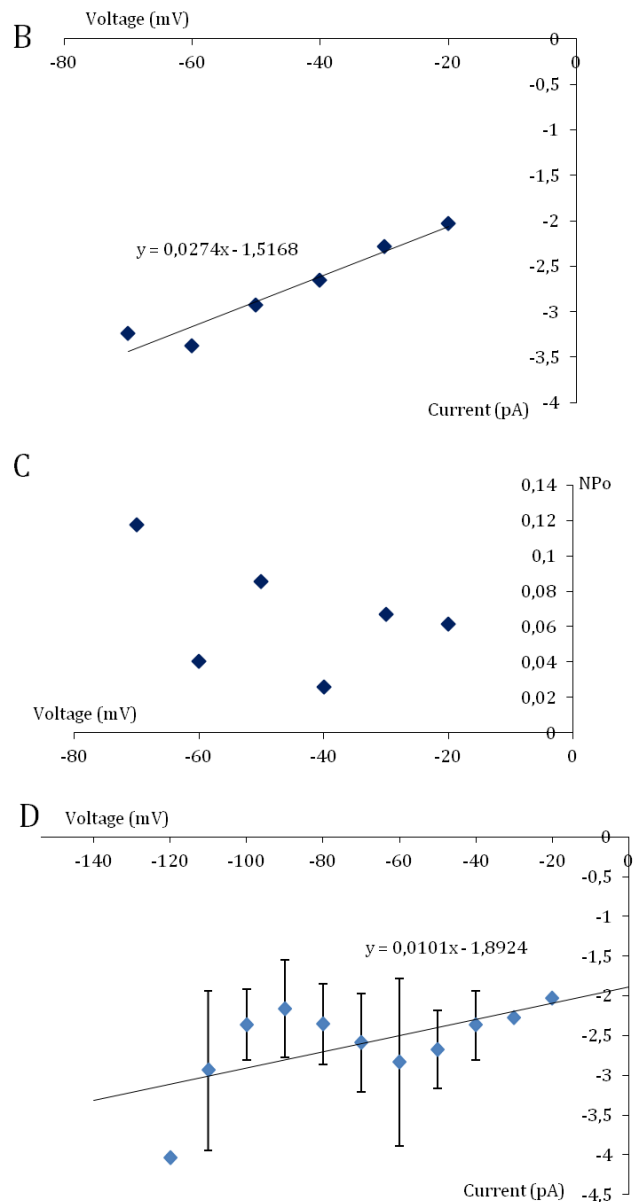


Figure 6.9: Current 3 in 7F2 cells cultured with adipogenic medium + ghrelin (excised inside-out) (part 2)

B: Corresponding current-voltage data plot. Lines of best fit yielded a conductance of 27.4 pS. Data points were derived from fitting amplitude histograms at each membrane potential. C: Corresponding open probability plot. NPo ($P_o/5$) was used as a measure of open probability, as there were at least 5 currents of the same type in this patch; NPo did not seem to vary with increasing pipette voltages. D: Current-voltage relationship for the current 3 in excised inside-out patches from 7F2 cells cultured with adipogenic medium + 20 nM ghrelin; each data point represents the average channel current calculated from amplitude histograms (mean \pm SD of 3 patches from different cells). Reversal potential was -55 ± 3.6 mV.

Chapter 6 – A comparison of the electrophysiological characteristics of osteoblasts and adipocytes, and the effects of ghrelin on these

A

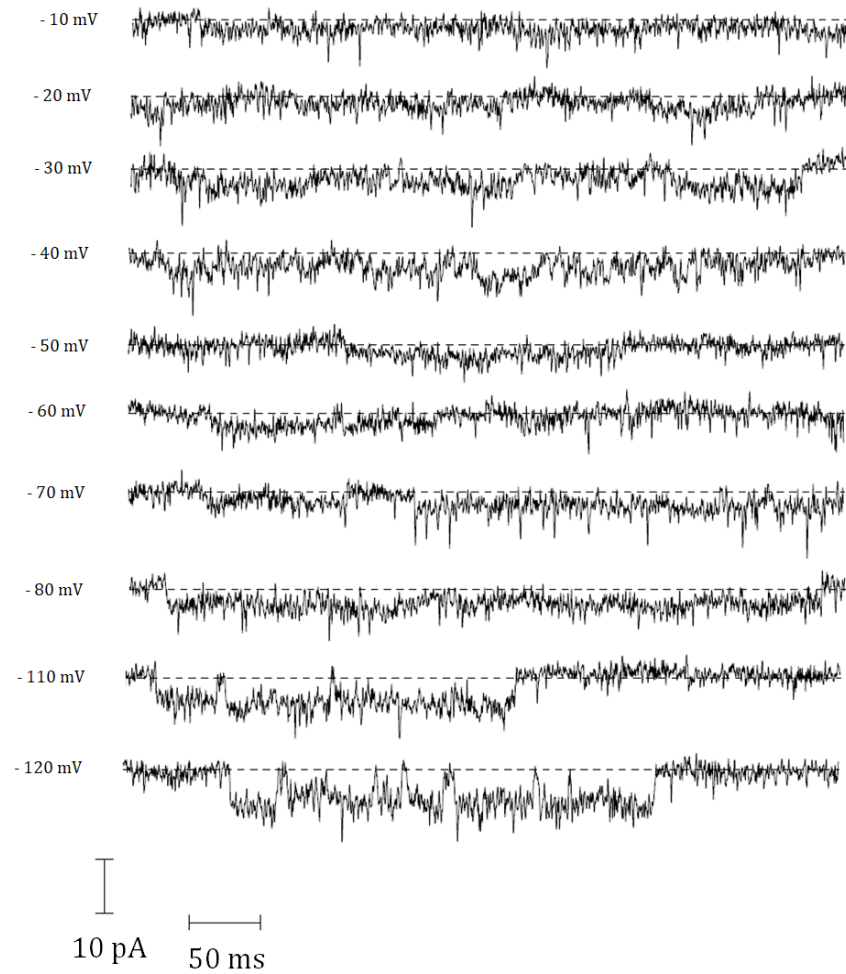


Figure 6.10: Current 3 in 7F2 cells cultured with basal medium + ghrelin (excised inside-out) (part 1)

A: Typical recordings of the current 3 in excised inside-out patch configuration. Bath solution was Na⁺ Locke and pipette solution was high-K⁺ medium. Downward deflections represent ion channel opening.

Chapter 6 – A comparison of the electrophysiological characteristics of osteoblasts and adipocytes, and the effects of ghrelin on these

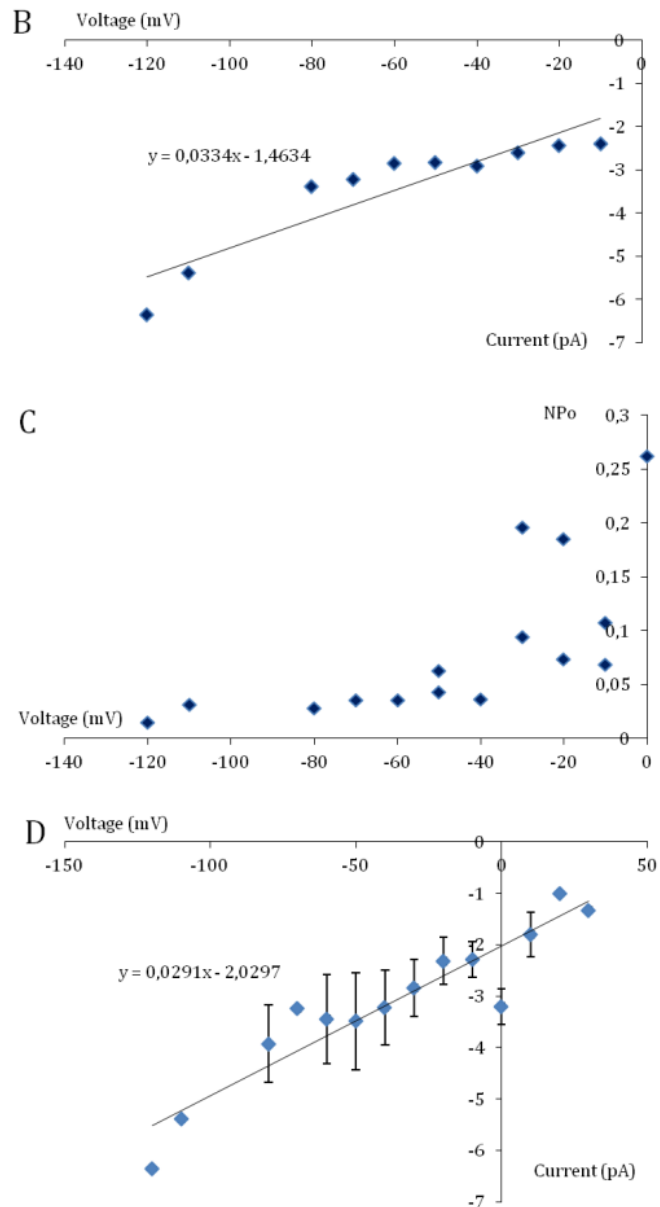


Figure 6.10: Current 3 in 7F2 cells cultured with basal medium + ghrelin (excised inside-out) (part 2)

B: Corresponding current-voltage data plot. Lines of best fit yielded a conductance of 33.4 pS. Data points were derived from fitting amplitude histograms at each membrane potential. C: Corresponding open probability plot. NPo (Po/3) was used as a measure of open probability; NPo decreased with increasing pipette voltage. D: Current-voltage relationship for the current 3 in excised inside-out patches from 7F2 cells cultured with adipogenic medium + 20 nM ghrelin; each data point represents the average channel current calculated from amplitude histograms (mean \pm SD of 3 patches from different cells). Reversal potential was -81 ± 6.1 mV.

Chapter 6 – A comparison of the electrophysiological characteristics of osteoblasts and adipocytes, and the effects of ghrelin on these

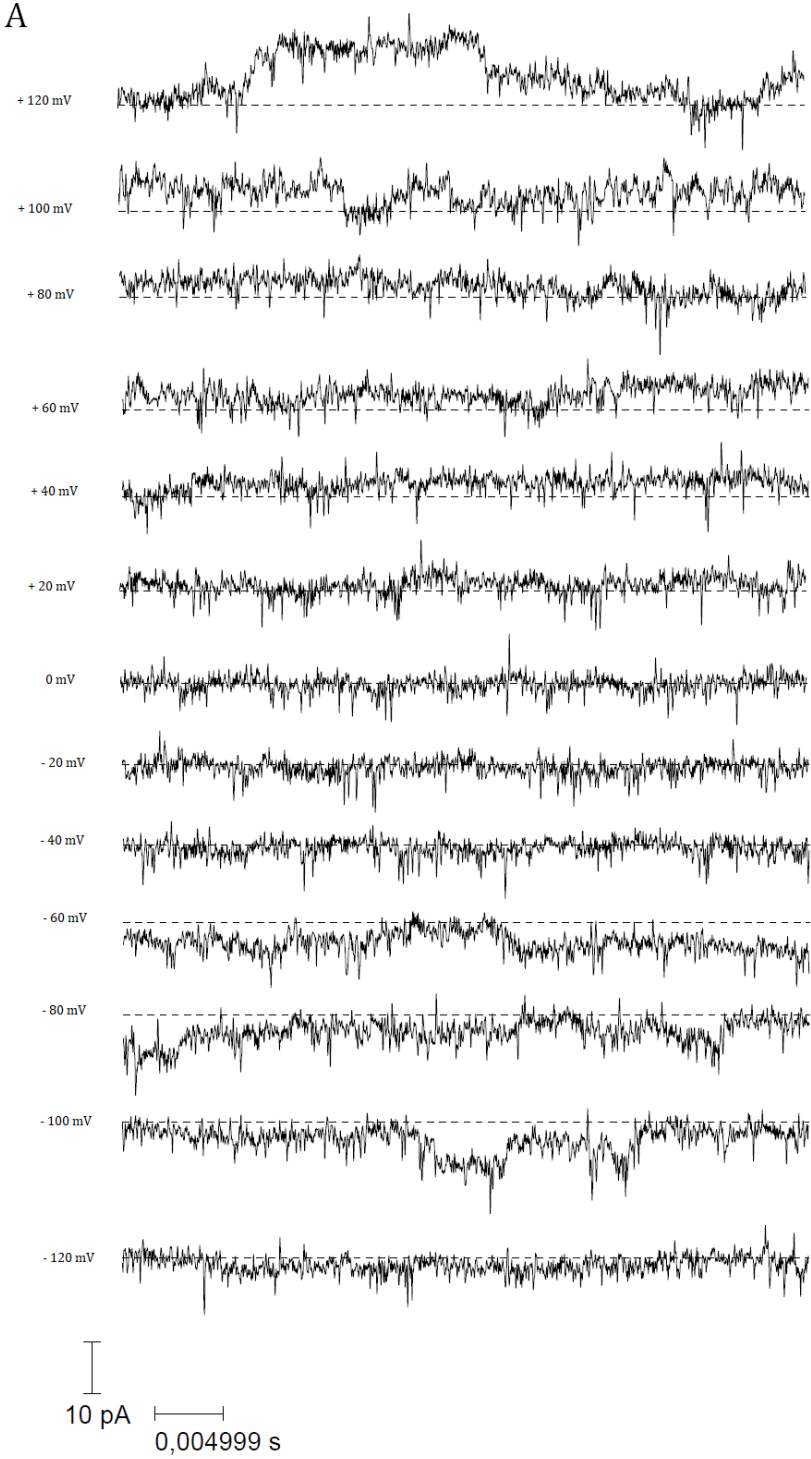


Figure 6.11: Current 4 in 7F2 cells cultured with basal medium (part 1)

A: Typical recordings of the current 4 in a cell-attached patch from a 7F2 cell cultured with basal medium. Bath solution was Na⁺ Locke and pipette solution was high-K⁺ medium. Downward deflections correspond to inward currents and upward deflections correspond to outward currents.

Chapter 6 – A comparison of the electrophysiological characteristics of osteoblasts and adipocytes, and the effects of ghrelin on these

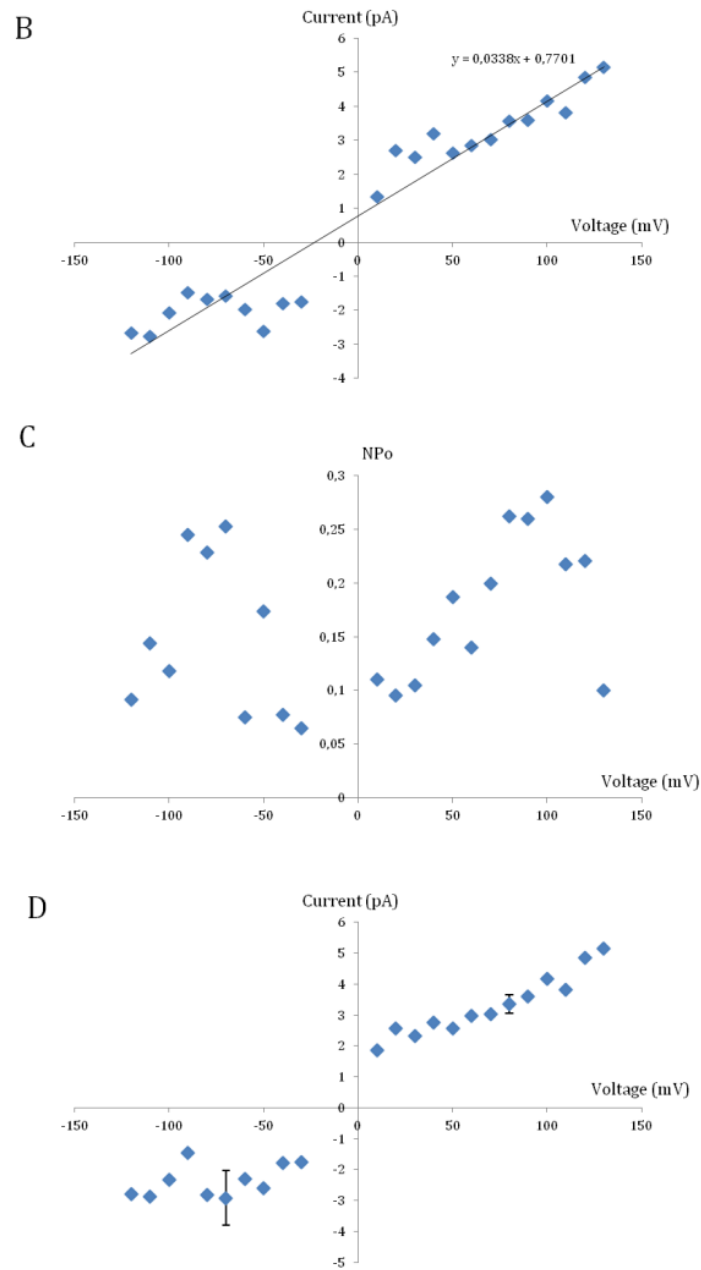


Figure 6.11: Current 4 in 7F2 cells cultured with basal medium (part 2)

B: Corresponding current-voltage plot. Data points were derived from fitting amplitude histograms at each membrane potential. C: Corresponding open probability; NPo ($P_o/3$) was used as there were at least three channels of same family in this patch; NPo decreased from -120 mV to 0 mV, increased from 0 mV to +100 mV, then decreased again, suggesting that this channel was voltage-sensitive. D: Current-voltage relationship for the current 4 in cell-attached patches from 7F2 cells cultured with basal medium; each data point represents the average channel current calculated from amplitude histograms (mean \pm SD of 2 patches from different cells). Reversal potential was -22.5 ± 0.7 mV.

Chapter 6 – A comparison of the electrophysiological characteristics of osteoblasts and adipocytes, and the effects of ghrelin on these

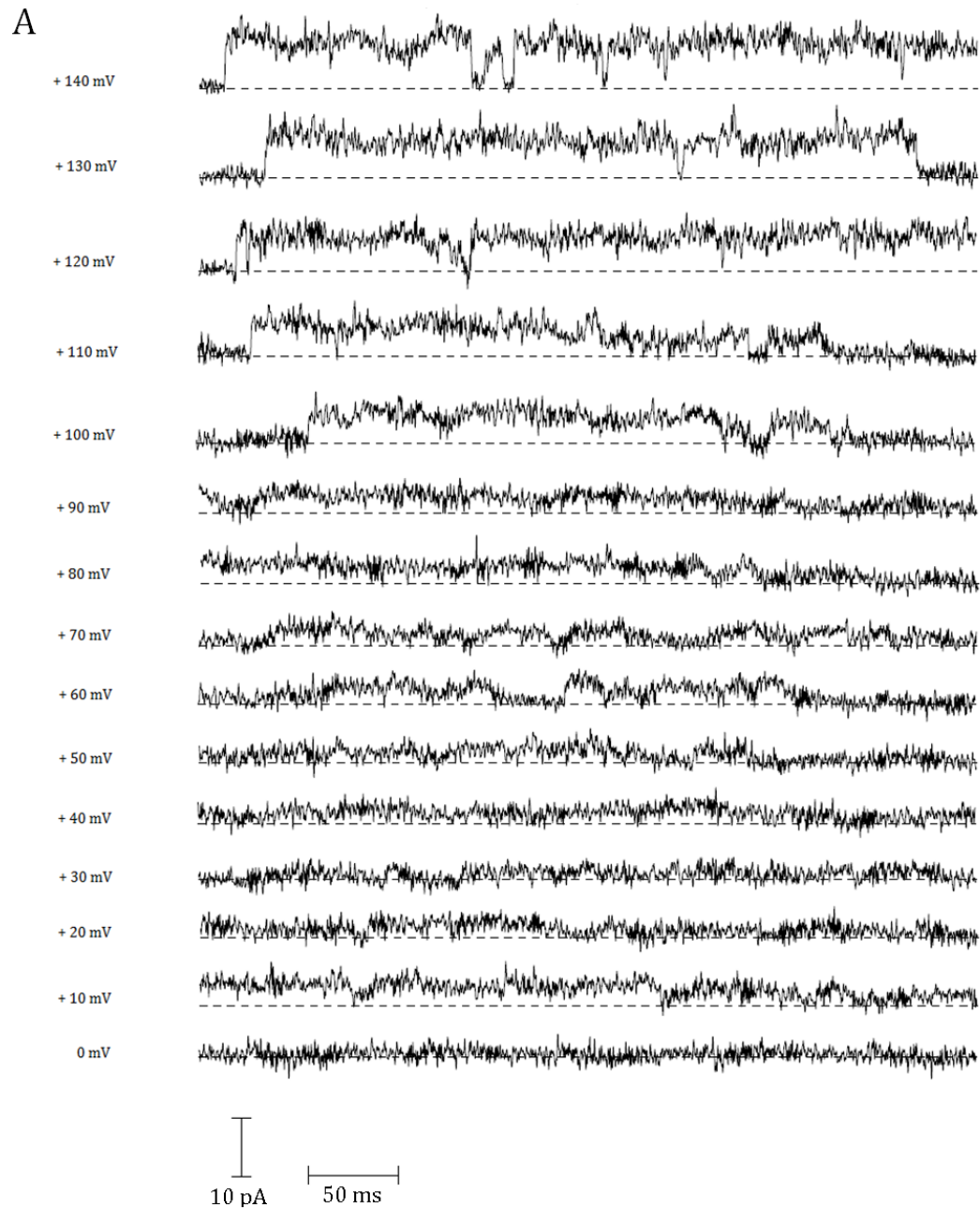


Figure 6.12: Current 5 in 7F2 cells cultured with basal medium (part 1)

A: Typical recordings of the current 5 in cell-attached patch configuration. Bath solution was Na⁺ Locke and pipette solution was high-K⁺ medium. Upward deflections represent ion channel opening.

Chapter 6 – A comparison of the electrophysiological characteristics of osteoblasts and adipocytes, and the effects of ghrelin on these

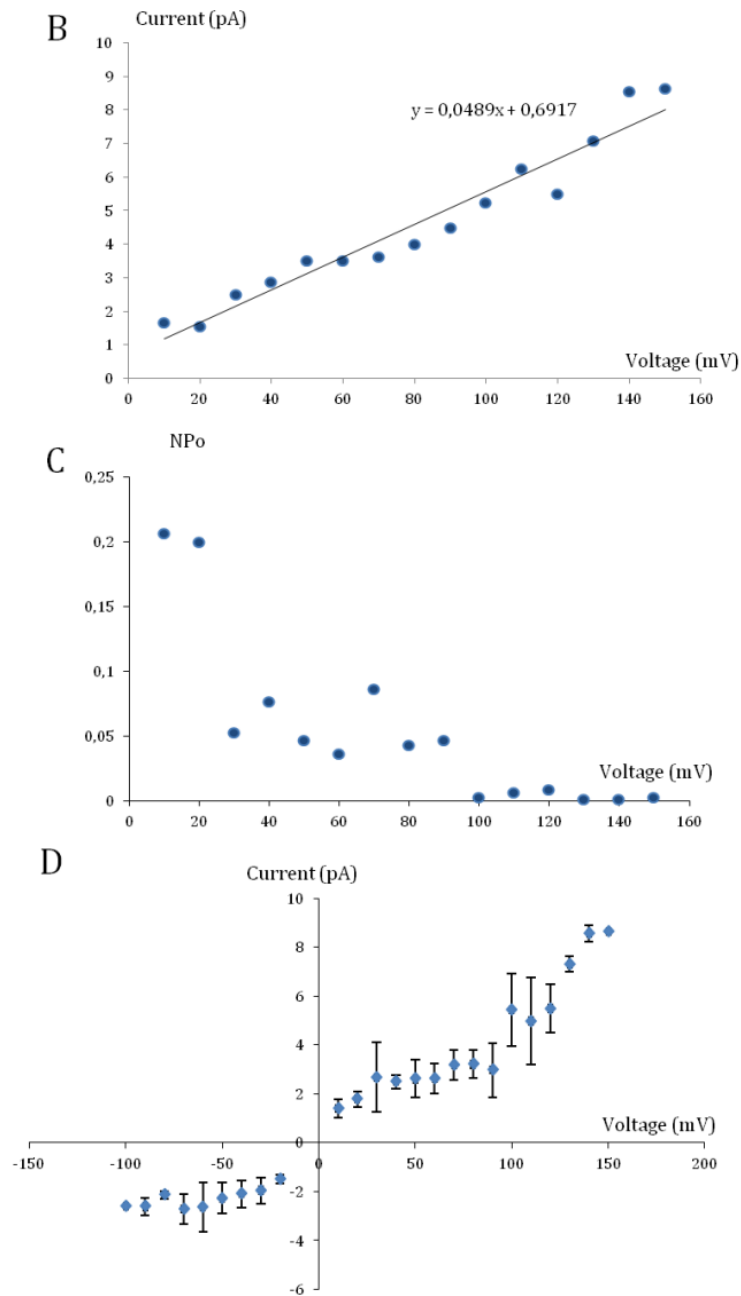


Figure 6.12: Current 5 in 7F2 cells cultured with basal medium (part 2)

B: Corresponding current-voltage data plot. Lines of best fit yielded a conductance of 49.2 pS. Data points were derived from fitting amplitude histograms at each membrane potential. C: Corresponding P_{open} plot. P_o tended to decrease with increasing pipette voltage, indicating that this channel was voltage-dependent. D: Pooled current-voltage relationship for the current 5 in cell-attached patches from 7F2 cells cultured with basal medium; each data point represents the average channel current calculated from amplitude histograms (mean \pm SD of 5 patches from different cells). Reversal potential was -2.4 ± 9.1 mV.

Chapter 6 – A comparison of the electrophysiological characteristics of osteoblasts and adipocytes, and the effects of ghrelin on these

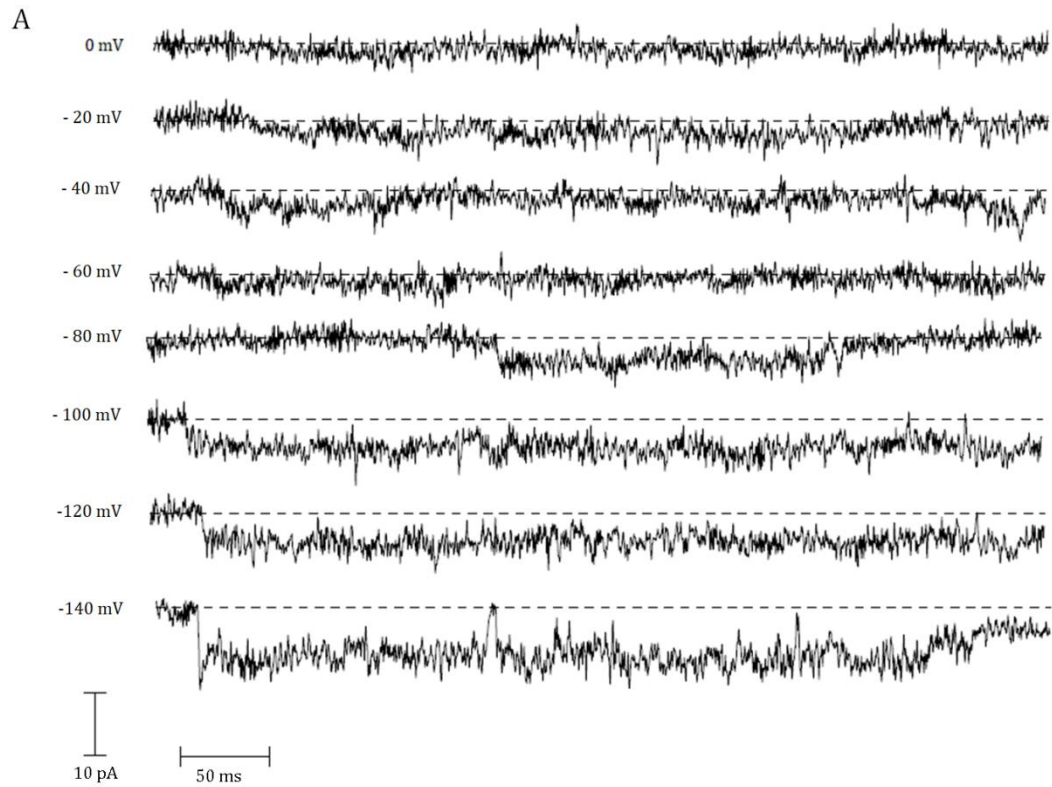


Figure 6.13: Current 5 in 7F2 cells cultured with adipogenic medium (part 1)

A: Typical recordings of the current 5 in excised inside-out patch configuration. Bath solution was Na⁺ Locke and pipette solution was high-K⁺ medium. Downward deflections represent ion channel opening.

Chapter 6 – A comparison of the electrophysiological characteristics of osteoblasts and adipocytes, and the effects of ghrelin on these

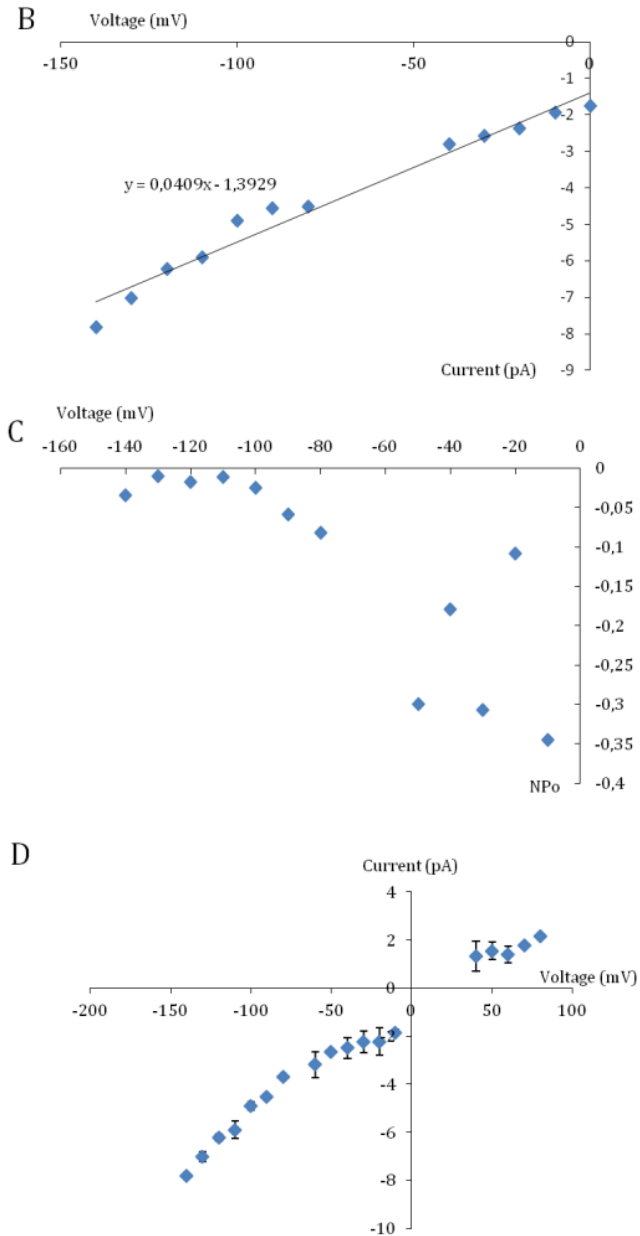


Figure 6.13: Current 5 in 7F2 cells cultured with adipogenic medium (part 2)

B: Corresponding current-voltage data plot. Lines of best fit yielded a conductance of 40.9 pS. Data points were derived from fitting amplitude histograms at each membrane potential. C: Corresponding P_{open} plot. P_{open} decreased with increasing pipette voltage, indicating that this channel was voltage-dependent. D: Pooled current-voltage relationship for the current 5 in cell-attached patches from 7F2 cells cultured with adipogenic medium ($n=3$); data are mean current (pA) \pm SD. Reversal potential was $+24 \pm 8.5$ mV.

Chapter 6 – A comparison of the electrophysiological characteristics of osteoblasts and adipocytes, and the effects of ghrelin on these

A

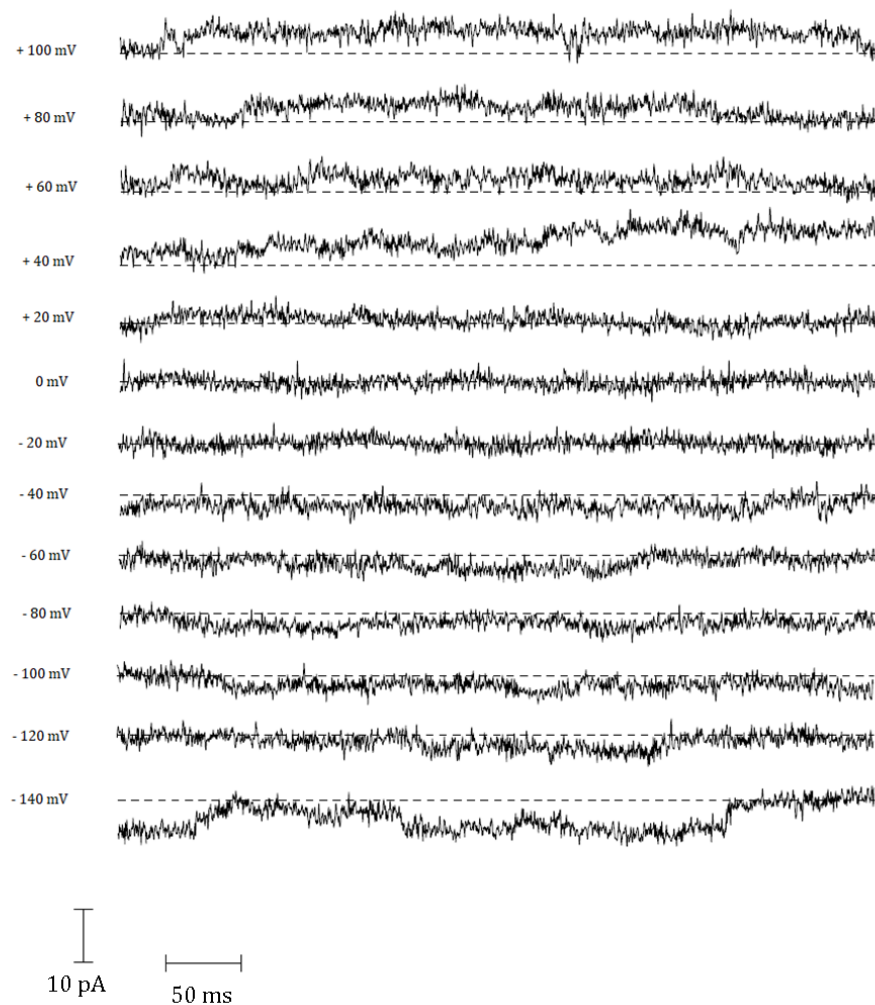


Figure 6.14: Current 5 in 7F2 cells cultured with adipogenic medium + ghrelin (part 1)

A: Typical recordings of the current 5. Bath solution was Na⁺ Locke and pipette solution was high-K⁺ medium. Inward and upward deflections from the dotted line represent ion channel opening.

Chapter 6 – A comparison of the electrophysiological characteristics of osteoblasts and adipocytes, and the effects of ghrelin on these

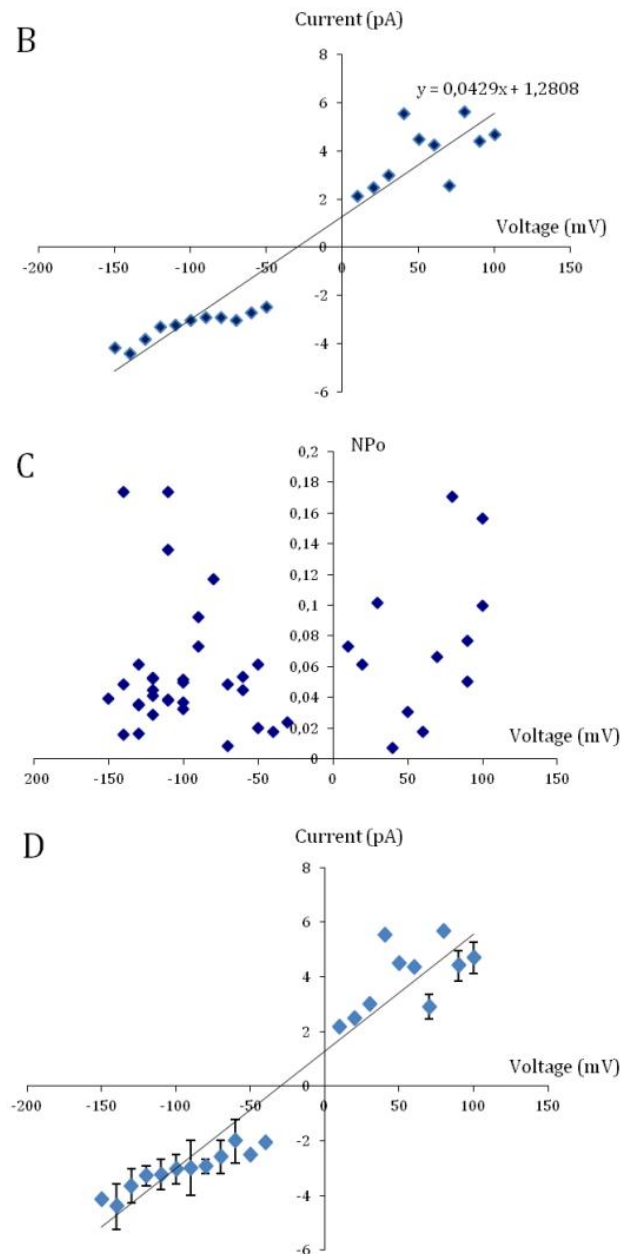


Figure 6.14: Current 5 in 7F2 cells cultured with adipogenic medium + ghrelin (part 2)

B: Corresponding current-voltage data plot. Lines of best fit yielded a conductance of 42.9 pS. Data points were derived from fitting amplitude histograms at each membrane potential. C: Corresponding open probability plot. NPo ($P_o/4$) was used as a measure of open probability; NPo decreased then increased again with increasing pipette voltages. D: Current-voltage relationship for the current 5 in cell-attached patches from 7F2 cells cultured with adipogenic medium + 20 nM ghrelin; each data point represents the average channel current calculated from amplitude histograms (mean \pm SD of 2 patches from different cells). Reversal potential was -21.5 ± 3.5 mV.

Chapter 6 – A comparison of the electrophysiological characteristics of osteoblasts and adipocytes, and the effects of ghrelin on these

A

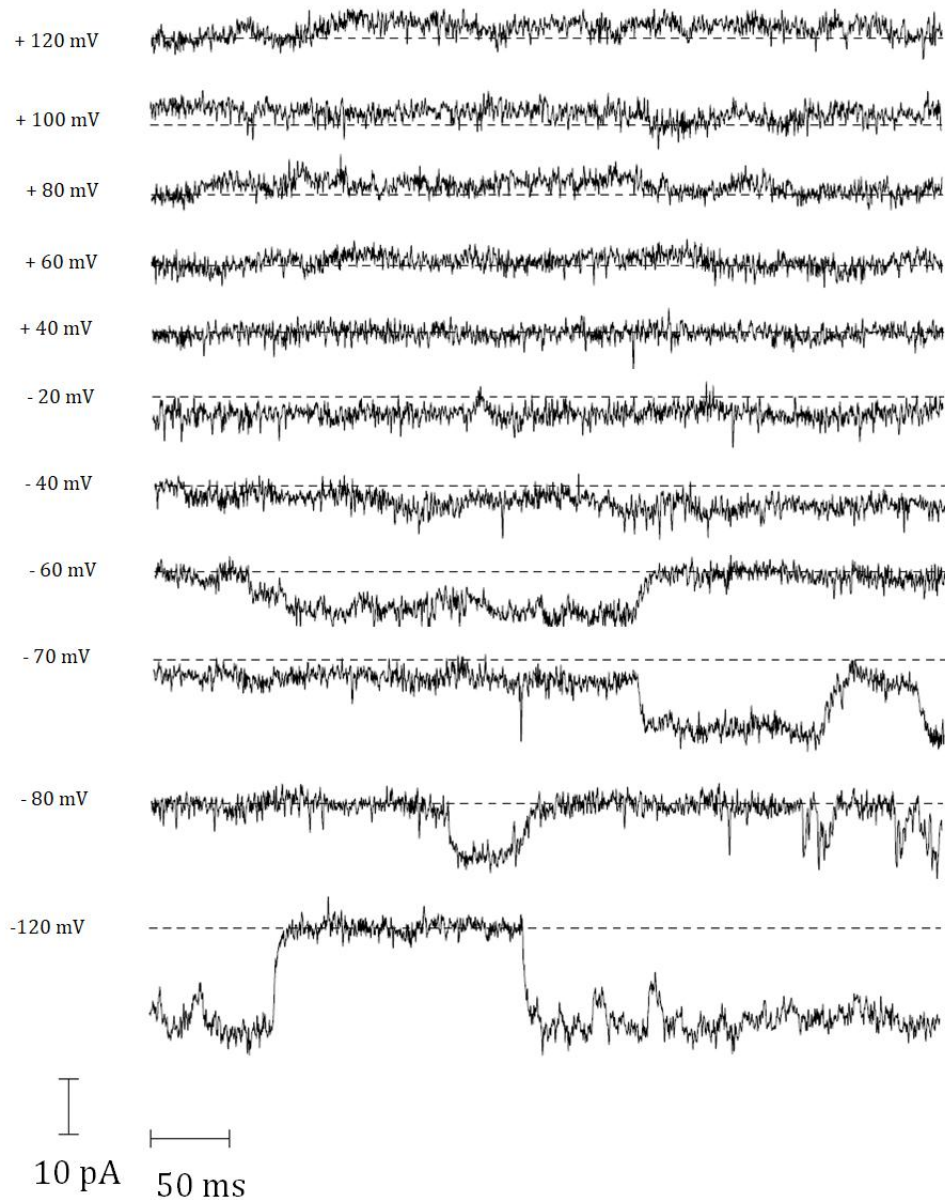


Figure 6.15: Current 6 in 7F2 cells cultured with adipogenic medium + ghrelin (part 1)

A: Typical recordings of the current 6 in excised inside-out configuration. Bath solution was Na⁺ Locke and pipette solution was high-K⁺ medium. Inward and upward deflections from the dotted line represent ion channel opening.

Chapter 6 – A comparison of the electrophysiological characteristics of osteoblasts and adipocytes, and the effects of ghrelin on these

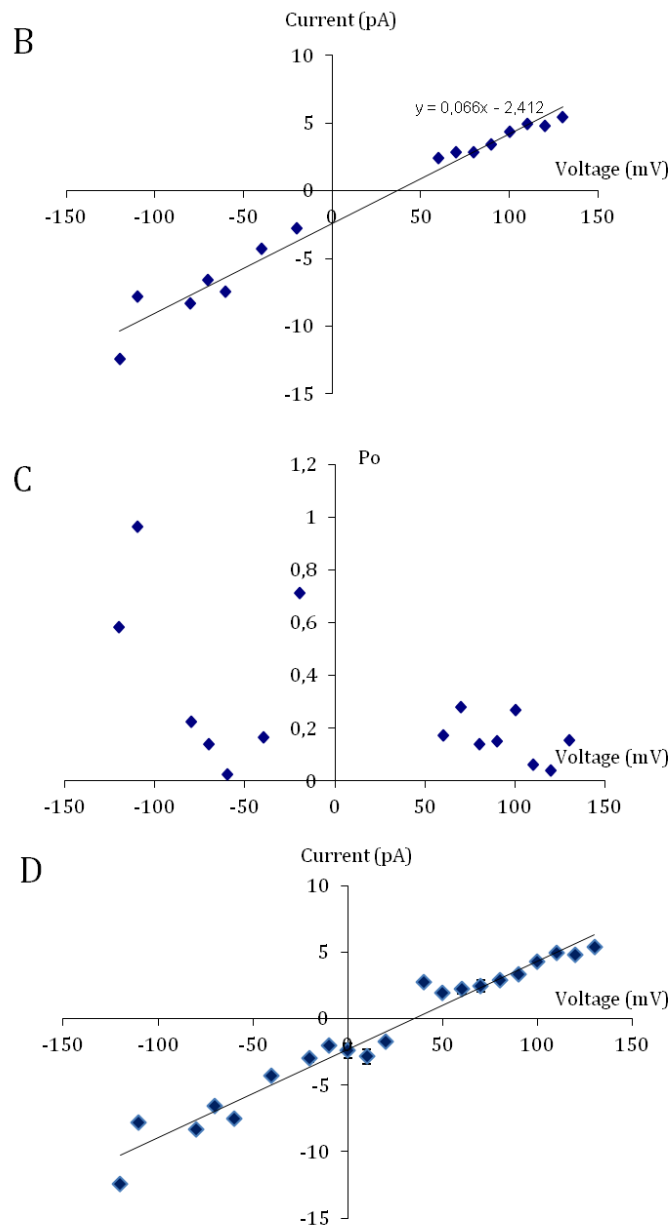


Figure 6.15: Current 6 in 7F2 cells cultured with adipogenic medium + ghrelin (part 2)

B: Corresponding current-voltage data plot. Lines of best fit yielded a conductance of 66 pS. Data points were derived from fitting amplitude histograms at each membrane potential. C: Corresponding open probability plot; P_{open} did not change with increasing pipette voltages.. D: Current-voltage relationship for the current 6 in excised inside-out patches from 7F2 cells cultured with adipogenic medium + 20 nM ghrelin; each data point represents the average channel current calculated from amplitude histograms (mean \pm SD of 2 patches from different cells). Reversal potential was -36 ± 1.4 mV.

Chapter 6 – A comparison of the electrophysiological characteristics of osteoblasts and adipocytes, and the effects of ghrelin on these

A

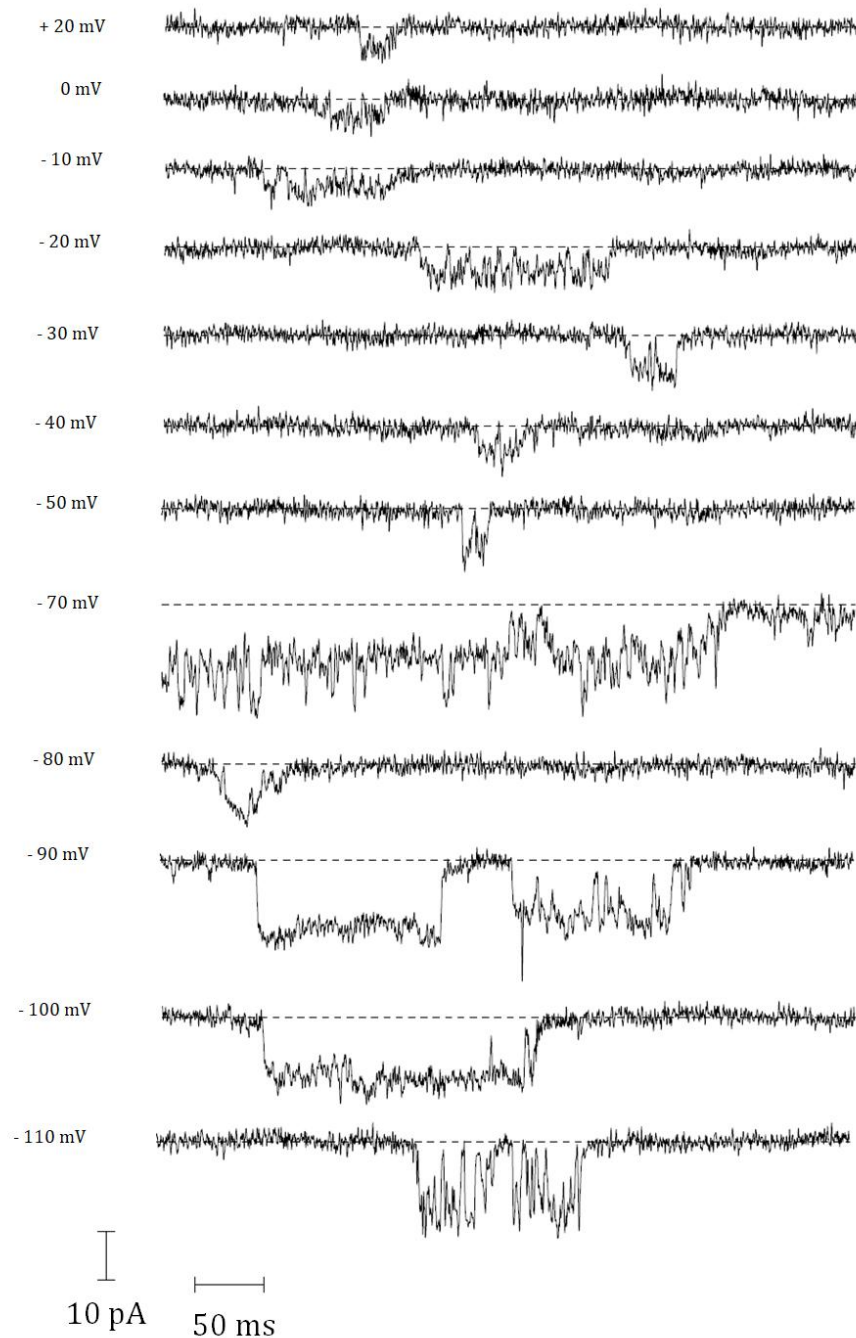


Figure 6.16: Current 7 in 7F2 cells cultured with basal medium + ghrelin (part 1)

A: Recordings of the current 7 in excised inside-out configuration. Bath solution was Na⁺ Locke and pipette solution was high-K⁺ medium. Upward deflections from the dotted line represent ion channel opening. Reversal potential was -60 mV.

Chapter 6 – A comparison of the electrophysiological characteristics of osteoblasts and adipocytes, and the effects of ghrelin on these

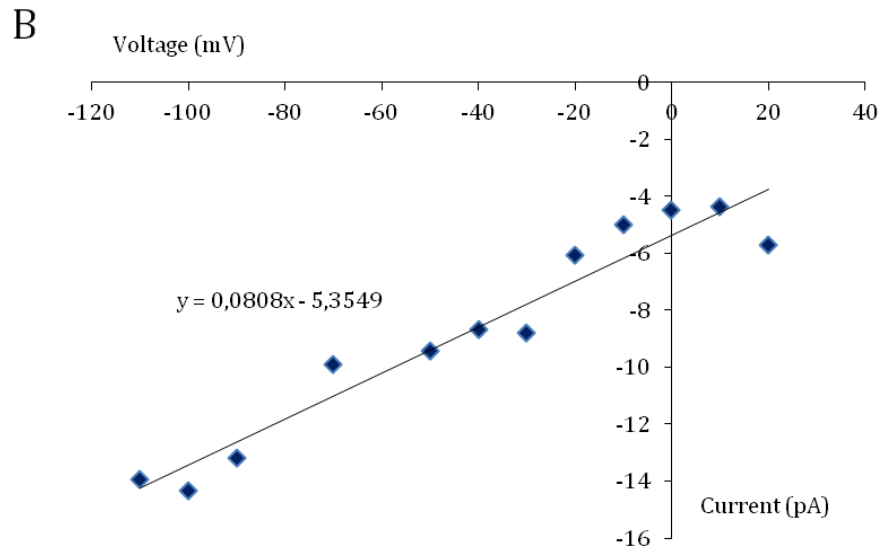


Figure 6.16: Current 7 in 7F2 cells cultured with basal medium + ghrelin (part 2)

B: Corresponding current-voltage data plot. Data points were derived from fitting amplitude histograms at each membrane potential. Open probability could not be analysed as there were several types of current in this patch.

Chapter 6 – A comparison of the electrophysiological characteristics of osteoblasts and adipocytes, and the effects of ghrelin on these

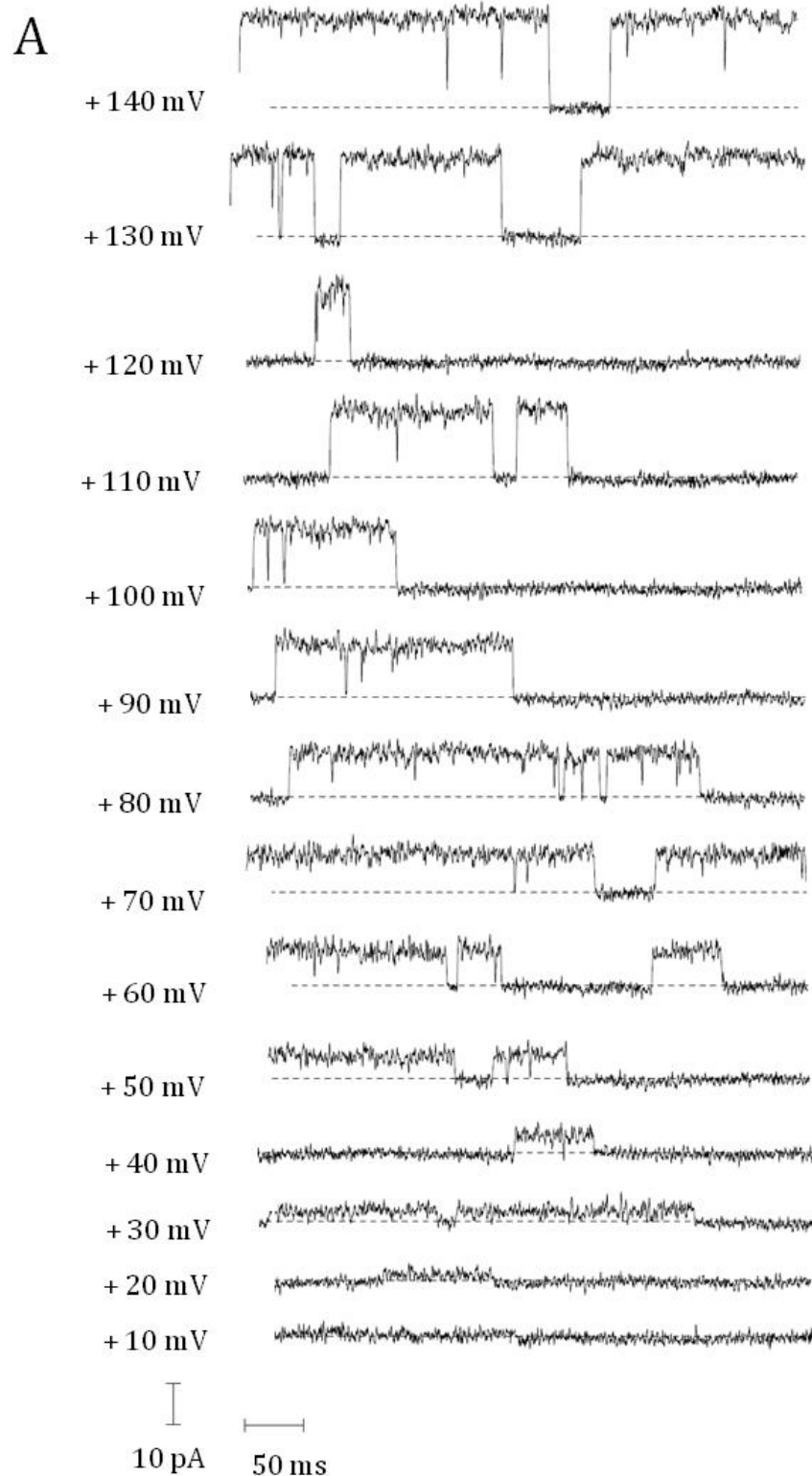
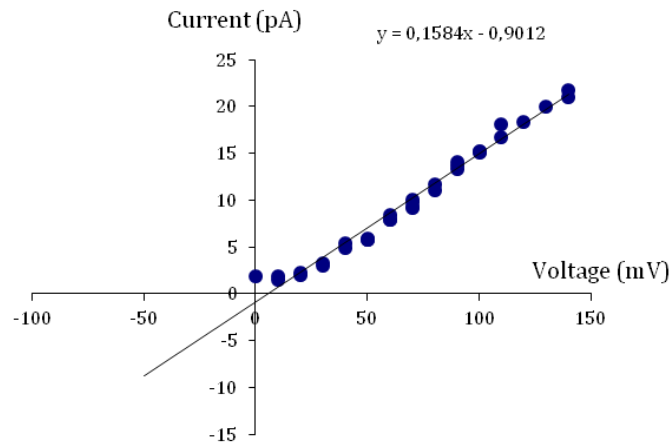


Figure 6.17: Current 8 in 7F2 cells cultured with basal medium (cell-attached) (part 1)

A: Current 8 in cell-attached patch from a 7F2 cell cultured with basal medium ($n = 1$). Bath solution was Na^+ Locke and pipette solution was high K^+ medium containing Amphotericin B (375 $\mu\text{g}/\text{ml}$). Upward deflections represent ion channel openings

B



C

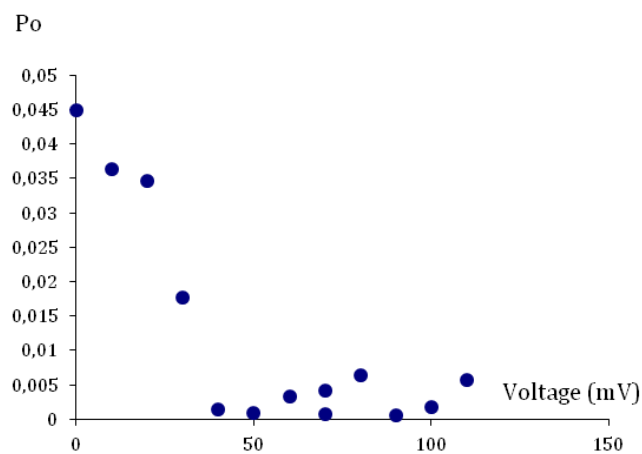


Figure 6.17: Current 8 in 7F2 cells cultured with basal medium (cell-attached) (part 2)

B: Corresponding current-voltage data plot. Data points were derived from fitting amplitude histograms at each membrane potential. Lines of best fit yielded a conductance of 158.4 pS. C: Corresponding open probability, which decreased with increasing pipette voltage, indicating that the current was voltage-sensitive.

Chapter 6 – A comparison of the electrophysiological characteristics of osteoblasts and adipocytes, and the effects of ghrelin on these

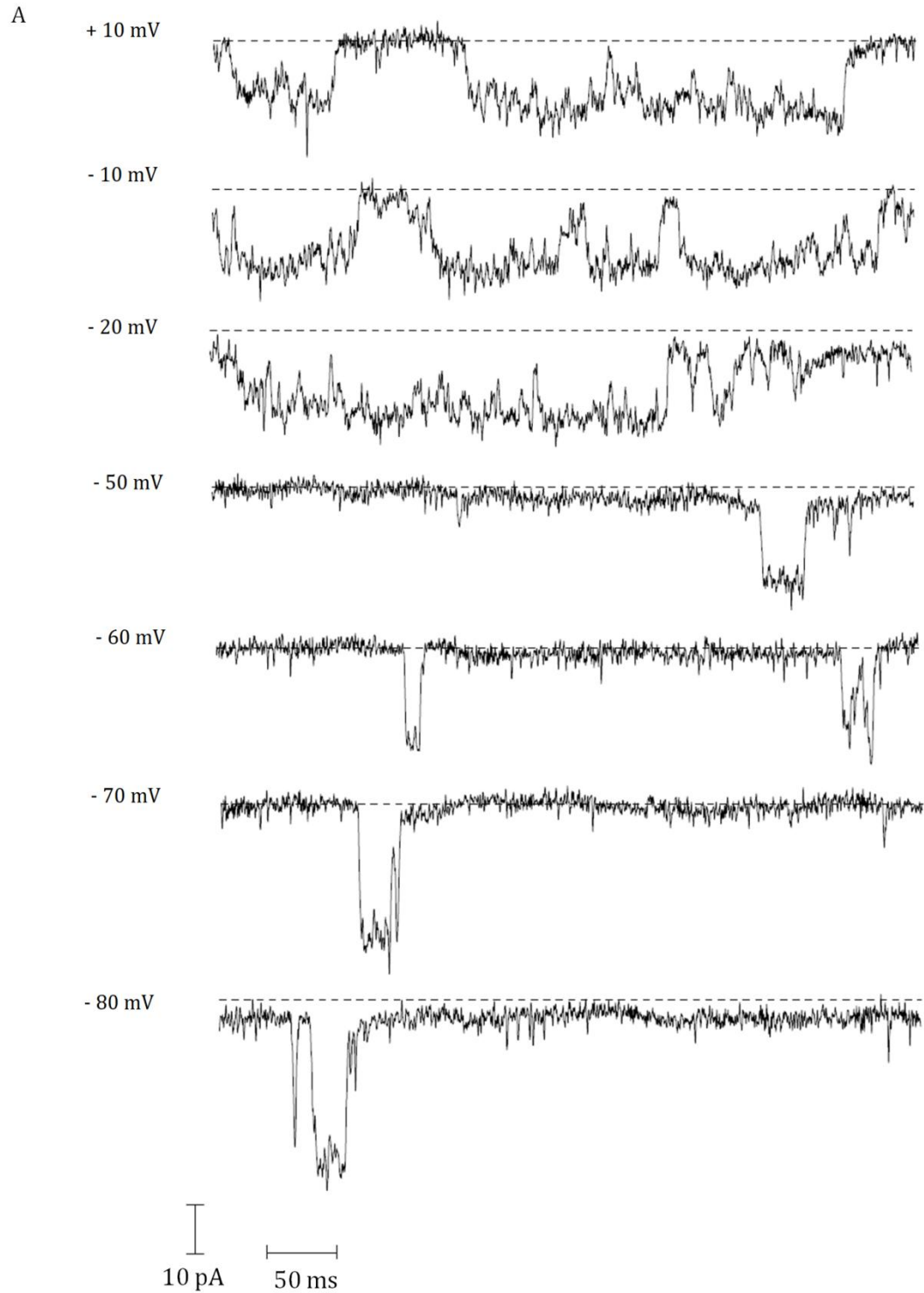


Figure 6.18: Current 8 in 7F2 cells cultured with basal medium (excised inside-out)
(part 1)

A: Current 8 in excised inside-out patch from a 7F2 cell cultured with basal medium ($n = 1$). Bath solution was Na^+ Locke and pipette solution was high K^+ medium. Upward deflections represent ion channel openings.

B

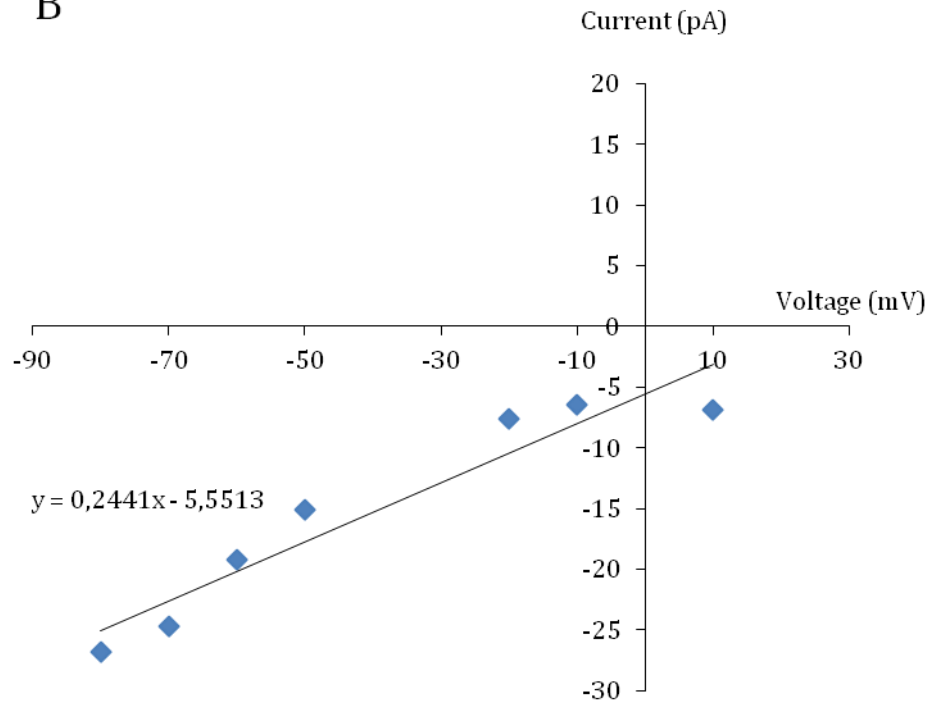


Figure 6.18: Current 8 in 7F2 cells cultured with basal medium (excised inside-out)
(part 2)

B: Current-voltage data for the current 8. Data points were derived from fitting amplitude histograms at each membrane potential. Lines of best fit yielded a conductance of 244.1 pS. Open probability could not be obtained for this channel, as the patch where it was recorded exhibited three families of ion channels.

Chapter 6 – A comparison of the electrophysiological characteristics of osteoblasts and adipocytes, and the effects of ghrelin on these

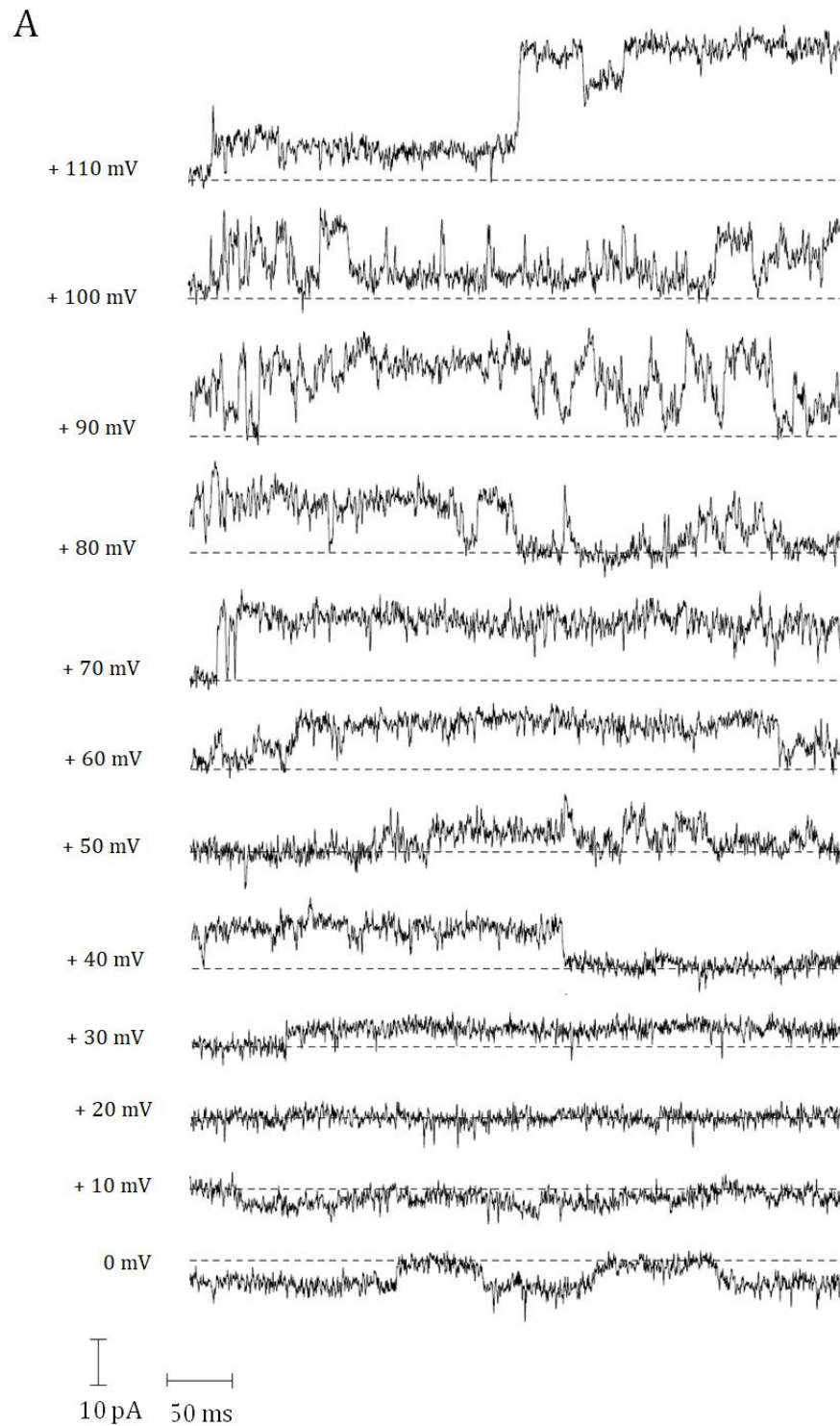


Figure 6.19: Current 9 in 7F2 cells cultured with basal medium + ghrelin (part 1)

A: Recordings of the large conductance channel current in excised inside-out configuration. Bath solution was Na⁺ Locke and pipette solution was high-K⁺ medium. Inward and upward deflections from the dotted line represent ion channel opening.

Chapter 6 – A comparison of the electrophysiological characteristics of osteoblasts and adipocytes, and the effects of ghrelin on these

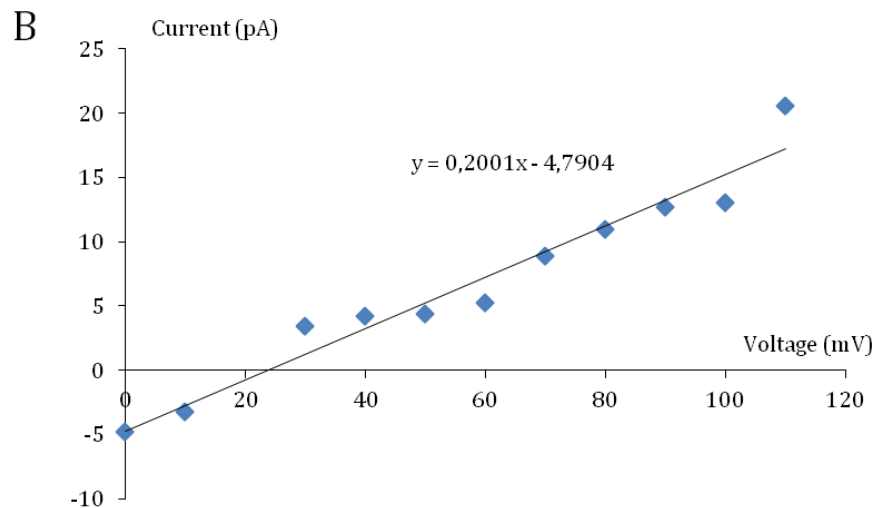


Figure 6.19: Current 9 in 7F2 cells cultured with basal medium + ghrelin (part 2)

B: Corresponding current-voltage data plot. Data points were derived from fitting amplitude histograms at each membrane potential. Open probability could not be analysed as there were several types of current in this patch. Reversal potential was +23 mV.

Chapter 6 – A comparison of the electrophysiological characteristics of osteoblasts and adipocytes, and the effects of ghrelin on these

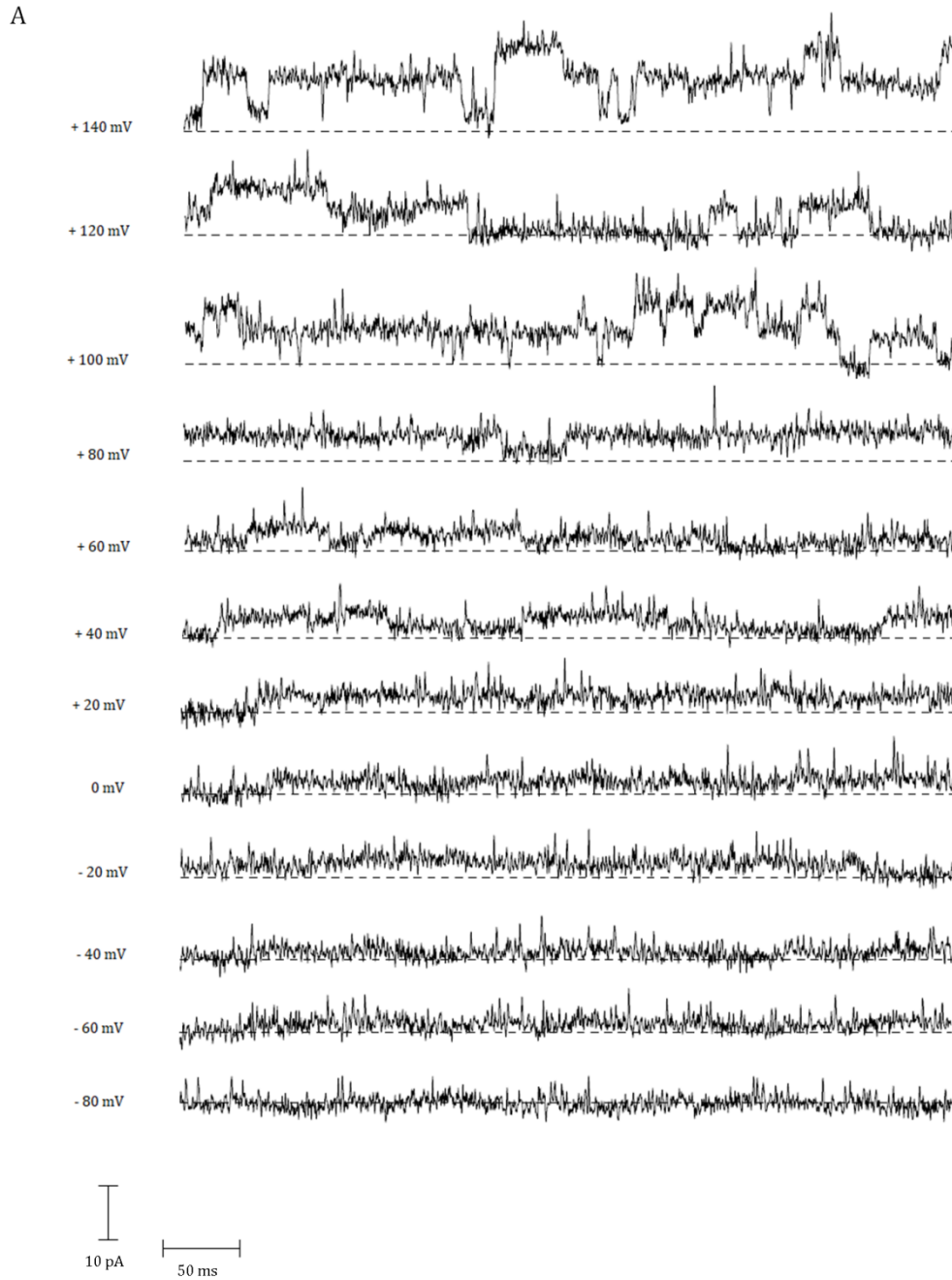


Figure 6.20: Current 10 in 7F2 cells cultured with basal medium (part 1)

A: Current 10 in a cell-attached patch from 7F2 cells ($n=1$). Bath solution was Na^+ Locke and pipette solution was high- K^+ medium. Upward deflections represent ion channel opening.

Chapter 6 – A comparison of the electrophysiological characteristics of osteoblasts and adipocytes, and the effects of ghrelin on these

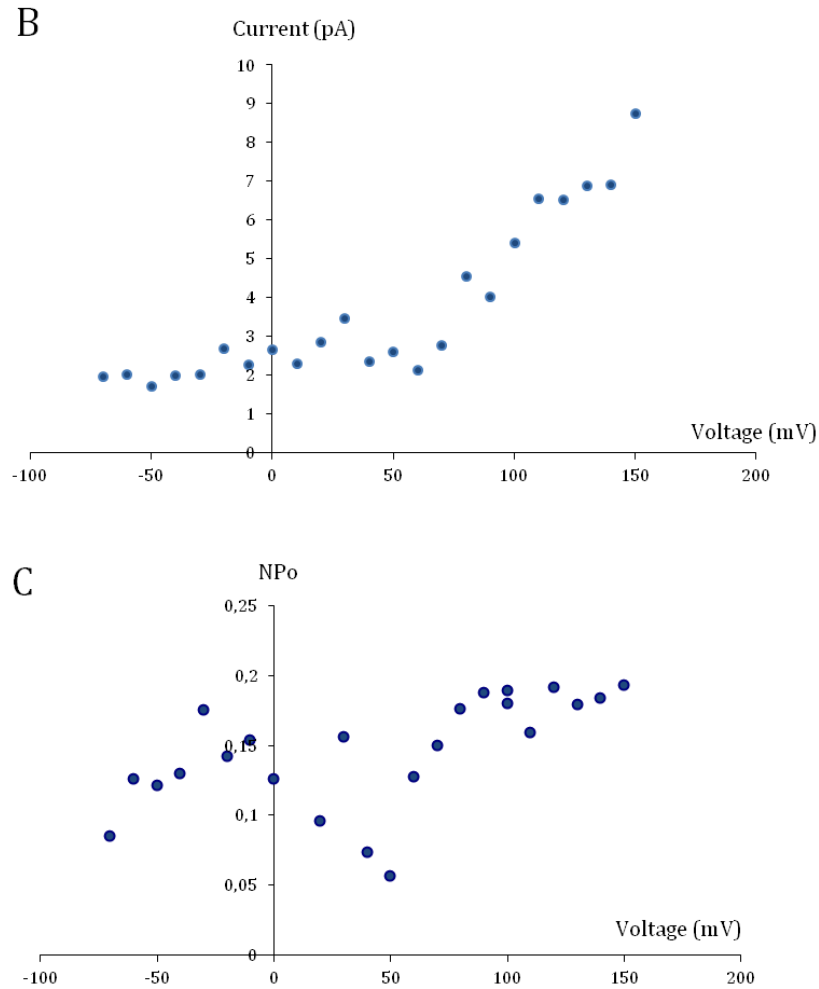


Figure 6.20: Current 10 in 7F2 cells cultured with basal medium (part 2)

B: Corresponding current-voltage plot. Data points were derived from fitting amplitude histograms at each membrane potential. C: Corresponding open probability; NPo ($P_o/2$) was used as there were two channels of same family in this patch. NPo increased with increasing pipette voltage, and several channels were active when pipette voltage was higher than 40 mV, indicating that this channel was voltage-sensitive.

Chapter 6 – A comparison of the electrophysiological characteristics of osteoblasts and adipocytes, and the effects of ghrelin on these

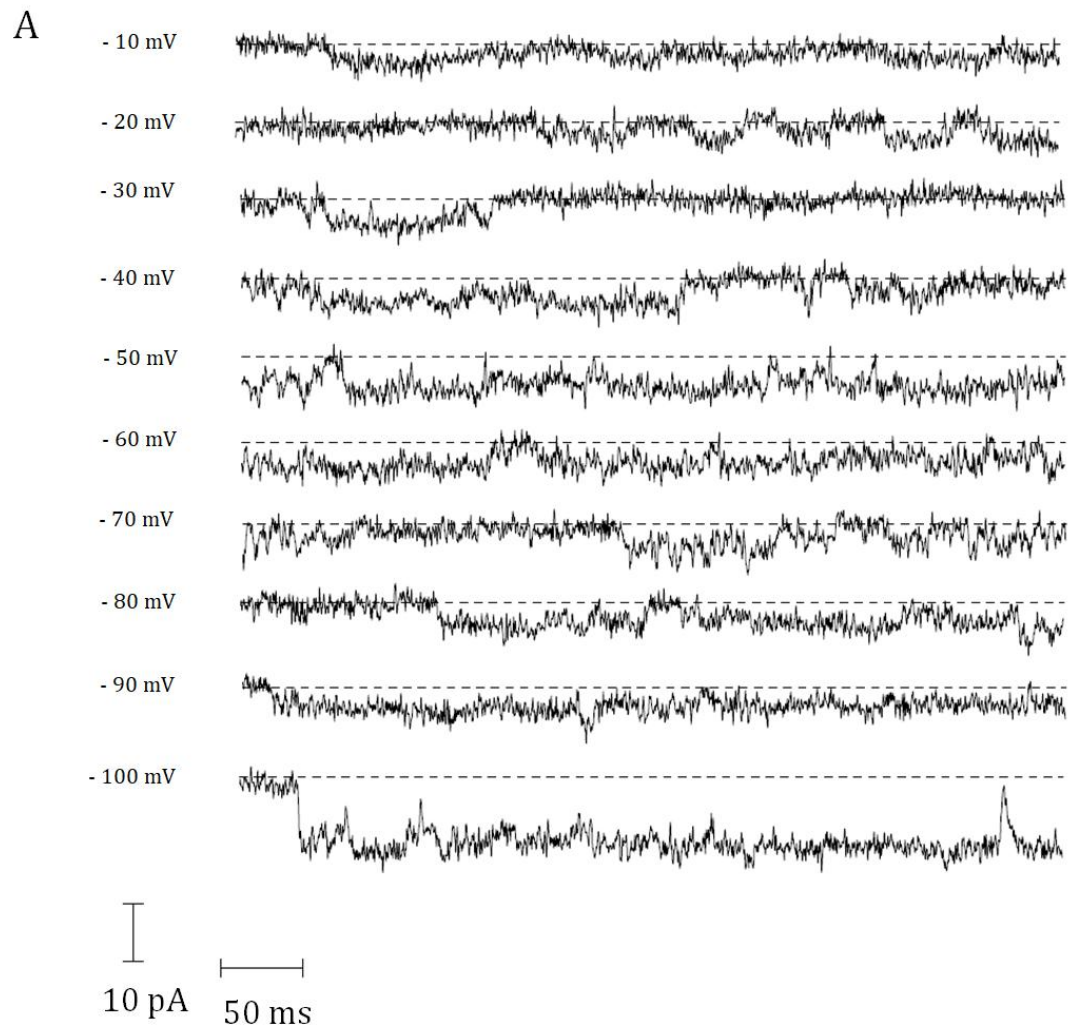


Figure 6.21: Current 10 in 7F2 cells cultured with adipogenic medium + ghrelin (part 1)

A: Recordings of the two conductance channel current in excised inside-out configuration. Bath solution was Na^+ Locke and pipette solution was high- K^+ medium. Upward deflections from the dotted line represent ion channel opening.

Chapter 6 – A comparison of the electrophysiological characteristics of osteoblasts and adipocytes, and the effects of ghrelin on these

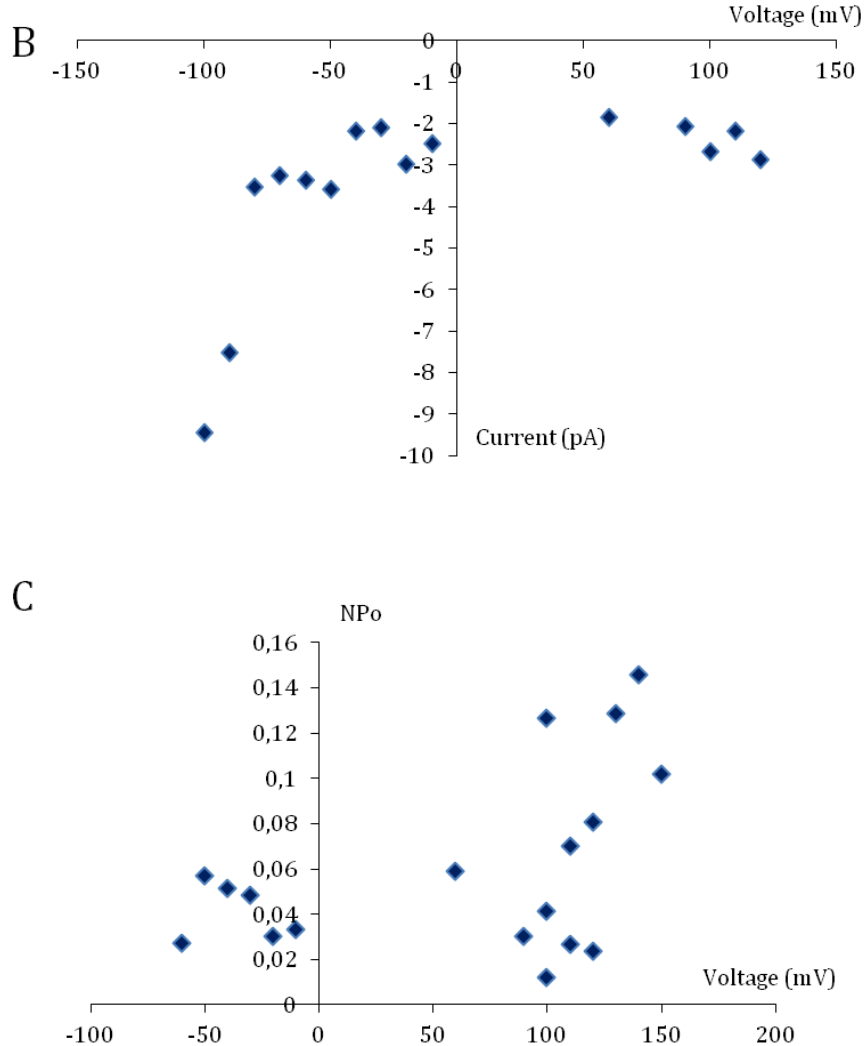


Figure 6.21: Current 10 in 7F2 cells cultured with adipogenic medium + ghrelin (part 2)

B: Corresponding current-voltage data plot. Data points were derived from fitting amplitude histograms at each membrane potential. C: Corresponding open probability plot. NPo (Po/5) was used as a measure of open probability. NPo increased from 0.02-0.06 to 0.15 with increasing pipette voltage.

Chapter 6 – A comparison of the electrophysiological characteristics of osteoblasts and adipocytes, and the effects of ghrelin on these

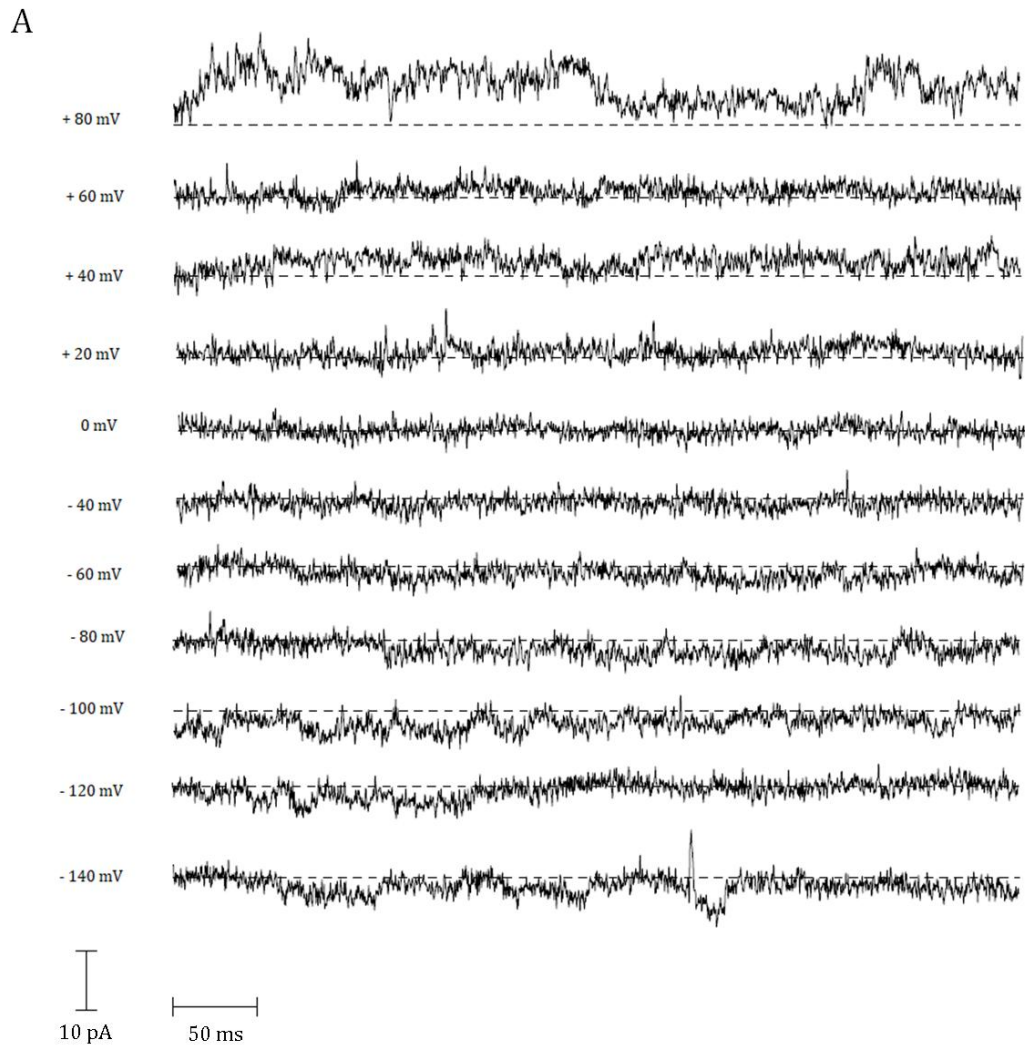


Figure 6.22: Current 11 in 7F2 cells cultured with adipogenic medium (part 1)

A: Typical recordings of the two conductance channel in a cell-attached patch from 7F2-cell derived adipocytes ($n=1$). Bath solution was Na^+ Locke and pipette solution was high- K^+ medium. Upward deflections represent ion channel opening.

Chapter 6 – A comparison of the electrophysiological characteristics of osteoblasts and adipocytes, and the effects of ghrelin on these

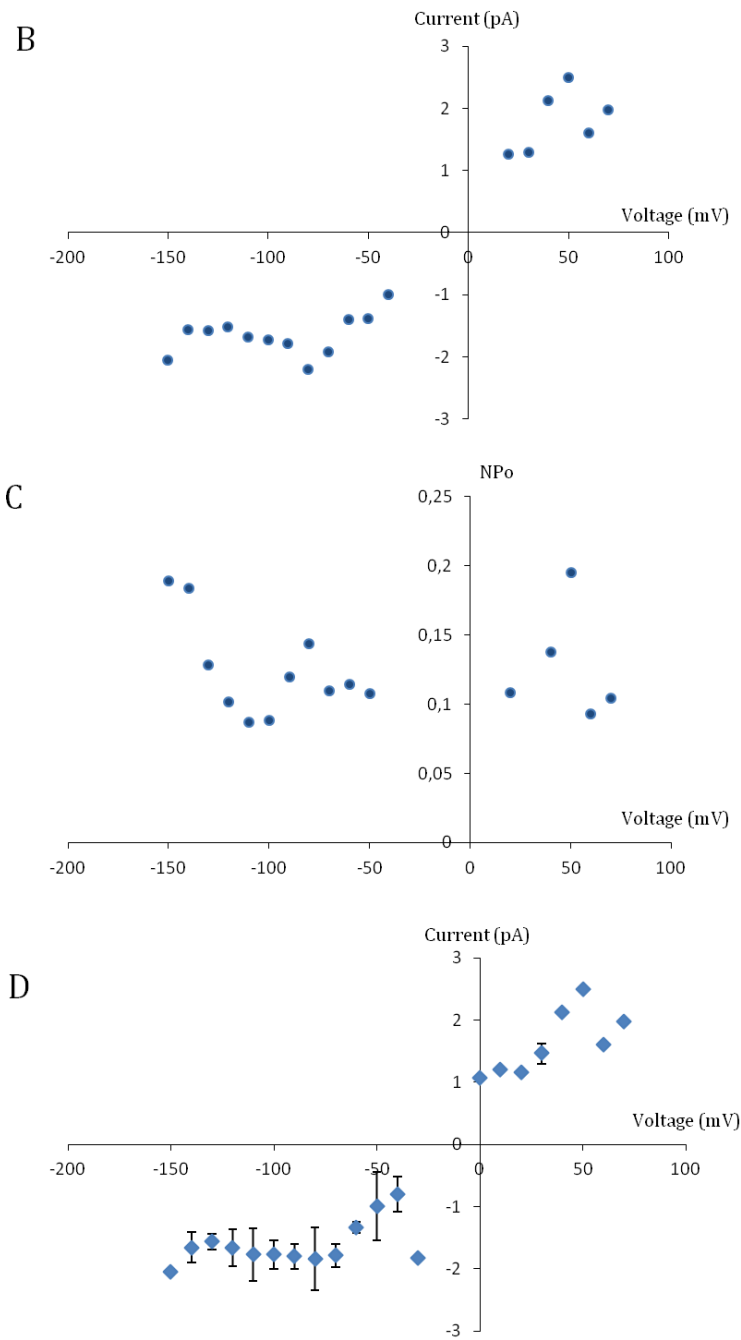


Figure 6.22: Current 11 in 7F2 cells cultured with adipogenic medium (part 2)

B: Corresponding current-voltage plot. Data points were derived from fitting amplitude histograms at each membrane potential. C: Corresponding open probability; NPo ($Po/3$) was used as there were two channels of same family in this patch. D: Current-voltage relationship for the two conductance channel in cell-attached patches from 7F2 cells cultured with adipogenic medium; each data point represents the average channel current calculated from amplitude histograms (mean \pm SD of 2 patches from different cells). Reversal potential was -16.5 ± 0.7 mV.

Chapter 6 – A comparison of the electrophysiological characteristics of osteoblasts and adipocytes, and the effects of ghrelin on these

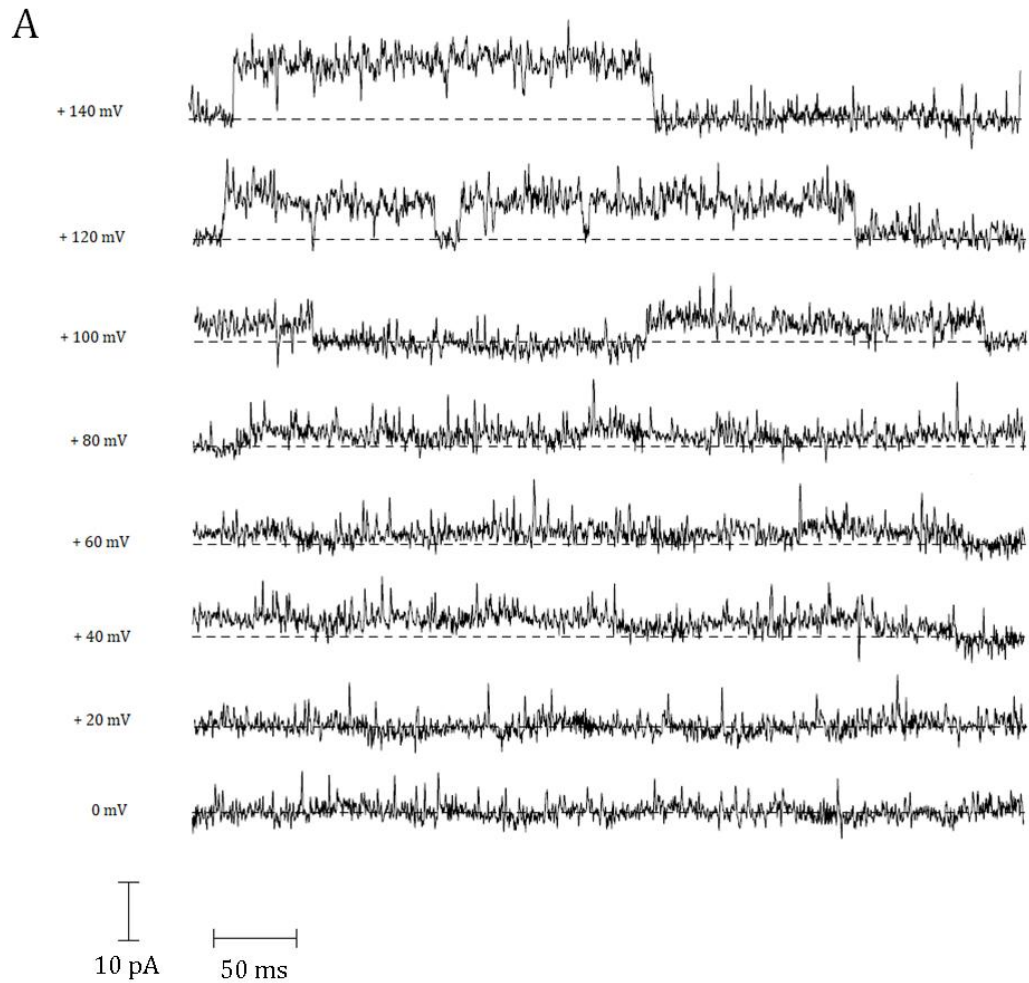


Figure 6.23: Current 12 in 7F2 cells cultured with adipogenic medium + ghrelin (part 1)

A: Recordings of the two conductance channel current (configuration unknown). Bath solution was Na⁺ Locke and pipette solution was high-K⁺ medium. Upward deflections from the dotted line represent ion channel opening.

Chapter 6 – A comparison of the electrophysiological characteristics of osteoblasts and adipocytes, and the effects of ghrelin on these

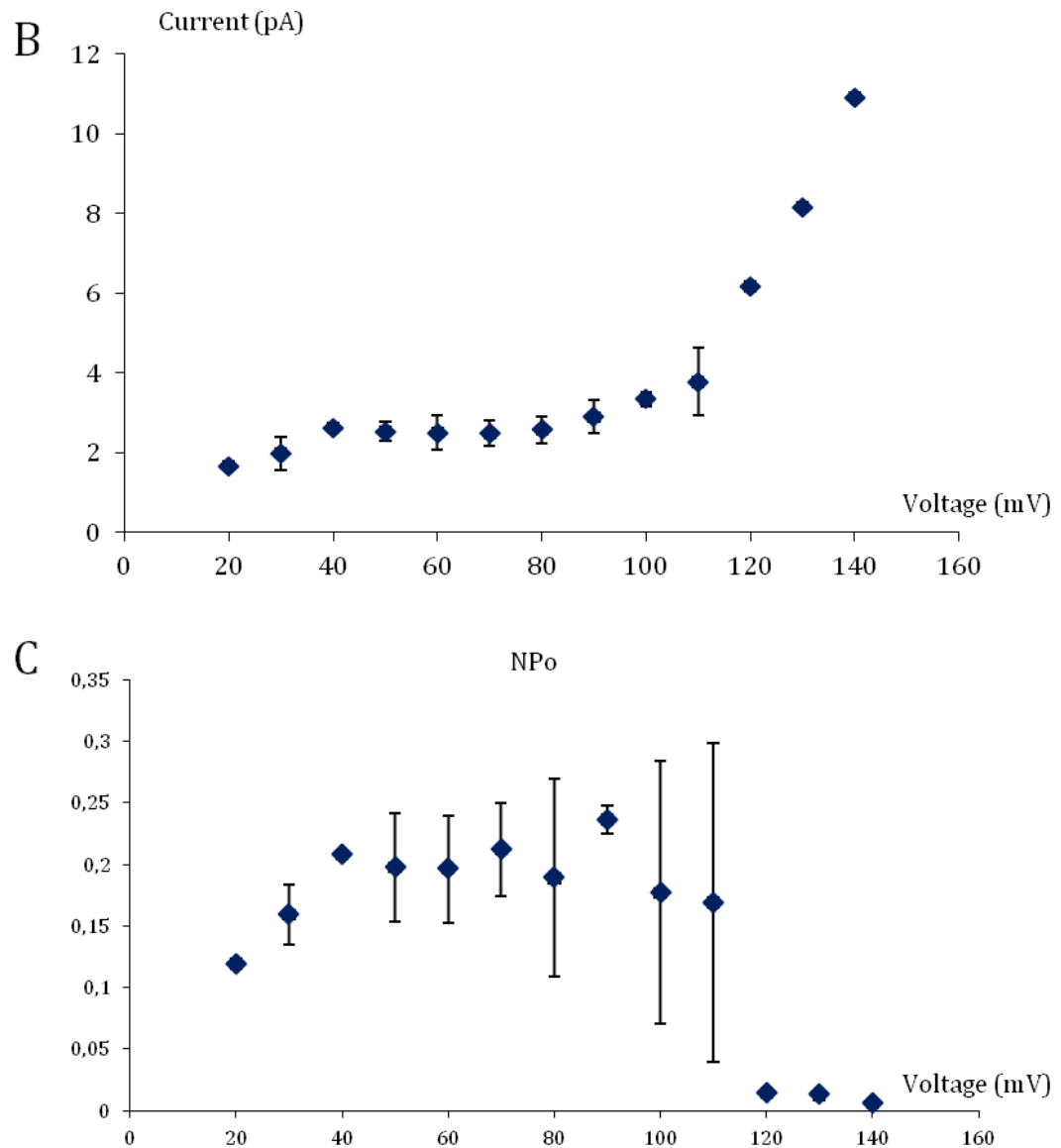


Figure 6.23: Current 12 in 7F2 cells cultured with adipogenic medium + ghrelin (part 2)

B: Corresponding current-voltage data plot. Each data point represents the average channel current calculated from amplitude histograms (mean \pm SD). C: Corresponding open probability plot. NPo ($P_o/4$) was used as a measure of open probability (mean \pm SD). NPo increased from 0.1 to 0.25 over the voltage range of 20 mV to 110 mV and then dropped to <0.05 .

Chapter 7 – General discussion and conclusions

7.1. Summary of Key Findings

The main aim of this thesis was to investigate the roles of ghrelin and ion channels, particularly K⁺ channels, in the adipogenic differentiation of 7F2 preosteoblastic cells. The key findings can be summarised as follows:

- Treatment with adipogenic medium increased the lipid content of the cells, significantly upregulated the mRNA expression of the adipocytic markers PPAR γ , C/EBP α and Glut4, and downregulated the expression of the osteoblastic markers osteocalcin and Runx2. ALP mRNA expression was not affected by adipogenic treatment.
- 7F2 osteoblastic cells and 7F2 cell-derived adipocytes expressed the three key genes from ghrelin signalling (*Ghsr*, *Ghrl* and *Mboat4*), including previously unreported variants isoforms of *Ghrl*, one of which contained exon 1, intron 1, exon 2, intron 2, exon 3, and may also contain exons 4, intron 4 and 5. mRNA of the variant isoform retaining intron 2 was much more abundant than that of native ghrelin, and was upregulated by treatment with 20 nM and 200 nM ghrelin.
- Ghrelin treatment did not seem to promote 7F2 cell proliferation, as there was no effect on cell numbers.
- Ghrelin treatment did not seem to inhibit the adipogenic differentiation of 7F2 cells; ghrelin treatment had no effect on the number and size of lipid droplets inside the cells, and it upregulated the mRNA expression of both osteoblastic and adipocytic markers, although the difference was not significant. This effect may be mediated by GHSR1a.
- 7F2 cells and 7F2 cell-derived adipocytes expressed several K⁺ channel subunits, including K_{ATP} channel subunits (Kir6.1/SUR2B) and BK channel subunits (KCNMA1/KCNMB2) at the mRNA level.
- Treatment with TEA, but not diazoxide, decreased 7F2 cell proliferation and adipogenic differentiation.
- 12 types of functional ion channels were detected in electrophysiology experiments, some of which may correspond to BK channels and K_{ATP} channels composed of Kir6.1/SUR2B. Several currents were only detected in 7F2 cells treated with ghrelin, and ghrelin treatment seemed to modify the open probabilities of some currents that were detected both in presence and in absence of ghrelin.

7.2. Discussion of findings

Ghrelin and ghrelin receptor agonists are emerging as promising therapeutic targets in the treatment of pathological conditions associated with aging, including the alterations in food intake, energy metabolism, cardiovascular function, neuronal activity, adaptive immunity and inflammation (Yin and Zhang, 2016). In particular, a decline in ghrelin activity may contribute to the aging-associated increase in adiposity, which is a common feature in several pathologies, including some forms of osteoporosis. Similarly, ion channels, and particularly potassium channels, have been shown to play an important role in regulating many cell processes such as proliferation, differentiation and apoptosis, but they are also involved in a number of pathologies, particularly in bone (Zhao *et al.*, 2009; Schulz *et al.*, 2010; O’Conor *et al.*, 2013; Loukin *et al.*, 2015). Hence, understanding the roles of ghrelin signalling and ion channels in pathological adipogenesis may provide new therapeutic targets to treat bone disorders such as osteoporosis.

In this study, adipogenic differentiation of 7F2 cells was induced by treatment with dexamethasone and indomethacin. 7F2 cells are already committed to the osteogenic lineage but were still able to differentiate into adipocytes, illustrating the degree of plasticity between these two lineages. Others have shown that osteoblasts can trans-differentiate into adipocytes and vice-versa (Song and Tuan, 2004; Kassem *et al.*, 2008; Berendsen and Olsen, 2014; Greco *et al.*, 2015). This may be relevant to humans, as some bone disorders such as osteoporosis are associated with increased bone marrow adipogenesis and decreased osteoblastogenesis and osteoblast function. BMSCs from elderly and osteoporotic patients tend to differentiate preferentially into adipocytes at the expense of osteoblasts (Rosen and Bouxsein, 2006; Sui *et al.*, 2016; Wang *et al.*, 2016). Although several studies have shown that BMSCs derived from dexamethasone-induced osteoporotic mice are more likely to differentiate into adipocytes (Li *et al.*, 2013a; Zhang *et al.*, 2015), others have shown that BMSCs retain their differentiation potential, as these cells are still able to differentiate into osteoblasts, to levels that are comparable to that of BMSCs from younger and non-osteoporotic patients (Justesen *et al.*, 2002; Stenderup *et al.*, 2003). The age-related increased adipogenic differentiation of BMSCs may result from changes in the bone marrow microenvironment (Justesen *et al.*, 2002; Stenderup *et al.*, 2003; Abdallah *et al.*, 2006; Kassem *et al.*, 2008), including changes in hormone and cytokines levels. In addition to altered BMSC differentiation, osteoporosis may also result from the trans-differentiation of osteoblasts and osteoblast-committed progenitor cells into adipocytes. Both dexamethasone and

indomethacin are known to increase the risk of osteoporosis and promote the adipogenic differentiation of MSCs (Styner *et al.*, 2010; Li *et al.*, 2013a; Zhang *et al.*, 2015); they may also downregulate preosteoblast differentiation by inducing them to undergo adipogenic differentiation.

7F2 cells expressed the three key genes from ghrelin signalling (*Ghrl*, *Ghsr* and *Mboat4*), suggesting that ghrelin plays a physiological role in these cells via autocrine/paracrine mechanisms, which is consistent with the literature (Fukushima *et al.*, 2005; Kim *et al.*, 2005; Maccarinelli *et al.*, 2005; Delhanty *et al.*, 2006). 7F2 cells expressed variant isoforms of ghrelin, which had never been reported in bone cells before; at least one of these variant isoforms was much more abundant than native ghrelin, and may encode a peptide that retains the first 12 amino acids of native ghrelin, suggesting that this variant, if expressed at the protein level, may be acylated by GOAT and activate GHSR1a. A number of variants of ghrelin have been identified in other tissues, including breast, ovary, testis, stomach, thymus, kidney, prostate, uterus, and brain (Hosoda *et al.*, 2000b; Jeffery *et al.*, 2005a; Yeh *et al.*, 2005; Seim *et al.*, 2007; Gahete *et al.*, 2010; Seim *et al.*, 2010; Gahete *et al.*, 2011; Seim *et al.*, 2013, 2016). Some of these variants have biological functions, such as In1-ghrelin which stimulates cancer cell proliferation and migration when overexpressed (Gahete *et al.*, 2011; Ibáñez-Costa *et al.*, 2015; Luque *et al.*, 2015; Hormaechea-Agulla *et al.*, 2017). Ghrelin variants may arise from tissue-specific alternative splicing. Ghrelin is known to have biological functions in a wide range of tissues; these effects may be mediated by these tissue-specific ghrelin variants. Identifying the ghrelin variants present in bone, particularly in MSCs and osteoblasts, may provide new therapeutic targets for bone disorders.

Despite the fact that 7F2 cells expressed genes from ghrelin signalling, the hypothesis that ghrelin could inhibit the adipogenic differentiation of 7F2 cells could not be verified, as ghrelin did not seem to have any effect on the number or size of lipid droplets inside 7F2 cell-derived adipocytes. The effects of ghrelin on 7F2 cells cultured with osteogenic medium was not tested in this study, as the subject was the role of ghrelin on the adipogenic differentiation of 7F2 cells. However, it would be interesting to test whether ghrelin favours a phenotype (osteoblastic or adipocytic) when 7F2 cells are cultured in the presence of both osteogenic and adipogenic media (Peng *et al.*, 2012; Cai *et al.*, 2014; Ghali *et al.*, 2015).

Although ghrelin did not inhibit the adipogenic differentiation of 7F2 cells, it upregulated the mRNA expression of both osteoblastic and adipocytic markers, in 7F2

cells cultured with basal medium or adipogenic medium, which seemed to be consistent with published data about the effects of ghrelin in bone and adipose tissues. On one hand, ghrelin stimulates the osteoblastic differentiation of preosteoblasts and primary osteoblasts, increasing the expression of osteoblastic markers such as Runx2, collagen $\alpha 1$ type 1, ALP, and osteocalcin (Fukushima *et al.*, 2005; Kim *et al.*, 2005; Maccarinelli *et al.*, 2005). On the other hand, ghrelin promotes adipogenesis, including bone marrow adipogenesis, with increased expression of adipogenic markers such as PPAR γ and fatty acid synthase (Choi *et al.*, 2003; Thompson *et al.*, 2004; Rodríguez *et al.*, 2009; Brown *et al.*, 2014). In these studies, it is unclear whether ghrelin may promote both osteogenic and adipogenic differentiation *in vivo*, as only one type of tissue (bone or adipose) is investigated individually. *In vivo* experiments have shown that *Ghsr* or *Ghrl* deficiency causes alterations of bone microarchitecture; *Ghsr*^{-/-} and *Ghrl*^{-/-} mice have lower trabecular and cortical bone mass, respectively (Delhanty *et al.*, 2014b), but it is not known whether bone marrow adipogenesis is affected. Here, treatment with 20 nM ghrelin increased the mRNA expression of both adipogenic and osteoblastic markers, suggesting that ghrelin may promote both lineages.

Contrary to ghrelin, treatment of 7F2 cells potassium channel ligands had an effect on cell proliferation and differentiation; in particular, treatment with TEA decreased cell number and limited the size of lipid droplets inside 7F2 cell-derived adipocytes, suggesting that voltage-gated potassium channels were involved in regulating cell proliferation and adipogenic differentiation. This is consistent with previous studies: in human BMSCs, blocking K_v currents with TEA significantly reduces lipid droplet formation and the expression of the adipogenic marker aP₂ (You *et al.*, 2013). However, there are a large number of K_v channels, and it is not known which ones were involved in regulating lipid content in 7F2 cells.

To help answering this question, the ionic mechanisms in 7F2 cells were investigated in electrophysiological experiments. A variety of currents corresponding to several types of ion channels were detected in 7F2 cells cultured for a few days with basal or adipogenic medium, in the presence or absence of ghrelin. Some currents were detected only in 7F2 osteoblastic cells, while others were detected only when 7F2 osteoblastic and adipocytic cells were treated with ghrelin. In addition, ghrelin treatment seemed to modify the open probabilities of some currents that were detected both in presence and in absence of ghrelin treatment. Ghrelin may exert effects in 7F2 cells by promoting the surface expression and activity of some ion channels. Other hormones have been shown to increase ion channel expression, such as insulin, which

may regulate adipogenesis by increasing potassium channel density in white adipocytes (Ramirez-Ponce *et al.*, 2002). Similarly, leptin may inhibit insulin secretion by causing a transient increase K_{ATP} and Kv2.1 channel density in rodent and human β -cells (Wu *et al.*, 2015). Interestingly, ghrelin also inhibits insulin secretion by activating Kv2.1 channels (Dezaki *et al.*, 2004, 2007), and these channels are expressed in rat MSCs and are implicated in regulating MSC proliferation (Li *et al.*, 2006; Deng *et al.*, 2007). As one of the currents detected in 7F2 cells may correspond to Kv2.1, this channel and its role in regulating 7F2 cell proliferation and adipogenic differentiation may be the focus of future investigations.

7.3. Limitations and assumptions

7.3.1. Cell culture assays

Firstly, as mentioned in the result chapters, there was a great variability between the repeats of Oil Red O staining assays; this variability may be explained by the effect of cell density, as adipogenesis was increased in areas of higher cell densities; but also by the Oil Red O crystals that artificially increased the amount of stain measured by absorbance, blunting the differences between cells cultured with basal medium and cells cultured with adipogenic medium, in the presence or absence of ghrelin.

Secondly, only short-term cultures were performed; 7 days of culture may not be a long enough period to reveal an effect of ghrelin on adipogenesis, and long-term cultures may be more sensitive. The decision to perform short-term cultures was made because of the proliferation rate in 7F2 cells cultured with basal medium; even with low seeding densities, after 7 days of culture the wells and flasks were confluent. Increasing the duration of culture resulted in the detachment and loss of these cells when replacing culture medium. In addition, it was not possible to passage 7F2 cells cultured with adipogenic medium, as this resulted in the loss of adipocytes.

Thirdly, only two concentrations of ghrelin were tested, 20 nM and 200 nM; it would have been helpful to use a larger range of concentrations, similarly to what was done in other studies (Kim and Chen, 2004; Liu *et al.*, 2009). In particular, lower concentrations of ghrelin (in the pM range) may have had stronger effects on adipogenic differentiation than 20 nM or 200 nM ghrelin. Also, the ghrelin used in this study was human, whereas 7F2 cells are murine.

7.3.2. Molecular biology

There was a great variability between qRT-PCR repeats; increasing the number of repeats would have been necessary to increase the statistical power of these experiments. Here, only 2 repeats were performed, with 3 replicate samples per condition in each repeat, and each of these samples were run in duplicate. Three house-keeping genes were chosen: GAPDH, HPRT1 – which are commonly used in qRT-PCR – and EEF2. GAPDH and HPRT1 tend to be differentially expressed depending on the experimental conditions and the type of tissue the cells originate from (Jonge *et al.*, 2007; Kouadjo *et al.*, 2007). Here, 7F2 osteoblastic cells and adipocytic cells originated from the same tissue – bone – but since they were differentiated into adipocytes *in vitro*, this may have had an influence on GAPDH and HPRT1 expression levels. EEF2 on the contrary was shown to have very stable expression levels (Jonge *et al.*, 2007; Kouadjo *et al.*, 2007); this gene is involved in translation and was evenly expressed between all tissues tested, particularly in mouse tissues (Kouadjo *et al.*, 2007). However, in some qRT-PCR repeats, the EEF2 expression levels varied significantly between the various samples, whereas HPRT1 expression levels seemed relatively even, which is why expression levels of the tested genes were normalised with both EEF2 and HPRT1 in the result sections.

Glut4 expression level was not measured by qRT-PCR analysis, because when its expression first tested by RT-PCR, it was not detected in 7F2 cells cultured with basal or adipogenic medium, despite running RT-PCR several times with various temperatures for the annealing step (56°C and 58°C), and increasing the number of cycles from 35 to 40. However, when tested again several months later, Glut4 mRNA was detected in 7F2 cells cultured with adipogenic medium. Similarly, osteocalcin expression was not measured by qRT-PCR, because the first set of primers that was used showed a low expression in RT-PCR experiments.

7.3.3. Electrophysiology

The main limitation of this study regarding electrophysiology data was the impossibility to obtain whole-cell patches, which caused several problems. Firstly, it prevented the pharmacological characterisation of the ion channels that were detected using single-channel patch clamping. Secondly, it prevented other types of experiments that would have provided useful data. In particular, it was not possible to test whether some ion channels opened in response to ghrelin binding to its receptor when adding ghrelin to the bathing solution, and to identify these ion channels using

pharmacological modulators. Thirdly, whole-cell patch may have allowed verifying that GHSR1a was the receptor ghrelin bound to, by using an antagonist of this receptor; if ghrelin bound to GHSR1a and triggered ion channel opening, then the corresponding currents may have been abolished by the addition of a GHSR1a antagonist.

The protocol used here favoured the detection of voltage-dependent and voltage-activated ion channels, by trying to detect currents when changing membrane voltage, but other types of ion channels exist that are activated by other stimuli, such as ligand-activated ion channels. In particular, some inwardly-rectifying K⁺ channels are coupled to GPCRs (Hibino *et al.*, 2010), which may have been relevant to this study, as GHSR1a is a GCPR (Camiña, 2006). These other types of ion channels may have been investigated using whole-cell patch clamping or perforated patch clamping, had those techniques been efficient with 7F2 cells.

This study focussed on the roles of K⁺ channels in this study, even though other families of ion channels such as Ca²⁺, Na⁺ or Cl⁻ channels are present and have biological functions in osteoblasts. PCR tools were used to detect expression of subunits of various K⁺ channels, but not other types of ion channels. However, in electrophysiology experiments, the recording solutions that were used also allowed detecting other families of ion channels, as they contained a non-negligible amount of other ions (Na⁺, Ca²⁺ and Cl⁻ in particular). The role of K⁺ channels in regulating 7F2 cell proliferation and adipogenic differentiation was investigated using TEA and diazoxide in cell culture assays, but using pharmacological modulators for other families of ion channels may have provided interesting data on the ionic mechanisms underlying 7F2 cell adipogenic differentiation.

7.4. Recommendations for future work

The findings presented in this study raise a number of questions that were not approached in this study due to lack of time or funding; these questions may be investigated in future work.

The transdifferentiation of 7F2 cells into adipocytes

Given the high degree of plasticity between the osteoblastic and adipocytic lineages, the work done on 7F2 cells in this study may be extended to other osteoblastic cells, especially primary osteoblasts and osteoblast cell lines from other species, including humans. Other differentiation markers may be tested, especially adipogenic markers such as secretion of leptin or adiponectin; it would be interesting to study whether 7F2

cell-derived adipocytes can secrete adipokines, which are known to regulate bone homeostasis.

The expression of differentiation markers was only tested at the mRNA level; future work may extend these results by analysing expression at the protein level, using western blotting.

Ghrelin signalling in 7F2 cells

7F2 cells express genes from ghrelin signalling, including several variant isoforms of ghrelin at the mRNA level, which raises several questions. Are these genes and the variant isoforms of ghrelin expressed at the protein level? Are ghrelin variants upregulated by ghrelin treatment, similarly to *Ghrl* mRNA? Other studies have shown that the ghrelin gene gives rise to a large number of isoforms whose expression pattern may be tissue-specific. Are the ghrelin variants detected in 7F2 cells expressed in other osteoblastic cells, such as primary osteoblasts? Are they expressed in osteoblasts from other species, especially humans?

The exact structure of the ghrelin variants in 7F2 cells could not be established due to the fact that PCR reaction with primers located on exons 1 and 5, or exons 1 and 4, did not work. These may be due to the fact that the PCR reaction needs to be optimised; or maybe there are several isoforms, one that contains exon 1 but not exons 4 and 5, and one that contains exons 4 and 5, but not exon 1. Further work is needed to establish the exact number and structure of the ghrelin variants detected in 7F2 cells.

Effect of ghrelin treatment on 7F2 cell adipogenic differentiation

Ghrelin treatment did not seem to inhibit 7F2 cell adipogenic differentiation, but upregulated both osteogenic and adipogenic marker mRNA expression. However, repeating qRT-PCR assays would be useful; here the effects of ghrelin on differentiation marker mRNA expression was only tested twice (with two different concentrations of ghrelin), and a great variability was observed between the two repeats.

If the ghrelin variants are expressed at the protein level, it would be interesting to study their effects on adipogenic differentiation of 7F2 cells, other osteoblastic cell lines or BMSCs. Overexpressing these variants may be used as an approach to test their effects on osteoblast formation and function.

Electrophysiological properties of 7F2 cells

Several functional ion channels were detected in 7F2 cells that could not be identified by pharmacological modulation during electrophysiological recording. To identify these ion channels, it may be helpful to investigate the mRNA expression the candidates that were proposed for the currents detected in 7F2 cells, including intermediate-conductance Ca^{2+} -activated K^+ channels (KCa3.1), which are expressed in mouse BMSCs; TRPV1 and the inward rectifier K^+ channel Kir2.1, which have been reported to regulate cell proliferation and differentiation in bone; and Kv2.1 which mediates ghrelin signalling in pancreatic β -cells. Analysing the kinetics of the currents, with less background noise in single-patch clamping experiments, will also help identify the corresponding ion channels.

The roles of K^+ channels in 7F2 cell proliferation and differentiation

The data in this study indicate that K^+ channels are involved in regulating 7F2 cell proliferation and adipogenic differentiation. Testing the effects of specific channel blockers or activators in cell culture assays should help identify the ion channels that are involved in regulating adipogenic differentiation. The channel blockers/openers may be selected based on RT-PCR and electrophysiological data.

K_{ATP} channels are involved in regulating the secretion of various hormones such as insulin and osteocalcin (Moreau *et al.*, 1997; Ashcroft, 2005). Here, diazoxide did not seem to affect cell proliferation and differentiation as measured by cell counting and Oil Red O staining, but it may affect other processes such as osteocalcin secretion by 7F2 cells.

Due to lack of time, the role of ion channels in mediating ghrelin signalling could not be tested. With electrophysiology techniques, since whole-cell and perforated-patch configurations could not be obtained, it was not possible to test whether adding ghrelin to the bathing solution could trigger ion channel activity or modify their kinetics. It may be interesting to test whether channel blockers/openers can attenuate the effects of ghrelin on the mRNA expression of differentiation markers and *Ghrl*.

7.5. Concluding statement

Understanding the mechanisms underlying pathological adipogenesis in bone is of importance to identify new therapeutic approaches to treat some forms of osteoporosis. The findings in this thesis provide data on the role of ghrelin signalling

Chapter 7 – General discussion and conclusions

and ionic mechanisms in osteoblast proliferation and adipogenic differentiation, but also raise many questions that will need to be answered in future studies.

Chapter 8 – Appendix

8.1. Oligonucleotide primers

8.1.1. Oligonucleotide primers for house-keeping genes

Oligonucleotide primers (see table 8.1 and figure 8.1) for three house-keeping genes: Hypoxanthine-guanine Phosphoribosyltransferase 1 (*Hprt1*), Glyceraldehyde 3-phosphate dehydrogenase (*Gapdh*) and Eukaryotic elongation factor 2 (*Eef2*), were designed from mouse gene sequences using FasterDB (Cancer Research Center of Lyon, CRCL) and Primer3 as follows: the FasterDB database was searched for genetic sequences in the mouse genome; part of mRNA sequences were selected so that they covered as many splicing isoforms as possible and copied into the 'source sequence box' of the web-based Primer3 primer design software. The software selected left and right primers for the given sequence without modification of the default software settings. Primer3-suggested primers were checked against the complete genetic sequence using the FasterDB 'in silico PCR' tool, to determine predicted amplicon sizes, especially when primer sequences were in different exons. Primers were obtained from Eurogentec.

Gene	Sequences	Product Size
<i>Hprt1</i>	F: ATTAGCGATGATGAACCAGGT	155 bp
	R: GCCTCCCATCTCCTTCATGA	
<i>Gapdh</i>	F: AAAGGGTCATCATCTCCGCC	170 bp
	R: CCCTTCCACAATGCCAAAGT	
<i>Eef2</i>	F: GGAGCTCTACCAGACCTTCC	186 bp
	R: GCCACATACATCTCCGCAA	

Table 8.1: Oligonucleotide primer details for differentiation markers

Hprt1

> [NM_013556](#) Mus musculus hypoxanthine guanine phosphoribosyl transferase (Hprt), mRNA

```

121 tttgccgcga gcgaccggt cccgtcatgc cgaccgcag tcccagcgtc gtgattagcg
181 atgatgaacc aggttatgac ctagatttgt tttgtatacc taatcattat gccgaggatt
241 tggaaaaagt gtttattcct catggactga ttatggacag gactgaaaga cttgctcgag
301 atgtcatgaa ggagatggga gccatcaca ttgtggcct ctgtgtgctc aaggggggct
    
```

Gapdh

> [NM_008084](#) Mus musculus glyceraldehyde-3-phosphate dehydrogenase (Gapdh), transcript variant 2, mRNA

```

541 accaccatgg agaaggccgg ggcccacttg aagggtggag ccaaagggt catcatctcc
601 gcccttctg ccgatgcccc catgtttgtg atgggtgtga accacgagaa atatgacaac
661 tcaactcaaga ttgtcagcaa tgcactctgc accaccaact gcttagcccc cctggccaag
721 gtcatccatg acaactttgg cattgtggaa gggctcatga ccacagtcca tgccatcact
    
```

Eef2

> [NM_007907](#) Mus musculus eukaryotic translation elongation factor 2 (Eef2), mRNA

```

601 ctggagcccg aggagcteta ccagaccttc cagcgcacgc tggagaacgt caacgtcatc
661 atctctacct acggcgaggg cgagagtggg cccatgggca atatcatgat tgacccccgc
721 ctgggcaccg taggctttgg ttctggcctg catggctggg ccttcaccct gaagcagttt
781 gccgagatgt atgtggc caa gtttgcagcc aagggtgagg gccagctgag cgcagccgag
    
```

Figure 8.1: Primers and amplification sequences for house-keeping genes.

Target primer sequences are shown in red.

8.1.2. Oligonucleotide primers for differentiation markers

Oligonucleotide primers (see table 8.2 and figure 8.2) for various adipocytic markers: peroxisome proliferator-activated receptor gamma (*Pparg*), Glucose transporter type 4 (*Glut4*) and CCAAT-enhancer-binding protein alpha (*Cebpa*); and osteoblastic markers: osteocalcin, Runt-related transcription factor 2 (*Runx2*), and alkaline phosphatase (*Alpl*), were designed as previously described (see above, section 8.1.1) and obtained from Eurogentec.

Gene	Sequences	Product Size
<i>Pparg</i>	F: AGAACCTGCATCTCCACCTT	155 bp
	R: TGCATCCTTCACAAGCATGA	
<i>Glut4</i>	F: CTTGGCTCCCTTCAGTTTG	130 bp
	R: TGCCTTGTGGGATGGAAT	
<i>Cebpa</i>	F: TACAACAGGCCAGGTTTCCT	206 bp
	R: AAGTTCCTTCAGCAACAGCG	
<i>Osteocalcin</i>	F: AGGTAGTGAACAGACTCCGG	162 bp
	R: ACTGTACAAGAGGCTCCAGG	
<i>Runx2</i>	F: TTCAACGATCTGAGATTTGTGGG	221 bp
	R: GGATGAGGAATGCGCCCTA	
<i>Alpl</i>	F: TCAGGGCAATGAGGTCACAT	161 bp
	R: CCTCTGGTGGCATCTCGTTA	

Table 8.2: Oligonucleotide primer details for differentiation markers

Pparg

> [NM_001127330.2](#) Mus musculus peroxisome proliferator activated receptor gamma (Pparg), transcript variant 1, mRNA: 155 bp

```

721 caaagtagaa cctgcatctc cacottatta ttctgaaaag acccagctct acaacaggcc
781 tcatgaagaa ctttctaact cctcatggc cattgagtgc cgagtctgtg gggataaagc
841 atcaggcttc cactatggag tcatgcttg tgaaggatgc aagggttttt tccgaagaac
901 catccgattg aagottatth atgataggtg tgatcttaac tgccggatcc acaaaaaaag

```

Also detects transcript variant 3 ([NM_001308352.1](#)) and 4 ([NM_001308354.1](#)), 155 bp

Glut4

> [NM_009204](#) Mus musculus solute carrier family 2 (facilitated glucose transporter), member 4 (Slc2a4), mRNA: 130 bp

```

301 ctgtgcttgg ctcccttcag tttgctata acattgggggt tatcaatgcc ccacagaagg
361 tgattgaaca gagctacaat gcaacgtggc tgggtaggca aggtcctggg ggaccggatt
421 ccatcccaca aggcaccctc actacgctct gggtctctc cgtggccatc ttctctgtgg
481 gtggcatgat ctcttctctt ctcaattggca tcatttctca atggttggga aggaaaaggg

```

Cebpa

> [NM_007678](#) Mus musculus CCAAT/enhancer binding protein (C/EBP), alpha (Cebpa), transcript variant 1, mRNA: 206 bp

```

1801 ccacctacat ccccccccc ccactcagct tacaacagge caggtttcoct gggtgagttc
1861 atggagaatg ggggcaccac cccagtcag accagaaagc tgagttgtga gttagccatg
1921 tggtaggaga cagagacctg ggtttctggg ctttctgggg tgggggatag gaggacacgg
1981 ggaccattag ccttctgtgt actgtatgct gccagccqct gttgctgaag gaacttgaag

```

Figure 8.2: Primers and amplification sequences for differentiation markers (part 1)

Target primer sequences are **underlined**.

Osteocalcin (1st set of primers)

> [BC069910](#) Mus musculus bone gamma-carboxyglutamate protein, related sequence 1, mRNA: 162 bp

```
241 cctcctgaac tcagaattac ctgaccttgt gtgtcttctc cacagccttc atgtccaage
301 aggagggcaa taaggtagtg aacagactcc ggcgctacct tgggtaagtg gccagagccc
361 ttagccttcc atattggtag ggaggagttg ttctggggta gtctctatga cccgcagagg
421 gctacacgtg caggccaatc cccaggtcca ggaccctgga gcctottgta cagtgtggga
```

Osteocalcin (2nd set of primers)

> [NM_007541](#) Mus musculus bone gamma carboxyglutamate protein (Bglap), mRNA (longer PolyA)

```
121 aagcccagcg gccctgagtc tgacaaagcc ttcattgtcca agcaggaggg caataaggta
181 gtgaacagac tccggcgcta ccttggagcc tcagtcccca gccagatcc cctggagccc
241 acccgggagc agtgtgagct taaccctgct tgtgacgagc taccagacca gtatggcttg
301 aagaccgcct acaaacgcat ctatggtatc actathtagg acctgtgctg ccctaaagcc
```

> [NM_001032298](#) Mus musculus bone gamma-carboxyglutamate protein 2 (Bglap2), mRNA

```
121 aagcccagcg gccctgagtc tgacaaagcc ttcattgtcca agcaggaggg caataggta
181 gtgaacagac tccggcgcta ccttggagcc tcagtcccca gccagatcc cctggagccc
241 acccgggagc agtgtgagct taaccctgct tgtgacgagc taccagacca gtatggcttg
301 aagaccgcct acaaacgcat ctacggtatc actathtagg acctgtgctg ccctaaagcc
```

Figure 8.2: Primers and amplification sequences for differentiation markers (part 2)

Target primer sequences are **underlined**.

Chapter 8 - Appendix

> [BC069910](#) Mus musculus bone gamma-carboxyglutamate protein, related sequence 1, mRNA (cDNA clone IMAGE:5250978), with apparent retained intron : 384/385 bp, intron retention between exon 3 and 4

```
421 gtgtcttoto cacagccttc atgtccaagc aggagggcaa t aaggtagtg aacagactcc
481 ggcgctacct tgggtaagtg gccagagccc ttagccttcc atagtggtag gaaggagtgtg
541 tgetggagtg gtctctatga cctgcagagg gctagacgtg caggtaaatc cccatgtcca
601 ggaccctgga goctcttgta cagtgtggga agagggtgtg tgtatccctg gtatattaat
661 gccactgtgt gttggttgat gttactttat gcttctcaga gctcagtcoc ccagcccaga
721 tcccctggag cccaccggg agcagtgtga gcttaaccct gcttgtagcag agctatcaga
781 ccagtatggc ttgaagaccg cctacaaacg catctatggt atcaactatttt aggacctgtg
841 ctgccctaaa gccaaactct ggcagctcgg ctttggtctgc tctccgggac ttgatccctc
```

Runx2

> [NM_001146038](#) Mus musculus runt related transcription factor 2 (Runx2), transcript variant 1, mRNA: 221 bp

```
781 atgaaaaacc aagtagccag gttcaacgat ctgagatttg tgggccggag cggacgaggc
841 aagagtttca ccttgaccat aacagtcttc acaaatcctc cccaagtggc cacttaccac
901 agagctatta aagtgacagt ggacggtooc cgggaaccaa gaaggcacag acagaagctt
961 gatgacteta aacctagttt gttctctgat cgcctcagtg atttagggcg cattcctcat
1021 cccagtatga gagtaggtgt cccgcctcag aaccacggc cctccctgaa ctctgcacca
```

Also detects transcript variants 2 ([NM_001145920](#)) and 3 ([NM_009820](#)), 221 bp

Alpl

> [NM_007431](#) Mus musculus alkaline phosphatase, liver/bone/kidney (Alpl), transcript variant 1, mRNA: 161 bp

```
661 aacaccacttc agggcaatga ggtcacatcc atcctgcgct gggccaagga tgetgggaag
721 tccgtgggca ttgtgactac cactcgggtg aaccacgcca caccagtgcc agcctacgca
781 cactcggccg atcgggactg gtactcggatt aacgagatgc caccagaggc tctgagccag
841 ggctgcaagg acatcgcata tcagctaata cacaaatca aggatatcga cgtgatcatg
901 ggtggcggcc ggaaatacat gtaccogaag aacagaactg atgtggaata cgaactggat
```

Figure 8.2: Primers and amplification sequences for differentiation markers (part 3)

Target primer sequences are **underlined**.

8.1.3. Oligonucleotide primers for ghrelin signalling genes

Oligonucleotide primers (see table 8.3 and figure 8.3) for Growth-Hormone Secretagogue Receptor (*Ghsr*), Ghrelin (*Ghrl*) and Ghrelin-O-Acyltransferase (*Mboat4*) were designed as previously described (section 8.1.1) and obtained from Eurogentec.

Gene	Sequences	Product Size
<i>Ghsr</i>	F: GGCAACGACTCACTCTCTGA	215 bp
	R: GGCATGCACAGGAAGATGAG	
<i>Ghrl</i>	F: GTCATCTGTCCTCACCACCA	220 bp
	R: TGCTTGTCTCTGTCCTCTG	
<i>Mboat4</i>	F: TGCCCTTCATCTCACCTAGC	240 bp
	R: GCCACACCTCCTAGTCCTTT	

Table 8.3: Oligonucleotide primer details for ghrelin signalling components

Ghsr

> [NM_177330](#) Mus musculus growth hormone secretagogue receptor (Ghsr), mRNA:
215 bp

```

301 cctggactgg gaogcttctc ccggcaacga ctcaactctct gacgaaactgc tgccactgtt
361 ccccgcgccg ctgctggcgg gcgtcaactgc cacctgcgtg gcgctcttcg tggtaggcac
421 ctggggcaac ctgctcacca tgctggtggt gtcccgttc cgogagctgc gcaccaccac
481 caacctctac ctatccagca tggccttctc cgatctgctc atcttctgt gcatgccgct

```

Ghrl

> [NM_021488](#) Mus musculus ghrelin (Ghrl), transcript variant 1, mRNA: 220 bp

```

1 atataaggag aagccggtga gcaggcacca catccccagg cattccaggt catctgtcct
61 caccaccaag accatgctgt cttcaggcac catctgcagt ttgctgtctac tcagcatgct
121 ctggatggac atggccatgg caggetccag cttcctgagc ccagagcacc agaaagccca
181 gcagagaaag gaatccaaga agccaccagc taaactgcag ccacgagctc tggaggctg
241 gctccaccca gaggacagag gacaagcaga agagacagag gaggagctgg agatcaggtt

```

Mboat4

> [NM_001126314](#) Mus musculus membrane bound O-acyltransferase domain containing 4 (Mboat4), mRNA: 240 bp

```

1381 cctggccttc atctcaccta gccattaaat actgcttagg aaatgccaga agatgccttg
1441 atgaataatg tatttaaac tattcatagt gaaagttttt aagtattgga tggataaacc
1501 tgatggctgg ccacagagat gtgtttctct tctgtggtgg tttgaatagt aatggctccc
1561 atatgtttat atatttaaat gcttagaggg tgacactact tgaaaggact aggaggtgtg
1621 gcttcatcgg aggaagtgtg tcactaggct ttgaagtttc aaaagcccag tcctagtta

```

Figure 8.3: Primers and amplification sequences for ghrelin signalling components.

Target primer sequences are **underlined**.

8.1.4. Oligonucleotide primers for ghrelin signalling genes

Oligonucleotide primers (see tables 8.4 and 8.5; and figure 8.4) spanning the various exons and intron 2 of the mouse ghrelin gene were obtained from Eurogentec. The primers were designed by (Kineman *et al.*, 2007), except for Ghrl458_E2f (Exon 2, forward) and Ghrl753_E3r (Exon 3, reverse), which were designed as previously described (section 8.1.1). All primers were obtained from Eurogentec.

Name	Sequence	Location	Direction
Ghrl30_E1f	ACATCCCCAGGCATTCCAG	Exon 1	Forward
Ghrl458_E2f	GTCATCTGTCCTCACCACCA	Exon 2	Forward
Ghrl698_E3f	TCCAAGAAGCCACCAGCTAA	Exon 3	Forward
Ghrl798_E3-4f	TCAGGTTCAATGCTCCCTTC	Exon 3/4	Forward
Ghrl2751_E4f	CAATGCTCCCTTCGATGTTG	Exon 4	Forward
Ghrl607_In2r	GTAGATGTGGGGGCTTAGGG	Intron 2	Reverse
Ghrl637_In2r	TTCTCTCTCTCTCACACACACAC	Intron 2	Reverse
Ghrl753_E3r	TGCTTGTCCTCTGTCCTCTG	Exon 3	Reverse
Ghrl2752_E4r	AACATCGAAGGGAGCATTGA	Exon 4	Reverse
Ghrl3657_E5r	AGGCCTGTCCGTGGTTACTT	Exon 5	Reverse

Table 8.4: Names, sequences and location of primers

Primer sets	Primer locations	Sequences	Product Size*
Ghrl30_E1f - Ghrl753_E3r	Ex1-Ex3	F: ACATCCCCAGGCATTCCAG	239 bp
		R: TGCTTGCCTCTGTCCTCTG	
Ghrl458_E2f - Ghrl607_In2r	Ex2-In2	F: GTCATCTGTCCTCACCACCA	169 bp
		R: GTAGATGTGGGGGCTTAGGG	
Ghrl458_E2f - Ghrl637_In2r	Ex2-In2	F: GTCATCTGTCCTCACCACCA	204 bp
		R: TTCTCTCTCTCACACACACACAC	
Ghrl458_E2f - Ghrl753_E3r	Ex2-Ex3	F: GTCATCTGTCCTCACCACCA	220 bp
		R: TGCTTGCCTCTGTCCTCTG	
Ghrl698_E3f - Ghrl2752_E4r	Ex3-Ex4	F: TCCAAGAAGCCACCAGCTAA	126 bp
		R: AACATCGAAGGGAGCATTGA	
Ghrl2751_E4f - Ghrl3657_E5r	Ex4-Ex5	F: CAATGCTCCCTTCGATGTTG	141 bp
		R: AGGCTGTCCGTGGTTACTT	

Table 8.5: Expected product size for each tested sets of primers

* sizes indicated are without any intron, except for when reverse primers are located within intron 2.

Ghrl (Exon 1 - Exon 3)

> [NM_021488](#) Mus musculus ghrelin (Ghrl), transcript variant 1, mRNA: 239 bp – Exon 1, Exon 2, Exon 3

```

1 atataaggag aagccggtga gcaggcacca catccccagg cattccaggt catctgtcct
61 caccaccaag accatgctgt cttcaggcac catctgcagt ttgctgctac tcagcatgct
121 ctggatggac atggccatgg caggetccag cttcctgagc ccagagcacc agaaagccca
181 gcagagaaag gaatccaaga agccaccagc taaactgcag ccacgagctc tggaaggctg
241 gctccaccca gaggacagag gacaagcaga agagacagag gaggagctgg agatcaggtt

```

Ghrl (Exon 2 - Intron 2, first primer set)

> [DQ993169](#) Mus musculus ghrelin variant mRNA sequence: 169 bp - Exon 2, Intron 2

```

1 gtcatctgtc ctcaccacca agaccatgct gtcttcagge accatctgca gtttgetgct
61 actcagcatg ctctggatgg acatggccat ggcaggetcc agcttctga gccagagca
121 ccagaaagcc caggtcagtc agtctgtctc cctaagcccc cacatctacc ccgatctgtg

```

Ghrl (Exon 2 - Intron 2, second primer set)

> [DQ993169](#) Mus musculus ghrelin variant mRNA sequence: 204 bp - Exon 2, Intron 2

```

1 gtcatctgtc ctcaccacca agaccatgct gtcttcagge accatctgca gtttgetgct
61 actcagcatg ctctggatgg acatggccat ggcaggetcc agcttctga gccagagca
121 ccagaaagcc caggtcagtc agtctgtctc cctaagcccc cacatctacc ccgatctgtg
181 tgtgtgtgtg tgagagagag agaaagagaa ccctcttttc ctttcagca gagaaaggaa

```

Figure 8.4: Primers and amplification sequences for the various regions of the ghrelin gene (part 1)

Target primer sequences are **underlined**. No intron included except for when reverse primer is located on intron 2.

Ghrl (Exon 2 - Exon 3)

> [NM_021488](#) Mus musculus ghrelin (Ghrl), transcript variant 1, mRNA: 220 bp - Exon 2, Exon 3 (no Intron 2)

```

1 atataaggag aagccggtga gcaggcacca catccccagg cattccaggt catctgtcct
61 caccaccaag accatgctgt cttcaggcac catctgcagt ttgctgctac tcagcatgct
121 ctggatggac atggccatgg caggctccag cttcctgagc ccagagcacc agaaagccca
181 gcagagaaaag gaatccaaga agccaccagc taaactgcag ccacgagctc tggaaggctg
241 gctccaccca gaggacagag gacaagcaga agagacagag gaggagctgg agatcaggtt

```

Ghrl (Exon 3 - Exon 4)

> [NM_021488](#) Mus musculus ghrelin (Ghrl), transcript variant 1, mRNA: 126 bp - Exon 3, Exon 4

```

181 gcagagaaaag gaattccaaga agccaccagc taaactgcag ccacgagctc tggaaggctg
241 gctccacca gaggacagag gacaagcaga agagacagag gaggagctgg agatcaggtt
301 caatgctccc ttcgatgttg gcatcaagct gtcaggagct cagtatcagc agcatggccg

```

Ghrl (Exon 4 - Exon 5)

> [NM_021488](#) Mus musculus ghrelin (Ghrl), transcript variant 1, mRNA: 141 bp - Exon 4, Exon 5

```

301 caatgctccc ttcgatgttg gcatcaagct gtcaggagct cagtatcagc agcatggccg
361 ggccctgggg aagtttcttc aggatatcct ctgggaagag gtcaaagagg cgccagctga
421 caagtaacca cggacaggcc tgacccccgt gctttccttc tctgagcaa gaactcacat

```

Figure 8.4: Primers and amplification sequences for the various regions of the ghrelin gene (part 2)

Target primer sequences are **underlined**. No intron included except for when reverse primer is located on intron 2.

8.1.5. Oligonucleotide primers for ion channels

Oligonucleotide primers (see table 8.6 and figure 8.5) for Kir6.1 (*Kcnj8*), Kir6.2 (*Kcnj11*), SUR1 (*Abcc8*), SUR2 (*Abcc9*), KCa1.1 (*Kcnma1*), KCa1.1 regulatory β subunits (*Kcnmb1-4*) and Kv4.2 (*Kcnd2*) were designed as previously described (section 8.1.1) and obtained from Eurogentec.

Gene	Sequences	Product Size
<i>Kcnj8</i>	F: CATGATCATTAGCGCCTCGG	155 bp
	R: CGTGGCAGATGATCAATGGG	
<i>Kcnj11</i>	F: CACCTCCTACCTAGCTGACG	249 bp
	R: ATGCTAAACTTGGGCTTGGC	
<i>Abcc8</i>	F: CCATTGATTACTGGCTGGCC	175 bp
	R: TCCACAGTGACAGAGGTGAC	
<i>Abcc9</i>	F: CCATCATCAGTGTTCAAAAGC	148 bp
	R: GGCTGCTTCCTGTTTATTGG	
<i>Abcc9</i>	F: ATCATGGATGAAGCCACTGC	SUR2A: 397 bp SUR2B: 221 bp
	R: AACGAGGCAAACACTCCATC	
<i>Kcnma1</i>	F: TGGTGGAGAATTCAGGGGAC	167 bp
	R: CCCGAGGATGAAGAAGACCA	
<i>Kcnmb1</i>	F: GGACAACTACCAGACAGCCT	164 bp
	R: TGGGCCAGAAGAAGGAGAAG	
<i>Kcnmb2</i>	F: TCGTGAGTGTCGTCATGGAA	155 bp
	R: CCCAGCCATCATACAAGTTGG	
<i>Kcnmb3</i>	F: AAATTCTAGAGGACCCCGC	217 bp
	R: ACCCTGTAGCGTGATTTGGA	
<i>Kcnmb4</i>	F: CTGTCCGTGCAGCAGATC	167 bp
	R: TTGGGGTTGGTCAGGAGC	
<i>Kcnd2</i>	F: GAACCGGCCTTCATAAGCAA	162 bp
	R: ACTGTGACTTGATGGGCGAT	

Table 8.6: Oligonucleotide primer details for ion channels

Kcnj8

> [NM_008428](#) Mus musculus potassium inwardly-rectifying channel, subfamily J, member 8 (Kcnj8), transcript variant 1, mRNA: 155 bp

```

1141 gggtgacctg aggaagagca tgatcattag cgctcggtg cgcattccagg tggtaagaa
1201 aaccacgacg ccagaagggg agtggtgccc tattcatcag caggacattc ctgttgataa
1261 tcccatcgag agcaataata tcttctagtg ggccccattg atcatctgcc acgtgattga
    
```

Also detects transcript variants 2 ([NM_001330363.1](#)) and 3 ([NM_001330366.1](#)), 155 bp

Kcnj11

> [NM_010602.3](#) Mus musculus potassium inwardly rectifying channel, subfamily J, member 11 (Kcnj11), transcript variant 1, mRNA: 249 bp

```

1201 ggaaggcgtg gtagaaacca cgggcatcac caccaggccc cgcaoctcct acctagetga
1261 cgagattcta tgggggcagc gctttgtccc cattgtggcc gaggaggacg gccgctattc
1321 tgtggactac tccaaatttg gtaacaccat taaagtgccc acaccactct gcacagcccg
1381 ccagcttgat gaggaccgca gtctgctgga tgccctgacc ctgcctcgt cgcgggggcc
1441 cctgcgcaag cgcagtgtgg ctgtggcgaa ggccaagccc aagtttagca tctctccaga
    
```

Also detects transcript variant 2 ([NM_001204411.1](#)), 249 bp

Abcc8

> [NM_011510.3](#) Mus musculus ATP-binding cassette, sub-family C (CFTR/MRP), member 8 (Abcc8), transcript variant 1, mRNA: 175 bp

```

3181 ttggtggcca ttgattactg gctggccaag tggacggaca gtgcctggt cctgagccct
3241 gctgccagga actgctccct cagccaggaa tgccgacctg accagttctgt ctatgceatg
3301 gtattcaccg tgctctgcag cctgggaatt gcaactgtgc ttgtcacctc tgtcaactgtg
3361 gagtggacag gactgaaggt ggccaagagg ctgcaccgca gctgctcaa tcgcatcacc
    
```

Also detects transcript variant 2 ([NM_001357538.1](#)), 175 bp

Figure 8.5: Primers and amplification sequences for ion channels (part 1)

Target primer sequences are **underlined**.

Abcc9 (first set of primers)

> [NM_011511.2](#) Mus musculus ATP-binding cassette, sub-family C (CFTR/MRP), member 9 (Abcc9), transcript variant 1, mRNA: 148 bp

```

1981 ggtggtcaga ttgcagtc aagccatcat cagtgttcaa aagctgaatg agttctctt
2041 gagcgatgag attggtgagg acagctggag gcccggggag gccacgctgc ctttcgagtc
2101 ctgtaagaag cacaccggag tgcaatcaaa accaataaac aggaagcagc ctggacggta
2161 ccacctggac agctacgagc aagcacggcg cctccggccc gctgagacgg aagacattgc
    
```

Also detects transcript variants 2 ([NM_021041.2](#)), 5 ([NM_001044720.1](#)) and 6 ([NM_001310143.1](#)), 148 bp

Abcc9 (second set of primers)

> [NM_011511.2](#) Mus musculus ATP-binding cassette, sub-family C (CFTR/MRP), member 9 (Abcc9), transcript variant 1, mRNA: 221 bp (isoform a, SUR2B)

```

4561 tggacagaga cagctgttct gcctggccag gccctttggt cggaaagagca gtatactcat
4621 catggatgaa gccactgctt ccacgacat gccacggaa aacatthtgc agaaagtgt
4681 catgacagcc tttgoggatc gcacggtogt aaccatagct catogggttc acaccattot
4741 gactgcagac ctggttattg tgatgaagag aggaaatatt ttggaatacg acaccocgga
4801 aagcctcttg gccacggaag atggagtgtt tgctctgctt gtccgtgcag acatgtgaca
    
```

> [NM_021041.2](#) Mus musculus ATP-binding cassette, sub-family C (CFTR/MRP), member 9 (Abcc9), transcript variant 2, mRNA: 397 bp (isoform b, SUR2A)

```

4561 tggacagaga cagctgttct gcctggccag gccctttggt cggaaagagca gtatactcat
4621 catggatgaa gccactgctt ccacgacat gccacggaa aacatthtgc agaaagtgt
4681 catgacagcc tttgoggatc gcacggtogt aaccatagct caccgtgtct cttctattgt
4741 ggatgcagcc cttgthtttag tctthttctga gggatthtta gtggagtgtg atactggtcc
4801 aaacctgctc cagcacaaga atggcctctt ttctactttg gtgatgacca acaagtagac
4861 cagcgtgac tgctccgaca agtgtctcat tctctgcac gccgttcacac cattctgaet
4921 gcagacctgg ttattgtgat gaagagagga aatathtttg aatacgacac cccggaagc
4981 ctcttgccc aggaagatgg agtgtttgcc tcgcttgtcc gtgcagacat gtgacaggat
    
```

Also detects transcript variants 4 ([NM_021042.2](#)) and 5 ([NM_001044720.1](#)), 397 bp; and transcript variant 6 ([NM_001310143.1](#)), 221 bp

Figure 8.5: Primers and amplification sequences for ion channels (part 2)

Target primer sequences are **underlined**.

Kcnma1

> [NM_001253358.1](#) Mus musculus potassium large conductance calcium-activated channel, subfamily M, alpha member 1 (Kcnma1), transcript variant 1, mRNA: 167 bp

```

1021 cagctggatt catccacttg gtggagaatt caggggaccc atgggaaaat ttccaaaaca
1081 accaggcaact tacgtactgg gaatgtgtct acttactcat ggtcacaatg tctacagtgg
1141 gttatgggga cgtttatgca aaaaccacac ttggacgcct ctccatggtc ttcttcaccc
1201 tcgggggact ggccatgttt gccagctacg tcctgaaat catagagtta ataggaaacc
    
```

Also detects all the other isoforms (transcript variants 2 to 21, same expected size for the PCR products) but not the transcript variant 18 ([NM_001253374.1](#)).

Kcnmb1

> [NM_031169.4](#) Mus musculus potassium large conductance calcium-activated channel, subfamily M, beta member 1 (Kcnmb1), mRNA: 164 bp

```

661 ggaacctgga caactaccag acagccttgg cagatgtgaa gaaggtcaga gccaatctct
721 ataagacca tgaattctat tgcctttctg cacctcaagt caacgagacc agcgtcgtgt
781 accagcgcct ctaogggccc caagtctctc tcttctcctt cttctggccc accttctctc
    
```

Kcnmb2

> [NM_028231.2](#) Mus musculus potassium large conductance calcium-activated channel, subfamily M, beta member 2 (Kcnmb2), mRNA: 155 bp

```

841 aactttgagg agtccatgtc tctcgtgagt gtctcatgg aaacttcag gagacaccaa
901 cacttcccct gctattctga ccagaagga aaccagaaga gtgtcatcct gaccaaactc
961 tacagctcca atgtgctggt ccattctctc ttctggccaa cttgtatgat ggctgggggt
    
```

Figure 8.5: Primers and amplification sequences for ion channels (part 3)

Target primer sequences are **underlined**.

Kcnmb3

> [NM_001195074.1](#) Mus musculus potassium large conductance calcium-activated channel, subfamily M, beta member 3 (Kcnmb3), mRNA: 217 bp

```
10741 cacctctcta ggaaacttct agaggacccc gcagotctg gatgcagcag gggctctggt
10801 gtctgtggct aggcaggaa ttggcaactc cctctgggac tccaactcog atgatgetta
10861 agcctoctgc gctctaaaag ggcacaactc aggcggggag catccgatcc agacatctcc
10921 tggcctcatg cagcccttca gcatccctgt ccaaatcacg ctacaggggtg gccggaggcg
```

Kcnmb4

> [NM_021452.1](#) Mus musculus potassium large conductance calcium-activated channel, subfamily M, beta member 4 (Kcnmb4), mRNA: 167 bp

```
121 tcagtcccg cttgcaggat ctgcaagcca cggcggccaa ctgcaccgtg ctgtcgggtgc
181 agcagatcgg cgaggtgttc gagtgcacct tcacctgtgg caccgactgc aggggcacct
241 cgcagtatcc ctgcgtccag gtgtacgtga acaactccga gtccaactcc agggcgctgc
301 tacacagcga ccagcaccag ctcctgacca accccaagtg ctctatatc ccgccctgta
```

Kcnd2

> [NM_019697.3](#) Mus musculus potassium voltage-gated channel, Shal-related family, member 2 (Kcnd2), mRNA: 162 bp

```
1561 gcagtcctcg gaggatgaac cggccttcat aagcaaatct ggatccagct ttgagacaca
1621 gcaccaccac ctgcttcaact gcctggagaa aaccacgaac catgagtttg tcgatgaaca
1681 agtctttgaa gaaagctgca tggaaagtgc caccgtcaat cgcccatcaa gtcacagtcc
```

Figure 8.5: Primers and amplification sequences for ion channels (part 4)

Target primer sequences are **underlined**.

8.2. Sequencing of *Ghrl* PCR products

The following figures show the raw data supplied by GATC Biotech (chromatographs), the sequence of the PCR product in FASTA format, and the alignment of that sequence with that of the mouse ghrelin gene, for each *Ghrl* PCR product that could be sequenced. These PCR products are presented in Chapter 4 (section 4.3.3.).

B

>24BA88

```
TCTGTATATGTGTGTATATATATGTATATATGTATATATGTATGCATGAACATGCAAGCTCACCGGGG
TCTAAATTATTCAGCACTGGTCATTCATAAGTGTGAGTACTGGTCAGCCTAATTAGCTCTGTC
ATCAGGCTCCTGAGGGCAAGGGACAAGCAACTGAAATGGACAACCCTCTATCACATCAGGCTCTGTC
TGCCTCCAAAGATTGAAAAAGCAGAGGTCAGCCTTCAGCTCCCACCCTTGAAAGATGGTGACAAGAGAG
CCTTGCTTCGTCAGCAGGTCTTACTTCTAGAAGCTTGCTGGATTCTAGCCTGAGCAAATTTCTAAGGC
ACATAACATGGAGATGAAGTAGGCTACCAGAAGACCCTCTCTCCCCAGGTCATCTGTCTCACCACCA
AGACCATGCTGTCTTCAGGCACCATCTGCAGTTTGCTGCTACTCAGCATGCTCTGGATGGACATGGCCA
TGGCAGGCTCCAGCTTCCTGAGCCAGAGCACCAGAAAGCCAGGTCAGTCAGTCTGTCTCCCTAAGCC
CCCACATGTACCCCGATCTGTGTGTGTGTGTGAGAGAGAGAGAAAGAGAACCCTCTTTTCCTTTCCA
GCAGAGAAAGGAA
```

Figure 8.6: Sequencing of the 741 bp band from PCR with primers located on exons 1 and 3 (part 2)

B: sequence of the PCR product, extracted from the chromatograph.

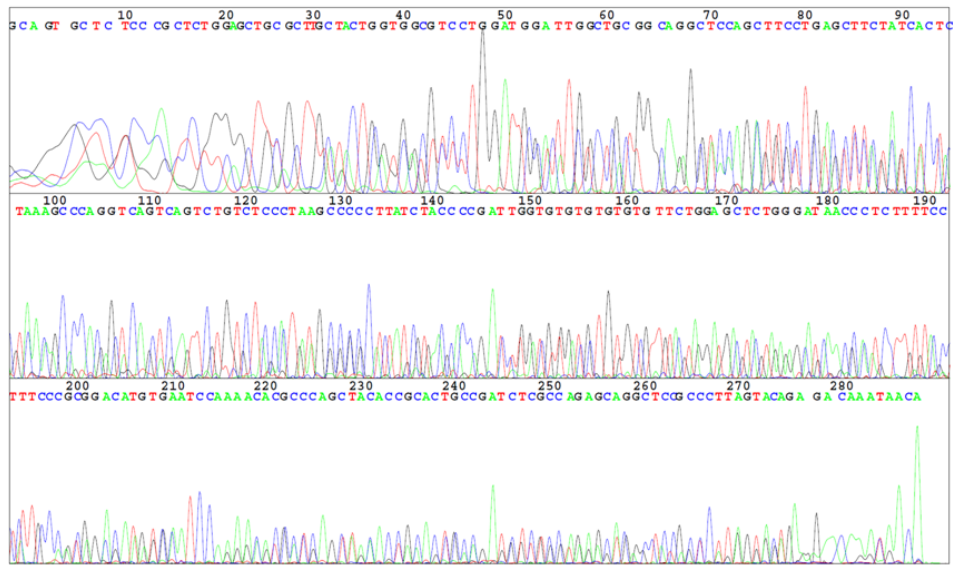


Figure 8.6: Sequencing of the 741 bp band from PCR with primers located on exons 1 and 3 (part 3)

C: sequence alignment between the ghrelin gene (mouse) and the PCR product sequence extracted from the chromatograph, using the Clustal Omega program (EBI-EMBL). Underlined= exons; dotted line= intronic sequence that has been found to be included in some ghrelin variants; perforated line= 8 repetitions of TG (Kineman *et al.*, 2007); highlighted = location of primers; * = matching bases; - = base missing in the PCR product.

A

Ex2 - Ex3 (Seq. ID 24BA89) - 315 bp



B

>24BA89

```
GCAGTGCTCTCCCGCTCTGGAGCTGCGCTTGCTACTGGTGGCGTCCTGGATGGATTGGCTGCG
GCAGGCTCCAGCTTCCTGAGCTTCTATCACTCTAAAGCCCAGGTCAGTCAGTCTGTCTCCCTA
AGCCCCCTTATCTACCCGATTGGTGTGTGTGTGTGTTCTGGAGCTCTGGGATAACCCCTTTT
CCTTTCCCGCGGACATGTGAATCCAAAACACGCCAGCTACACCGCACTGCCGATCTCGCCAG
AGCAGGCTCCGCCCTTAGTACAGAGACAAATAAC
```

Figure 8.7: Sequencing of the 315 bp band from PCR with primers located on exons 2 and 3 (part 1)

A: chromatograph supplied by GATC Biotech; N indicates unidentified bases (Phred quality score < 10). B: sequence of the PCR product, extracted from the chromatograph.

C

CLUSTAL O (1.2.4) multiple sequence alignment

```

24BA89 -----GCAGTGCTCTCCCGCTCTGGAGCTGCGCTTGCT
Ghrelin GTCATCTGTCCTCACCACCAAGACCATGCTGTCTTCAGGCACCATCTGCAGTTTGCTGCT
                                         ** ** * * * *
24BA89 A-CTGGTGGCGTCCTGGATGGATTGGCTGCGGCAGGCTCCAGCTTCCTGAGCTTCTATCA
Ghrelin ACTCAGCATGCTCTGGATGGACATGGCCATGGCAGGCTCCAGCTTCCTGAGCCCAGAGCA
* * ** * * **** ***** * **
24BA89 CTCTAAAGCCCAGGTCAGTCAGTCTGTCTCCCTAAGCCCCCTTATCTACCCGATTG-GTG
Ghrelin CCAGAAAGCCCAGGTCAGTCAGTCTGTCTCCCTAAGCCCCACATCTACCCGATCTGTG
* ***** ***** * **
24BA89 TGTGTGTGTGTTCTGGAG-CTCTGGGATAACCTCTTTTCCTTTCCCGCGACATGTGAA
Ghrelin TGTGTGTGTGTGAGAGAGAGAGAAAGAGAACCCTCTTTTCCTTTCCAGCAGAGAAAGGAA
***** ** ** ***** ** * * **
24BA89 TCCAAAACACGCCAGCTACACCGCACTGCCGATCTCGCCAGAGCAGGCTCCGCCCTTAG
Ghrelin TCCAAGAAGCCACCAGCTAAACTGCAGCCACGAGCTCTGGAAGGCTGGCTCCACCCAGAG
***** * * ***** ** ** *** ** * ** ***** ** **
24BA89 TACAGAGACAAATAAC
Ghrelin GACAGAGGACAAGCAG
***** ** *

```

Figure 8.7: Sequencing of the 315 bp band from PCR with primers located on exons 2 and 3 (part 2)

C: sequence alignment between the ghrelin gene (mouse) and the PCR product sequence extracted from the chromatograph, using the Clustal Omega program (EBI-EMBL). Underlined= exons; perforated line= 8 repetitions of TG (Kineman *et al.*, 2007); **highlighted** = location of primers; * = matching bases; - = base missing in the PCR product

A

Ex4 - Ex5 (Seq. ID 24BA90) - 924 bp



Figure 8.8: Sequencing of the 924 bp band from PCR with primers located on exons 4 and 5 (part 1)

A: chromatograph supplied by GATC Biotech; N indicates unidentified bases (Phred quality score < 10).

B

>24BA90

```
AACGTACGACTCCTGAGATCAGCTCGGTCTGCCCTGGGGCTTTTCTGCCGGAATCCTCTGTT
ACAGGTCATGGGTGGCTCAATCTGAACTGGACCTGATTGGGGGTATGAAGGATGCAAATTTT
CTCCCCTAGCCCCACTCCTGATGTTCTAATCTTCCTGACTATCTTTGGGGAAGGGTGTGACC
TGGGTGTGTATCAACCCAGGAAAGCTGGATAGCCTGGTCCATCTTCCACAGCCCTGTGTTCCA
GGGATTGTGTTATCTAGCTGTCATGCCCCATCTGACCCTCAGTCCTCTAACTGTGAGGCTGTG
CTGAGGCCTATTTCCGGCATTTCAAATTATCTGGCTTTAAAGCATCTTTACAGTATAACTTC
ACTTCGGGAATCTGTGCCCACTACCCTGAAAACGCCAGCAGACACATAAGGATCTTAGGG
GTTTTTGTGTAGTGTGGGATGAAGACCAAGGCCTCGTGCATTCTGAACAAGCACACTAACA
CTAAGCTGCACCCCTGGTCTTCATTACACTCTGACTTTGTGAAAAGGATACCCAGGCCTTCC
CTGATGGAGAAAGCAAAGATCTCAAGAACAAGTTGCATTCTTTCCCTAAGCACTTCCTCACA
AATATGGCAATCACACATACCTCACGATTCATATCACACAGCAAGATTTGCGGACATCAGGA
CACTCATCCAAGAGCACACTCACATGCCATCTTCCAAATCCAGGCCAGTAACACCCACCCAC
CCATATCACGACTGCTTGCCTCTTGCACACCACGGTGACGACAGTCACTTTTGATGACATGCA
AGATTGTACTAGAACACTGACTTGATCTCTTGCTTGTACATACGCGCCGCTGACACTACGGAG
GAGGAGCATAATAA
```

Figure 8.8: Sequencing of the 924 bp band from PCR with primers located on exons 4 and 5 (part 2)

B: sequence of the PCR product, extracted from the chromatograph.

C

CLUSTAL O (1.2.4) multiple sequence alignment

```

24BA90 -----AACGTACGACTCCTGAGATCAGCTCGGTC
Ghrelin CAATGCTCCCTTCGATGTTGGCATCAAGCTGTGAGGAGCTCAGTATCAGCAGCATGGCCG
                * * * * *
24BA90 GCCCCTGGGGCTTTTCTGC--CGGAATCCTCTGTACAGGTCATGGGTGGCTCAATCTG
Ghrelin GGCCCTGGGGAAAGTTTCTTCAGGATATCCTCTGGGAAGAGGTCAAAGGTGAGTCAATCTG
                * * * * *
24BA90 AACTGGA-CCTGATTGGGGTATGAAGGATGCAAAATTTTCTCCCTAGCCCCACTCCTGA
Ghrelin AAATGGAGCTTAACCTATTTATGAATGATACAAATTTTCTCCCTAGCCCCACTCCTGA
                ** * * * *
24BA90 TGTCTAATCTTCTGACTATCTTTGGGGAAGGTTGTGACCTGGTGTGTATCAACCA
Ghrelin GGTCTAATCTTCTGACTATCTGTGGGGAAGGTTGTGAGCTGGTGTGTAGCAACCA
                *****
24BA90 GGAAAGCTGGATAGCCTGGTCCATCTTCCACAGCCCTGTGTTCCAGGATTGTGTTATCT
Ghrelin GGAAAGCTGGATAGCCAGTCCATCTTCCACAGCCCTGTGTTCCAGGATTGTGTTAGCT
                *****
24BA90 AGCTGTCATGCCCATCTGACCCTCAGTCTCTAACTGTGAGGCTGTGCTGAGGCCTATT
Ghrelin AGCTGTCAGGCCCATCTGAGCCTCAGTCTCTAACTGTGAGGCTGTGCTGAGGCCTATT
                *****
24BA90 TCCGGCATTCAAATTAATCTGGCTTTAAAGCATCTTACAGTATAACTTCACTTCGGGAA
Ghrelin TCCAGCATTCAAATTAATCTGGCTTTAAAGCATCTTACAGTATAACTTCACTTCGGGAA
                ***
24BA90 TCTGTGCCCACTACCACTGAAAACGCCAGCAGACATAAGGATCTTAGGGTTTTTGT
Ghrelin TCTGTGCCCAGTAGCACTGAAAACGCCAGCAGACATAAGGATCTTAGGGTTTTTGT
                *****
24BA90
Ghrelin
24BA90 GTAGTGCTGGGATGAAGACCAAGGCCTCGTGCATTCTGAACAAGCACACTAACACTAAGC
Ghrelin GTAGTGCTGGGATGAAGACCAAGGCCTCGTGCATTCTGAACAAGCACACTAGCCTAAGC
                *****
24BA90 TGCACCCCTGGTCTTCATTACACTCTGACTTTGTGAAAAGGATACCCAGGCGTTTCCTG
Ghrelin TGCACCCCTGGTCTTCAGTACACTCTGACTTTGTGAAAAGGATACCCAGGCGTTTCATG
                *****
24BA90 ATGGAGAAAGCAAAGATCTCAAGAACAAGTTGCATTCTTCCCTAAGCACTTCCTCACAA
Ghrelin ATGGAGAAAGCAAAGATCTCAAGAACAAGTTGCATTCTTCCCTAAGCACTTCCTCACAA
                *****
24BA90 ATATGGCAATCACACATACCTCACGATTCATATCACACAGCAAGATTTGCGGACATCAGG
Ghrelin ATATGGCAATCACACATACCTCACGATTCAGATCAGAAAGCAAGACTTTGGGACACAAAG
                *****
24BA90 ACACCTCATCCAAGAGCACACTCACATGCCATCTTCCAAATCCAGGCCAGTAACACCCAC-
Ghrelin ACACCTCATCCAAGAGCACACTCAAATGCCATCTTCCAAATCCAGGCCAGTAACACCCAC
                *****
24BA90 --CCCACCATATCAGGACTGCTTGCCTCTTGACACACAGGAGGACAGTCACTTTTG
Ghrelin CCCACCCCAATCACGACATGCTTGCCTCTAGCATACCATGGGAAGGAAAGTCACTTTTG
                * * * * *
24BA90 ATGACATGCAAGATTGTACTAGAACACTGACTTGATCTTGTCTTGTCATACGCGCCGCT
Ghrelin ATGACATGCAAGATTGTACTAGAAGACTGACTTGATCTTGTCTTTTCAGAGGCCCGCAGC
                *****
24BA90 GACACTACGGAGGAGGACATAATAA-----
Ghrelin TGACAAGTAACCAAGGACAGGCTGACCCCGTGCTTTCCTTCTCCTGAGCAAGAACTCA
                *** * *
24BA90 -----
Ghrelin CATCCGCC

```

Figure 8.8: Sequencing of the 924 bp band from PCR with primers located on exons 4 and 5 (part 3)

C: sequence alignment between the ghrelin gene (mouse) and the PCR product sequence extracted from the chromatograph, using the Clustal Omega program (EBI-EMBL). Underlined= exons; **highlighted** = location of primers; * = matching bases; - = base missing in the PCR product.

A

Ex 3/4 – Ex5 (Seq. ID 24BA45) – 2088 bp

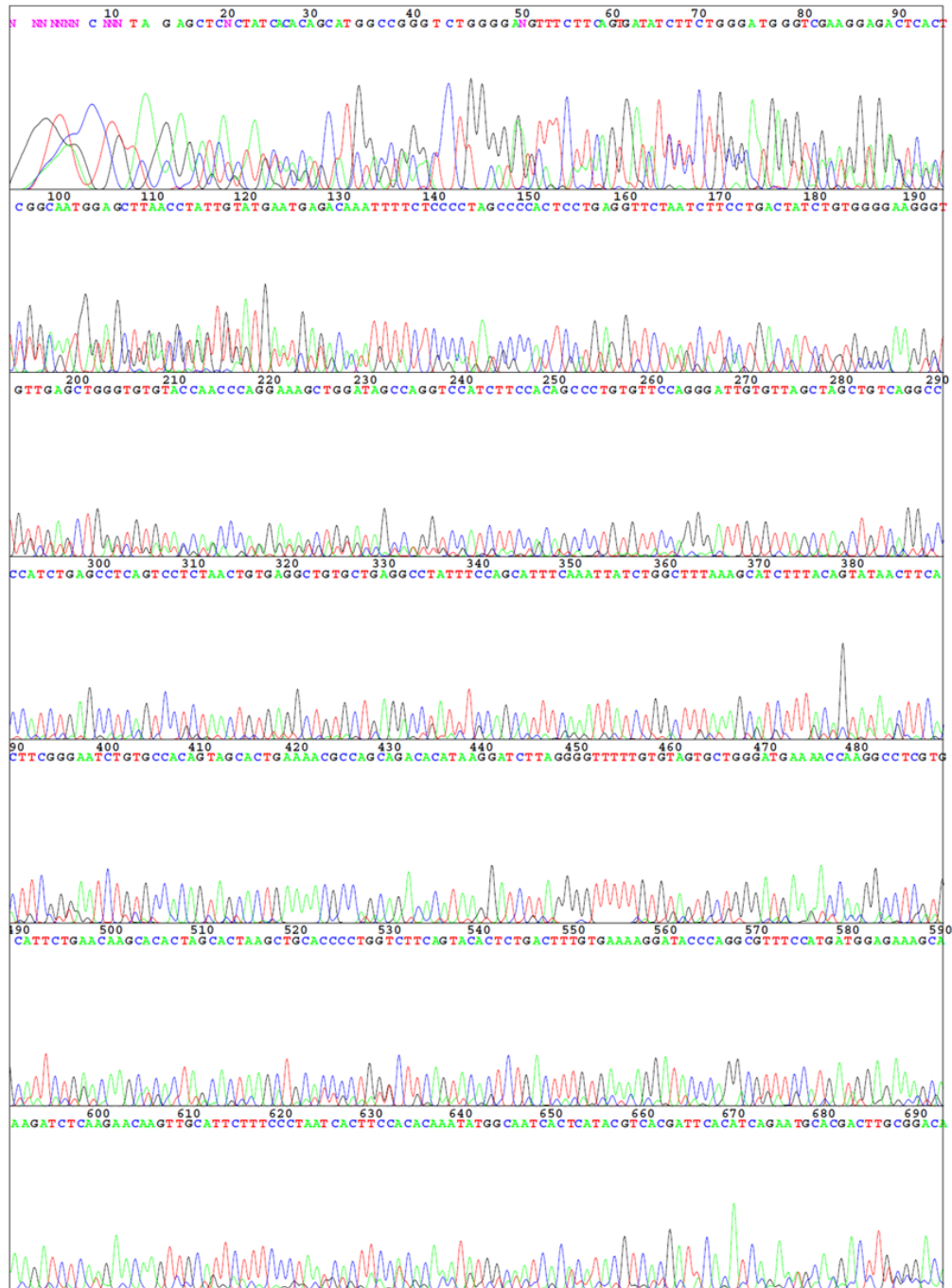


Figure 8.9: Sequencing of the 2088 bp band from PCR with primers located on exons 3/4 and 5 (part 1)

A: chromatograph supplied by GATC Biotech; N indicates unidentified bases (Phred quality score < 10).

B
>24BA45

```
NNNNNNNCNNNTAGAGCTCNCTATCACACAGCATGGCCGGGTCTGGGGANGTTTCTTCAGT
GATATCTTCTGGGATGGGTCTGAAGGAGACTCACTCGGCAATGGAGCTTACCTATTGTATGAA
TGAGACAAATTTTCTCCCCTAGCCCCACTCCTGAGGTTCTAATCTTCCTGACTATCTGTGGGG
AAGGGTGTGAGCTGGGTGTGTACCACCCAGGAAAGCTGGATAGCCAGGTCCATCTTCCACA
GCCCTGTGTTCCAGGGATTGTGTTAGCTAGCTGTCAGGCCCATCTGAGCCTCAGTCCTCTAA
CTGTGAGGCTGTGCTGAGGCCTATTTCCAGCATTTCAAATTATCTGGCTTTAAAGCATCTTT
ACAGTATAACTTCACTTCGGGATCTGTGCCACAGTAGCACTGAAAACGCCAGCAGACACATA
AGGATCTTAGGGGTTTTTGTGTAGTGCTGGGATGAAAACCAAGGCCTCGTGCATTCTGAACA
AGCACACTAGCACTAAGCTGCACCCCTGGTCTTCAGTACACTCTGACTTTGTGAAAAGGATA
CCCAGGCGTTTCCATGATGGAGAAAGCAAAGATCTCAAGAACAAGTTGCATTCTTCCCTAA
TCACTTCCACACAAATATGGCAATCACTCATACGTCACGATTCACATCAGAATGCACGACTT
GCGGACACAAGGACACTCATCNNAGAGCACACTCGAATGCCATCTTCCAAATCCAGGCCAGT
AACACCCACCCACCCCAATCACGACTTGCTTGCTCTNCATACCACGCGAAGGAAAGTCAC
TTTTGATGACATGCAAGATTGTACTAGAAGACTGACTTGATCTCTTGCTTTNAANGGCGCCG
CTGACAGTAACAGGGTNAGGGCCTAAAANNAAA
```

Figure 8.9: Sequencing of the 2088 bp band from PCR with primers located on exons
3/4 and 5 (part 2)

B: sequence of the PCR product, extracted from the chromatograph.

C

CLUSTAL O (1.2.4) multiple sequence alignment

```

24BA45 -----|-----
Ghrelin AGAGGACAAGCAGAAGAGACAGAGGAGGAGCTGGAGATCAGG|TTCAATGCTCCCTTCGAT
                                     |
24BA45 -----NNNNNNNNTAGAGCTCNCCTATCACACAGCATGGCCGGGTCTGGGGANGTTT
Ghrelin GTTCAGCATCAAGCTGTCAGGAGCTCAGTATCAGCAGCATGGCCGGGCCCTGGGGAAGTTT
                *****   * * *   *****   * * *
24BA45 CTTCAGTGATATCTTCTGGGATGGGTCTGAAGGAGACTCACTCGGCAATGGA-GCTTACCT
Ghrelin CTTCAGGATATCCTCTGGGAAGAGTCAAAGGTGAGTCAATCTGAAATGGAGCTTAACCT
                *****   * * *   *****   * * *
24BA45 ATTGTATGAATGAGACAAATTTTCTCCCTAGCCCCACTCCTGAGGTTCTAATCTTCCTG
Ghrelin ATTTTATGAATGATACAAATTTTCTCCCTAGCCCCACTCCTGAGGTTCTAATCTTCCTG
                ***   *****   *****   *****   *****   *****
24BA45 ACTATCTGTGGGAAGGGTGTGAGCTGGGTGTACCA-CCCAGGAAAGCTGGATAGCC
Ghrelin ACTATCTGTGGGAAGGGTGTGAGCTGGGTGTAGCAACCAGGAAAGCTGGATAGCC
                *****   *****   *****   *****
24BA45 AGGTCCATCTTCCACAGCCCTGTGTTCCAGGATTGTGTTAGCTAGCTGTCAGGCCCAT
Ghrelin AGGTCCATCTTCCACAGCCCTGTGTTCCAGGATTGTGTTAGCTAGCTGTCAGGCCCAT
                *****
24BA45 CTGAGCCTCAGTCTTAACTGTGAGGCTGTGCTGAGGCCATTTCCAGCATTTCAAATT
Ghrelin CTGAGCCTCAGTCTTAACTGTGAGGCTGTGCTGAGGCCATTTCCAGCATTTCAAATT
                *****
24BA45 ATCTGGCTTTAAAGCATCTTTACAGTATAACTTCACTTCGG-GATCTGTGCCAGTAGC
Ghrelin ATCTGGCTTTAAAGCATCTTTACAGTATAACTTCACTTCGGGAATCTGTGCCAGTAGC
                *****
24BA45 ACTGAAAACGCCAGCAGACACATAAGGATCTTAGGGGTTTTTGTGTAGTGCTGGGATGAA
Ghrelin ACTGAAAACGCCAGCAGACACATAAGGATCTTAGGGGTTTTTGTGTAGTGCTGGGATGAA
                *****
24BA45 AACCAAGGCCTCGTGCAATCTGAACAAGCACACTAGCACTAAGCTGCACCCCTGGCTTC
Ghrelin GACCAAGGCCTCGTGCAATCTGAACAAGCACACTAGCACTAAGCTGCACCCCTGGCTTC
                *****
24BA45 AGTACACTCTGACTTGTGAAAAGGATACCCAGGCGTTTCCATGATGGAGAAAGCAAAGA
Ghrelin AGTACACTCTGACTTGTGAAAAGGATACCCAGGCGTTTCCATGATGGAGAAAGCAAAGA
                *****
24BA45 TCTCAAGAACAAGTTGCATTCTTCCCTAATCACTTCCACACAAATATGGCAATCACTCA
Ghrelin TCTCAAGAACAAGTTGCATTCTTCCCTAATCACTTCCACACAAATATGGCAATCACTCA
                *****
24BA45 TACGTCACGATTCACATCAGAAATGCAGACTTGCGGACACAAGGACACTCATCENAGAGC
Ghrelin TACGTCACGATTCACATCAGAAATGCAGACTTGCGGACACAAGGACACTCATCENAGAGC
                *****
24BA45 ACACTCGAATGCCATCTTCCAAATCCAGG-CCAGTAACACCCACCCCAATCAGG
Ghrelin ACACTCGAATGCCATCTTCCAAATCCAGG-CCAGTAACACCCACCCCAATCAGG
                *****
24BA45 ACTTGCTTGCCCTCT-NCATACCACGCGAAGGAAAGTCACTTTTGATGACATGCAAGATTG
Ghrelin ACTTGCTTGCCCTCT-NCATACCACGCGAAGGAAAGTCACTTTTGATGACATGCAAGATTG
                *****
24BA45 TACTAGAAGACTGACTTGATCTCTTGCTTTNAANGGCGCGCTGACAGTAACAGGGTNAG
Ghrelin TACTAGAAGACTGACTTGATCTCTTGCTTTNAANGGCGCGCTGACAGTAACAGGGTNAG
                *****

```

Figure 8.9: Sequencing of the 2088 bp band from PCR with primers located on exons 3/4 and 5 (part 3)

C: sequence alignment between the ghrelin gene (mouse) and the PCR product sequence extracted from the chromatograph, using the Clustal Omega program (EBI-EMBL). Underlined= exons; |: junction between exon 3 and exon 4; * = matching bases; - = base missing in the PCR product.

Chapter 9 – References

Abbott, M.J., Roth, T.M., Ho, L., Wang, L., O'Carroll, D. and Nissenson, R.A., (2015) Negative Skeletal Effects of Locally Produced Adiponectin. *PLoS ONE*, 107, p.e0134290.

Abdallah, B.M., Haack-Sørensen, M., Burns, J.S., Elsnab, B., Jakob, F., Hokland, P. and Kassem, M., (2005) Maintenance of differentiation potential of human bone marrow mesenchymal stem cells immortalized by human telomerase reverse transcriptase gene despite of extensive proliferation. *Biochemical and Biophysical Research Communications*, 3263, pp.527–538.

Abdallah, B.M., Haack-Sørensen, M., Fink, T. and Kassem, M., (2006) Inhibition of osteoblast differentiation but not adipocyte differentiation of mesenchymal stem cells by sera obtained from aged females. *Bone*, 391, pp.181–188.

Abdanipour, A., Shahsavandi, B., Alipour, M. and Feizi, H., (2018) Ghrelin Upregulates Hoxb4 Gene Expression in Rat Bone Marrow Stromal Cells. *Cell Journal*, 202, pp.183–187.

Adams, D.S. and Levin, M., (2013) Endogenous voltage gradients as mediators of cell-cell communication: strategies for investigating bioelectrical signals during pattern formation. *Cell and Tissue Research*, 3521, pp.95–122.

Akune, T., Ohba, S., Kamekura, S., Yamaguchi, M., Chung, U., Kubota, N., Terauchi, Y., Harada, Y., Azuma, Y., Nakamura, K., Kadowaki, T. and Kawaguchi, H., (2004) PPAR γ insufficiency enhances osteogenesis through osteoblast formation from bone marrow progenitors. *Journal of Clinical Investigation*, 1136, pp.846–855.

Alamri, B.N., Shin, K., Chappe, V. and Anini, Y., (2016) The role of ghrelin in the regulation of glucose homeostasis. *Hormone Molecular Biology and Clinical Investigation*, 261, pp.3–11.

Alexander, S., Mathie, A. and Peters, J., (2011a) Ion Channels. *British Journal of Pharmacology*, 164, pp.S137–S174.

Alexander SPH, Mathie A and Peters JA, (2011b) Guide to Receptors and Channels (GRAC), 5th edition. *British Journal of Pharmacology*, 164s1, pp.S1–S2.

- Alexander Stephen PH, Striessnig Jörg, Kelly Eamonn, Marrion Neil V, Peters John A, Faccenda Elena, Harding Simon D, Pawson Adam J, Sharman Joanna L, Southan Christopher, Davies Jamie A and null null, (2017) THE CONCISE GUIDE TO PHARMACOLOGY 2017/18: Voltage-gated ion channels. *British Journal of Pharmacology*, 174S1, pp.S160–S194.
- Ali, A.T., Hochfeld, W.E., Myburgh, R. and Pepper, M.S., (2013) Adipocyte and adipogenesis. *European Journal of Cell Biology*, 926–7, pp.229–236.
- An, J., Yang, H., Zhang, Q., Liu, C., Zhao, J., Zhang, L. and Chen, B., (2016) Natural products for treatment of osteoporosis: The effects and mechanisms on promoting osteoblast-mediated bone formation. *Life Sciences*, 147Supplement C, pp.46–58.
- Ashcroft, F.M., (2005) ATP-sensitive potassium channelopathies: focus on insulin secretion. *Journal of Clinical Investigation*, 1158, pp.2047–2058.
- Aubin, J.E. and Triffitt, J.T., (n.d.) Mesenchymal stem cells and osteoblast differentiation. In: *Principles of Bone Biology (Second Edition)*. San Diego: Academic Press, pp.59–81.
- Babenko, A.P., Gonzalez, G. and Bryan, J., (2000) Pharmacology of Sulfonylurea Receptors SEPARATE DOMAINS OF THE REGULATORY SUBUNITS OF K⁺ ATP CHANNEL ISOFORMS ARE REQUIRED FOR SELECTIVE INTERACTION WITH K⁺ CHANNEL OPENERS. *Journal of Biological Chemistry*, 275, pp.717–720.
- Banks, W.A., Tschöp, M., Robinson, S.M. and Heiman, M.L., (2002) Extent and Direction of Ghrelin Transport Across the Blood-Brain Barrier Is Determined by Its Unique Primary Structure. *Journal of Pharmacology and Experimental Therapeutics*, 302, pp.822–827.
- Bailey, A.R., von Engelhardt, N., Von Engelhardt, N., Leng, G., Smith, R.G. and Dickson, S.L., (2000) Growth hormone secretagogue activation of the arcuate nucleus and brainstem occurs via a non-noradrenergic pathway. *Journal of Neuroendocrinology*, 123, pp.191–197.
- Barradas, A.M.C., Fernandes, H.A.M., Groen, N., Chai, Y.C., Schrooten, J., van de Peppel, J., van Leeuwen, J.P.T.M., van Blitterswijk, C.A. and de Boer, J., (2012) A calcium-induced signaling cascade leading to osteogenic differentiation of human bone marrow-derived mesenchymal stromal cells. *Biomaterials*, 33, pp.3205–3215.

- Bartl, R. and Bartl, C., (2017) Subgroups of Osteoporosis. In: *Bone Disorders*. [online] Springer, Cham, pp.115–121. Available at: https://link.springer.com/chapter/10.1007/978-3-319-29182-6_19 [Accessed 2 Aug. 2018].
- Benayahu, D., Peled, A. and Zipori, D., (1994) Myeloblastic cell line expresses osteoclastic properties following coculture with marrow stromal adipocytes. *Journal of Cellular Biochemistry*, 563, pp.374–384.
- Berendsen, A.D. and Olsen, B.R., (2014) Osteoblast–adipocyte lineage plasticity in tissue development, maintenance and pathology. *Cellular and Molecular Life Sciences*, 713, pp.493–497.
- Beresford, J.N., Bennett, J.H., Devlin, C., Leboy, P.S. and Owen, M.E., (1992) Evidence for an inverse relationship between the differentiation of adipocytic and osteogenic cells in rat marrow stromal cell cultures. *Journal of Cell Science*, 1022, pp.341–351.
- Best, L., Brown, P.D., Sener, A. and Malaisse, W.J., (2010) Electrical activity in pancreatic islet cells: The VRAC hypothesis. *Islets*, 22, pp.59–64.
- Bethel, M., Chitteti, B.R., Srour, E.F. and Kacena, M.A., (2013) The Changing Balance Between Osteoblastogenesis and Adipogenesis in Aging and its Impact on Hematopoiesis. *Current osteoporosis reports*, 112, pp.99–106.
- Bianco, P., Riminucci, M., Gronthos, S. and Robey, P.G., (2001) Bone Marrow Stromal Stem Cells: Nature, Biology, and Potential Applications. *STEM CELLS*, 193, pp.180–192.
- Bianco, P., Robey, P.G. and Simmons, P.J., (2008) Mesenchymal Stem Cells: Revisiting History, Concepts, and Assays. *Cell Stem Cell*, 24, pp.313–319.
- Binggeli, R. and Weinstein, R.C., (1986) Membrane potentials and sodium channels: Hypotheses for growth regulation and cancer formation based on changes in sodium channels and gap junctions. *Journal of Theoretical Biology*, 1234, pp.377–401.
- Bitar, M., Brown, R.A., Salih, V., Kidane, A.G., Knowles, J.C. and Nazhat, S.N., (2008) Effect of Cell Density on Osteoblastic Differentiation and Matrix Degradation of Biomimetic Dense Collagen Scaffolds. *Biomacromolecules*, 91, pp.129–135.

- Björninen, M., Siljander, A., Pelto, J., Hyttinen, J., Kellomäki, M., Miettinen, S., Seppänen, R. and Haimi, S., (2014) Comparison of Chondroitin Sulfate and Hyaluronic Acid Doped Conductive Polypyrrole Films for Adipose Stem Cells. *Annals of Biomedical Engineering*, 429, pp.1889–1900.
- Blackiston, D.J., McLaughlin, K.A. and Levin, M., (2009) Bioelectric controls of cell proliferation: ion channels, membrane voltage and the cell cycle. *Cell Cycle (Georgetown, Tex.)*, 821, pp.3527–3536.
- Blair, H.C., Robinson, L.J. and Zaidi, M., (2005) Osteoclast signalling pathways. *Biochemical and Biophysical Research Communications*, 3283, pp.728–738.
- Boskey, A.L. and Coleman, R., (2010) Aging and bone. *Journal of Dental Research*, 8912, pp.1333–1348.
- Bozec, A. and Hannemann, N., (2016) Mechanism of Regulation of Adipocyte Numbers in Adult Organisms Through Differentiation and Apoptosis Homeostasis. *Journal of Visualized Experiments : JoVE*, [online] 112. Available at: <https://www.ncbi.nlm.nih.gov/pmc/articles/PMC4927764/> [Accessed 28 Aug. 2018].
- Brennan-Speranza, T.C. and Conigrave, A.D., (2015) Osteocalcin: An Osteoblast-Derived Polypeptide Hormone that Modulates Whole Body Energy Metabolism. *Calcified Tissue International*, 961, pp.1–10.
- Briot, K. and Roux, C., (2015) Glucocorticoid-induced osteoporosis. *RMD Open*, [online] 11. Available at: <http://www.ncbi.nlm.nih.gov/pmc/articles/PMC4613168/>.
- Brown, R.C., Hopkins, A.L., Lewis, C.L., Guschina, I.A., Davies, J.S., Christian, H.C. and Wells, T., (2014) Unacylated ghrelin promotes adipogenesis in rodent bone marrow via the action of ghrelin o-acyl transferase and the growth hormone secretagogue receptor. *Proceedings of The Physiological Society*, [online] Proc Physiol Soc 32. Available at: <http://www.physoc.org/proceedings/abstract/Proc%20Physiol%20Soc%2032PC030> [Accessed 11 Feb. 2016].
- Cai, R., Nakamoto, T., Hoshiba, T., Kawazoe, N. and Chen, G., (2014) Control of Simultaneous Osteogenic and Adipogenic Differentiation of Mesenchymal Stem Cells. *Journal of Stem Cell Research & Therapy*, 48, pp.1–9.

- Callaghan, B. and Furness, J.B., (2014) Novel and Conventional Receptors for Ghrelin, Desacyl-Ghrelin, and Pharmacologically Related Compounds. *Pharmacological Reviews*, 664, pp.984–1001.
- Camiña, J.P., (2006) Cell Biology of the Ghrelin Receptor. *Journal of Neuroendocrinology*, 181, pp.65–76.
- Capiod, T., (2011) Cell proliferation, calcium influx and calcium channels. *Biochimie*, 9312, pp.2075–2079.
- Cawthorn, W.P., Scheller, E.L., Learman, B.S., Parlee, S.D., Simon, B.R., Mori, H., Ning, X., Bree, A.J., Schell, B., Broome, D.T., Soliman, S.S., DelProposto, J.L., Lumeng, C.N., Mitra, A., Pandit, S.V., Gallagher, K.A., Miller, J.D., Krishnan, V., Hui, S.K., Bredella, M.A., Fazeli, P.K., Klibanski, A., Horowitz, M.C., Rosen, C.J. and MacDougald, O.A., (2014) Bone Marrow Adipose Tissue Is an Endocrine Organ that Contributes to Increased Circulating Adiponectin during Caloric Restriction. *Cell Metabolism*, 202, pp.368–375.
- Cheng, S.L., Yang, J.W., Rifas, L., Zhang, S.F. and Avioli, L.V., (1994) Differentiation of human bone marrow osteogenic stromal cells in vitro: induction of the osteoblast phenotype by dexamethasone. *Endocrinology*, 1341, pp.277–286.
- Choi, H.J., Ki, K.H., Yang, J.-Y., Jang, B.Y., Song, J.A., Baek, W.-Y., Kim, J.H., An, J.H., Kim, S.W., Kim, S.Y., Kim, J.-E. and Shin, C.S., (2013) Chronic Central Administration of Ghrelin Increases Bone Mass through a Mechanism Independent of Appetite Regulation. *PLoS ONE*, 87, p.e65505.
- Choi, K., Roh, S.-G., Hong, Y.-H., Shrestha, Y.B., Hishikawa, D., Chen, C., Kojima, M., Kangawa, K. and Sasaki, S.-I., (2003) The Role of Ghrelin and Growth Hormone Secretagogues Receptor on Rat Adipogenesis. *Endocrinology*, 1443, pp.754–759.
- Chubinskiy-Nadezhdin, V.I., Vasileva, V.Y., Pugovkina, N.A., Vassilieva, I.O., Morachevskaya, E.A., Nikolsky, N.N. and Negulyaev, Y.A., (2017) Local calcium signalling is mediated by mechanosensitive ion channels in mesenchymal stem cells. *Biochemical and Biophysical Research Communications*, 4824, pp.563–568.
- Clemens, T.L. and Karsenty, G., (2011) The osteoblast: An insulin target cell controlling glucose homeostasis. *Journal of Bone and Mineral Research*, 264, pp.677–680.
- Clunie, G. and Keen, R.W., (2014) *Osteoporosis*. Oxford University Press.

Chapter 9 – References

- Cock, T.-A., Back, J., Elefteriou, F., Karsenty, G., Kastner, P., Chan, S. and Auwerx, J., (2004) Enhanced bone formation in lipodystrophic PPAR γ hyp/hyp mice relocates haematopoiesis to the spleen. *EMBO Reports*, 510, pp.1007–1012.
- Colaïanni, G., (2014) Osteoporosis and obesity: Role of Wnt pathway in human and murine models. *World Journal of Orthopedics*, 53, p.242.
- Compston, J.E., Flahive, J., Hosmer, D.W., Watts, N.B., Siris, E.S., Silverman, S., Saag, K.G., Roux, C., Rossini, M., Pfeilschifter, J., Nieves, J.W., Netelenbos, J.C., March, L., LaCroix, A.Z., Hooven, F.H., Greenspan, S.L., Gehlbach, S.H., Díez-Pérez, A., Cooper, C., Chapurlat, R.D., Boonen, S., Anderson, F.A., Adami, S. and Adachi, J.D., (2014) Relationship of Weight, Height, and Body Mass Index with Fracture Risk at Different Sites in Postmenopausal Women: The Global Longitudinal study of Osteoporosis in Women (GLOW). *Journal of bone and mineral research: the official journal of the American Society for Bone and Mineral Research*, 292, pp.487–493.
- Contador, D., Ezquer, F., Espinosa, M., Arango-Rodriguez, M., Puebla, C., Sobrevia, L. and Conget, P., (2015) Featured Article: Dexamethasone and rosiglitazone are sufficient and necessary for producing functional adipocytes from mesenchymal stem cells. *Experimental Biology and Medicine*, 2409, pp.1235–1246.
- Corre, J., Planat-Benard, V., Corberand, J.X., Pénicaud, L., Casteilla, L. and Laharrague, P., (2004) Human bone marrow adipocytes support complete myeloid and lymphoid differentiation from human CD34+ cells. *British Journal of Haematology*, 1273, pp.344–347.
- Costa, J.L., Naot, D., Lin, J.-M., Watson, M., Callon, K.E., Reid, I.R., Grey, A.B. and Cornish, J., (2011) Ghrelin is an Osteoblast Mitogen and Increases Osteoclastic Bone Resorption In Vitro. *International Journal of Peptides*, 2011, p.e605193.
- Datta, H.K., Ng, W.F., Walker, J.A., Tuck, S.P. and Varanasi, S.S., (2008) The cell biology of bone metabolism. *Journal of Clinical Pathology*, 615, pp.577–587.
- Davenport, A.P., Bonner, T.I., Foord, S.M., Harmar, A.J., Neubig, R.R., Pin, J.-P., Spedding, M., Kojima, M. and Kangawa, K., (2005) International Union of Pharmacology. LVI. Ghrelin Receptor Nomenclature, Distribution, and Function. *Pharmacological Reviews*, 574, pp.541–546.

- David, C.J. and Manley, J.L., (2010) Alternative pre-mRNA splicing regulation in cancer: pathways and programs unhinged. *Genes & Development*, 2421, pp.2343–2364.
- Davies, J.S., Kotokorpi, P., Eccles, S.R., Barnes, S.K., Tokarczuk, P.F., Allen, S.K., Whitworth, H.S., Guschina, I.A., Evans, B.A.J., Mode, A., Zigman, J.M. and Wells, T., (2009) Ghrelin Induces Abdominal Obesity Via GHS-R-Dependent Lipid Retention. *Molecular Endocrinology*, 236, pp.914–924.
- De Vriese, C., Gregoire, F., Lema-Kisoka, R., Waelbroeck, M., Robberecht, P. and Delporte, C., (2004) Ghrelin Degradation by Serum and Tissue Homogenates: Identification of the Cleavage Sites. *Endocrinology*, 14511, pp.4997–5005.
- Delhanty, P.J.D., van der Eerden, B.C.J. and van Leeuwen, J.P.T.M., (2014a) Ghrelin and bone. *BioFactors*, 401, pp.41–48.
- Delhanty, P.J.D., Eerden, B.C.J. van der, Velde, M. van der, Gauna, C., Pols, H. a. P., Jahr, H., Chiba, H., Lely, A.J. van der and Leeuwen, J.P.T.M. van, (2006) Ghrelin and unacylated ghrelin stimulate human osteoblast growth via mitogen-activated protein kinase (MAPK)/phosphoinositide 3-kinase (PI3K) pathways in the absence of GHS-R1a. *Journal of Endocrinology*, 1881, pp.37–47.
- Delhanty, P.J.D., Neggers, S.J. and Lely, A.J. van der, (2012) Mechanisms in Endocrinology: Ghrelin: the differences between acyl- and des-acyl ghrelin. *European Journal of Endocrinology*, 1675, pp.601–608.
- Delhanty, P.J.D., van der Velde, M., van der Eerden, B.C.J., Sun, Y., Geminn, J.M.M., van der Lely, A.-J., Smith, R.G. and van Leeuwen, J.P.T.M., (2014b) Genetic Manipulation of the Ghrelin Signaling System in Male Mice Reveals Bone Compartment Specificity of Acylated and Unacylated Ghrelin in the Regulation of Bone Remodeling. *Endocrinology*, 15511, pp.4287–4295.
- Delporte, C., (2013) Structure and Physiological Actions of Ghrelin. *Scientifica*, *Scientifica*, 2013, 2013, p.e518909.
- Deng, F., Ling, J., Ma, J., Liu, C. and Zhang, W., (2008) Stimulation of intramembranous bone repair in rats by ghrelin. *Experimental Physiology*, 937, pp.872–879.

- Deng, X.L., Lau, C.P., Lai, K., Cheung, K.F., Lau, G.K. and Li, G.R., (2007) Cell cycle-dependent expression of potassium channels and cell proliferation in rat mesenchymal stem cells from bone marrow. *Cell Proliferation*, 405, pp.656–670.
- Dezaki, K., Hosoda, H., Kakei, M., Hashiguchi, S., Watanabe, M., Kangawa, K. and Yada, T., (2004) Endogenous Ghrelin in Pancreatic Islets Restricts Insulin Release by Attenuating Ca²⁺ Signaling in β -Cells Implication in the Glycemic Control in Rodents. *Diabetes*, 5312, pp.3142–3151.
- Dezaki, K., Kakei, M. and Yada, T., (2007) Ghrelin Uses Gai2 and Activates Voltage-Dependent K⁺ Channels to Attenuate Glucose-Induced Ca²⁺ Signaling and Insulin Release in Islet β -Cells Novel Signal Transduction of Ghrelin. *Diabetes*, 569, pp.2319–2327.
- Díaz-Lezama, N., Hernández-Elvira, M., Sandoval, A., Monroy, A., Felix, R. and Monjaraz, E., (2010) Ghrelin inhibits proliferation and increases T-type Ca²⁺ channel expression in PC-3 human prostate carcinoma cells. *Biochemical and Biophysical Research Communications*, 4031, pp.24–29.
- Diehlmann, A., Bork, S., Saffrich, R., Veh, R.W., Wagner, W. and Derst, C., (2011) KATP channels in mesenchymal stromal stem cells: strong up-regulation of Kir6.2 subunits upon osteogenic differentiation. *Tissue & Cell*, 435, pp.331–336.
- Dixit, V.D., Yang, H., Sun, Y., Weeraratna, A.T., Youm, Y.-H., Smith, R.G. and Taub, D.D., (2007) Ghrelin promotes thymopoiesis during aging. *Journal of Clinical Investigation*, 11710, pp.2778–2790.
- Dong, W. and Day, R., (2013) Gene Expression of Proprotein Convertases in Individual Rat Anterior Pituitary Cells and Their Regulation in Corticotrophs Mediated by Glucocorticoids. *Endocrinology*. [online] Available at: http://press.endocrine.org/doi/10.1210/endo.143.1.8570?url_ver=Z39.88-2003&rfr_id=ori:rid:crossref.org&rfr_dat=cr_pub%3dpubmed [Accessed 23 Sep. 2015].
- Dorheim, M.-A., Sullivan, M., Dandapani, V., Wu, X., Hudson, J., Segarini, P.R., Rosen, D.M., Aulthouse, A.L. and Gimble, J.M., (1993) Osteoblastic gene expression during adipogenesis in hematopoietic supporting murine bone marrow stromal cells. *Journal of Cellular Physiology*, 1542, pp.317–328.

Chapter 9 – References

- Duan, D., Winter, C., Cowley, S., Hume, J.R. and Horowitz, B., (1997) Molecular identification of a volume-regulated chloride channel. *Nature*, 3906658, pp.417–421.
- Ducy, P., Zhang, R., Geoffroy, V., Ridall, A.L. and Karsenty, G., (1997) *Osf2/Cbfa1*: A Transcriptional Activator of Osteoblast Differentiation. *Cell*, 895, pp.747–754.
- Duque, G., (2007) As a matter of fat: New perspectives on the understanding of age-related bone loss. *BoneKEy-Osteovision*, 44, pp.129–140.
- Evans, B.A.J., Bull, M.J., Kench, R.C., Fox, R.E., Morgan, L.D., Stevenson, A.E., Gevers, E.F., Perry, M.J. and Wells, T., (2011) The influence of leptin on trabecular architecture and marrow adiposity in GH-deficient rats. *Journal of Endocrinology*, 2081, pp.69–79.
- Ferron, M., Hinoi, E., Karsenty, G. and Ducy, P., (2008) Osteocalcin differentially regulates β cell and adipocyte gene expression and affects the development of metabolic diseases in wild-type mice. *Proceedings of the National Academy of Sciences of the United States of America*, 10513, pp.5266–5270.
- Ferron, M., Wei, J., Yoshizawa, T., Fattore, A.D., DePinho, R.A., Teti, A., Ducy, P. and Karsenty, G., (2010) Insulin Signaling in Osteoblasts Integrates Bone Remodeling and Energy Metabolism. *Cell*, 1422, pp.296–308.
- Fischer, M., Janssen, A.G.H. and Fahlke, C., (2010) Barttin Activates ClC-K Channel Function by Modulating Gating. *Journal of the American Society of Nephrology*, 218, pp.1281–1289.
- Florencio-Silva, R., Sasso, G.R. da S., Sasso-Cerri, E., Simões, M.J. and Cerri, P.S., (2015) Biology of Bone Tissue: Structure, Function, and Factors That Influence Bone Cells. *BioMed Research International*, [online] 2015. Available at: <https://www.ncbi.nlm.nih.gov/pmc/articles/PMC4515490/>.
- Frost, H.M., (2001) Why should many skeletal scientists and clinicians learn the Utah paradigm of skeletal physiology? *J Musculoskelet Neuronal Interact*, 2, pp.121–130.
- Fukushima, N., Hanada, R., Teranishi, H., Fukue, Y., Tachibana, T., Ishikawa, H., Takeda, S., Takeuchi, Y., Fukumoto, S., Kangawa, K., Nagata, K. and Kojima, M., (2005) Ghrelin directly regulates bone formation. *Journal of Bone and Mineral Research: The Official Journal of the American Society for Bone and Mineral Research*, 205, pp.790–798.

Chapter 9 – References

- Fulzele, K., Riddle, R.C., Cao, X., Wan, C., Chen, D., Faugere, M.-C., Aja, S., Hussain, M.A., Brüning, J.C. and Clemens, T.L., (2010) Insulin receptor signaling in osteoblasts regulates postnatal bone acquisition and body composition. *Cell*, 1422, pp.309–319.
- Gabrielsson, B.G., Karlsson, A.C., Lönn, M., Olofsson, L.E., Johansson, J.M., Torgerson, J.S., Sjöström, L., Carlsson, B., Edén, S. and Carlsson, L.M.S., (2004) Molecular characterization of a local sulfonylurea system in human adipose tissue. *Molecular and Cellular Biochemistry*, 2581–2, pp.65–71.
- Gahete, M.D., Córdoba-Chacón, J., Hergueta-Redondo, M., Martínez-Fuentes, A.J., Kineman, R.D., Moreno-Bueno, G., Luque, R.M. and Castaño, J.P., (2011) A Novel Human Ghrelin Variant (In1-Ghrelin) and Ghrelin-O-Acyltransferase Are Overexpressed in Breast Cancer: Potential Pathophysiological Relevance. *PLoS ONE*, 68, p.e23302.
- Gahete, M.D., Córdoba-Chacón, J., Salvatori, R., Castaño, J.P., Kineman, R.D. and Luque, R.M., (2010) Metabolic regulation of ghrelin O-acyl transferase (GOAT) expression in the mouse hypothalamus, pituitary, and stomach. *Molecular and Cellular Endocrinology*, 3171–2, pp.154–160.
- Gao, B., Huang, Q., Lin, Y.-S., Wei, B.-Y., Guo, Y.-S., Sun, Z., Wang, L., Fan, J., Zhang, H.-Y., Han, Y.-H., Li, X.-J., Shi, J., Liu, J., Yang, L. and Luo, Z.-J., (2014) Dose-Dependent Effect of Estrogen Suppresses the Osteo-Adipogenic Transdifferentiation of Osteoblasts via Canonical Wnt Signaling Pathway. *PLOS ONE*, 96, p.e99137.
- Ge, L., Hoa, N.T., Wilson, Z., Arismendi-Morillo, G., Kong, X.-T., Tajhya, R.B., Beeton, C. and Jadus, M.R., (2014) Big Potassium (BK) ion channels in biology, disease and possible targets for cancer immunotherapy. *International Immunopharmacology*, 222, pp.427–443.
- Ghali, O., Broux, O., Falgayrac, G., Haren, N., van Leeuwen, J.P., Penel, G., Hardouin, P. and Chauveau, C., (2015) Dexamethasone in osteogenic medium strongly induces adipocyte differentiation of mouse bone marrow stromal cells and increases osteoblast differentiation. *BMC Cell Biology*, [online] 16. Available at: <http://www.ncbi.nlm.nih.gov/pmc/articles/PMC4359404/> [Accessed 11 Jan. 2016].
- Gimble, J.M., (2011) Leptin's balancing act between bone and fat. *Journal of Bone and Mineral Research*, 268, pp.1694–1697.

Gimble, J.M., Morgan, C., Kelly, K., Wu, X., Dandapani, V., Wang, C.-S. and Rosen, V., (1995) Bone morphogenetic proteins inhibit adipocyte differentiation by bone marrow stromal cells. *Journal of Cellular Biochemistry*, 583, pp.393–402.

Giovambattista, A., Gaillard, R.C. and Spinedi, E., (2007) Ghrelin Gene-Related Peptides Modulate Rat White Adiposity. In: B.-V.& Hormones, ed., Ghrelin. [online] Academic Press, pp.171–205. Available at: <http://www.sciencedirect.com/science/article/pii/S008367290677008X> [Accessed 7 Feb. 2016].

Gloyn, A.L., Pearson, E.R., Antcliff, J.F., Proks, P., Bruining, G.J., Slingerland, A.S., Howard, N., Srinivasan, S., Silva, J.M.C.L., Molnes, J., Edghill, E.L., Frayling, T.M., Temple, I.K., Mackay, D., Shield, J.P.H., Sumnik, Z., van Rhijn, A., Wales, J.K.H., Clark, P., Gorman, S., Aisenberg, J., Ellard, S., Njølstad, P.R., Ashcroft, F.M. and Hattersley, A.T., (2004) Activating Mutations in the Gene Encoding the ATP-Sensitive Potassium-Channel Subunit Kir6.2 and Permanent Neonatal Diabetes. *New England Journal of Medicine*, 35018, pp.1838–1849.

Gnanapavan, S., Kola, B., Bustin, S.A., Morris, D.G., McGee, P., Fairclough, P., Bhattacharya, S., Carpenter, R., Grossman, A.B. and Korbonits, M., (2002) The Tissue Distribution of the mRNA of Ghrelin and Subtypes of Its Receptor, GHS-R, in Humans. *The Journal of Clinical Endocrinology & Metabolism*, 876, pp.2988–2991.

Goldstein, M.F., Fallon, J.J. and Harning, R., (1999) Chronic Glucocorticoid Therapy-Induced Osteoporosis in Patients With Obstructive Lung Disease. *Chest*, 1166, pp.1733–1749.

Goujon, M., McWilliam, H., Li, W., Valentin, F., Squizzato, S., Paern, J. and Lopez, R., (2010) A new bioinformatics analysis tools framework at EMBL–EBI. *Nucleic Acids Research*, 38suppl_2, pp.W695–W699.

Grabauskas, G., Wu, X., Lu, Y., Heldsinger, A., Song, I., Zhou, S.-Y. and Owyang, C., (2015) KATP channels in the nodose ganglia mediate the orexigenic actions of ghrelin. *The Journal of Physiology*, 59317, pp.3973–3989.

Greco, E.A., Lenzi, A. and Migliaccio, S., (2015) The obesity of bone. *Therapeutic Advances in Endocrinology and Metabolism*, 66, pp.273–286.

Chapter 9 – References

- Gregoire, F.M., (2001) Adipocyte differentiation: from fibroblast to endocrine cell. *Experimental Biology and Medicine (Maywood, N.J.)*, 22611, pp.997–1002.
- Gribble Fiona M., Tucker Stephen J. and Ashcroft Frances M., (1997) The essential role of the Walker A motifs of SUR1 in K-ATP channel activation by Mg-ADP and diazoxide. *The EMBO Journal*, 166, pp.1145–1152.
- Gu, Y., Preston, M.R., El Haj, A.J., Howl, J.D. and Publicover, S.J., (2001a) Three types of K⁺ currents in murine osteocyte-like cells (MLO-Y4). *Bone*, 281, pp.29–37.
- Gu, Y., Preston, M.R., Magnay, J., El Haj, A.J. and Publicover, S.J., (2001b) Hormonally-Regulated Expression of Voltage-Operated Ca²⁺ Channels in Osteocytic (MLO-Y4) Cells. *Biochemical and Biophysical Research Communications*, 2822, pp.536–542.
- Gualillo, O., Caminos, J.E., Kojima, M., Kangawa, K., Arvat, E., Ghigo, E., Casanueva, F.F. and Dieguez, C., (2001) Gender and gonadal influences on ghrelin mRNA levels in rat stomach. *European Journal of Endocrinology*, 1446, pp.687–690.
- Guan, X.-M., Yu, H., Palyha, O.C., McKee, K.K., Feighner, S.D., Sirinathsinghji, D.J.S., Smith, R.G., Van der Ploeg, L.H.T. and Howard, A.D., (1997) Distribution of mRNA encoding the growth hormone secretagogue receptor in brain and peripheral tissues. *Molecular Brain Research*, 481, pp.23–29.
- Gutierrez, J.A., Solenberg, P.J., Perkins, D.R., Willency, J.A., Knierman, M.D., Jin, Z., Witcher, D.R., Luo, S., Onyia, J.E. and Hale, J.E., (2008) Ghrelin octanoylation mediated by an orphan lipid transferase. *Proceedings of the National Academy of Sciences of the United States of America*, 10517, pp.6320–6325.
- Han, Y., Cowin, S.C., Schaffler, M.B. and Weinbaum, S., (2004) Mechanotransduction and strain amplification in osteocyte cell processes. *Proceedings of the National Academy of Sciences of the United States of America*, 10147, pp.16689–16694.
- Harada, S. and Rodan, G.A., (2003) Control of osteoblast function and regulation of bone mass. *Nature*. [online] Available at: <https://www.nature.com/articles/nature01660> [Accessed 25 Jan. 2018].
- Hardaway, A.L., Herroon, M.K., Rajagurubandara, E. and Podgorski, I., (2014) Bone marrow fat: linking adipocyte-induced inflammation with skeletal metastases. *Cancer and Metastasis Reviews*, 332–3, pp.527–543.

Hardouin, P., Rharass, T. and Lucas, S., (2016) Bone Marrow Adipose Tissue: To Be or Not To Be a Typical Adipose Tissue? *Bone Research*, p.85.

Hauschka, P.V., Lian, J.B., Cole, D.E. and Gundberg, C.M., (1989) Osteocalcin and matrix Gla protein: vitamin K-dependent proteins in bone. *Physiological Reviews*, 693, pp.990–1047.

Hei, H., Gao, J., Dong, J., Tao, J., Tian, L., Pan, W., Wang, H. and Zhang, X., (2016) BK Knockout by TALEN-Mediated Gene Targeting in Osteoblasts: KCNMA1 Determines the Proliferation and Differentiation of Osteoblasts. *Molecules and Cells*, 397, pp.530–535.

Hemmingsen, M., Vedel, S., Skafted-Pedersen, P., Sabourin, D., Collas, P., Bruus, H. and Dufva, M., (2013) The Role of Paracrine and Autocrine Signaling in the Early Phase of Adipogenic Differentiation of Adipose-derived Stem Cells. *PLOS ONE*, 85, p.e63638.

Henney, N.C., (2008) *Expression and characteristics of ion channels in osteoblasts: putative roles for TRP and K⁺ channels*. [phd] Cardiff University. Available at: <http://orca.cf.ac.uk/54500/> [Accessed 17 Sep. 2014].

Henney, N.C., Li, B., Elford, C., Reviriego, P., Campbell, A.K., Wann, K.T. and Evans, B.A.J., (2009) A large-conductance (BK) potassium channel subtype affects both growth and mineralization of human osteoblasts. *American Journal of Physiology - Cell Physiology*, 2976, pp.C1397–C1408.

Heubach, J.F., Graf, E.M., Leutheuser, J., Bock, M., Balana, B., Zahanich, I., Christ, T., Boxberger, S., Wettwer, E. and Ravens, U., (2004) Electrophysiological properties of human mesenchymal stem cells. *The Journal of Physiology*, 5543, pp.659–672.

Hibino, H., Inanobe, A., Furutani, K., Murakami, S., Findlay, I. and Kurachi, Y., (2010) Inwardly Rectifying Potassium Channels: Their Structure, Function, and Physiological Roles. *Physiological Reviews*, 901, pp.291–366.

Hirukawa, K., Muraki, K., Ohya, S., Imaizumi, Y. and Togari, A., (2008) Electrophysiological Properties of a Novel Ca²⁺-Activated K⁺ Channel Expressed in Human Osteoblasts. *Calcified Tissue International*, 833, pp.222–229.

Ho, K., Nichols, C.G., Lederer, W.J., Lytton, J., Vassilev, P.M., Kanazirska, M.V. and Hebert, S.C., (1993) Cloning and expression of an inwardly rectifying ATP-regulated potassium channel. *Nature*, 3626415, pp.31–38.

Chapter 9 – References

- Hoffmann, E.K., Holm, N.B. and Lambert, I.H., (2014) Functions of volume-sensitive and calcium-activated chloride channels. *IUBMB Life*, 664, pp.257–267.
- Hofmann, K., (2000) A superfamily of membrane-bound O-acyltransferases with implications for Wnt signaling. *Trends in Biochemical Sciences*, 253, pp.111–112.
- Holick, M.F., (2009) Vitamin D and Health: Evolution, Biologic Functions, and Recommended Dietary Intakes for Vitamin D. *Clinical Reviews in Bone and Mineral Metabolism*, 71, pp.2–19.
- Holst, B., Cygankiewicz, A., Jensen, T.H., Ankersen, M. and Schwartz, T.W., (2003) High Constitutive Signaling of the Ghrelin Receptor—Identification of a Potent Inverse Agonist. *Molecular Endocrinology*, 1711, pp.2201–2210.
- Hong, J.-H., Hwang, E.S., McManus, M.T., Amsterdam, A., Tian, Y., Kalmukova, R., Mueller, E., Benjamin, T., Spiegelman, B.M., Sharp, P.A., Hopkins, N. and Yaffe, M.B., (2005) TAZ, a Transcriptional Modulator of Mesenchymal Stem Cell Differentiation. *Science*, 3095737, pp.1074–1078.
- Hopkins, A.L., Nelson, T.A.S., Guschina, I.A., Parsons, L.C., Lewis, C.L., Brown, R.C., Christian, H.C., Davies, J.S. and Wells, T., (2017) Unacylated ghrelin promotes adipogenesis in rodent bone marrow via ghrelin O-acyl transferase and GHS-R1a activity: evidence for target cell-induced acylation. *Scientific Reports*, 7, p.srep45541.
- Hormaechea-Agulla, D., Gahete, M.D., Jiménez-Vacas, J.M., Gómez-Gómez, E., Ibáñez-Costa, A., L-López, F., Rivero-Cortés, E., Sarmiento-Cabral, A., Valero-Rosa, J., Carrasco-Valiente, J., Sánchez-Sánchez, R., Ortega-Salas, R., Moreno, M.M., Tsomaia, N., Swanson, S.M., Culler, M.D., Requena, M.J., Castaño, J.P. and Luque, R.M., (2017) The oncogenic role of the In1-ghrelin splicing variant in prostate cancer aggressiveness. *Molecular Cancer*, 16, p.146.
- Hosoda, H., Kojima, M., Matsuo, H. and Kangawa, K., (2000a) Ghrelin and Des-acyl Ghrelin: Two Major Forms of Rat Ghrelin Peptide in Gastrointestinal Tissue. *Biochemical and Biophysical Research Communications*, 2793, pp.909–913.
- Hosoda, H., Kojima, M., Matsuo, H. and Kangawa, K., (2000b) Purification and Characterization of Rat des-Gln14-Ghrelin, a Second Endogenous Ligand for the Growth Hormone Secretagogue Receptor. *Journal of Biological Chemistry*, 27529, pp.21995–22000.

Chapter 9 – References

- Howard, A.D., Feighner, S.D., Cully, D.F., Arena, J.P., Liberators, P.A., Rosenblum, C.I., Hamelin, M., Hreniuk, D.L., Palyha, O.C., Anderson, J., Paresse, P.S., Diaz, C., Chou, M., Liu, K.K., McKee, K.K., Pong, S.-S., Chaung, L.-Y., Elbrecht, A., Dashkevich, M., Heavens, R., Rigby, M., Sirinathsinghji, D.J.S., Dean, D.C., Melillo, D.G., Patchett, A.A., Nargund, R., Griffin, P.R., DeMartino, J.A., Gupta, S.K., Schaeffer, J.M., Smith, R.G. and Ploeg, L.H.T.V. (1996) A Receptor in Pituitary and Hypothalamus That Functions in Growth Hormone Release. *Science*, 273:5277, pp.974–977.
- Hu, H., He, M.-L., Tao, R., Sun, H.-Y., Hu, R., Zang, W.-J., Yuan, B.-X., Lau, C.-P., Tse, H.-F. and Li, G.-R., (2009) Characterization of ion channels in human preadipocytes. *Journal of Cellular Physiology*, 218:2, pp.427–435.
- Hu, K., Sun, H., Gui, B. and Sui, C., (2017) TRPV4 functions in flow shear stress induced early osteogenic differentiation of human bone marrow mesenchymal stem cells. *Biomedicine & Pharmacotherapy*, 91:Supplement C, pp.841–848.
- Hughes, S., Magnay, J., Foreman, M., Publicover, S.J., Dobson, J.P. and El Haj, A.J., (2006) Expression of the mechanosensitive 2PK⁺ channel TREK-1 in human osteoblasts. *Journal of Cellular Physiology*, 206:3, pp.738–748.
- Ibáñez-Costa, A., Gahete, M.D., Rivero-Cortés, E., Rincón-Fernández, D., Nelson, R., Beltrán, M., de la Riva, A., Japón, M.A., Venegas-Moreno, E., Gálvez, M.Á., García-Arnés, J.A., Soto-Moreno, A., Morgan, J., Tsomaia, N., Culler, M.D., Dieguez, C., Castaño, J.P. and Luque, R.M., (2015) In1-ghrelin splicing variant is overexpressed in pituitary adenomas and increases their aggressive features. *Scientific Reports*, 5, p.8714.
- Iguchi, G., Okimura, Y., Takahashi, T., Mizuno, I., Fumoto, M., Takahashi, Y., Kaji, H., Abe, H. and Chihara, K., (1999) Cloning and Characterization of the 5'-Flanking Region of the Human Growth Hormone-releasing Hormone Receptor Gene. *Journal of Biological Chemistry*, 274:17, pp.12108–12114.
- Ikeda, S.R. and Korn, S.J., (1995) Influence of permeating ions on potassium channel block by external tetraethylammonium. *The Journal of Physiology*, 486:2, pp.267–272.
- Im, W.B. and Quandt, F.N., (1992) Mechanism of asymmetric block of K channels by tetraalkylammonium ions in mouse neuroblastoma cells. *The Journal of Membrane Biology*, 130:2, pp.115–124.

- Inagaki, N., Gono, T., Iv, J.P.C., Wang, C.-Z., Aguilar-Bryan, L., Bryan, J. and Seino, S., (1996) A Family of Sulfonylurea Receptors Determines the Pharmacological Properties of ATP-Sensitive K⁺ Channels. *Neuron*, 165, pp.1011–1017.
- Inazumi, T., Shirata, N., Morimoto, K., Takano, H., Segi-Nishida, E. and Sugimoto, Y., (2011) Prostaglandin E2-EP4 signaling suppresses adipocyte differentiation in mouse embryonic fibroblasts via an autocrine mechanism. *Journal of Lipid Research*, p.jlr.M013615.
- Isabelle, G., Ronan, B., Françoise, C.-A., Nicolas, B. and Jean, P.S., (2013) Ghrelin differentiates human osteoblasts via GHS-R1a receptor. *Bone Abstracts*. [online] Available at: <http://www.bone-abstracts.org/ba/0002/ba0002P131.htm> [Accessed 15 Oct. 2014].
- Ishibashi, H., Moorhouse, A. and Nabekura, J., (2012) Perforated Whole-Cell Patch-Clamp Technique: A User's Guide. In: Y. Okada, ed., *Patch Clamp Techniques*, Springer Protocols Handbooks. [online] Springer Japan, pp.71–83. Available at: http://dx.doi.org/10.1007/978-4-431-53993-3_4 [Accessed 22 Sep. 2016].
- Ito, S., Suzuki, N., Kato, S., Takahashi, T. and Takagi, M., (2007) Glucocorticoids induce the differentiation of a mesenchymal progenitor cell line, ROB-C26 into adipocytes and osteoblasts, but fail to induce terminal osteoblast differentiation. *Bone*, 401, pp.84–92.
- James, A.W., (2013) Review of Signaling Pathways Governing MSC Osteogenic and Adipogenic Differentiation. *Scientifica*, 2013, p.e684736.
- Jeffery, P.L., Duncan, R.P., Yeh, A.H., Jaskolski, R.A., Hammond, D.S., Herington, A.C. and Chopin, L.K., (2005a) Expression of the Ghrelin Axis in the Mouse: An Exon 4-Deleted Mouse Proghrelin Variant Encodes a Novel C Terminal Peptide. *Endocrinology*, 1461, pp.432–440.
- Jeffery, P.L., Herington, A.C. and Chopin, L.K., (2002) Expression and action of the growth hormone releasing peptide ghrelin and its receptor in prostate cancer cell lines. *Journal of Endocrinology*, 1723, pp.R7-11.
- Jeffery, P.L., Herington, A.C. and Chopin, L.K., (2003) The potential autocrine/paracrine roles of ghrelin and its receptor in hormone-dependent cancer. *Cytokine & Growth Factor Reviews*, 142, pp.113–122.

Jeffery, P.L., Murray, R.E., Yeh, A.H., McNamara, J.F., Duncan, R.P., Francis, G.D., Herington, A.C. and Chopin, L.K., (2005b) Expression and function of the ghrelin axis, including a novel preproghrelin isoform, in human breast cancer tissues and cell lines. *Endocrine-Related Cancer*, 124, pp.839–850.

Jiang, Y., Mishima, H., Sakai, S., Liu, Y., Ohyabu, Y. and Uemura, T., (2008) Gene expression analysis of major lineage-defining factors in human bone marrow cells: Effect of aging, gender, and age-related disorders. *Journal of Orthopaedic Research*, 267, pp.910–917.

Jilka, R.L., Weinstein, R.S., Bellido, T., Roberson, P., Parfitt, A.M. and Manolagas, S.C., (1999) Increased bone formation by prevention of osteoblast apoptosis with parathyroid hormone. *The Journal of Clinical Investigation*, 1044, pp.439–446.

Jilka, R.L., Weinstein, R.S., Parfitt, A.M. and Manolagas, S.C., (2007) Perspective: Quantifying Osteoblast and Osteocyte Apoptosis: Challenges and Rewards. *Journal of Bone and Mineral Research*, 2210, pp.1492–1501.

Jing, W., Smith, A.A., Liu, B., Li, J., Hunter, D.J., Dhamdhare, G., Salmon, B., Jiang, J., Cheng, D., Johnson, C.A., Chen, S., Lee, K., Singh, G. and Helms, J.A., (2015) Reengineering autologous bone grafts with the stem cell activator WNT3A. *Biomaterials*, 47Supplement C, pp.29–40.

Jonge, H.J.M. de, Fehrmann, R.S.N., Bont, E.S.J.M. de, Hofstra, R.M.W., Gerbens, F., Kamps, W.A., Vries, E.G.E. de, Zee, A.G.J. van der, Meerman, G.J. te and Elst, A. ter, (2007) Evidence Based Selection of Housekeeping Genes. *PLOS ONE*, 29, p.e898.

Justesen, J., Pedersen, S.B., Stenderup, K. and Kassem, M., (2004) Subcutaneous Adipocytes Can Differentiate into Bone-Forming Cells in Vitro and in Vivo. *Tissue Engineering*, 103–4, pp.381–391.

Justesen, J., Stenderup, K., Ebbesen, E.N., Mosekilde, L., Steiniche, T. and Kassem, M., (2001) Adipocyte tissue volume in bone marrow is increased with aging and in patients with osteoporosis. *Biogerontology*, 23, pp.165–171.

Justesen, J., Stenderup, K., Eriksen, E.F. and Kassem, M., (2002) Maintenance of Osteoblastic and Adipocytic Differentiation Potential with Age and Osteoporosis in Human Marrow Stromal Cell Cultures. *Calcified Tissue International*, 711, pp.36–44.

Chapter 9 – References

- Kaiya, H., Kangawa, K. and Miyazato, M., (2013) Ghrelin Receptors in Non-Mammalian Vertebrates. *Frontiers in Endocrinology*, [online] 4. Available at: <http://journal.frontiersin.org/article/10.3389/fendo.2013.00081/abstract> [Accessed 29 Mar. 2017].
- Kamegai, J., Tamura, H., Ishii, S., Sugihara, H. and Wakabayashi, I., (2001) Thyroid Hormones Regulate Pituitary Growth Hormone Secretagogue Receptor Gene Expression. *Journal of Neuroendocrinology*, 133, pp.275–278.
- Kanamoto, N., Akamizu, T., Hosoda, H., Hataya, Y., Ariyasu, H., Takaya, K., Hosoda, K., Saijo, M., Moriyama, K., Shimatsu, A., Kojima, M., Kangawa, K. and Nakao, K., (2011) Substantial Production of Ghrelin by a Human Medullary Thyroid Carcinoma Cell Line. *The Journal of Clinical Endocrinology & Metabolism*. [online] Available at: <http://press.endocrine.org/doi/10.1210/jcem.86.10.7891> [Accessed 29 Aug. 2017].
- Karsenty, G., (2006) Convergence between bone and energy homeostases: Leptin regulation of bone mass. *Cell Metabolism*, 45, pp.341–348.
- Kassem, M., Abdallah, B.M. and Saeed, H., (2008) Osteoblastic cells: Differentiation and trans-differentiation. *Archives of Biochemistry and Biophysics*, 4732, pp.183–187.
- Kawai, M., de Paula, F.J.A. and Rosen, C.J., (2012) New insights into osteoporosis: the bone–fat connection. *Journal of Internal Medicine*, 2724, pp.317–329.
- Kawamura, K., Sato, N., Fukuda, J., Kodama, H., Kumagai, J., Tanikawa, H., Nakamura, A., Honda, Y., Sato, T. and Tanaka, T., (2003) Ghrelin Inhibits the Development of Mouse Preimplantation Embryos *in Vitro*. *Endocrinology*, 1446, pp.2623–2633.
- Kawamura, N., Kugimiya, F., Oshima, Y., Ohba, S., Ikeda, T., Saito, T., Shinoda, Y., Kawasaki, Y., Ogata, N., Hoshi, K., Akiyama, T., Chen, W.S., Hay, N., Tobe, K., Kadowaki, T., Azuma, Y., Tanaka, S., Nakamura, K., Chung, U. and Kawaguchi, H., (2007) Akt1 in Osteoblasts and Osteoclasts Controls Bone Remodeling. *PLOS ONE*, 210, p.e1058.
- Kelly, K.A., Tanaka, S., Baron, R. and Gimble, J.M., (1998) Murine Bone Marrow Stromally Derived BMS2 Adipocytes Support Differentiation and Function of Osteoclast-Like Cells *in Vitro*. *Endocrinology*, 1394, pp.2092–2101.

- Kim, J.E. and Chen, J., (2004) Regulation of Peroxisome Proliferator-Activated Receptor- γ Activity by Mammalian Target of Rapamycin and Amino Acids in Adipogenesis. *Diabetes*, 5311, pp.2748–2756.
- Kim, K.-C., Shin, D.-H., Lee, S.-Y., Im, J.-A. and Lee, D.-C., (2010) Relation between Obesity and Bone Mineral Density and Vertebral Fractures in Korean Postmenopausal Women. *Yonsei Medical Journal*, 516, pp.857–863.
- Kim, K.H., Song, M.J., Yoo, E.J., Choe, S.S., Park, S.D. and Kim, J.B., (2004) Regulatory Role of Glycogen Synthase Kinase 3 for Transcriptional Activity of ADD1/SREBP1c. *Journal of Biological Chemistry*, 27950, pp.51999–52006.
- Kim, S.W., Choi, O.K., Jung, J.Y., Yang, J.-Y., Cho, S.W., Shin, C.S., Park, K.S. and Kim, S.Y., (2009) Ghrelin inhibits early osteogenic differentiation of C3H10T1/2 cells by suppressing Runx2 expression and enhancing PPAR γ and C/EBP α expression. *Journal of Cellular Biochemistry*, 1064, pp.626–632.
- Kim, S.W., Her, S.J., Park, S.J., Kim, D., Park, K.S., Lee, H.K., Han, B.H., Kim, M.S., Shin, C.S. and Kim, S.Y., (2005) Ghrelin stimulates proliferation and differentiation and inhibits apoptosis in osteoblastic MC3T3-E1 cells. *Bone*, 373, pp.359–369.
- Kineman, R.D., Gahete, M.D. and Luque, R.M., (2007) Identification of a mouse ghrelin gene transcript that contains intron 2 and is regulated in the pituitary and hypothalamus in response to metabolic stress. *Journal of Molecular Endocrinology*, 385, pp.511–521.
- Köhler, R., Wulff, H., Eichler, I., Kneifel, M., Neumann, D., Knorr, A., Grgic, I., Kämpfe, D., Si, H., Wibawa, J., Real, R., Borner, K., Brakemeier, S., Orzechowski, H.-D., Reusch, H.-P., Paul, M., Chandy, K.G. and Hoyer, J., (2003) Blockade of the Intermediate-Conductance Calcium-Activated Potassium Channel as a New Therapeutic Strategy for Restenosis. *Circulation*, 1089, pp.1119–1125.
- Kohno, D., Gao, H.-Z., Muroya, S., Kikuyama, S. and Yada, T., (2003) Ghrelin Directly Interacts With Neuropeptide-Y-Containing Neurons in the Rat Arcuate Nucleus Ca²⁺ Signaling via Protein Kinase A and N-Type Channel-Dependent Mechanisms and Cross-Talk With Leptin and Orexin. *Diabetes*, 524, pp.948–956.

Chapter 9 – References

- Kojima, M., Hosoda, H., Date, Y., Nakazato, M., Matsuo, H. and Kangawa, K., (1999) Ghrelin is a growth-hormone-releasing acylated peptide from stomach. *Nature*, 4026762, pp.656–660.
- Kojima, M. and Kangawa, K., (2005) Ghrelin: Structure and Function. *Physiological Reviews*, 852, pp.495–522.
- Komori, T., (2013) Functions of the osteocyte network in the regulation of bone mass. *Cell and Tissue Research*, 3522, pp.191–198.
- Komori, T., Yagi, H., Nomura, S., Yamaguchi, A., Sasaki, K., Deguchi, K., Shimizu, Y., Bronson, R.T., Gao, Y.-H., Inada, M., Sato, M., Okamoto, R., Kitamura, Y., Yoshiki, S. and Kishimoto, T., (1997) Targeted Disruption of Cbfa1 Results in a Complete Lack of Bone Formation owing to Maturational Arrest of Osteoblasts. *Cell*, 895, pp.755–764.
- Koromila, T., Baniwal, S.K., Song, Y.S., Martin, A., Xiong, J. and Frenkel, B., (2014) Glucocorticoids Antagonize RUNX2 During Osteoblast Differentiation in Cultures of ST2 Pluripotent Mesenchymal Cells. *Journal of Cellular Biochemistry*, 1151, pp.27–33.
- Kos, K., Harte, A.L., O’Hare, P.J., Kumar, S. and McTernan, P.G., (2009) Ghrelin and the differential regulation of des-acyl (DSG) and oct-anoyl ghrelin (OTG) in human adipose tissue (AT). *Clinical Endocrinology*, 703, pp.383–389.
- Kouadjo, K.E., Nishida, Y., Cadrin-Girard, J.F., Yoshioka, M. and St-Amand, J., (2007) Housekeeping and tissue-specific genes in mouse tissues. *BMC Genomics*, 8, p.127.
- Kozłowski, R.Z., Hales, C.N. and Ashford, M.L.J., (1989) Dual effects of diazoxide on ATP-K⁺ currents recorded from an insulin-secreting cell line. *British Journal of Pharmacology*, 974, pp.1039–1050.
- Kyle, B.D. and Braun, A.P., (2014) The regulation of BK channel activity by pre- and post-translational modifications. *Frontiers in Physiology*, [online] 5. Available at: <https://www.ncbi.nlm.nih.gov/pmc/articles/PMC4141542/> [Accessed 13 Jun. 2018].
- Lampiasi, N., Russo, R. and Zito, F., (2016) The Alternative Faces of Macrophage Generate Osteoclasts. *BioMed Research International*, 2016, p.e9089610.
- Lane, N.E., Yao, W., Balooch, M., Nalla, R.K., Balooch, G., Habelitz, S., Kinney, J.H. and Bonewald, L.F., (2006) Glucocorticoid-Treated Mice Have Localized Changes in

Trabecular Bone Material Properties and Osteocyte Lacunar Size That Are Not Observed in Placebo-Treated or Estrogen-Deficient Mice. *Journal of Bone and Mineral Research*, 213, pp.466–476.

Larsson, O., Ammälä, C., Bokvist, K., Fredholm, B. and Rorsman, P., (1993) Stimulation of the KATP channel by ADP and diazoxide requires nucleotide hydrolysis in mouse pancreatic beta-cells. *The Journal of Physiology*, 463, pp.349–365.

Lecka-Czernik, B., (2012) Marrow fat metabolism is linked to the systemic energy metabolism. *Bone*, 502, pp.534–539.

Lecka-Czernik, B., Moerman, E.J., Grant, D.F., Lehmann, J.M., Manolagas, S.C. and Jilka, R.L., (2002) Divergent Effects of Selective Peroxisome Proliferator-Activated Receptor- γ 2 Ligands on Adipocyte Versus Osteoblast Differentiation. *Endocrinology*, 1436, pp.2376–2384.

Leclerc, N., Noh, T., Cogan, J., Samarawickrama, D.B., Smith, E. and Frenkel, B., (2008) Opposing effects of glucocorticoids and Wnt signaling on Krox20 and mineral deposition in osteoblast cultures. *Journal of Cellular Biochemistry*, 1036, pp.1938–1951.

Lee, K.-S., Kim, H.-J., Li, Q.-L., Chi, X.-Z., Ueta, C., Komori, T., Wozney, J.M., Kim, E.-G., Choi, J.-Y., Ryoo, H.-M. and Bae, S.-C., (2000) Runx2 Is a Common Target of Transforming Growth Factor β 1 and Bone Morphogenetic Protein 2, and Cooperation between Runx2 and Smad5 Induces Osteoblast-Specific Gene Expression in the Pluripotent Mesenchymal Precursor Cell Line C2C12. *Molecular and Cellular Biology*, 2023, pp.8783–8792.

Lee, N.K., Sowa, H., Hinoi, E., Ferron, M., Ahn, J.D., Confavreux, C., Dacquin, R., Mee, P.J., McKee, M.D., Jung, D.Y., Zhang, Z., Kim, J.K., Mauvais-Jarvis, F., Ducy, P. and Karsenty, G., (2007) Endocrine Regulation of Energy Metabolism by the Skeleton. *Cell*, 1303, pp.456–469.

Lee, U.S. and Cui, J., (2010) BK channel activation: structural and functional insights. *Trends in neurosciences*, 339, pp.415–423.

Leonoudakis, D., Gray, A.T., Winegar, B.D., Kindler, C.H., Harada, M., Taylor, D.M., Chavez, R.A., Forsayeth, J.R. and Yost, C.S., (1998) An Open Rectifier Potassium Channel with Two Pore Domains in Tandem Cloned from Rat Cerebellum. *Journal of Neuroscience*, 183, pp.868–877.

- Levin, M., (2007) Large-scale biophysics: ion flows and regeneration. *Trends in Cell Biology*, 176, pp.261–270.
- Levin, M., (2013) Reprogramming cells and tissue patterning via bioelectrical pathways: molecular mechanisms and biomedical opportunities. *Wiley Interdisciplinary Reviews: Systems Biology and Medicine*, 56, pp.657–676.
- L’Hoste, S., Diakov, A., Andrini, O., Genete, M., Pinelli, L., Grand, T., Keck, M., Paulais, M., Beck, L., Korbmacher, C., Teulon, J. and Lourdel, S., (2013) Characterization of the mouse ClC-K1/Barttin chloride channel. *Biochimica et Biophysica Acta (BBA) - Biomembranes*, 182811, pp.2399–2409.
- Li, B., (2012) *The role of BK channel in cellular proliferation and differentiation in human osteoblast and osteoblast-like cells*. [phd] Cardiff University. Available at: <http://orca.cf.ac.uk/35876/> [Accessed 17 Sep. 2014].
- Li, G.-R., Deng, X.-L., Sun, H., Chung, S.S.M., Tse, H.-F. and Lau, C.-P., (2006) Ion Channels in Mesenchymal Stem Cells from Rat Bone Marrow. *STEM CELLS*, 246, pp.1519–1528.
- Li, G.-R., Sun, H., Deng, X. and Lau, C.-P., (2005) Characterization of Ionic Currents in Human Mesenchymal Stem Cells from Bone Marrow. *STEM CELLS*, 233, pp.371–382.
- Li, J., Zhang, N., Huang, X., Xu, J., Fernandes, J.C., Dai, K. and Zhang, X., (2013a) Dexamethasone shifts bone marrow stromal cells from osteoblasts to adipocytes by C/EBPalpha promoter methylation. *Cell Death & Disease*, 410, p.e832.
- Li, Q. and Yan, J., (2016) Modulation of BK Channel Function by Auxiliary Beta and Gamma Subunits. *International Review of Neurobiology*, 128, pp.51–90.
- Li, W., Wei, S., Liu, C., Song, M., Wu, H. and Yang, Y., (2016a) Regulation of the osteogenic and adipogenic differentiation of bone marrow-derived stromal cells by extracellular uridine triphosphate: The role of P2Y2 receptor and ERK1/2 signaling. *International Journal of Molecular Medicine*, 371, pp.63–73.
- Li, X., Zheng, S., Dong, X. and Xiao, J., (2013b) 17 β -Estradiol Inhibits Outward Voltage-Gated K⁺ Currents in Human Osteoblast-Like MG63 Cells. *The Journal of Membrane Biology*, 2461, pp.39–45.

- Li, Z., Mulholland, M. and Zhang, W., (2016b) Ghrelin O-acyltransferase (GOAT) and energy metabolism. *Science China Life Sciences*, pp.1–11.
- Lian, J.B., Stein, G.S., van Wijnen, A.J., Stein, J.L., Hassan, M.Q., Gaur, T. and Zhang, Y., (2012) MicroRNA control of bone formation and homeostasis. *Nature reviews. Endocrinology*, 84, pp.212–227.
- Liang, Q.-H., Jiang, Y., Zhu, X., Cui, R.-R., Liu, G.-Y., Liu, Y., Wu, S.-S., Liao, X.-B., Xie, H., Zhou, H.-D., Wu, X.-P., Yuan, L.-Q. and Liao, E.-Y., (2012) Ghrelin Attenuates the Osteoblastic Differentiation of Vascular Smooth Muscle Cells through the ERK Pathway. *PLoS ONE*, 74, p.e33126.
- Lim, C.T., Kola, B., Grossman, A. and Korbonits, M., (2011) The expression of ghrelin O-acyltransferase (GOAT) in human tissues. *Endocrine Journal*, 588, pp.707–710.
- Lin, L., Saha, P.K., Ma, X., Henshaw, I.O., Shao, L., Chang, B.H.J., Buras, E.D., Tong, Q., Chan, L., McGuinness, O.P. and Sun, Y., (2011) Ablation of ghrelin receptor reduces adiposity and improves insulin sensitivity during aging by regulating fat metabolism in white and brown adipose tissues. *Aging Cell*, 106, pp.996–1010.
- Linley, J., (2013) Perforated Whole-Cell Patch-Clamp Recording. In: N. Gamper, ed., *Ion Channels*, Methods in Molecular Biology. [online] Humana Press, pp.149–157. Available at: http://dx.doi.org/10.1007/978-1-62703-351-0_11 [Accessed 19 Sep. 2016].
- Lippiat, J., (2009) Whole-Cell Recording Using the Perforated Patch Clamp Technique. In: J. Lippiat, ed., *Potassium Channels*, Methods in Molecular Biology. [online] Humana Press, pp.141–149. Available at: http://dx.doi.org/10.1007/978-1-59745-526-8_11 [Accessed 19 Sep. 2016].
- Liu, J., Lin, H., Cheng, P., Hu, X. and Lu, H., (2009) Effects of ghrelin on the proliferation and differentiation of 3T3-L1 preadipocytes. *Journal of Huazhong University of Science and Technology [Medical Sciences]*, 292, pp.227–230.
- Liu, L.-F., Shen, W.-J., Zhang, Z.H., Wang, L.J. and Kraemer, F.B., (2010) Adipocytes decrease Runx2 expression in osteoblastic cells: roles of PPAR γ and adiponectin. *Journal of Cellular Physiology*, 2253, pp.837–845.
- Liu, Y., Porta, A., Peng, X., Gengaro, K., Cunningham, E.B., Li, H., Dominguez, L.A., Bellido, T. and Christakos, S., (2004) Prevention of Glucocorticoid-Induced Apoptosis in

Osteocytes and Osteoblasts by Calbindin-D28k. *Journal of Bone and Mineral Research*, 193, pp.479–490.

Livak, K.J. and Schmittgen, T.D., (2001) Analysis of Relative Gene Expression Data Using Real-Time Quantitative PCR and the $2^{-\Delta\Delta CT}$ Method. *Methods*, 254, pp.402–408.

Lopatin, A.N., Makhina, E.N. and Nichols, C.G., (1994) Potassium channel block by cytoplasmic polyamines as the mechanism of intrinsic rectification. *Nature*, 3726504, pp.366–369.

Loukin, S.H., Teng, J. and Kung, C., (2015) A channelopathy mechanism revealed by direct calmodulin activation of TrpV4. *Proceedings of the National Academy of Sciences*, 11230, pp.9400–9405.

Luque, R., Sampedro-Nuñez, M., Gahete, M., Ramos-Levi, A., Ibáñez-Costa, A., Rivero-Cortés, E., Serrano-Somavilla, A., Adrados, M., Culler, M., Castaño, J., Marazuela, M., Luque, R., Sampedro-Nuñez, M., Gahete, M., Ramos-Levi, A., Ibáñez-Costa, A., Rivero-Cortés, E., Serrano-Somavilla, A., Adrados, M., Culler, M., Castaño, J. and Marazuela, M., (2015) In1-ghrelin, a splice variant of ghrelin gene, is associated with the evolution and aggressiveness of human neuroendocrine tumors: Evidence from clinical, cellular and molecular parameters. *Oncotarget*, 623, pp.19619–19633.

Ma, C., Fukuda, T., Ochi, H., Sunamura, S., Xu, C., Xu, R., Okawa, A. and Takeda, S., (2015) Genetic determination of the cellular basis of the ghrelin-dependent bone remodeling. *Molecular Metabolism*, 43, pp.175–185.

Ma, X., Lin, L., Yue, J., Pradhan, G., Qin, G., Minze, L.J., Wu, H., Sheikh-Hamad, D., Smith, C.W. and Sun, Y., (2013) Ghrelin receptor regulates HFCS-induced adipose inflammation and insulin resistance. *Nutrition & Diabetes*, 312, p.e99.

Maccarinelli, G., Sibilina, V., Torsello, A., Raimondo, F., Pitto, M., Giustina, A., Netti, C. and Cocchi, D., (2005) Ghrelin regulates proliferation and differentiation of osteoblastic cells. *Journal of Endocrinology*, 1841, pp.249–256.

MacDonald, D.P.E. and Wheeler, M.B., (2003) Voltage-dependent K⁺ channels in pancreatic beta cells: Role, regulation and potential as therapeutic targets. *Diabetologia*, 468, pp.1046–1062.

Chapter 9 – References

- Mackie, E.J., (2003) Osteoblasts: novel roles in orchestration of skeletal architecture. *The International Journal of Biochemistry & Cell Biology*, 359, pp.1301–1305.
- Macro, J.A., Dimaline, R. and Dockray, G.J., (1996) Identification and expression of prohormone-converting enzymes in the rat stomach. *The American Journal of Physiology*, 2701 Pt 1, pp.G87-93.
- Mammalian Gene Collection (MGC) Program Team, (2002) Generation and initial analysis of more than 15,000 full-length human and mouse cDNA sequences. *Proceedings of the National Academy of Sciences of the United States of America*, 9926, pp.16899–16903.
- Mangiafico, S.S., (2015). *An R Companion for the Handbook of Biological Statistics*. Version 1.3.2. Available at : rcompanion.org/rcompanion/.
- Manolagas, S.C., (2000) Osteoporosis. In: *Principles of Molecular Rheumatology*, Current Molecular Medicine. [online] Humana Press, Totowa, NJ, pp.413–422. Available at: https://link.springer.com/chapter/10.1007/978-1-59259-018-6_26 [Accessed 15 Feb. 2018].
- Manolagas, S.C. and Parfitt, A.M., (2010) What old means to bone. *Trends in endocrinology and metabolism: TEM*, 216, pp.369–374.
- Marchigiano, G., (1997) Osteoporosis: Primary prevention and intervention strategies for women at risk. *Home Care Provider*, 22, pp.76–81.
- Marie, P.J., (2008) Transcription factors controlling osteoblastogenesis. *Archives of Biochemistry and Biophysics*, 4732, pp.98–105.
- Marks, S.C. and Odgren, P.R., (2002) Structure and Development of the Skeleton. In: *Principles of Bone Biology (Second Edition)*. Academic Press, pp.3–15.
- Marotti, G., (2000) The osteocyte as a wiring transmission system. *Journal of Musculoskeletal & Neuronal Interactions*, 12, pp.133–136.
- Matic, I., Matthews, B.G., Wang, X., Dymant, N.A., Worthley, D.L., Rowe, D.W., Grcevic, D. and Kalajzic, I., (2016) Quiescent Bone Lining Cells Are a Major Source of Osteoblasts During Adulthood. *Stem cells (Dayton, Ohio)*, 3412, pp.2930–2942.

Chapter 9 – References

- Mauney, J.R., Volloch, V. and Kaplan, D.L., (2005) Matrix-mediated retention of adipogenic differentiation potential by human adult bone marrow-derived mesenchymal stem cells during ex vivo expansion. *Biomaterials*, 2631, pp.6167–6175.
- McBeath, R., Pirone, D.M., Nelson, C.M., Bhadriraju, K. and Chen, C.S., (2004) Cell Shape, Cytoskeletal Tension, and RhoA Regulate Stem Cell Lineage Commitment. *Developmental Cell*, 64, pp.483–495.
- McDonald, J.H., (2014) *Handbook of Biological Statistics*. 3rd ed. Sparky House Publishing, Baltimore, Maryland. Available at: <http://www.biostathandbook.com/outline.html>
- McKee, K.K., Palyha, O.C., Feighner, S.D., Hreniuk, D.L., Tan, C.P., Phillips, M.S., Smith, R.G., Ploeg, V. der, T, L.H. and Howard, A.D., (1997) Molecular Analysis of Rat Pituitary and Hypothalamic Growth Hormone Secretagogue Receptors. *Molecular Endocrinology*, 114, pp.415–423.
- McWilliam, H., Li, W., Uludag, M., Squizzato, S., Park, Y.M., Buso, N., Cowley, A.P. and Lopez, R., (2013) Analysis Tool Web Services from the EMBL-EBI. *Nucleic Acids Research*, 41W1, pp.W597–W600.
- Meyer, M.B., Benkusky, N.A., Sen, B., Rubin, J. and Pike, J.W., (2016) Epigenetic Plasticity Drives Adipogenic and Osteogenic Differentiation of Marrow-derived Mesenchymal Stem Cells. *Journal of Biological Chemistry*, 29134, pp.17829–17847.
- Mikami, Y., Lee, M., Irie, S. and Honda, M.J., (2011) Dexamethasone modulates osteogenesis and adipogenesis with regulation of osterix expression in rat calvaria-derived cells. *Journal of Cellular Physiology*, 2263, pp.739–748.
- Miller, S.C., de Saint-Georges, L., Bowman, B.M. and Jee, W.S., (1989) Bone lining cells: structure and function. *Scanning Microscopy*, 33, pp.953–960; discussion 960-961.
- Moazed, B., Quest, D. and Gopalakrishnan, V., (2009) Des-acyl ghrelin fragments evoke endothelium-dependent vasodilatation of rat mesenteric vascular bed via activation of potassium channels. *European Journal of Pharmacology*, 6041–3, pp.79–86.
- Moerman, E.J., Teng, K., Lipschitz, D.A. and Lecka-Czernik, B., (2004) Aging activates adipogenic and suppresses osteogenic programs in mesenchymal marrow stroma/stem

cells: the role of PPAR- γ 2 transcription factor and TGF- β /BMP signaling pathways. *Aging Cell*, 36, pp.379–389.

Molchadsky, A., Ezra, O., Amendola, P.G., Krantz, D., Kogan-Sakin, I., Buganim, Y., Rivlin, N., Goldfinger, N., Folgiero, V., Falcioni, R., Sarig, R. and Rotter, V., (2013) p53 is required for brown adipogenic differentiation and has a protective role against diet-induced obesity. *Cell Death and Differentiation*, 205, pp.774–783.

Monteil, A., Chemin, J., Bourinet, E., Mennessier, G., Lory, P. and Nargeot, J., (2000) Molecular and Functional Properties of the Human α 1G Subunit That Forms T-type Calcium Channels. *Journal of Biological Chemistry*, 2759, pp.6090–6100.

Moreau, R., Aubin, R., Lapointe, J.Y. and Lajeunesse, D., (1997) Pharmacological and Biochemical Evidence for the Regulation of Osteocalcin Secretion by Potassium Channels in Human Osteoblast-like MG-63 Cells. *Journal of Bone and Mineral Research*, 1212, pp.1984–1992.

Morimoto, E., Li, M., Khalid, A.B., Krum, S.A., Ching, N.O. and Frenkel, B., (2017) Glucocorticoids Hijack Runx2 to Stimulate Wif1 for Suppression of Osteoblast Growth and Differentiation., Glucocorticoids Hijack Runx2 to Stimulate Wif1 for Suppression of Osteoblast Growth and Differentiation. *Journal of cellular physiology, Journal of cellular physiology*, 232, 2321, 1, pp.145, 145–153.

Morris, E.V. and Edwards, C.M., (2016) Bone Marrow Adipose Tissue: A New Player in Cancer Metastasis to Bone. *Bone Research*, p.90.

Moseti, D., Regassa, A. and Kim, W.-K., (2016) Molecular Regulation of Adipogenesis and Potential Anti-Adipogenic Bioactive Molecules. *International Journal of Molecular Sciences*, [online] 171. Available at: <http://www.ncbi.nlm.nih.gov/pmc/articles/PMC4730365/> [Accessed 1 Mar. 2016].

Moutsatsou, P., Kassi, E. and Papavassiliou, A.G., (2012) Glucocorticoid receptor signaling in bone cells. *Trends in Molecular Medicine*, 186, pp.348–359.

Müller, T.D., Nogueiras, R., Andermann, M.L., Andrews, Z.B., Anker, S.D., Argente, J., Batterham, R.L., Benoit, S.C., Bowers, C.Y., Broglio, F., Casanueva, F.F., D'Alessio, D., Depoortere, I., Geliebter, A., Ghigo, E., Cole, P.A., Cowley, M., Cummings, D.E., Dagher, A., Diano, S., Dickson, S.L., Diéguez, C., Granata, R., Grill, H.J., Grove, K., Habegger, K.M., Heppner, K., Heiman, M.L., Holsen, L., Holst, B., Inui, A., Jansson, J.O., Kirchner, H.,

Chapter 9 – References

- Korbonits, M., Laferrère, B., LeRoux, C.W., Lopez, M., Morin, S., Nakazato, M., Nass, R., Perez-Tilve, D., Pfluger, P.T., Schwartz, T.W., Seeley, R.J., Sleeman, M., Sun, Y., Sussel, L., Tong, J., Thorner, M.O., van der Lely, A.J., van der Ploeg, L.H.T., Zigman, J.M., Kojima, M., Kangawa, K., Smith, R.G., Horvath, T. and Tschöp, M.H., (2015) Ghrelin. *Molecular Metabolism*, 46, pp.437–460.
- Murphy, K.D., Lee, J.O. and Herndon, D.N., (2003) Current pharmacotherapy for the treatment of severe burns. *Expert Opinion on Pharmacotherapy*, 43, pp.369–384.
- Muruganandan, S., Parlee, S.D., Rourke, J.L., Ernst, M.C., Goralski, K.B. and Sinal, C.J., (2011) Chemerin, a Novel Peroxisome Proliferator-activated Receptor γ (PPAR γ) Target Gene That Promotes Mesenchymal Stem Cell Adipogenesis. *Journal of Biological Chemistry*, 28627, pp.23982–23995.
- Muruganandan, S., Roman, A.A. and Sinal, C.J., (2009) Adipocyte differentiation of bone marrow-derived mesenchymal stem cells: Cross talk with the osteoblastogenic program. *Cellular and Molecular Life Sciences*, 662, pp.236–253.
- Muruganandan, S., Roman, A.A. and Sinal, C.J., (2010) Role of chemerin/CMKLR1 signaling in adipogenesis and osteoblastogenesis of bone marrow stem cells. *Journal of Bone and Mineral Research*, 252, pp.222–234.
- Nakashima, K., Zhou, X., Kunkel, G., Zhang, Z., Deng, J.M., Behringer, R.R. and de Crombrughe, B., (2002) The Novel Zinc Finger-Containing Transcription Factor Osterix Is Required for Osteoblast Differentiation and Bone Formation. *Cell*, 1081, pp.17–29.
- Naot, D. and Cornish, J., (2014) Cytokines and hormones that contribute to the positive association between fat and bone. *Bone Research*, 5, p.70.
- National Osteoporosis Society, (2018) *Hormone Replacement Therapy (HRT) for women and osteoporosis*. Available at: <https://nos.org.uk/media/99720/hormone-replacement-therapy-for-women-and-osteoporosis-factsheet.pdf>.
- National Osteoporosis Society, (2018) *What Is Osteoporosis?* <https://nos.org.uk/about-osteoporosis/what-is-osteoporosis/>. [online] Available at: <https://nos.org.uk/about-osteoporosis/what-is-osteoporosis/> [Accessed 8 Feb. 2018].

Chapter 9 – References

- Neuhuber, B., Swanger, S.A., Howard, L., Mackay, A. and Fischer, I., (2008) Effects of plating density and culture time on bone marrow stromal cell characteristics. *Experimental Hematology*, 369, pp.1176–1185.
- Nikolopoulos, D., Theocharis, S. and Kouraklis, G., (2010) Ghrelin, another factor affecting bone metabolism. *Medical Science Monitor: International Medical Journal of Experimental and Clinical Research*, 167, pp.RA147-162.
- Nillni, E.A., (2007) Regulation of Prohormone Convertases in Hypothalamic Neurons: Implications for ProThyrotropin-Releasing Hormone and Proopiomelanocortin. *Endocrinology*, 1489, pp.4191–4200.
- Nuttall, M.E. and Gimble, J.M., (2004) Controlling the balance between osteoblastogenesis and adipogenesis and the consequent therapeutic implications. *Current Opinion in Pharmacology*, 43, pp.290–294.
- Nuttall, M.E., Patton, A.J., Olivera, D.L., Nadeau, D.P. and Gowen, M., (1998) Human Trabecular Bone Cells Are Able to Express Both Osteoblastic and Adipocytic Phenotype: Implications for Osteopenic Disorders. *Journal of Bone and Mineral Research*, 133, pp.371–382.
- O'Brien, C.A., Jia, D., Plotkin, L.I., Bellido, T., Powers, C.C., Stewart, S.A., Manolagas, S.C. and Weinstein, R.S., (2004) Glucocorticoids Act Directly on Osteoblasts and Osteocytes to Induce Their Apoptosis and Reduce Bone Formation and Strength. *Endocrinology*, 1454, pp.1835–1841.
- O'Connor, C.J., Griffin, T.M., Liedtke, W. and Guilak, F., (2013) Increased susceptibility of Trpv4-deficient mice to obesity and obesity-induced osteoarthritis with very high-fat diet. *Annals of the Rheumatic Diseases*, 722, pp.300–304.
- Ogata, Y., Yamauchi, M., Kim, R.H., Li, J.J., Freedman, L.P. and Sodek, J., (1995) Glucocorticoid Regulation of Bone Sialoprotein (BSP) Gene Expression. *European Journal of Biochemistry*, 2301, pp.183–192.
- Ogden, D. and Stanfield, P., (1994) Patch clamp techniques for single channel and whole-cell recording.

- Ohnaka, K., Tanabe, M., Kawate, H., Nawata, H. and Takayanagi, R., (2005) Glucocorticoid suppresses the canonical Wnt signal in cultured human osteoblasts. *Biochemical and Biophysical Research Communications*, 3291, pp.177–181.
- Otto, F., Thornell, A.P., Crompton, T., Denzel, A., Gilmour, K.C., Rosewell, I.R., Stamp, G.W.H., Beddington, R.S.P., Mundlos, S., Olsen, B.R., Selby, P.B. and Owen, M.J., (1997) Cbfa1, a Candidate Gene for Cleidocranial Dysplasia Syndrome, Is Essential for Osteoblast Differentiation and Bone Development. *Cell*, 895, pp.765–771.
- Pal, S., Gupta, R. and Davuluri, R.V., (2012) Alternative transcription and alternative splicing in cancer. *Pharmacology & Therapeutics*, 1363, pp.283–294.
- Pangalos, M., Bintig, W., Schlingmann, B., Feyerabend, F., Witte, F., Begandt, D., Heisterkamp, A. and Ngezahayo, A., (2011) Action potentials in primary osteoblasts and in the MG-63 osteoblast-like cell line. *Journal of Bioenergetics and Biomembranes*, 433, pp.311–322.
- Parsons, L.C., Brown, R.C., Hopkins, A.L., Lewis, C.L., Thompson, A., Davies, J. and Wells, T., (2015) Ghrelin O-acyl transferase and the growth hormone secretagogue receptor mediate the adipogenic action of unacylated ghrelin in murine bone marrow revealing a novel endocrine mechanism. *Proceedings of The Physiological Society*, [online] Proc Physiol Soc 34. Available at: <http://www.physoc.org/proceedings/abstract/Proc%20Physiol%20Soc%2034C63> [Accessed 11 Feb. 2016].
- Patel, A. and Honoré, E., (2002) The TREK two P domain K⁺ channels. *The Journal of Physiology*, 539Pt 3, p.647.
- Pelto, J., Björninen, M., Pälli, A., Talvitie, E., Hyttinen, J., Mannerström, B., Seppänen, R.S., Kellomäki, M., Miettinen, S. and Haimi, S., (2013) Novel Polypyrrole-Coated Polylactide Scaffolds Enhance Adipose Stem Cell Proliferation and Early Osteogenic Differentiation. *Tissue Engineering. Part A*, 197–8, p.882.
- Peng, R., Yao, X., Cao, B., Tang, J. and Ding, J., (2012) The effect of culture conditions on the adipogenic and osteogenic inductions of mesenchymal stem cells on micropatterned surfaces. *Biomaterials*, 3326, pp.6008–6019.
- van de Peppel, J., Strini, T., Tilburg, J., Westerhoff, H., van Wijnen, A.J. and van Leeuwen, J.P., (2017) Identification of Three Early Phases of Cell-Fate Determination during

Osteogenic and Adipogenic Differentiation by Transcription Factor Dynamics. *Stem Cell Reports*, 84, pp.947–960.

Pereira, R.C., Delany, A.M. and Canalis, E., (2002) Effects of cortisol and bone morphogenetic protein-2 on stromal cell differentiation: correlation with CCAAT-enhancer binding protein expression. *Bone*, 305, pp.685–691.

Petersenn, S., Rasch, A.C., Penschorn, M., Beil, F.U. and Schulte, H.M., (2001) Genomic Structure and Transcriptional Regulation of the Human Growth Hormone Secretagogue Receptor. *Endocrinology*, 1426, pp.2649–2659.

Piek, E., Sleumer, L.S., van Someren, E.P., Heuver, L., de Haan, J.R., de Grijjs, I., Gilissen, C., Hendriks, J.M., van Ravestein-van Os, R.I., Bauerschmidt, S., Dechering, K.J. and van Zoelen, E.J., (2010) Osteo-transcriptomics of human mesenchymal stem cells: Accelerated gene expression and osteoblast differentiation induced by vitamin D reveals c-MYC as an enhancer of BMP2-induced osteogenesis. *Bone*, 463, pp.613–627.

Piters, E., Boudin, E. and Van Hul, W., (2008) Wnt signaling: A win for bone. *Archives of Biochemistry and Biophysics*, 4732, pp.112–116.

Pittenger, M.F., Mackay, A.M., Beck, S.C., Jaiswal, R.K., Douglas, R., Mosca, J.D., Moorman, M.A., Simonetti, D.W., Craig, S. and Marshak, D.R., (1999) Multilineage Potential of Adult Human Mesenchymal Stem Cells. *Science*, 2845411, pp.143–147.

Pizzorno, L., (2016a) Bariatric Surgery: Bad to the Bone, Part 1. *Integrative Medicine: A Clinician's Journal*, 151, pp.48–54.

Pizzorno, L., (2016b) Bariatric Surgery: Bad to the Bone, Part 2. *Integrative Medicine: A Clinician's Journal*, 152, pp.35–46.

Porter, R.L. and Calvi, L.M., (2008) Communications between bone cells and hematopoietic stem cells. *Archives of Biochemistry and Biophysics*, 4732, pp.193–200.

Pountney, D.J., Sun, Z.-Q., Porter, L.M., Nitabach, M.N., Nakamura, T.Y., Holmes, D., Rosner, E., Kaneko, M., Manaris, T., Holmes, T.C. and Coetzee, W.A., (2001) Is the Molecular Composition of KATP Channels more Complex than Originally Thought? *Journal of Molecular and Cellular Cardiology*, 338, pp.1541–1546.

Chapter 9 – References

- Pramojanee, S.N., Phimphilai, M., Chattipakorn, N. and Chattipakorn, S.C., (2014) Possible roles of insulin signaling in osteoblasts. *Endocrine Research*, 394, pp.144–151.
- Quandt, F.N. and Im, W.B., (1992) Tetraalkylammonium ion block of potassium currents in mouse neuroblastoma cells. *Journal of Pharmacology and Experimental Therapeutics*, 2603, pp.1379–1385.
- Rajan, S., Plant, L.D., Rabin, M.L., Butler, M.H. and Goldstein, S.A.N., (2005) Sumoylation Silences the Plasma Membrane Leak K⁺ Channel K2P1. *Cell*, 1211, pp.37–47.
- Ramirez-Ponce, M.P., Mateos, J.C. and Bellido, J.A., (2002) Insulin increases the density of potassium channels in white adipocytes: possible role in adipogenesis. *Journal of Endocrinology*, 1742, pp.299–307.
- Rawlinson, S.C., Pitsillides, A.A. and Lanyon, L.E., (1996) Involvement of different ion channels in osteoblasts' and osteocytes' early responses to mechanical strain. *Bone*, 196, pp.609–614.
- Reagan, M.R., Liaw, L., Rosen, C.J. and Ghobrial, I.M., (2015) Dynamic interplay between bone and multiple myeloma: Emerging roles of the osteoblast. *Bone*, 75, pp.161–169.
- Resende, R.R., Andrade, L.M., Oliveira, A.G., Guimarães, E.S., Guatimosim, S. and Leite, M.F., (2013) Nucleoplasmic calcium signaling and cell proliferation: calcium signaling in the nucleus. *Cell Communication and Signaling*, 11, p.14.
- Rhea, E.M., Salameh, T.S., Gray, S., Niu, J., Banks, W.A. and Tong, J., (2018) Ghrelin transport across the blood–brain barrier can occur independently of the growth hormone secretagogue receptor. *Molecular Metabolism*, 18, pp.88–96.
- Rodeheffer, M.S. and Horowitz, M.C., (2016) Fat Decisions: Leptin Regulates Bone versus Fat in the Marrow. *Cell Stem Cell*, 186, pp.684–686.
- Rodríguez, A., Gómez-Ambrosi, J., Catalán, V., Gil, M.J., Becerril, S., Sáinz, N., Silva, C., Salvador, J., Colina, I. and Frühbeck, G., (2009) Acylated and desacyl ghrelin stimulate lipid accumulation in human visceral adipocytes. *International Journal of Obesity*, 335, pp.541–552.

Chapter 9 – References

- Rodriguez, J., Astudillo, P., Rios, S. and Pino, A., (2008) Involvement of Adipogenic Potential of Human Bone Marrow Mesenchymal Stem Cells (MSCs) in Osteoporosis. *Current Stem Cell Research & Therapy*, 33, pp.208–218.
- Romero, A., Kirchner, H., Heppner, K., Pfluger, P.T., Tschöp, M.H. and Nogueiras, R., (2010) GOAT: the master switch for the ghrelin system? *European Journal of Endocrinology*, 1631, pp.1–8.
- Rorsman, P. and Ashcroft, F.M., (2018) Pancreatic β -Cell Electrical Activity and Insulin Secretion: of Mice and Men. *Physiological reviews*, 981, pp.117–214.
- Rosen, C.J., Ackert-Bicknell, C., Rodriguez, J.P. and Pino, A.M., (2009) Marrow Fat and the Bone Microenvironment: Developmental, Functional, and Pathological Implications. *Critical reviews in eukaryotic gene expression*, 192, pp.109–124.
- Rosen, C.J. and Bouxsein, M.L., (2006) Mechanisms of Disease: is osteoporosis the obesity of bone? *Nature Clinical Practice Rheumatology*, 21, pp.35–43.
- Rosen, E.D. and MacDougald, O.A., (2006) Adipocyte differentiation from the inside out. *Nature Reviews Molecular Cell Biology*, 712, pp.885–896.
- Roux, C., (2011) Osteoporosis in inflammatory joint diseases. *Osteoporosis International*, 222, pp.421–433.
- Rzonca, S.O., Suva, L.J., Gaddy, D., Montague, D.C. and Lecka-Czernik, B., (2004) Bone Is a Target for the Antidiabetic Compound Rosiglitazone. *Endocrinology*, 1451, pp.401–406.
- Sadie-Van Gijsen, H., Hough, F.S. and Ferris, W.F., (2013) Determinants of bone marrow adiposity: The modulation of peroxisome proliferator-activated receptor- γ 2 activity as a central mechanism. *Bone*, 562, pp.255–265.
- Sakaguchi, K., Morita, I. and Murota, S., (2000) Relationship between the ability to support differentiation of osteoclast-like cells and adipogenesis in murine stromal cells derived from bone marrow. *Prostaglandins, Leukotrienes and Essential Fatty Acids (PLEFA)*, 625, pp.319–327.
- Sangiao-Alvarellos, S., Vázquez, M.J., Varela, L., Nogueiras, R., Saha, A.K., Cordido, F., López, M. and Diéguez, C., (2009) Central Ghrelin Regulates Peripheral Lipid Metabolism in a Growth Hormone-Independent Fashion. *Endocrinology*, 15010, pp.4562–4574.

Chapter 9 – References

- Sato, T., Oishi, K., Ida, T. and Kojima, M., (2015) Physiological Functions and Pathology of Ghrelin. *American Journal of Life Sciences*, 33, p.8.
- Schatz, M. and Hamilos, D., (1995) Osteoporosis in Glucocorticoid-Dependent Asthmatic Patients. *Clinical Immunotherapeutics*, 43, pp.180–196.
- Schmittgen, T.D. and Livak, K.J., (2008) Analyzing real-time PCR data by the comparative CT method. *Nature Protocols*, 36, pp.1101–1108.
- Schulz, P., Werner, J., Stauber, T., Henriksen, K. and Fendler, K., (2010) The G215R Mutation in the Cl⁻/H⁺-Antiporter ClC-7 Found in ADO II Osteopetrosis Does Not Abolish Function but Causes a Severe Trafficking Defect. *PLOS ONE*, 59, p.e12585.
- Scott, M.A., Nguyen, V.T., Levi, B. and James, A.W., (2011) Current Methods of Adipogenic Differentiation of Mesenchymal Stem Cells. *Stem Cells and Development*, 2010, pp.1793–1804.
- Seim, I., Amorim, L., Walpole, C., Carter, S., Chopin, L.K. and Herington, A.C., (2010) Ghrelin gene-related peptides: Multifunctional endocrine/autocrine modulators in health and disease. *Clinical and Experimental Pharmacology and Physiology*, 371, pp.125–131.
- Seim, I., Collet, C., Herington, A.C. and Chopin, L.K., (2007) Revised genomic structure of the human ghrelin gene and identification of novel exons, alternative splice variants and natural antisense transcripts. *BMC Genomics*, 8, p.298.
- Seim, I., Jeffery, P.L., Thomas, P.B., Walpole, C.M., Maugham, M., Fung, J.N.T., Yap, P.-Y., O’Keeffe, A.J., Lai, J., Whiteside, E.J., Herington, A.C. and Chopin, L.K., (2016) Multi-species sequence comparison reveals conservation of ghrelin gene-derived splice variants encoding a truncated ghrelin peptide. *Endocrine*, 523, pp.609–617.
- Seim, I., Lubik, A.A., Lehman, M.L., Tomlinson, N., Whiteside, E.J., Herington, A.C., Nelson, C.C. and Chopin, L.K., (2013) Cloning of a novel insulin-regulated ghrelin transcript in prostate cancer. *Journal of Molecular Endocrinology*, 502, pp.179–191.
- Seino, S., Iwanaga, T., Nagashima, K. and Miki, T., (2000) Diverse roles of K(ATP) channels learned from Kir6.2 genetically engineered mice. *Diabetes*, 493, pp.311–318.

- Sekiya, I., Larson, B.L., Vuoristo, J.T., Cui, J.-G. and Prockop, D.J., (2004) Adipogenic Differentiation of Human Adult Stem Cells From Bone Marrow Stroma (MSCs). *Journal of Bone and Mineral Research*, 192, pp.256–264.
- Shefrin, A.E. and Goldman, R.D., (2009) Use of dexamethasone and prednisone in acute asthma exacerbations in pediatric patients. *Canadian Family Physician*, 557, pp.704–706.
- Shuto, Y., Shibasaki, T., Otagiri, A., Kuriyama, H., Ohata, H., Tamura, H., Kamegai, J., Sugihara, H., Oikawa, S. and Wakabayashi, I., (2002) Hypothalamic growth hormone secretagogue receptor regulates growth hormone secretion, feeding, and adiposity. *Journal of Clinical Investigation*, 10911, pp.1429–1436.
- Shuto, Y., Shibasaki, T., Wada, K., Parhar, I., Kamegai, J., Sugihara, H., Oikawa, S. and Wakabayashi, I., (2001) Generation of polyclonal antiserum against the growth hormone secretagogue receptor (GHS-R): Evidence that the GHS-R exists in the hypothalamus, pituitary and stomach of rats. *Life Sciences*, 689, pp.991–996.
- Shyng, S.-L., Ferrigni, T. and Nichols, C.G., (1997) Regulation of KATP Channel Activity by Diazoxide and MgADP : Distinct Functions of the Two Nucleotide Binding Folds of the Sulfonylurea Receptor. *The Journal of General Physiology*, 1106, pp.643–654.
- Siddappa, R., Licht, R., van Blitterswijk, C. and de Boer, J., (2007) Donor variation and loss of multipotency during in vitro expansion of human mesenchymal stem cells for bone tissue engineering. *Journal of Orthopaedic Research*, 258, pp.1029–1041.
- Sievers, F., Wilm, A., Dineen, D., Gibson, T.J., Karplus, K., Li, W., Lopez, R., McWilliam, H., Remmert, M., Söding, J., Thompson, J.D. and Higgins, D.G., (2011) Fast, scalable generation of high-quality protein multiple sequence alignments using Clustal Omega. *Molecular Systems Biology*, 71, p.539.
- Smith, R.G., Feighner, S., Prendergast, K., Guan, X. and Howard, A., (1999) A New Orphan Receptor Involved in Pulsatile Growth Hormone Release. *Trends in Endocrinology & Metabolism*, 104, pp.128–135.
- Song, L. and Tuan, R.S., (2004) Transdifferentiation potential of human mesenchymal stem cells derived from bone marrow. *FASEB journal: official publication of the Federation of American Societies for Experimental Biology*, 189, pp.980–982.

- Song, M., Zhao, D., Wei, S., Liu, C., Liu, Y., Wang, B., Zhao, W., Yang, K., Yang, Y. and Wu, H., (2014) The effect of electromagnetic fields on the proliferation and the osteogenic or adipogenic differentiation of mesenchymal stem cells modulated by dexamethasone. *Bioelectromagnetics*, 357, pp.479–490.
- Sottile, V., Seuwen, K. and Kneissel, M., (2004) Enhanced Marrow Adipogenesis and Bone Resorption in Estrogen-Deprived Rats Treated with the PPARgamma Agonist BRL49653 (Rosiglitazone). *Calcified Tissue International*, 754, pp.329–337.
- Staa, T.P. van, Staa, T.P. van, Staa, T.P. van, Leufkens, H.G.M. and Cooper, C., (2002) The Epidemiology of Corticosteroid-Induced Osteoporosis: a Meta-analysis. *Osteoporosis International*, 1310, pp.777–787.
- Staa, T.P.V., Geusens, P., Bijlsma, J.W.J., Leufkens, H.G.M. and Cooper, C., (2006) Clinical assessment of the long-term risk of fracture in patients with rheumatoid arthritis. *Arthritis & Rheumatism*, 5410, pp.3104–3112.
- Standridge, M., Alemzadeh, R., Zemel, M., Koontz, J. and Moustaid-Moussa, N., (2000) Diazoxide down-regulates leptin and lipid metabolizing enzymes in adipose tissue of Zucker rats. *The FASEB Journal*, 143, pp.455–460.
- Stenderup, K., Justesen, J., Clausen, C. and Kassem, M., (2003) Aging is associated with decreased maximal life span and accelerated senescence of bone marrow stromal cells. *Bone*, 336, pp.919–926.
- Steward, A.J. and Kelly, D.J., (2015) Mechanical regulation of mesenchymal stem cell differentiation. *Journal of Anatomy*, 2276, pp.717–731.
- Styner, M., Sen, B., Xie, Z., Case, N. and Rubin, J., (2010) Indomethacin promotes adipogenesis of mesenchymal stem cells through a cyclooxygenase independent mechanism. *Journal of Cellular Biochemistry*, 1114, pp.1042–1050.
- Suchacki, K.J., Cawthorn, W.P. and Rosen, C.J., (2016) Bone marrow adipose tissue: formation, function and regulation. *Current opinion in pharmacology*, 28, pp.50–56.
- Sui, B., Hu, C., Liao, L., Chen, Y., Zhang, X., Fu, X., Zheng, C., Li, M., Wu, L., Zhao, X. and Jin, Y., (2016) Mesenchymal progenitors in osteopenias of diverse pathologies: differential characteristics in the common shift from osteoblastogenesis to adipogenesis. *Scientific Reports*, 6, p.30186.

Chapter 9 – References

- Sun, Y., Ahmed, S. and Smith, R.G., (2003) Deletion of Ghrelin Impairs neither Growth nor Appetite. *Molecular and Cellular Biology*, 2322, pp.7973–7981.
- Sun, Y., Garcia, J.M. and Smith, R.G., (2007) Ghrelin and Growth Hormone Secretagogue Receptor Expression in Mice during Aging. *Endocrinology*, 1483, pp.1323–1329.
- Sun, Y., Wang, P., Zheng, H. and Smith, R.G., (2004) Ghrelin stimulation of growth hormone release and appetite is mediated through the growth hormone secretagogue receptor. *Proceedings of the National Academy of Sciences of the United States of America*, 10113, pp.4679–4684.
- Sundelacruz, S., Levin, M. and Kaplan, D.L., (2008) Membrane potential controls adipogenic and osteogenic differentiation of mesenchymal stem cells. *PLoS One*, 311, p.e3737.
- Sundelacruz, S., Levin, M. and Kaplan, D.L., (2009) Role of membrane potential in the regulation of cell proliferation and differentiation. *Stem Cell Reviews*, 53, pp.231–246.
- Svedbom, A., Hernlund, E., Ivergård, M., Compston, J., Cooper, C., Stenmark, J., McCloskey, E.V., Jönsson, B. and Kanis, J.A., (2013) Osteoporosis in the European Union: a compendium of country-specific reports. *Archives of Osteoporosis*, [online] 81–2. Available at: <https://www.ncbi.nlm.nih.gov/pmc/articles/PMC3880492/>.
- Swanson, C., Lorentzon, M., Conaway, H.H. and Lerner, U.H., (2006) Glucocorticoid Regulation of Osteoclast Differentiation and Expression of Receptor Activator of Nuclear Factor- κ B (NF- κ B) Ligand, Osteoprotegerin, and Receptor Activator of NF- κ B in Mouse Calvarial Bones. *Endocrinology*, 1477, pp.3613–3622.
- Takeshita, S., Fumoto, T., Naoe, Y. and Ikeda, K., (2014) Age-related marrow adipogenesis is linked to increased expression of RANKL. *Journal of Biological Chemistry*, p.jbc.M114.547919.
- Tamura, H., Kamegai, J., Sugihara, H., Kineman, R.D., Frohman, L.A. and Wakabayashi, I., (2000) Glucocorticoids Regulate Pituitary Growth Hormone Secretagogue Receptor Gene Expression. *Journal of Neuroendocrinology*, 126, pp.481–485.
- Tanaka, M., Hayashida, Y., Iguchi, T., Nakao, N., Nakai, N. and Nakashima, K., (2001a) Organization of the Mouse Ghrelin Gene and Promoter: Occurrence of a Short Noncoding First Exon. *Endocrinology*. [online] Available at:

- http://press.endocrine.org/doi/10.1210/endo.142.8.8433?url_ver=Z39.88-2003&rfr_id=ori:rid:crossref.org&rfr_dat=cr_pub%3dpubmed [Accessed 15 Sep. 2015].
- Tanaka, M., Hayashida, Y., Nakao, N., Nakai, N. and Nakashima, K., (2001b) Testis-specific and developmentally induced expression of a ghrelin gene-derived transcript that encodes a novel polypeptide in the mouse. *Biochimica et Biophysica Acta (BBA) - Gene Structure and Expression*, 15221, pp.62–65.
- Tao, R., Lau, C.-P., Tse, H.-F. and Li, G.-R., (2007) Functional ion channels in mouse bone marrow mesenchymal stem cells. *American Journal of Physiology - Cell Physiology*, 2935, pp.C1561–C1567.
- Tao, R., Lau, C.-P., Tse, H.-F. and Li, G.-R., (2008) Regulation of cell proliferation by intermediate-conductance Ca²⁺-activated potassium and volume-sensitive chloride channels in mouse mesenchymal stem cells. *American Journal of Physiology - Cell Physiology*, 2955, pp.C1409–C1416.
- Taub, D.D., Murphy, W.J. and Longo, D.L., (2010) Rejuvenation of the aging thymus: growth hormone-mediated and ghrelin-mediated signaling pathways. *Current Opinion in Pharmacology*, 104, pp.408–424.
- Teitelbaum, S.L. and Ross, F.P., (2003) Genetic regulation of osteoclast development and function. *Nature Reviews Genetics*, 48, p.638.
- Tharp, D.L., Wamhoff, B.R., Turk, J.R. and Bowles, D.K., (2006) Upregulation of intermediate-conductance Ca²⁺-activated K⁺ channel (IKCa1) mediates phenotypic modulation of coronary smooth muscle. *American Journal of Physiology-Heart and Circulatory Physiology*, 2915, pp.H2493–H2503.
- Theander-Carrillo, C., Wiedmer, P., Cettour-Rose, P., Nogueiras, R., Perez-Tilve, D., Pfluger, P., Castaneda, T.R., Muzzin, P., Schürmann, A., Szanto, I., Tschöp, M.H. and Rohner-Jeanrenaud, F., (2006) Ghrelin action in the brain controls adipocyte metabolism. *Journal of Clinical Investigation*, 1167, pp.1983–1993.
- Thompson, D.L., Lum, K.D., Nygaard, S.C., Kuestner, R.E., Kelly, K.A., Gimble, J.M. and Moore, E.E., (1998) The Derivation and Characterization of Stromal Cell Lines from the Bone Marrow of p53^{-/-} Mice: New Insights into Osteoblast and Adipocyte Differentiation. *Journal of Bone and Mineral Research*, 132, pp.195–204.

- Thompson, N.M., Gill, D.A.S., Davies, R., Loveridge, N., Houston, P.A., Robinson, I.C.A.F. and Wells, T., (2004) Ghrelin and Des-Octanoyl Ghrelin Promote Adipogenesis Directly in Vivo by a Mechanism Independent of the Type 1a Growth Hormone Secretagogue Receptor. *Endocrinology*, 1451, pp.234–242.
- Ton, F.N., Gunawardene, S.C., Lee, H. and Neer, R.M., (2005) Effects of Low-Dose Prednisone on Bone Metabolism. *Journal of Bone and Mineral Research*, 203, pp.464–470.
- Toogood, J.H., (2004) Asthma and Therapeutics: Inhaled Corticosteroids, Corticosteroid Osteoporosis, and the Risk of Fracture in Chronic Asthma. *Allergy, Asthma & Clinical Immunology*, 11, p.28.
- Tornvig, L., Mosekilde, L., Justesen, J., Falk, E. and Kassem, M., (2001) Troglitazone Treatment Increases Bone Marrow Adipose Tissue Volume but Does not Affect Trabecular Bone Volume in Mice. *Calcified Tissue International*, 691, pp.46–50.
- Tschöp, M., Flora, D.B., Mayer, J.P. and Heiman, M.L., (2002) Hypophysectomy prevents ghrelin-induced adiposity and increases gastric ghrelin secretion in rats. *Obesity Research*, 1010, pp.991–999.
- Tschöp, M., Smiley, D.L. and Heiman, M.L., (2000) Ghrelin induces adiposity in rodents. *Nature*, 4076806, pp.908–913.
- van der Velde, M., Eerden, V.D., C.j, B., Sun, Y., Almering, J.M.M., van der Lely, A.-J., Delhanty, P.J.D., Smith, R.G., Leeuwen, V. and P.t.m, J., (2012) An Age-Dependent Interaction with Leptin Unmasks Ghrelin's Bone-Protective Effects. *Endocrinology*, 1538, pp.3593–3602.
- Venables, J.P., Klinck, R., Koh, C., Gervais-Bird, J., Bramard, A., Inkel, L., Durand, M., Couture, S., Froehlich, U., Lapointe, E., Lucier, J.-F., Thibault, P., Rancourt, C., Tremblay, K., Prinos, P., Chabot, B. and Elela, S.A., (2009) Cancer-associated regulation of alternative splicing. *Nature Structural & Molecular Biology*, 166, pp.670–676.
- Verma, S., Rajaratnam, J.H., Denton, J., Hoyland, J.A. and Byers, R.J., (2002) Adipocytic proportion of bone marrow is inversely related to bone formation in osteoporosis. *Journal of Clinical Pathology*, 559, pp.693–698.

- Wang, B., Jaffe, D.B. and Brenner, R., (2014) Current understanding of iberiotoxin-resistant BK channels in the nervous system. *Frontiers in Physiology*, [online] 5. Available at: <https://www.frontiersin.org/articles/10.3389/fphys.2014.00382/full> [Accessed 29 Aug. 2018].
- Wang, C., Meng, H., Wang, X., Zhao, C., Peng, J. and Wang, Y., (2016) Differentiation of Bone Marrow Mesenchymal Stem Cells in Osteoblasts and Adipocytes and its Role in Treatment of Osteoporosis. *Medical Science Monitor: International Medical Journal of Experimental and Clinical Research*, 22, pp.226–233.
- Wang, D., Haile, A. and Jones, L.C., (2013) Dexamethasone-induced lipolysis increases the adverse effect of adipocytes on osteoblasts using cells derived from human mesenchymal stem cells. *Bone*, 532, pp.520–530.
- Wang, F.-S., Lin, C.-L., Chen, Y.-J., Wang, C.-J., Yang, K.D., Huang, Y.-T., Sun, Y.-C. and Huang, H.-C., (2005) Secreted Frizzled-Related Protein 1 Modulates Glucocorticoid Attenuation of Osteogenic Activities and Bone Mass. *Endocrinology*, 1465, pp.2415–2423.
- Wang, S.-P., Wang, J.-A., Luo, R.-H., Cui, W.-Y. and Wang, H., (2008) Potassium channel currents in rat mesenchymal stem cells and their possible roles in cell proliferation. *Clinical and Experimental Pharmacology & Physiology*, 359, pp.1077–1084.
- Wang, Y.-H., Zheng, H.-Y., Qin, N.-L., Yu, S.-B. and Liu, S.-Y., (2007) Involvement of ATP-sensitive potassium channels in proliferation and differentiation of rat preadipocytes. *Sheng Li Xue Bao: [Acta Physiologica Sinica]*, 591, pp.8–12.
- Wann, K.T., Henney, N.C., Prajerová, I., Boolaky, U.V. and Evans, B.A.J., (2004) *Single channels in human osteoblast-like cells*. [online] Available at: <http://www.physoc.org/proceedings/abstract/J%20Physiol%20555PPC59> [Accessed 30 Oct. 2014].
- Wee, N.K.Y. and Baldock, P.A., (2014) The hunger games of skeletal metabolism. *BoneKEy Reports*, 3, p.588.
- Wei, W., Motoike, T., Krzeszinski, J.Y., Jin, Z., Xie, X.-J., Dechow, P.C., Yanagisawa, M. and Wan, Y., (2014) Orexin Regulates Bone Remodeling via a Dominant Positive Central Action and a Subordinate Negative Peripheral Action. *Cell Metabolism*, 196, pp.927–940.

Chapter 9 – References

- Weinstein, R.S., (2012) Glucocorticoid-Induced Osteoporosis and Osteonecrosis. *Endocrinology and metabolism clinics of North America*, 413, pp.595–611.
- Wells, T., (2009) Ghrelin – Defender of fat. *Progress in Lipid Research*, 485, pp.257–274.
- Willert, K., Brown, J.D., Danenberg, E., Duncan, A.W., Weissman, I.L., Reya, T., Yates, J.R. and Nusse, R., (2003) Wnt proteins are lipid-modified and can act as stem cell growth factors. *Nature*, 4236938, pp.448–452.
- Wortley, K.E., Rincon, J.-P. del, Murray, J.D., Garcia, K., Iida, K., Thorner, M.O. and Sleeman, M.W., (2005) Absence of ghrelin protects against early-onset obesity. *The Journal of Clinical Investigation*, 11512, pp.3573–3578.
- Wren, A.M., Small, C.J., Ward, H.L., Murphy, K.G., Dakin, C.L., Taheri, S., Kennedy, A.R., Roberts, G.H., Morgan, D.G.A., Ghatei, M.A. and Bloom, S.R., (2000) The Novel Hypothalamic Peptide Ghrelin Stimulates Food Intake and Growth Hormone Secretion. *Endocrinology*, 14111, pp.4325–4328.
- Wu, Y., Shyng, S.-L. and Chen, P.-C., (2015) Concerted Trafficking Regulation of Kv2.1 and KATP Channels by Leptin in Pancreatic β -Cells. *Journal of Biological Chemistry*, 29050, pp.29676–29690.
- Yada, T., Damdindorj, B., Rita, R.S., Kurashina, T., Ando, A., Taguchi, M., Koizumi, M., Sone, H., Nakata, M., Kakei, M. and Dezaki, K., (2014) Ghrelin signalling in β -cells regulates insulin secretion and blood glucose. *Diabetes, Obesity and Metabolism*, 16S1, pp.111–117.
- Yamada, M., Isomoto, S., Matsumoto, S., Kondo, C., Shindo, T., Horio, Y. and Kurachi, Y., (1997) Sulphonylurea receptor 2B and Kir6.1 form a sulphonylurea-sensitive but ATP-insensitive K⁺ channel. *The Journal of Physiology*, 499Pt 3, pp.715–720.
- Yang, J., Brown, M.S., Liang, G., Grishin, N.V. and Goldstein, J.L., (2008) Identification of the Acyltransferase that Octanoylates Ghrelin, an Appetite-Stimulating Peptide Hormone. *Cell*, 1323, pp.387–396.
- Yao, W., Cheng, Z., Busse, C., Pham, A., Nakamura, M.C. and Lane, N.E., (2008) Glucocorticoid excess in mice results in early activation of osteoclastogenesis and adipogenesis and prolonged suppression of osteogenesis: A longitudinal study of gene

expression in bone tissue from glucocorticoid-treated mice. *Arthritis & Rheumatism*, 586, pp.1674–1686.

Yasuda, T., Cuny, H. and Adams, D.J., (2013) Kv3.1 channels stimulate adult neural precursor cell proliferation and neuronal differentiation. *The Journal of Physiology*, 59110, pp.2579–2591.

Ye, N. and Jiang, D., (2015) Ghrelin accelerates the growth and osteogenic differentiation of rabbit mesenchymal stem cells through the ERK1/2 pathway. *BMC Biotechnology*, 15, p.51.

Yeh, A.H., Jeffery, P.L., Duncan, R.P., Herington, A.C. and Chopin, L.K., (2005) Ghrelin and a Novel Preproghrelin Isoform Are Highly Expressed in Prostate Cancer and Ghrelin Activates Mitogen-Activated Protein Kinase in Prostate Cancer. *Clinical Cancer Research*, 1123, pp.8295–8303.

Yellowley, C.E., Hancox, J.C., Skerry, T.M. and Levi, A.J., (1998) Whole-cell membrane currents from human osteoblast-like cells. *Calcified Tissue International*, 622, pp.122–132.

Yeon, J.-T., Kim, K.-J., Chun, S.W., Lee, H.I., Lim, J.Y., Son, Y.-J., Kim, S.H. and Choi, S.-W., (2015) KCNK1 inhibits osteoclastogenesis by blocking the Ca²⁺ oscillation and JNK–NFATc1 signaling axis. *J Cell Sci*, 12818, pp.3411–3419.

Yin, L., Li, Y. and Wang, Y., (2006) Dexamethasone-induced adipogenesis in primary marrow stromal cell cultures: mechanism of steroid-induced osteonecrosis. *Chinese Medical Journal*, 1197, pp.581–588.

Yin, Y. and Zhang, W., (2016) The Role of Ghrelin in Senescence: A Mini-Review. *Gerontology*, 622, pp.155–162.

Yogui, F.C., Momesso, G.A.C., Faverani, L.P., Polo, T.O.B., Ramalho-Ferreira, G., Hassumi, J.S., Rossi, A.C., Freire, A.R., Prado, F.B. and Okamoto, R., (2018) A SERM increasing the expression of the osteoblastogenesis and mineralization-related proteins and improving quality of bone tissue in an experimental model of osteoporosis. *Journal of Applied Oral Science*, [online] 26. Available at: <https://www.ncbi.nlm.nih.gov/pmc/articles/PMC5933824/> [Accessed 2 Aug. 2018].

Chapter 9 – References

- You, M., Song, M.S., Lee, S.K., Ryu, P.D., Lee, S.Y. and Kim, D., (2013) Voltage-gated K⁺ channels in adipogenic differentiation of bone marrow-derived human mesenchymal stem cells. *Acta Pharmacologica Sinica*, 341, pp.129–136.
- Youm, Y.-H., Yang, H., Sun, Y., Smith, R.G., Manley, N.R., Vandanmagsar, B. and Dixit, V.D., (2009) Deficient Ghrelin Receptor-mediated Signaling Compromises Thymic Stromal Cell Microenvironment by Accelerating Thymic Adiposity. *Journal of Biological Chemistry*, 28411, pp.7068–7077.
- Yu, M., Liu, S., Sun, P., Pan, H., Tian, C. and Zhang, L., (2016) Peptide toxins and small-molecule blockers of BK channels. *Acta Pharmacologica Sinica*, 371, pp.56–66.
- Yuan, Z., Li, Q., Luo, S., Liu, Z., Luo, D., Zhang, B., Zhang, D., Rao, P. and Xiao, J., (2015) PPAR γ and Wnt Signaling in Adipogenic and Osteogenic Differentiation of Mesenchymal Stem Cells. *Current Stem Cell Research & Therapy*.
- Yue, R., Zhou, B.O., Shimada, I.S., Zhao, Z. and Morrison, S.J., (2016) Leptin Receptor Promotes Adipogenesis and Reduces Osteogenesis by Regulating Mesenchymal Stromal Cells in Adult Bone Marrow. *Cell Stem Cell*, 186, pp.782–796.
- Zhang, J., Li, M., Kang, E.-T. and Neoh, K.G., (2016) Electrical stimulation of adipose-derived mesenchymal stem cells in conductive scaffolds and the roles of voltage-gated ion channels. *Acta Biomaterialia*, 32Supplement C, pp.46–56.
- Zhang, W., Yang, G.-J., Wu, S.-X., Li, D.-Q., Xu, Y.-B., Ma, C.-H., Wang, J.-L. and Chen, W.-W., (2018) The guiding role of bone metabolism test in osteoporosis treatment. *American Journal of Clinical and Experimental Immunology*, 72, pp.40–49.
- Zhang, W., Zhao, L., Lin, T.R., Chai, B., Fan, Y., Gantz, I. and Mulholland, M.W., (2004) Inhibition of Adipogenesis by Ghrelin. *Molecular Biology of the Cell*, 155, pp.2484–2491.
- Zhang, X., Yang, M., Lin, L., Chen, P., Ma, K.T., Zhou, C.Y. and Ao, Y.F., (2006) Runx2 Overexpression Enhances Osteoblastic Differentiation and Mineralization in Adipose-Derived Stem Cells in vitro and in vivo. *Calcified Tissue International*, 793, pp.169–178.
- Zhang, X.-H., Zhang, Y.-Y., Sun, H.-Y., Jin, M.-W. and Li, G.-R., (2012) Functional ion channels and cell proliferation in 3T3-L1 preadipocytes. *Journal of Cellular Physiology*, 2275, pp.1972–1979.

Chapter 9 – References

- Zhang, Y., Ma, C., Liu, X., Wu, Z., Yan, P., Ma, N., Fan, Q. and Zhao, Q., (2015) Epigenetic landscape in PPAR γ 2 in the enhancement of adipogenesis of mouse osteoporotic bone marrow stromal cell. *Biochimica et Biophysica Acta (BBA) - Molecular Basis of Disease*, 185211, pp.2504–2516.
- Zhang, Y., Marsboom, G., Toth, P.T. and Rehman, J., (2013) Mitochondrial Respiration Regulates Adipogenic Differentiation of Human Mesenchymal Stem Cells. *PLOS ONE*, 810, p.e77077.
- Zhang, Y.-Y., Yue, J., Che, H., Sun, H.-Y., Tse, H.-F. and Li, G.-R., (2014) BKCa and hEag1 Channels Regulate Cell Proliferation and Differentiation in Human Bone Marrow-Derived Mesenchymal Stem Cells. *Journal of Cellular Physiology*, 2292, pp.202–212.
- Zhao, L.-J., Jiang, H., Papasian, C.J., Maulik, D., Drees, B., Hamilton, J. and Deng, H.-W., (2008) Correlation of Obesity and Osteoporosis: Effect of Fat Mass on the Determination of Osteoporosis. *Journal of Bone and Mineral Research*, 231, pp.17–29.
- Zhao, Q., Wei, Q., He, A., Jia, R. and Xiao, Y., (2009) CLC-7: A potential therapeutic target for the treatment of osteoporosis and neurodegeneration. *Biochemical and Biophysical Research Communications*, 3843, pp.277–279.
- Zhao, S., Kato, Y., Zhang, Y., Harris, S., Ahuja, S.S. and Bonewald, L.F., (2002) MLO-Y4 Osteocyte-Like Cells Support Osteoclast Formation and Activation. *Journal of Bone and Mineral Research*, 1711, pp.2068–2079.
- Zhou, H., Lu, S.S. and Dempster, D.W., (2010) Chapter 2 - Bone Remodeling: Cellular Activities in Bone. In: E.S. Orwoll, J.P. Bilezikian and D. Vanderschueren, eds., *Osteoporosis in Men (Second Edition)*. [online] San Diego: Academic Press, pp.15–24. Available at: <http://www.sciencedirect.com/science/article/pii/B978012374602300002X>.
- Zhou, X., Zhang, Z., Feng, J.Q., Dusevich, V.M., Sinha, K., Zhang, H., Darnay, B.G. and Crombrughe, B. de, (2010) Multiple functions of Osterix are required for bone growth and homeostasis in postnatal mice. *Proceedings of the National Academy of Sciences*, 10729, pp.12919–12924.
- Zhu, X., Cao, Y., Voodg, K. and Steiner, D.F., (2006) On the Processing of Proghrelin to Ghrelin. *Journal of Biological Chemistry*, 28150, pp.38867–38870.

Chapter 9 – References

Zigman, J.M., Nakano, Y., Coppari, R., Balthasar, N., Marcus, J.N., Lee, C.E., Jones, J.E., Deysher, A.E., Waxman, A.R., White, R.D., Williams, T.D., Lachey, J.L., Seeley, R.J., Lowell, B.B. and Elmquist, J.K., (2005) Mice lacking ghrelin receptors resist the development of diet-induced obesity. *The Journal of Clinical Investigation*, 11512, pp.3564–3572.

Zych, J., Stimamiglio, M.A., Senegaglia, A.C., Brofman, P.R.S., Dallagiovanna, B., Goldenberg, S., Correa, A., Zych, J., Stimamiglio, M.A., Senegaglia, A.C., Brofman, P.R.S., Dallagiovanna, B., Goldenberg, S. and Correa, A., (2013) The epigenetic modifiers 5-aza-2'-deoxycytidine and trichostatin A influence adipocyte differentiation in human mesenchymal stem cells. *Brazilian Journal of Medical and Biological Research*, 465, pp.405–416.

